

**Generation and functional characterization of specific receptor inhibitors based
on an analysis of the VEGFR-2 activation mechanism**

Inauguraldissertation

zur

Erlangung der Würde eines Doktors der Philosophie

vorgelegt der

Philosophisch-Naturwissenschaftlichen Fakultät

der Universität Basel

von Alexandra Giese

aus Freiburg im Brsg., Deutschland

Basel, 2012

Originaldokument gespeichert auf dem Dokumentenserver der Universität Basel

edoc.unibas.ch



Dieses Werk ist unter dem Vertrag „Creative Commons Namensnennung-Keine kommerzielle Nutzung-Keine Bearbeitung 2.5 Schweiz“ lizenziert. Die vollständige Lizenz kann unter

creativecommons.org/licences/by-nc-nd/2.5/ch

eingesehen werden.

Genehmigt von der Philosophisch-Naturwissenschaftlichen Fakultät auf Antrag der Professoren:

Prof. Kurt Ballmer-Hofer

Prof. Thérèse Resink

Basel, den 24.05.2011

Prof. Dr. Martin Spiess
Dekan



Namensnennung-Keine kommerzielle Nutzung-Keine Bearbeitung 2.5 Schweiz

Sie dürfen:



das Werk vervielfältigen, verbreiten und öffentlich zugänglich machen

Zu den folgenden Bedingungen:



Namensnennung. Sie müssen den Namen des Autors/Rechteinhabers in der von ihm festgelegten Weise nennen (wodurch aber nicht der Eindruck entstehen darf, Sie oder die Nutzung des Werkes durch Sie würden entlohnt).



Keine kommerzielle Nutzung. Dieses Werk darf nicht für kommerzielle Zwecke verwendet werden.



Keine Bearbeitung. Dieses Werk darf nicht bearbeitet oder in anderer Weise verändert werden.

- Im Falle einer Verbreitung müssen Sie anderen die Lizenzbedingungen, unter welche dieses Werk fällt, mitteilen. Am Einfachsten ist es, einen Link auf diese Seite einzubinden.
- Jede der vorgenannten Bedingungen kann aufgehoben werden, sofern Sie die Einwilligung des Rechteinhabers dazu erhalten.
- Diese Lizenz lässt die Urheberpersönlichkeitsrechte unberührt.

Die gesetzlichen Schranken des Urheberrechts bleiben hiervon unberührt.

Die Commons Deed ist eine Zusammenfassung des Lizenzvertrags in allgemeinverständlicher Sprache: <http://creativecommons.org/licenses/by-nc-nd/2.5/ch/legalcode.de>

Haftungsausschluss:

Die Commons Deed ist kein Lizenzvertrag. Sie ist lediglich ein Referenztext, der den zugrundeliegenden Lizenzvertrag übersichtlich und in allgemeinverständlicher Sprache wiedergibt. Die Deed selbst entfaltet keine juristische Wirkung und erscheint im eigentlichen Lizenzvertrag nicht. Creative Commons ist keine Rechtsanwaltsgesellschaft und leistet keine Rechtsberatung. Die Weitergabe und Verlinkung des Commons Deeds führt zu keinem Mandatsverhältnis.

TABLE OF CONTENTS

Summary	i
Zusammenfassung	iii
1 Introduction	1
1.1 Angiogenesis.....	1
1.1.1 Physiological and pathological angiogenesis	1
1.1.2 Growth Factors, Receptors, Coreceptors in angiogenesis.....	2
1.2 Vascular Endothelial Growth Factor Receptor-2.....	3
1.2.1 Vascular Endothelial Growth Factor Receptor-2 properties and signaling.....	3
1.2.2 Structure of VEGFs and VEGFR-2 extracellular domain.....	5
1.3 Anti-angiogenic therapy.....	7
1.3.1 Available drugs for anti-angiogenic therapy	7
1.3.2 Antibodies in the clinic.....	8
1.3.2.1 Definition of an antibody	8
1.3.2.2 Phage Display.....	9
1.3.2.3 ETH-2 Gold Library.....	11
1.3.3 Designed Ankyrin Repeat Proteins	13
1.3.3.1 Definition of a Designed Ankyrin Repeat Protein	13
1.3.3.2 Ribosome Display	15
1.4 Aim of the thesis	16
2 Structure–function analysis of VEGF receptor activation and the role of coreceptors in angiogenic signaling	17
3 Inhibition of receptor activation by Designed Ankyrin Repeat Proteins specific for the Ig-homology domain 4 of VEGFR-2 extracellular domain	19
3.1 Abstract.....	20
3.2 Introduction.....	20
3.3 Materials and Methods.....	22

3.3.1	Cloning of VEGFR-2 mutants.....	22
3.3.2	Cell culture	22
3.3.3	Transfection of HEK293 and COS-1 cells	23
3.3.4	Generation of Stably Transfected PAE-Cells by Retroviral Transduction	23
3.3.5	VEGF Receptor Activation	23
3.3.6	Immunocytochemistry.....	24
3.3.7	Sprouting of BAECs.....	24
3.3.8	Cloning of Expression Plasmids.....	25
3.3.9	Production and Purification of Recombinant Proteins.....	25
3.3.10	Size Exclusion Chromatography coupled Multi-Angle Light Scattering (SEC-MALS).....	26
3.3.11	Ribosome Display	26
3.3.12	Epitope-mapping ELISA.....	26
3.4	Results.....	27
3.4.1	Role of membrane-proximal Ig-homology domains 4 and 7 in receptor activation	27
3.4.2	Isolation and characterization of Ig-homology domain-specific DARPins	30
3.4.3	Effect of DARPins on ligand-mediated receptor dimerization	32
3.4.4	Functional characterization of receptor-inhibitory DARPins	34
3.5	Discussion	39
3.6	Supplementary Information	43
4	Isolation of single chain variable fragment antibodies against Ig-homology domain 7 of the VEGFR-2 extracellular domain	51
4.1	Introduction.....	51
4.2	Materials and Methods.....	52
4.2.1	Phage selection on immobilized antigen.....	52
4.2.2	Enzyme linked Immunosorbent Assay.....	52
4.2.3	Expression and Purification of scFv.....	53
4.2.4	Receptor kinase Inhibition Assay.....	53
4.3	Results.....	54
4.3.1	Production and purification of VEGFR-2 D7	54
4.3.2	Phage display selection of scFvs against VEGFR-2 ECD D7	54
4.3.3	Functional characterization of anti-VEGFR-2 D7 scFv 3B1	58

4.4	Discussion	59
5	Novel functional germline variations in the vascular endothelial growth factor receptor 2 gene and their effect on gene expression and microvessel density in lung cancer	61
6	Monitoring Migration of Endothelial Cells on Micropatterned Biochips	63
6.1	Abstract	63
6.2	Introduction	63
6.3	Materials and Methods	65
6.3.1	Materials	65
6.3.2	Molecular-Assembly Patterning after Lift-Off	65
6.3.3	Microfluidics	66
6.3.4	Cell culture	66
6.4	Results	67
6.4.1	VEGF Immobilization through Molecular-Assembly Patterning by Lift-Off (MAPL)	67
6.4.2	Cell attachment to immobilized VEGF-A ₁₆₅	70
6.4.3	Generation of a protein gradient through microfluidics	72
6.4.4	Cell growth on VEGF-A gradients	74
6.5	Discussion	75
7	Conclusions and Outlook	77
8	Abbreviations	79
9	References	83
10	Acknowledgements	93
11	List of Publications	95
12	Curriculum Vitae	97

13 APPENDIX A	99
14 APPENDIX B	114
15 APPENDIX C	158

TABLE OF FIGURES

Figure 1-1:	VEGFR-2 signaling and phosphorylation sites.	4
Figure 1-2:	Model for the activation of VEGFR-2.	6
Figure 1-3:	Homotypic VEGFR-2 domain 7 interface.	6
Figure 1-4:	Selection of single chain Fvs from a phage display library.	11
Figure 1-5:	Variable heavy and light chain sequence design in a scFv (ETH-Gold-2 library).	12
Figure 1-6:	pHEN1 expression plasmid.	13
Figure 1-7:	Scheme of DARPin library design.	14
Figure 1-8:	Ribosome display technology.	15
Figure 3-1:	Schematic representation of the β E- β F loop in VEGFR-2 D7 and sequences of generated mutants.	27
Figure 3-2:	The conserved dimerization motif in D7 is crucial for ligand-induced activation of VEGFR-2.	28
Figure 3-3:	D4 is essential for ligand-induced VEGFR-2 activation.	29
Figure 3-4:	DARPin specificity for VEGFR-2.	30
Figure 3-5:	DARPin 6C8 binds to D4 and DARPin 6G9 to D2-3.	31
Figure 3-6:	DARPin 6C8 does not interfere with dimerization of VEGFR-2 ECD whereas DARPin 6G9 prevents dimerization in the presence of VEGF.	33
Figure 3-7:	DARPins 6G9 and 6C8 inhibit VEGFR-2 activation and downstream signaling.	34
Figure 3-8:	DARPins 6G9 and 6C8 inhibit VEGFR-2 internalization after stimulation.	35
Figure 3-9:	DARPins 6G9 and 6C8 inhibit sprouting of BAECs in the EC-spheroid assay.	36
Figure 3-10:	Endothelial cell sprouting over time.	37
Figure 3-11:	Inhibition of endothelial cell sprouting by DARPin 6C8.	38
Figure 3-12:	Schematic representation of VEGFR-2 mutants.	43
Figure 3-13:	Ligand-induced activation of VEGFR-2 is compromised by mutation of D4 and D7.	44
Figure 3-14:	Ligand-induced activation of VEGFR-2 is compromised by mutation of D4.	45
Figure 3-15:	Stainings of VEGFR-2 on cells with DARPins are specific.	46
Figure 3-16:	DARPins 3C8, 6G9, and 6C8 inhibit VEGFR-2 activation.	47

Figure 4-1:	Binding specificities of anti-VEGFR-2 D7 scFv clones.	55
Figure 4-2:	Purification of anti-VEGFR-2 D7 scFv 3B1.	56
Figure 4-3:	ScFvs 3B1 in its current form does not inhibit VEGFR-2 activation.	58
Figure 5-1:	VEGFR-2 phosphorylation in HEK293 cells and effect of four non-synonymous variants.	61
Figure 6-1:	Molecular patterning after Lift-Off strategy for the immobilization of VEGF-A ₁₆₅	67
Figure 6-2:	Immobilization of Streptavidin-Alexa488 on the PLL-g-PEG biotin pattern produced by MAPL.	68
Figure 6-3:	Immobilization of VEGF-A ₁₆₅ via heparin on the PLL-g-PEG biotin pattern.	69
Figure 6-4:	PAE-VEGFR-2 cells grown on VEGF-A ₁₆₅ patterned coverslips.	70
Figure 6-5:	Migration of PAE cells on VEGF-A ₁₆₅ patterns	71
Figure 6-6:	Microfluidics strategy for the generation of a VEGF-A gradient on coverslips.	73
Figure 6-7:	PAE-VEGFR-2 cells grown on VEGF-A ₁₆₅ gradients.	74

Summary

Angiogenesis, the formation of new blood vessels from preexisting vasculature, mainly occurs during embryonic development. In the adult it takes place in the female reproductive system and during wound healing. Unregulated angiogenesis is associated with various diseases such as atherosclerosis, retinopathies, lymphoproliferative or rheumatoid disease, and cancer. Tumor neovascularization enables cancer cells to enter the blood circulation and to metastasize to other organs and is a hallmark of many types of cancer.

Vascular Endothelial Growth Factors (VEGFs) constitute a family of proteins that play an important role in blood and lymphatic vessel development. VEGFs interact with three type V receptor tyrosine kinases, VEGFR-1, -2, and -3 promoting endothelial cell survival, migration, proliferation, and differentiation. VEGFR-2 is the major mediator of angiogenic signaling in endothelial cells and its activity is regulated at multiple levels. Ligand binding to the extracellular domain (ECD) of VEGFR-2 leads to receptor dimerization followed by activation of the intracellular kinase domain and downstream signaling. However, at present the specific structural changes in the ECD and the exact molecular mechanisms underlying kinase activation are only partially understood. In this study, we investigated the role of ECD Immunoglobulin (Ig)-homology domains D4 and D7 in receptor dimerization and activation. We expressed a series of receptor ECD mutants in tissue culture cells and determined receptor activation. Mutation or deletion of D4 or D7 drastically reduced receptor activation. We interpret these data as the demonstration that Ig-homology domains 4 and 7 are required for correctly aligning receptor monomers in active dimers and are thus indispensable for kinase activation.

Based on our insights into the activation mechanism of VEGFR-2, we generated two types of ECD binders, single chain Fvs (scFvs) and Designed Ankyrin Repeat Proteins (DARPs), specifically interacting with single Ig-homology domains. We tested these reagents for inhibition of ligand-stimulated receptor activation. We identified several DARPs interacting with D2-3 and thereby blocking ligand binding and receptor activation. Most interestingly, DARPs binding to D4 inhibited receptor activation without interfering with receptor dimerization and therefore behave as allosteric regulators of VEGFR-2. Furthermore, scFvs specifically binding to D7 were identified. These new reagents will be useful for *in vivo* studies aiming at vessel imaging or for inhibiting VEGFR-2.

We furthermore characterized variations in the VEGFR-2 gene which might contribute to the phenotypic variability in tumor endothelial function and, consequently, may affect cancer progression and the susceptibility of tumors to VEGFR-2 inhibitors. VEGFR-2 genomic sequencing

in three different ethnic groups led to the discovery of 120 genetic variants, single nucleotide polymorphisms (SNPs), of which 25 had not been previously reported. The functionality of the genetic variants was assessed by phosphorylation assays, mRNA and protein expression arrays, as well as by the measurement of microvessel density in non-small cell lung cancer (NSCLC) tumor samples. The correlations found may have important implications for understanding the molecular basis of genetic associations between VEGFR-2 variation and clinical phenotypes related to VEGFR-2 function.

Finally, we were interested in the influence of extracellular matrix components on VEGF-induced angiogenesis. *In vivo*, endothelial cells are exposed to concentration gradients of soluble growth factors and matrix immobilized guidance cues. To better mimic the complexity of angiogenic tissues *in vitro*, we generated micropatterned coverslips derivatized with VEGF for the cultivation of endothelial cells and the monitoring of their migration. Immobilized VEGF was shown to be biologically active and endothelial cells migrated and adhered to the patterned surfaces. The micropatterned coverslips present a robust and reproducible platform for the characterization of complex cellular behaviors generated by multiple VEGF isoforms.

Zusammenfassung

Die Bildung neuer Blutgefäße aus der bereits vorhandenen Vaskulatur, die sogenannte Angiogenese, tritt hauptsächlich während der Embryonalentwicklung auf. Beim erwachsenen Menschen kommt die Angiogenese sowohl im Fortpflanzungstrakt der Frau als auch in der Wundheilung auf natürliche Art und Weise vor. Unkontrollierte Angiogenese ist mit einer Vielzahl von Erkrankungen wie z.B. Arteriosklerose, Retinopathien, lymphoproliferative oder rheumatoide Krankheiten sowie Krebs verbunden. Blutgefäßneubildung im Tumor ermöglichen es den Tumorzellen in den Blutkreislauf zu gelangen und in andere lebenswichtige Organe zu metastasieren. Dieser Prozess ist ein Markenzeichen vieler Krebsarten.

Vascular Endothelial Growth Factors (VEGFs) gehören zu einer Familie von Proteinen, die eine wichtige Rolle in der Bildung von Blut- und Lymphgefäßen spielt. VEGFs interagieren mit drei Typ V Rezeptor Tyrosin Kinasen, den VEGFR-1, -2, und -3 und fördern das Überleben, die Migration, die Proliferation, und die Differenzierung von Endothelzellen. Der VEGFR-2 ist das hauptverantwortliche Protein in der Signalübertragung der Angiogenese und seine Aktivierung wird auf vielen verschiedenen Ebenen reguliert. Die Bindung seines Liganden an die extrazelluläre Domäne (ECD) des VEGFR-2 führt zu Dimerisierung des Rezeptors, gefolgt von der Aktivierung der intrazellulären Kinase-Domäne und des darunterliegenden Signaltransportweges. Die spezifischen, dabei zugrundeliegenden strukturellen Veränderungen in der ECD als auch die molekularen Mechanismen und Details der Kinase Aktivierung sind gegenwärtig jedoch nur teilweise erforscht. In meinem Forschungsprojekt haben wir die Rolle der extrazellulären Immunglobulin-ähnlichen Domänen 4 und 7 in der Rezeptor Dimerisierung und seiner Aktivierung untersucht. Verschiedene Rezeptor-ECD Mutanten wurden in kultivierten Zellen exprimiert und deren Grad der Rezeptor-Aktivierung bestimmt. Mutationen oder eine Deletion in der D4 beziehungsweise D7 führten zu einer Reduktion der Rezeptor-Aktivierung. Wir interpretieren unsere Daten als Beweis dafür, dass die Ig-Homologie Domänen 4 und 7 für die korrekte Ausrichtung der Rezeptor Monomere, eine Grundvoraussetzung für die Aktivierung einer Kinase, in den aktiven Dimeren unverzichtbar sind.

Basierend auf unseren Erkenntnissen über den Aktivierungsmechanismus des VEGFR-2 haben wir zwei verschiedene Arten von ECD bindenden Reagenzien entwickelt, single chain Fvs (scFvs) und Designed Ankyrin Repeat Proteins (DARPs). Diese interagieren mit einzelnen Ig-Homologie Domänen mit hoher Spezifität und wurden auf ihre Fähigkeit der Inhibition der Liganden-stimulierten Rezeptor Aktivierung getestet. Es wurden mehrere DARPs identifiziert, welche die Bindung des Liganden in D2-3 blockierten und so eine Aktivierung des Rezeptors

verhinderten. Interessanterweise inhibierten D4 bindende DARPins die Rezeptor Aktivierung ohne gleichzeitig Einfluss auf die Dimerisierung des Rezeptors zu nehmen. Dieses Phänomen ähnelt einer Art allosterischen VEGFR-2 Regulation. Solche neuen Reagenzien sind sehr nützlich für die Bildanalyse von Blutgefäßen oder das Inhibieren der VEGFR-2 Aktivierung *in vivo*.

Darüber hinaus haben wir Variationen des VEGFR-2 Gens charakterisiert, welche bei der phänotypischen Variabilität in der Funktion des Tumorendothels und infolgedessen auch auf die Entwicklung von Krebserkrankungen wirken könnten. Diese Genvarianten könnten ausserdem die Empfindlichkeit gegenüber VEGFR-2 Inhibitoren beeinflussen. Sequenzierung von VEGFR-2 in der Keimbahn führte zur Entdeckung von 120 genetischen Varianten, sogenannter single nucleotide polymorphisms (SNPs). Davon waren bisher 25 nicht beschrieben. Die Funktionalität dieser genetischen Varianten wurde mit Hilfe von Phosphorylierungsassays, mRNA- und Proteinexpressionsassays bestimmt. Ausserdem wurde die Dichte der Mikrovaskulatur in non-small cell lung cancer (NSCLC) Tumorproben gemessen. Die beschriebenen Korrelationen könnten in der Zukunft helfen, die molekulare Basis genetischer Variationen zwischen VEGFR-2 Aktivierung und klinischen mit der VEGFR-2 Funktion assoziierten Phänotypen zu verstehen.

Abschliessend interessierte uns der Einfluss von Bestandteilen der extrazellulären Matrix auf die VEGF-induzierte Angiogenese. Konzentrationsgradienten von Wachstumsfaktoren und matrix-immobilisierten Botenstoffe stellen die natürliche Umgebung von Endothelzellen *in vivo* dar. Um den komplexen Aufbau von angiogenem Gewebe in Zukunft besser *in vitro* imitieren zu können, generierten wir VEGF derivatisierte Mikromuster auf Deckgläsern. Diese Deckgläser dienten der Kultivierung von Endothelzellen und ermöglichten das Verfolgen der Zellmigration. Es konnte gezeigt werden, dass immobilisiertes VEGF weiterhin biologisch aktiv ist und dass Endothelzellen zu den vorgefertigten VEGF-Mustern migrieren und sich dort anheften. Unsere mit VEGF derivatisierten Deckgläser stellen eine robuste und reproduzierbare Plattform für die Charakterisierung von komplexen zellulären Verhalten dar, welche durch die vielfachen VEGF Isoformen generiert werden.

1 Introduction

1.1 Angiogenesis

1.1.1 Physiological and pathological angiogenesis

The cardiovascular system is crucial for ensuring the delivery of nutrients and oxygen to all organs and tissues while at the same time being responsible for the disposal of catabolic products. The vasculature is also a major communication system between distant organs and tissues. Vasculogenesis and angiogenesis are the two key processes involved in the formation, development and maturation of the vascular system.

Vasculogenesis is defined as the process of vessel formation in early development during which endothelial precursor cells, also known as angioblasts, differentiate into endothelial cells and form a primitive vascular plexus (Schmidt *et al.*, 2007). Angiogenesis is the formation of new blood vessels from pre-existing vasculature. The process involves two main mechanisms known as splitting or intussusception and sprouting of vessels. During sprouting, endothelial cells of existing blood vessels secrete proteases which will degrade the underlying vessel basement membrane. Following degradation of the extracellular matrix (ECM), endothelial cells proliferate and extend “sprouts” into the surrounding tissue and towards the source of the angiogenic stimulus. The “leader” endothelial cells or non-dividing tip cells are followed by proliferating cells (Gerhardt *et al.*, 2003). Finally, sprouting tubes fuse and form loops to build up a fully fledged vessel lumen that allows directional blood flow. Nascent vessels are stabilized by the recruitment of mural cells and vascular smooth muscle cells (Liekens *et al.*, 2001).

Physiological angiogenesis is not only observed in embryogenesis but also in the adult during the female reproductive cycle where follicular growth and corpus luteum formation require the proliferation of blood vessels (Hyder and Stancel, 1999). Vascular Endothelial Growth Factor (VEGF) is the main growth factor involved here (Ferrara *et al.*, 1998). Furthermore, newly formed blood vessels also participate in the process of wound healing (Li *et al.*, 2003). Fibroblast Growth Factor (FGF) and VEGF regulate neovascularization here (Ortega *et al.*, 1998) (Nissen *et al.*, 1998).

In contrast, unregulated or pathological angiogenesis is a hallmark of various (over 20) malignant, ischemic, inflammatory, and infectious diseases. Insufficient angiogenesis contributes to ischemic heart disease (Shiojima *et al.*, 2005), stroke (Krupinski *et al.*, 1994), preeclampsia (Luttun and Carmeliet, 2003), and amyotrophic lateral sclerosis (Brockington *et al.*, 2004). Excessive

angiogenesis may lead to rheumatoid arthritis (Paleolog, 2002), psoriasis (Detmar, 2004), diabetic retinopathy (Shams and Ianchulev, 2006), and atherosclerosis (Celletti *et al.*, 2001). A very serious disease accompanied by abnormal and excessive angiogenesis is cancer. Oxygen and nutrient supply guaranteed through an extensive network of capillaries is crucial for the growth of a tumor. When the tumor reaches a size of 1-2 mm in diameter, its demand for oxygen and nutrients exceeds the local supply. Limited oxygen supply from the surrounding blood vessels leads to a hypoxic microenvironment (Carmeliet and Jain, 2000). Subsequently, the hypoxia-inducible transcription factor HIF-1 α is upregulated and activates the expression of many genes involved in angiogenesis such as *VEGF* and *VEGFR-2* (Carmeliet *et al.*, 1998). Many of the processes involved in tumor angiogenesis are similar to those occurring during physiological angiogenesis. However, due to tumor-secreted factors and tumor hypoxia, the angiogenic cascade in tumors is persistent and unresolved (Chung *et al.*, 2010). The overproduction of VEGF leads to a leaky and haemorrhagic tumor vasculature. Another difference is the morphology of tumor vessels, which are disorganized and do not follow the hierarchical branching pattern of normal vascular networks. The newly formed blood vasculature in tumors enables the tumor cells to enter the blood circulation and metastasize to other organs (Fidler, 2000).

Lymphangiogenesis, the formation of lymphatic vessels from pre-existing lymphatic vessels, plays a crucial role in homeostasis, metabolism, and immune surveillance of the body (Alitalo *et al.*, 2005). It has been implicated in numerous pathologies (Jurisic and Detmar, 2009). Recently, it was shown that tumors can induce lymphangiogenesis by secreting growth factors which will then be drained to the sentinel nodes. Here, they lead to the formation of premetastatic niches (Hirakawa *et al.*, 2007).

1.1.2 Growth Factors, Receptors, Coreceptors in angiogenesis

A detailed overview of coreceptors involved in VEGFR-mediated responses can be found in our review “Structure-function analysis of VEGF receptor activation and the role of coreceptors in angiogenic signaling” in appendix A (Grünewald *et al.*, 2010).

1.2 Vascular Endothelial Growth Factor Receptor-2

1.2.1 Vascular Endothelial Growth Factor Receptor-2 properties and signaling

Vascular Endothelial Growth Factor Receptor-2 (VEGFR-2), originally known as Kinase insert domain-containing receptor (KDR) or fetal liver kinase-1 (Flk-1) is the central mediator of survival, migration, proliferation, maturation, and differentiation of endothelial cells. It binds VEGF-A, -C, -D, -E, and -F. VEGFR-2 is expressed on vascular and lymphatic endothelial and hematopoietic precursor cells, mature capillary endothelial cells, and neuronal cells. Gene-targeting of *VEGFR-2* in the mouse leads to lethality at embryonic day (E) 8.5 due to defective blood island formation and arrested endothelial and hematopoietic development (Shalaby *et al.*, 1995). The receptor is composed of seven Immunoglobulin (Ig)-homology domains in the extracellular domain (ECD), a single transmembrane region and a tyrosine kinase sequence interrupted by a kinase insert domain. Signaling by VEGFRs is initiated upon binding of a covalently linked ligand dimer to the extracellular receptor domain. This interaction promotes receptor homo- and heterodimerization followed by activation of the intracellular kinase domain. We have recently shown how VEGF induces dimerization of the extracellular receptor domain (Ruch *et al.*, 2007). VEGFR-2 monomers are dimerized upon ligand binding to Ig-homology domains 2 and 3 and dimers are further stabilized by receptor-receptor contacts mediated by Ig-homology domains 4 and 7. Similar results were published by Schlessinger's laboratory for the related Kit, PDGF-, and VEGF-receptors (Yuzawa *et al.*, 2007) (Yang *et al.*, 2008) (Yang *et al.*, 2010). We further demonstrated that artificial dimerization-promoting transmembrane domains (TMDs) derived from oncogenic variants of ErbB receptors activate VEGFR-2. Such TMD constructs orient receptor monomers by intra-membrane interactions mediated by charged amino acids (Dell'Era Dosch and Ballmer-Hofer, 2009). Receptor tyrosine kinase (RTK) activation thus requires specific orientation of receptor monomers in an active dimer which results from ligand-induced ECD rearrangement.

Activation of RTKs leads to phosphorylation of specific tyrosine residues located in the intracellular juxtamembrane domain, the kinase domain, the kinase insert domain and the carboxyterminal tail of the receptor (Fig. 1-1). The subsequent interaction between VEGFRs and downstream signaling effectors is mediated through Src homology-2 (SH-2) and phosphotyrosine-binding (PTB) domains (reviewed in (Schlessinger and Lemmon, 2003)). Signaling by VEGF receptors has been reviewed comprehensively in recent review articles (Cébe-Suarez *et al.*, 2006b) (Shibuya and Claesson-Welsh, 2005); here we therefore refer only to some of the hallmarks of VEGFR-2 activation.

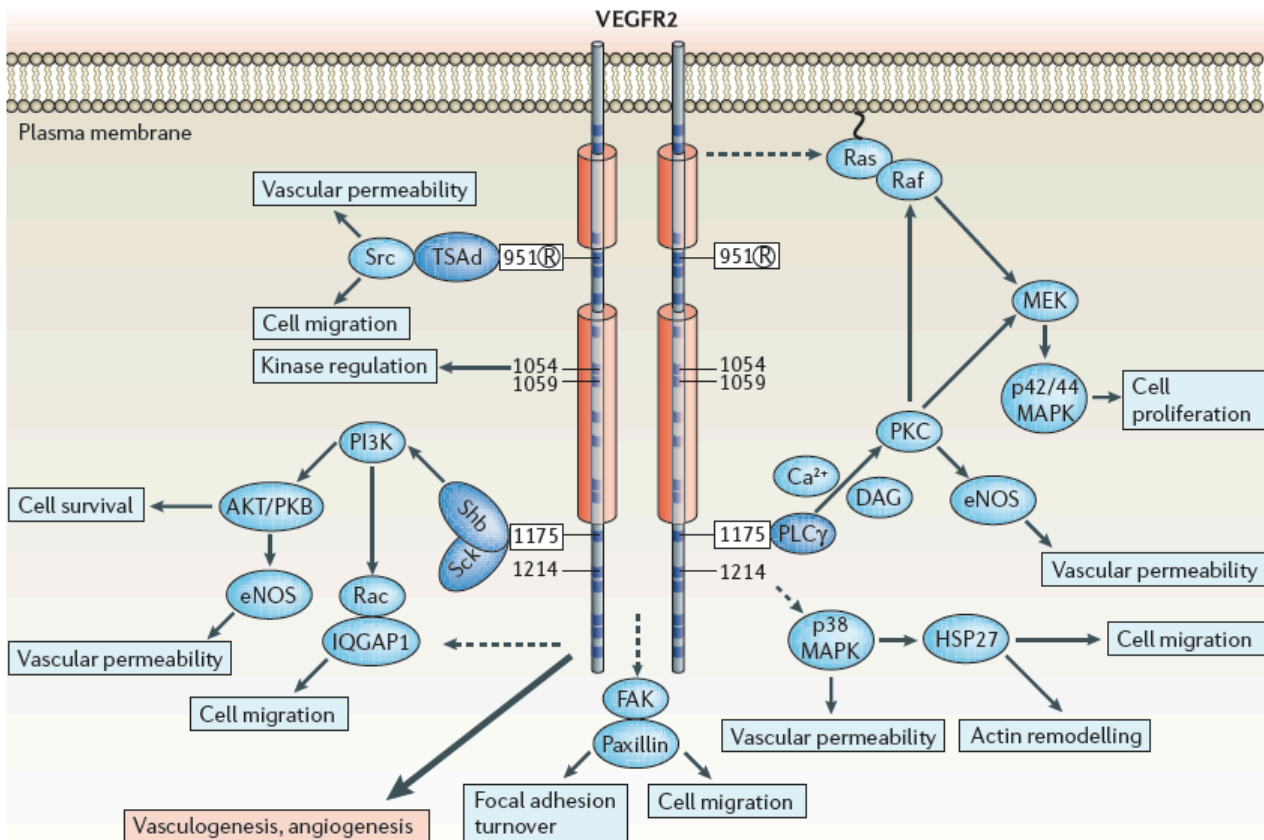


Figure 1-1: VEGFR-2 signaling and phosphorylation sites.

Reprinted from (Olsson *et al.*, 2006).

Y951, Y1054, Y1059, Y1175 and Y1214 were identified as the most prominent phosphorylation sites of hVEGFR-2 (Matsumoto *et al.*, 2005). Y1054 and Y1059 located in the activation loop of the kinase domain were classified as autophosphorylation sites important for the catalytic activity of the receptor kinase (Kendall *et al.*, 1999). Site-directed mutagenesis led to the identification of Y801 and Y1175 as binding sites of phospholipase C- γ (PLC- γ 1) (Cunningham *et al.*, 1997). Phosphorylation and activation of PLC- γ 1 gives rise to diacylglycerol and inositol trisphosphate which stimulate protein kinase C (PKC) (Nishizuka, 1984). Mitogenic signaling by VEGFR-2 is Ras independent and mediated by PKC via Erk kinases (Takahashi *et al.*, 1999) (Doanes *et al.*, 1999) (Wu *et al.*, 2000a). VEGF-induced endothelial cell migration is mediated by the adaptor protein VRAP, also known as T cell-specific adaptor (TSAd) (Wu *et al.*, 2000b). VRAP binding to Y951 leads to its phosphorylation and recruitment of Src kinase which promotes actin reorganization and cell migration (Matsumoto *et al.*, 2005). Additionally, the adapter protein Shb binds to phosphorylated Y1175 and leads to phosphoinositide-3-kinase (PI3-kinase)-mediated

cytoskeleton reorganization as well as activation of focal adhesion kinase (FAK) (Holmqvist *et al.*, 2004). Cell migration and capillary formation are regulated by VEGF through Gab1, which acts as an adaptor for Grb2, PI 3-kinase and the tyrosine phosphatase SHP2 (Laramee *et al.*, 2007) (Dance *et al.*, 2006). VEGF-induced actin remodeling is also triggered through the sequential activation of the small GTPase Cdc42 and stress activated protein kinase (SAPK/p38) following phosphorylation of Y1214 (Lamallice *et al.*, 2004). This leads to phosphorylation and release of heat-shock protein 27 (HSP27). Early molecular events in cytoskeleton reorganization include recruitment of the adaptor protein Nck and the Src family kinase Fyn to VEGFR-2 and triggers phosphorylation of p21-activated protein kinase-2 (PAK2) and activation of Cdc42 and p38 MAPK (Lamallice *et al.*, 2006). An additional important function of VEGF is survival signaling via activation of PI3-kinase and phosphorylation of Akt (Gerber *et al.*, 1998). Finally, signaling by VEGFR-2 is important for endothelial cell specification, a process that might require activation of the Ras-Erk pathway (Kawasaki *et al.*, 2008).

1.2.2 Structure of VEGFs and VEGFR-2 extracellular domain

Structural information on the ECD of VEGFRs is limited to the crystal structure of the Ig-homology domain 2 of VEGFR-1 in complex with VEGF-A (Wiesmann *et al.*, 1997) (Starovasnik *et al.*, 1999) or PlGF (Christinger *et al.*, 2004), the Ig-homology domains 2 and 3 of VEGFR-2 in complex with VEGF-C (Leppanen *et al.*, 2010), and the Ig-homology domain 7 of VEGFR-2 (Yang *et al.*, 2010). D7 folds into a β -sandwich made up of two four-stranded sheets, the one composed of strands A, B, D, and E and the other of strands A', G, F, and C. Hydrogen bonds are formed between A and B and A' and G. The hydrophobic core buries a disulfide bridge between Cys688 in β B and Cys737 β F that connects the two β -sheets. A disulfide bridge is found between Cys740 in the β F and Cys745 in β G. Homotypic interactions suggested by the EM-structure of VEGFR-2 ECD (Ruch *et al.*, 2007) (Fig. 1-2) have now been confirmed in the crystal structure.

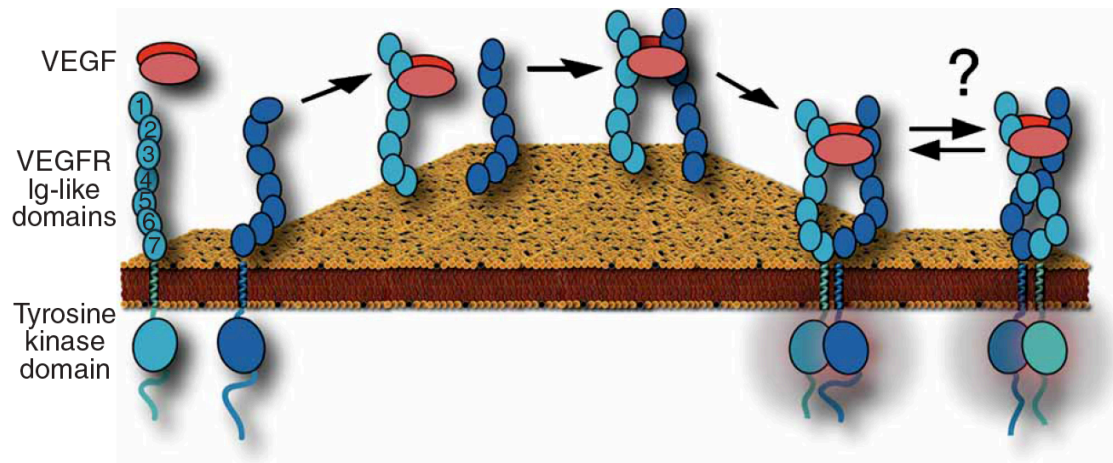


Figure 1-2: Model for the activation of VEGFR-2.

VEGF binds to VEGFR-2 and leads to dimerization of the receptor. Homotypic interactions in D7 and probably also D4 stabilize the dimers. Reprinted from (Ruch *et al.*, 2007).

Interactions are mediated by salt bridges formed between the positively charged Arg726 of one protomer and the negatively charged Asp731 of the other protomer in the loop region linking the β^E and β^F strands (Fig. 1-3). The contacts very strongly resemble the ones seen between D4 of the Kit receptor (Yuzawa *et al.*, 2007).

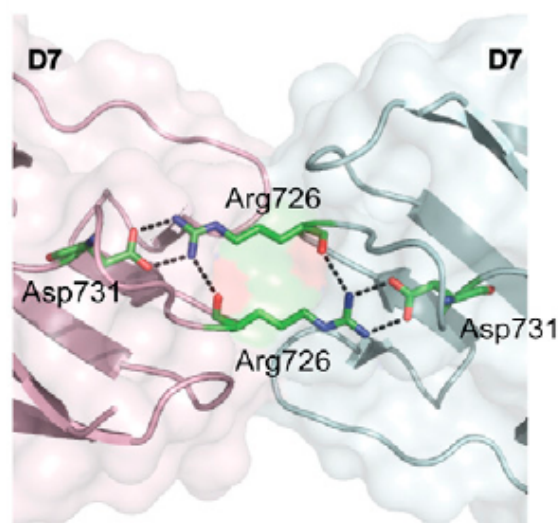


Figure 1-3: Homotypic VEGFR-2 domain 7 interface.

Salt bridges are formed between Arg726 and Asp731 in the loop region between β^E and β^F strands in Ig-homology domain 7 of VEGFR-2. Reprinted from (Yang *et al.*, 2010).

1.3 Anti-angiogenic therapy

1.3.1 Available drugs for anti-angiogenic therapy

In the 1970s, Dr. Judah Folkman of the Harvard Medical School suggested inhibiting new blood vessel formation as a way to fight cancer (Folkman, 1971). In the following years several therapies blocking angiogenesis have been developed and the first anti-angiogenic agents have now been approved for clinical use (reviewed in (Jain *et al.*, 2006)). Inhibitors of the VEGF-pathway include monoclonal antibodies against the growth factors, small-molecule tyrosine kinase inhibitors (TKIs), and antibodies targeting the extracellular domain of the receptors.

An example of an anti-angiogenesis drug targeting the growth factor is bevacizumab, a humanized monoclonal antibody against human VEGF-A (Presta *et al.*, 1997) present on the market under the name Avastin® (Genentech, Inc., San Francisco, USA). Bevacizumab is intravenously administered to cancer patients and binds to all VEGF-A isoforms preventing their interaction with the receptors (VEGFR-1, -2, Nrp-1, and -2). This leads to inhibition of VEGFR-2 activation and blocks downstream signaling. As a result, angiogenesis at the tumor site is reduced and tumor growth slowed down. Bevacizumab has received Food and Drug Administration (FDA) approval for use in combination with chemotherapy in metastatic colorectal cancer (CRC) (Willett *et al.*, 2004) (Hurwitz, 2004), recurrent or metastatic non-small cell lung cancer (NSCLC) (Sandler, 2007), metastatic breast cancer (Miller *et al.*, 2007) and renal cancer, and as a single agent in recurrent glioblastoma (GBM) (Friedman *et al.*, 2009). It has been suggested that instead of blocking angiogenesis at the tumor site, bevacizumab rather leads to the normalization of abnormal blood vessels in the tumor environment and in this way allows an easier and more efficient delivery of jointly administered chemotherapeutics to the tumor (Jain, 2005) (Yang *et al.*, 2005). In addition, bevacizumab is also used off-label to treat neovascular age-related macular degeneration (AMD) (Ciulla and Rosenfeld, 2009). AMD is caused by abnormal blood vessel growth beneath the macula which leads to severe loss of vision upon irreversible damage to the photoreceptors. An affinity-matured Fab fragment variant of bevacizumab known as ranibizumab (Lucentis®) has also received FDA-approval for the treatment of AMD (Ciulla *et al.*, 2009).

Tyrosine kinase inhibitors, the second group of anti-angiogenesis agents, target the ATP-binding site of the receptor tyrosine kinase (Traxler, 2003). Although TKIs such as sorafenib (Nexavar®, Bayer AG) and sunitinib (Sutent®, Pfizer) used against renal cell carcinoma have demonstrated antitumor activities, they present the disadvantage that they inhibit many kinase targets in addition to the VEGFRs. The lack of specificity for VEGFRs leads to a number of

“off-target” adverse effects in their long-term use (Shepard and Garcia, 2009). Therefore, one of the challenges is to develop more specific inhibitors against the individual VEGFRs. Since the different TKs are structurally very similar, a better option would be to target receptors at other unique site.

The most clinically advanced VEGFR-2 inhibitor so far is Ramucirumab (IMC-1121B, ImClone Systems, New York, USA), a fully human monoclonal antibody against the ligand-binding domain of VEGFR-2 (Spratlin, 2011). It was developed from IMC-1C11, a mouse-human chimeric antibody which proved to be successful but showed side effects associated with chimeric antibodies in early clinical trials. To circumvent these adverse effects, IMC-1C11 was later fully humanized to IMC-1121B. IMC-1121B will shortly be entering phase II and III clinical trials. However, the main disadvantage of inhibitors that bind to the ligand-binding domain of receptors is that they need to compete with the ligand and are therefore only effective when ligand-concentration is low.

Despite the success of anti-angiogenic drugs in prolonging the life of cancer patients, two studies have now shown that VEGF-targeted drugs inhibit primary tumor growth but elicit tumor invasiveness and metastasis (Paez-Ribes *et al.*, 2009) (Ebos *et al.*, 2009). Explanations for this could be that compared to normal cells tumor cells tolerate hypoxia better but are also capable of escaping hypoxia (discussed in (Loges *et al.*, 2009)). Escape mechanisms include metabolic reprogramming to glucose addiction in hypoxic conditions (Brahimi-Horn *et al.*, 2001), co-option of existing vasculature (Bergers and Hanahan, 2008), or selection of hypoxia-tolerant tumor cell clones (Brahimi-Horn *et al.*, 2001). Drug resistance may also arise from compensatory activation or the overexpression of a different cell signaling protein. A VEGF-independent vascular regrowth has been observed with concurrent upregulation of FGF family ligands. A potential strategy against this resistance could be to target multiple angiogenic signaling pathways simultaneously.

1.3.2 Antibodies in the clinic

1.3.2.1 Definition of an antibody

Antibodies are proteins involved in specific immune recognition and their functions are to bind specifically to pathogens (bacteria, virus) and to recruit other cells are required to destroy pathogens or pathogen containing host cells. Antibodies are produced by B cells and occur in two forms, either soluble or membrane-bound. They consist of two parts, the variable region which is the antigen-binding region and the constant region which is responsible for engaging the effector functions of the immune system. An antibody molecule is made up of two heavy (50 kDa each) and

two light chains (25 kDa each) joined by disulfide bridges. Each heavy chain is linked to a light chain and the two heavy chains are linked to each other. The heavy chains are composed of a variable (V_H) and three constant domains (C_{H1-3}) whereas the light chains consist of one variable (V_L) and one constant domain (C_L). The variable regions V_H and V_L contain the so-called hypervariable regions or complementary determining regions (CDRs) which form the antigen binding site and determine antibody specificity.

Fully human monoclonal antibodies (mAbs) are a promising and rapidly growing category of targeted therapeutic agents. In 1975, Köhler and Milstein established the method of generating monoclonal antibodies by hybridomas (Kohler and Milstein, 1975). For this, spleen cells of an immunized mouse are fused to cells of a mouse myeloma, a common tumor of plasma cells. These hybrid myeloma cells or hybridomas proliferate indefinitely and secrete antibodies specific for the antigen used to immunize the mouse. For therapeutic applications in humans, the disadvantages of murine antibodies are their safety as well as the immunogenicity of the mouse-derived protein sequences. Establishing human hybridomas and the production of human mAbs from human cell lines proved to be difficult (Cole *et al.*, 1984) (Pasqualini and Arap, 2004). Therefore, several alternative strategies have been followed to produce human mAbs. To reduce the immunogenicity of murine antibodies, chimeric and humanized mAbs containing murine variable regions linked to human constant regions were engineered (Riechmann *et al.*, 1988). Another approach to obtain humanized antibodies is the production of monoclonal antibodies in so-called “Xenomice”, transgenic mice that carry human immunoglobulin gene loci (Green, 1999).

Finally, antibodies can be obtained by selection of human antibody fragments from phage-display libraries (McCafferty *et al.*, 1990).

1.3.2.2 Phage Display

Phage display libraries may be used to raise human antibodies against a variety of antigens, including toxic, highly pathogenic, or non-immunogenic targets. The gene encoding a specific antibody-like polypeptide is inserted into the genome of a phage and as a result the peptide is displayed on the phage surface. Large repertoires, so-called phage libraries, can be generated where each polypeptide expressed on the surface of a phage has a different sequence (Pini *et al.*, 1998). Filamentous bacteriophages such as M13 are used for the technology of phage display and allow the linking of phenotype (displayed protein) to genotype (inserted gene encoding the protein). M13 is a bacterial virus that infects many gram-negative bacteria. The phage is composed of five coat

proteins (pIII, pVI, pVII, pVIII, and pIX) of which the minor coat protein pIII is most often used for the phage display fusions. pIII is expressed in five copies at the tip of the phage and is responsible for attachment of the phage to the f pilus of bacteria during infection. Following attachment, the viral ssDNA is translocated into the bacterial cytoplasm, converted into dsDNA from which phage genes are subsequently expressed. New virions are now assembled and secreted from the bacteria. Phagemid vectors containing only the gene III, cloning sites and packaging signal, have nowadays replaced the initial phage vectors. Since phagemid vectors lack some of the phage genes, superinfection of the *E.coli* with helper phages such as VCSM13 or M13KO7 is required for the production of functional phage particles. The antigen of interest is immobilized onto a support such as a plastic tube for example and the library of single chain Fv (scFv)-displaying phages is run over it. After panning, unbound phages are washed away and specific phages are eluted and collected. They are amplified by infection of bacteria and used for further rounds of selection (Fig. 1-4). Usually after two to three selection rounds, clones are tested for their specificity by enzyme-linked immunosorbant assay (ELISA). Instead of selecting antibodies against immobilized antigens, antigens can be biotinylated and antibodies selected in solution. This circumvents the problem that in some cases antigens change their conformation when immobilized on solid surfaces.

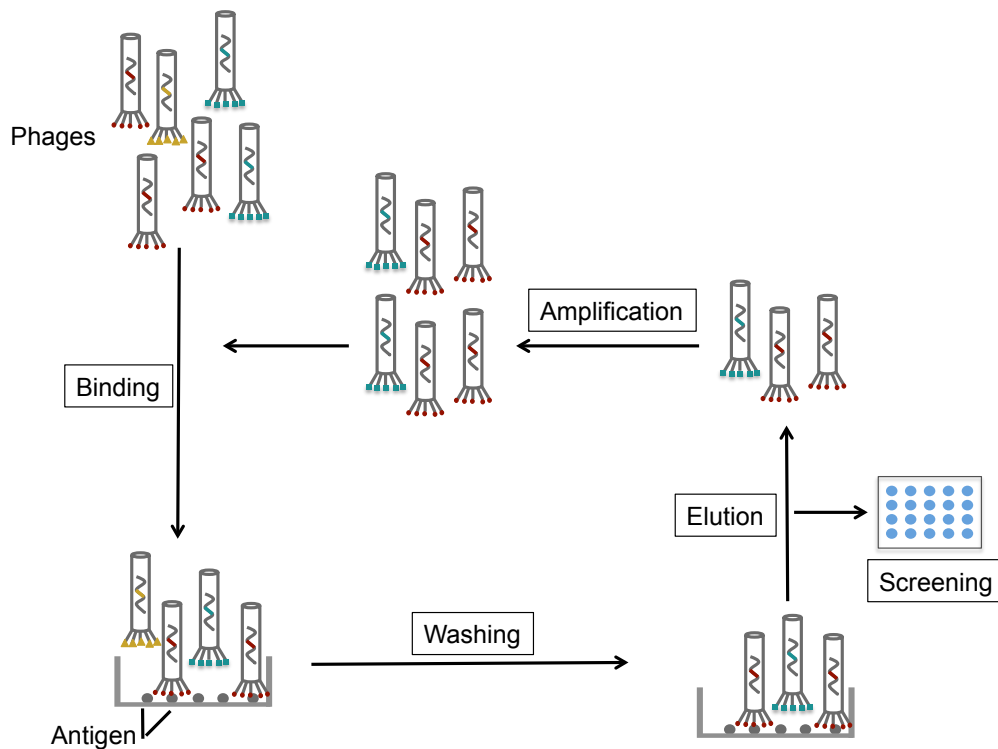


Figure 1-4: Selection of single chain Fvs from a phage display library.

Phages displaying binding proteins (red, green, yellow) on their surface are captured on immobilized antigen. Unbound phages are washed away and binding phages are eluted. Amplification occurs in *E.coli* after infection of the bacteria with the eluted phages. Enriched phages are used for further rounds of selection. Screening of eluted binders is performed after two to three selection rounds. Original artwork inspired by (Marasco and Sui, 2007).

1.3.2.3 ETH-2 Gold Library

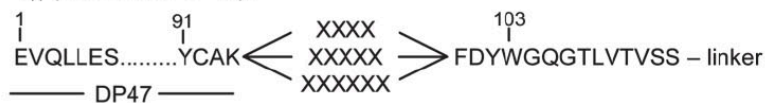
The ETH-2 Gold antibody phage display library is a synthetic human antibody library in the single-chain Fv (scFv) format. The library was established and constructed in the group of Prof. Dario Neri at the ETHZ (Silacci *et al.*, 2005). A scFv fragment is made up of a single polypeptide chain consisting of an antibody heavy variable domain (VH) linked by a flexible polypeptide linker to a light chain variable domain (VL). ScFvs have a molecular weight of about 30 kDa and are not glycosylated. In order to obtain the 3×10^9 individual clones that make up a complex library, sequence variability was introduced into the CDR3 regions of both the heavy and the light chains. PCR with partially degenerate primers was used to generate random mutations in the CDR3 of the heavy chain DP47 and the CDR3 of the light chains DPL16 or DPK22. Variability

in the CDR3 of the DP47 segment consists of four to six randomized amino acids at positions 95-100. In the CDR3 of DPL16, six amino acids were randomized with at least one residue being a proline. In the CDR3 of DPK22, the second or third residue of the six is a glycine and the fifth residue a proline (Fig. 1-5). The flexible polypeptide Gly₄SerGly₄SerGly₄ (Huston *et al.*, 1988) was used as a linker between the two variable fragments.

scFv sequence:



V_H (based on DP47):



V_L (based on DPK22):



V_L (based on DPL16):



Figure 1-5: Variable heavy and light chain sequence design in a scFv (ETH-Gold-2 library).

Variability is obtained by random sequences (X) in the human V_H (DP47) and V_L (DPK22 or DPL16) antibody germline segments as indicated. V_H and V_L sequences are joined by a linker. ScFvs carry a myc affinity-tag. pIII encodes the phage coat protein to which the scFv is fused. An amber stop codon is found between the scFv- and the pIII-sequence. Reprinted from (Silacci *et al.*, 2005).

The V_H - V_L combinations were cloned into the phagemid vector (pHEN1) (Hoogenboom, 1991). The pHEN1 vector is composed of an upstream bacterial periplasmic secretion signal (*pelB*), a downstream myc-tag (EKQLISEEDL) fused to the C-terminus of the scFv, a suppressible amber stop codon (TAG) and the phage coat protein gene pIII (Fig. 1-6).

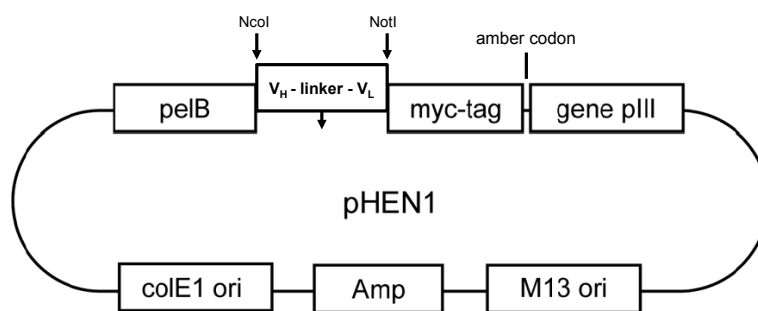


Figure 1-6: pHEN1 expression plasmid.

The pHEN1 phagemid containing a bacterial periplasmic secretion signal (pelB), a colE1 ori, and an M13 phage origin of replication is used for the expression of scFvs (V_H -linker- V_L). Modified from (Silacci *et al.*, 2005).

When amber- or *supE*-suppressor *E. coli* strains are infected with phage, the translation will read through the amber stop codon and a fusion protein consisting of the scFv and the pIII coat protein will be produced. In a non-*supE* suppressor strain, only soluble scFv protein will be produced and secreted into the periplasmic space. ScFvs will leak into the supernatant in part due to their cytotoxicity in *E. coli*. Protein A can be used to purify the scFvs from the supernatant via affinity chromatography.

1.3.3 Designed Ankyrin Repeat Proteins

1.3.3.1 Definition of a Designed Ankyrin Repeat Protein

Designed Ankyrin Repeat Proteins (DARPin)s are genetically engineered antibody mimetic proteins derived from natural ankyrin proteins (Fig. 1-7). They were developed at the University of Zürich by the group of Prof. Plückthun (Binz *et al.*, 2003). Like their natural counterparts, DARPins bind specifically and with high-affinity to target proteins. They consist of two to four repeat motifs which are genetically fused and flanked by an N- and a C- capping repeat. The role of the caps is to bury the hydrophobic core. Each library module consists of an ankyrin repeat of 33 amino acids of which seven are variable. The molecular mass of DARPins ranges from 14 to 21 kDa, depending on the number of modules. DARPins show very high expression levels in *E. coli*, are soluble and exhibit high stability (Binz *et al.*, 2003). The DARPins scaffold does not contain any cysteines, these can therefore be added for site-directed coupling of a variety of chemicals such as cytotoxins for

example. This opens the possibility to use DARPins as therapeutic agents. DARPin[®] MP0112 a potent VEGF-A inhibitor developed by Molecular Partners AG, has now entered clinical trials for the treatment of Diabetic Macular Edema (<http://www.clinicaltrials.gov/show/NCT01042678>) and Wet Age-Related Macular Degeneration (<http://www.clinicaltrials.gov/ct2/show/NCT01086761>).

Advantages of therapeutic DARPins over antibodies include higher stability, low-cost production, better tissue penetration due to the smaller size of the DARPins (18 kDa versus 150 kDa for an IgG), and the absence of effector function and therefore low risk of immunogenicity (Stumpp and Amstutz, 2007) (Stumpp *et al.*, 2008). In most of the cases, DARPins bind their target proteins on a conformational epitope. The protein is therefore forced to remain in this specific conformation and in this way allows allosteric inhibition through the DARPIn.

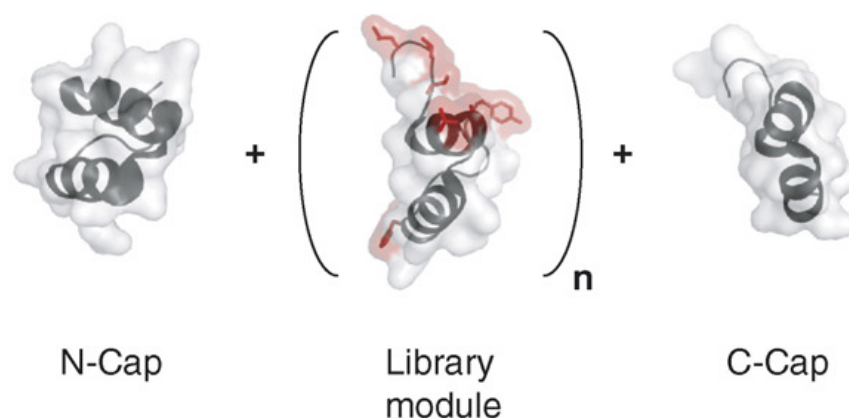


Figure 1-7: Scheme of DARPIn library design.

Two caps (N- and C-Cap) and a variable number of library modules ($n=2-4$) make up a DARPIn molecule. Library modules consist of an ankyrin repeat of 33 amino acids with seven variable positions. The size of a DARPIn molecule typically ranges between 14 and 21 kDa.

Reprinted from (Stumpp *et al.*, 2008) .

1.3.3.2 Ribosome Display

The technique of ribosome display was first described by Mattheakis et al. in 1994 (Mattheakis *et al.*, 1994). Ribosome display begins with the transcription of linear DNA fragments encoding a protein library (Fig. 1-8). Subsequently, translation of the mRNA takes place *in vitro*. Due to the absence of a stop codon in the mRNA (Hanes and Pluckthun, 1997), the ribosome does not detach from the mRNA and a ternary complex composed of the ribosome, the mRNA and the nascent polypeptide is formed. The complex is stabilized by lowering the temperature and adding cations. It is directly used for affinity selection with a ligand which is either immobilized or in solution. The mRNA contained in the bound ribosomal complexes is eluted by addition of EDTA. It is then purified, reverse-transcribed, and amplified by PCR. Like phage display, this technique allows the coupling of genotype (RNA, DNA) and phenotype (protein). Being an *in vitro* display technology, ribosome display has two advantages over other selection strategies. First, very high library diversity can be achieved since there is no limitation arising from the transformation efficiency of bacterial cells. Second, mutations leading to a high diversity can easily be introduced by PCR-based mutagenesis during the PCR step in the selection round.

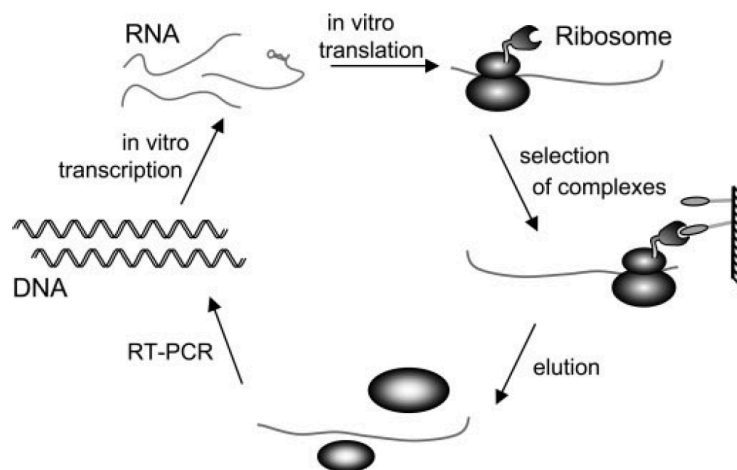


Figure 1-8: Ribosome display technology.

Transcription of DNA fragments encoding a protein library is followed by translation. Since the mRNA does not contain a stop codon, the ribosome will not dissociate and forms a stable complex with the translated protein and the mRNA. The ternary complex of mRNA, ribosome, and nascent polypeptide is used for selection. Eluted mRNA is reverse transcribed and DNA used for the next selection round. Reprinted from (Zahnd *et al.*, 2004).

1.4 Aim of the thesis

The inhibition of new blood vessel formation is a very promising therapeutic approach in the fight against cancer. Given the key importance of VEGFR-2 in angiogenesis, promising anti-angiogenic therapies aim at targeting this receptor and blocking its downstream signaling. A detailed understanding of the VEGFR-2 activation mechanism is a crucial prerequisite for the development of specific anti-angiogenic drugs in biomedical research.

VEGFR-2 is activated upon ligand-binding to the extracellular domain (ECD). Receptor dimerization follows ligand-binding and promotes activation of the intracellular kinase domain which leads to downstream signaling. At present, the specific structural changes in the ECD and the exact mechanisms responsible for kinase activation are only partially understood. The work presented in my thesis is focused on an investigation of the activation mechanism of VEGFR-2 aiming at a detailed functional investigation of the role of ECD membrane-proximal Ig-homology domains 4 and 7 in VEGFR-2 activation. Based on our functional analysis of VEGFR-2 activation, we further aimed at the generation of specific inhibitors binding to D4 and D7 of the ECD that might block receptor activation. We generated two different types of inhibitors. We used the synthetic ETH-2 gold library to identify scFv inhibitors against D7 and, in collaboration with Molecular Partners AG in Schlieren, we developed DARPins interacting with the receptor ECD.

In a second project, we were interested in characterizing variations in the VEGFR-2 gene which might contribute to the phenotypic variability in tumor endothelial function and, consequently, may affect cancer progression and the susceptibility of tumors to VEGFR-2 inhibitors.

My third project aimed at the development of a new cell culture technology based on growing cells on micropatterned substrates for monitoring VEGF-induced angiogenesis *in vitro*. I used two different methodologies to generate micropatterned coverslips for cultivation of endothelial cells. These substrates mimic the *in vivo* environment and allow the application of gradients of different VEGF isoforms to endothelial cell cultures. Different concentrations of soluble or matrix-bound VEGF will be used for monitoring endothelial cell migration.

2 Structure–function analysis of VEGF receptor activation and the role of coreceptors in angiogenic signaling

The full manuscript can be found in appendix A.

My contribution to this manuscript was the writing of chapter “VEGF receptor activation and signaling” (1.3.).

3 Inhibition of receptor activation by Designed Ankyrin Repeat Proteins specific for the Ig-homology domain 4 of VEGFR-2 extracellular domain

Alexandra Giese^{1%}, Edward Stutfeld^{1%}, Kaspar Binz² and Kurt Ballmer-Hofer^{1*}

¹Biomolecular Research, Molecular Cell Biology, Paul Scherrer Institute, CH-5232 Villigen PSI, Switzerland and ²Molecular Partners AG, Wagistrasse 14, 8952 Zürich-Schlieren, Switzerland

(Manuscript in preparation)

% These authors equally contributed to this paper

*To whom correspondence should be addressed:

Phone: +41 56 310 4165

Fax: +41 56 310 5288

e-mail: kurt.ballmer@psi.ch

3.1 Abstract

Vascular Endothelial Growth Factors (VEGFs) regulate blood and lymph vessel formation by activating three receptor tyrosine kinases, VEGFR-1, -2 and -3. The extracellular ligand-binding domain of VEGFRs consists of seven immunoglobulin homology domains (Ig domains) connected by a transmembrane helix to the intracellular tyrosine kinase domain. VEGF family ligands interact with Ig domains 2 and 3 thereby inducing receptor dimerization. Low resolution structural information and biophysical data show that specific orientation of receptor monomers in active dimers is further controlled by homotypic receptor contacts mediated through membrane-proximal Ig domains. Investigating the role of this membrane proximal part of the extracellular domain in receptor activation we found that Ig domains 4 and 7 are required for properly aligning receptor monomers in active dimers and are thus indispensable for kinase activation. We developed Designed Ankyrin Repeat Proteins (DARPs) specifically binding to the extracellular receptor domain. DARPs specific for Ig domains 2 and 3 inhibited ligand binding while DARPs specific for Ig domain 4 prevented kinase activation without interfering with dimerization. These data reveal a crucial role for the membrane-proximal receptor domain in ligand-mediated activation of VEGFR-2.

3.2 Introduction

Receptor tyrosine kinases (RTKs) fulfill essential functions in a wide variety of biological processes such as cell growth, differentiation, migration and survival. Regulation of RTKs is the subject of intense research since it holds promise for the development of new drugs aiming at diseases caused by deregulation of RTK activity. Vascular Endothelial Growth Factors, VEGFs, comprise a family of proteins interacting with three type V RTKs, VEGFR-1 (Flt-1), VEGFR-2 (KDR/Flk-1), and VEGFR-3 (Flt-4) (Pajusola *et al.*, 1992; Shibuya *et al.*, 1990; Terman *et al.*, 1991). VEGFs promote endothelial cell survival, migration, proliferation, and differentiation, and are thus indispensable for blood and lymph vessel formation. In addition, VEGFs regulate endothelial cell permeability and vessel contraction. Like all RTKs, VEGFRs are activated following ligand-induced structural changes in the receptor extracellular domain (ECD) (reviewed in (Grünewald *et al.*, 2010). VEGFR-2 is the major mediator of angiogenic signaling in endothelial cells (Shalaby *et al.*, 1995) and its activity is regulated at multiple levels. We have also shown that receptor

dimerization is necessary, but not sufficient, for receptor kinase activation (Dell'Era Dosch *et al.*, 2009). These data clearly demonstrate that specific orientation of receptor monomers in the active dimers is required to instigate transmembrane signaling and kinase activation.

High resolution structures of ligand-receptor complexes of VEGFRs show that Ig homology domains 2 and 3 comprise the ligand binding site (Christinger *et al.*, 2004; Leppanen *et al.*, 2010; Wiesmann *et al.*, 1997). In addition, our laboratory published an electron microscopy structure of the full length ECD of VEGFR-2 bound to VEGF (Ruch *et al.*, 2007). This structure was recently confirmed by a structural model derived from a small angle solution scattering (SAXS) analysis (Kisko *et al.* accepted). Taken together, our data demonstrate that receptor monomers are not only held together by ligand binding to Ig domains 2 and 3, but by additional homotypic receptor contacts formed by the membrane-proximal part of the ECD.

Here we extend earlier studies investigating the role played by the individual extracellular Ig homology domains in ligand binding (Shinkai *et al.*, 1998) and receptor activation (Tao *et al.*, 2001; Yang *et al.*, 2010). Based on our own work (Ruch *et al.*, 2007), we analyzed the function of Ig homology domains D4 and D7 in receptor dimerization and activation. We created a series of receptor ECD mutants that were expressed in tissue culture cells for determining receptor activity. Mutation or deletion of D4 and D7 drastically reduced receptor activity. Based on these results we developed new ECD binders, Designed Ankyrin Repeat Proteins (DARPs), specifically interacting with single Ig homology domains. By testing these reagents for inhibition of ligand-stimulated receptor activity we identified several DARPs binding to D2-3 and thereby blocking ligand binding and receptor activation. Most interestingly, DARPs binding to D4 efficiently inhibited receptor activation without interfering with dimerization. These new reagents will be useful for *in vivo* studies aiming at imaging or inhibiting VEGFR-2.

3.3 Materials and Methods

3.3.1 Cloning of VEGFR-2 mutants

The pcDNA5/FRT vector (Invitrogen) was used for the expression of VEGFR-2 mutants in HEK293 and COS-1 cells. The pcDNA5/FRT VEGFR-2 3/5 construct was generated by PCR-subcloning (Geiser *et al.*, 2001). Ig-homology D5 was PCR-amplified from the pcDNA3.1 VEGFR-2 wt construct (in-house) using the primers listed in the appendix table 1 and subcloned into the pcDNA5 FRT VEGFR-2 wt plasmid to replace D4. The pcDNA5 FRT VEGFR-2 Δ 4 and K868M constructs were kindly provided by Claudia Ruch (in-house).

Mutations R726A, D731, RD/AA, and xD7EF were introduced into the pcDNA5 FRT VEGFR-2 wt construct by PCR-subcloning (Geiser *et al.*, 2001) with primers containing the mutations (Suppl. Table 3-1).

The pLIB vector derived from Moloney murine leukemia virus was used for the retroviral transduction of PAE cells. The pLIB LN VEGFR-2 and the pVSV-G plasmids were kindly provided by Ralph Graeser (ProKinase GmbH Freiburg, Germany). For generating pLIB LN VEGFR-2 wt, 3/5, R, D, RD, and xD7EF constructs, the sequences were PCR-amplified from the respective constructs in the pcDNA5/FRT vector by simultaneously introducing a Sall restriction site. Primers are listed in Suppl. Table 3-2. Insert and pLIB LN vector were joined by standard ligation process.

Mutations RRR/AAA, RRRK/AAAS, ED/AA, and EDE/AAA were introduced into both the pcDNA5 FRT VEGFR-2 wt and pLIB LN VEGFR-2 wt constructs by PCR-subcloning (Geiser *et al.*, 2001) with primers containing the mutations (Suppl. Table 3-3).

3.3.2 Cell culture

Human embryonic kidney epithelial cells 293 (HEK 293), COS-1 monkey kidney cells and bovine aortic endothelial cells (BAECs) were grown in Dulbecco's modified Eagle's medium (DMEM, BioConcept) supplemented with 10% fetal bovine serum (FBS) or 10% newborn calf serum (NCS) in the case of the BAECs. Porcine aortic endothelial cells (PAE cells) were maintained in Ham's F12 medium (BioConcept) containing 10% FBS. Cells were grown in a humidified atmosphere at 37 °C and 5% CO₂.

3.3.3 Transfection of HEK293 and COS-1 cells

Transfection of HEK293 cells or COS-1 cells with FuGENE (FuGENE HD Transfection Reagent, Roche) was performed according to manufacturer's protocol. For the DNA titration experiments, different amounts of DNA were used to form the transfection complex.

3.3.4 Generation of Stably Transfected PAE-Cells by Retroviral Transduction

HEK293 Ampho (5×10^6) cells were plated in 10-cm cell culture dishes and cultured in Dulbecco's modified Eagle's medium (DMEM, Sigma) supplemented with 10% fetal bovine serum (FBS). Cells were transfected with 10 μ g pLib LN VEGFR-2 plasmid and 10 μ g pVSV-G plasmid by $\text{Ca}_3(\text{PO}_4)_2$ precipitation. Cells were then transferred to an S2 laboratory. Medium was replaced 5 h later with 20 ml of fresh DMEM. Target PAE cells were seeded in 10-cm cell culture dishes in Ham's F12 medium (Bioconcept) containing 10% FBS. After 24 h, the supernatant of the transfected HEK293 Ampho cells was filtered through a 45 μ m-nitroacetate filter and added to the PAE cells. To increase the efficiency of infection, polybrene (Hexadimethrine bromide, Sigma H9268) was added to a final concentration of 4 μ g/ml. Fresh DMEM was added to the HEK293 Ampho cells. Infection of PAE cells was repeated the next day. After 48 h, PAE cells were split 1/6 and selected with 1 mg/ml G418. Selection medium was added every 3 days. After 2 weeks, cells were checked for expression.

3.3.5 VEGF Receptor Activation

HEK293 (5×10^5) cells were plated into 6-cm cell culture dishes, grown for 24 h in DMEM with 10% FBS, and transfected with $\text{Ca}_3(\text{PO}_4)_2$ precipitation. At 30 h after transfection, cells were starved overnight in DMEM supplemented with 1% BSA. Transfected cells were stimulated with 1.5 nM VEGF-A₁₆₅ for 10 min at 37°C. Cells were rinsed once with ice-cold PBS followed by lysis in 200 μ l lysis buffer (50 mM Tris, pH 7.5; 100 mM NaCl; and 0.5% w/v Triton X-100) containing protease inhibitor cocktail (Roche), phosphatase inhibitors (200 μ M Na_3VO_4 , 10 mM NaF, 10 mM sodium pyrophosphate, 30 mM paranitrophenylphosphate, 80 mM glycerophosphate, and 20 μ M phenylarsine oxide), and 10% glycerol. Cell lysates were boiled in Lämmli buffer (20 mM Tris, pH 6.8; 5% SDS; 10% mercaptoethanol; and 0.02% bromophenol blue) and resolved on 8% SDS gels, blotted to PVDF membranes, and immunodecorated with phospho-specific antibody pY1175 or VEGFR-2 specific antibody (Cell Signaling). All experiments were performed in triplicates and

immunoblots were quantified by densitometric scanning using the ImageQuant TL software (Molecular Dynamics, GE Healthcare).

3.3.6 Immunocytochemistry

HEK293, COS-1, or stably transfected PAE cells were grown on glass coverslips to a density of approximately 60%. HEK293 and COS-1 cells were transfected with the VEGFR-2 constructs. Cells were fixed with 3.7% formaldehyde in PBS for 10 min at 37 °C followed by extensive washing with PBS. Cells were permeabilized with 1% NP40 in PBS for 10 min at RT. The first antibody diluted in PBS was added to the cells for 2 h at room temperature followed by incubation with fluorescence-labeled secondary antibody for 1 h. Samples were washed with PBS before they were embedded in gelvatol (15% gelvatol, 33% glycerol, 0.1% sodium azide). Images were acquired on an Olympus IX81 epifluorescence microscope and processed using spectral unmixing and 3D deconvolution software (Olympus Cell[^]R).

3.3.7 Sprouting of BAECs

BAECs were cultured in DMEM supplemented with 10% normal calf serum (NCS). A total of 500 cells were used to generate one hanging drop. Hanging drops were incubated upside down at 37 °C. After 24 h, spheroids were collected and pooled by centrifugation (100 rcf, 3 min). On ice, 8 volumes of collagen I stock (BD Biosciences) were mixed with one volume of 10 x PBS and 0.023 volumes of 1 N NaOH. Basal medium was added up to ten volumes. Spheroids were resuspended in basal growth medium with inclusion of DARPIn (100 nM) and mixed 1:1 with the collagen-containing medium. Spheroids were transferred to a prewarmed 24-well plate (500 µl, 20 spheroids per well) and polymerization was induced by incubation at 37 °C for 2 h. Gels were overlaid with 500 µl of normal growth medium supplemented with 1% FCS with VEGF-A₁₆₅ (1.5 nM final concentration) and incubated for 24 h. Spheroids were fixed with 3.7% formaldehyde at 37 °C o/n. After washing with PBS spheroids were stained with phalloidin-rhodamin (Cell Signaling) and imaged. In the spheroid assay the length and number of sprouts was determined using the Image J software (NIH). Sprouts from two independent experiments were statistically analysed for each condition.

Live-cell imaging was performed by incubating a spheroid in a Ludin-chamber at 37 °C during 24 h.

3.3.8 Cloning of Expression Plasmids

Mammalian expression plasmids for VEGFR-2-D7 (aa 663-764) and VEGFR-2-D6-7 (aa 549-764) production were generated using PCR-subcloning (Geiser *et al.*, 2001). Ig-homology domain 7 was PCR-amplified from pcDNA3-VEGFR-2-D7-GCN4 using the forward primer 5'- ATGGAGAGCAAGGTGCTGC-3' and the reverse primer 5'- GTGATGCTGGAAGTAGAGGTTCTCCAAGTTCGTCTTTTCCTGGGC -3'. Ig-homology domains 6-7 were amplified from pcDNA3-VEGFR-2-D1-7 using the forward primer 5'- CGCCTCTGTGGGTTTGCCTAGGGGTCCTGAAATTACTTTGC -3' and the reverse primer 5'- GTGATGCTGGAAGTAGAGGTTCTCCAAGTTCGTCTTTTCCTGGGC -3'. The PCR-products were then subcloned back into the templates used for the amplification reaction, thereby deleting Ig-homology domains 1-5 or the sequence coding for a GCN4-zipper. VEGFR-2-D1-7 (residue 1-764) was cloned into the pFASTBAC plasmid (Invitrogen) for expression in Sf21 cells as described (Brozzo *et al.*, 2011).

3.3.9 Production and Purification of Recombinant Proteins

VEGFR-2-ECD was produced and purified as described (Brozzo *et al.*, 2011). Briefly, Sf21 cells, maintained in serum-free Insect-Express (Lonza) media at 27 °C, were used to produce recombinant virus. When the cells reached a density of 10⁶ cells/ml, they were infected with recombinant baculovirus at high multiplicity. Three days after infection, the supernatant was harvested by centrifugation at 900 g, concentrated and dialyzed against 20 mM sodium-phosphate buffer pH 7.4 and 500 mM NaCl. The conditioned medium was loaded onto a Ni²⁺-NTA agarose column (GE Healthcare). The His₆-tagged protein was eluted with a gradient from 40-500 mM imidazole and further purified by gel filtration on a Superdex 200HR 10/30 column (GE Healthcare) equilibrated with 25 mM HEPES pH 7.5 containing 150 mM NaCl.

VEGFR-2-D7 and VEGFR-2-D6-7 were produced in transiently transfected HEK293T cells as described (Aricescu *et al.*, 2006 #139). When the cells reached ~90% confluency, the medium was changed from DMEM containing 10% fetal bovine serum to DMEM containing 0.5% fetal bovine serum. The preincubated DNA-polyethylenimine complex (at a 1:1.5 ratio) diluted in serum-free DMEM was added to the cells. Three days after transfection the medium was harvested, cleared by centrifugation, and concentrated. The His₆-tagged proteins were purified by IMAC as described above. The buffer was exchanged to 25 mM HEPES pH 7.5, 150 mM NaCl using centrifugal protein concentrators (Sartorius Stedim Biotech).

3.3.10 Size Exclusion Chromatography coupled Multi-Angle Light Scattering (SEC-MALS)

The SEC-MALS experiments were conducted on an Agilent 1100 HPLC-system (Agilent Technologies) with an analytical-grade Superdex 200HR 10/30 column (GE Healthcare) coupled to the Wyatt miniDAWN Tristar (Wyatt Technologies). The system was equilibrated in 25 mM HEPES pH 7.5, 150 mM NaCl at 20°C prior to the experiments. For each run around 100 µg of VEGFR-2-ECD alone, VEGF-A₁₂₁ alone, VEGFR-2-ECD/VEGF-A₁₂₁ complex, VEGFR-2-ECD/6C8/VEGF-A₁₂₁ complex, and VEGFR-2-ECD/6G9/VEGF-A₁₂₁ were loaded onto the SEC-column. The elution profiles were recorded as UV-absorbance at 280 nm and as the intensity of Rayleigh scattering at three different angles. In the case of VEGFR-2-ECD/6C8/VEGF-A₁₂₁ and VEGFR-2-ECD/6G9/VEGF-A₁₂₁, VEGFR-2-ECD was mixed with the inhibitor at a 1:3 molar ratio and incubated for 60 min at 4 °C. VEGF-A₁₂₁ was added to the receptor at a molar ratio of 1:1.1 (receptor : ligand). The ASTRA™ software (Wyatt Technologies) was used to calculate the weight average Molecular masses (M_w).

3.3.11 Ribosome Display

Ribosome display was performed by Molecular Partners AG, Schlieren, as described in (Zahnd *et al.*, 2007) and (Binz *et al.*, 2004).


3.3.12 Epitope-mapping ELISA

Epitope-mapping ELISA was performed by Molecular Partners AG, Schlieren, using Surface Plasmon Resonance (ProteOn XPR36, Biorad, Switzerland) (Reference: Dr. Kaspar Binz, Molecular Partners AG, Zürich-Schlieren, Switzerland).

3.4 Results

3.4.1 Role of membrane-proximal Ig-homology domains 4 and 7 in receptor activation

In the crystal structure of the c-Kit receptor, two amino acids Arg381 and Glu386 in the EF loop of D4 were identified that form salt bridges mediating homotypic interaction of receptor monomers. Sequence alignment showed that this dimerization motif is conserved among several type III and type V RTKs and is also found in D7 of VEGFR-2. Based on this alignment, we generated a series of VEGFR-2 D7 mutants where parts of or the entire loop containing this dimerization motif were mutated (Fig. 3-1).



VEGFR-2 WT:	(715)	LKDGNRNLT	RRVRKEDE	GLYTCQACSVL	(743)
VEGFR-2 xD7EF:	(715)	LKDGNRNLT	AAVASAAE	GLYTCQACSVL	(743)
VEGFR-2 R726A:	(715)	LKDGNRNLT	RAVRKEDE	GLYTCQACSVL	(743)
VEGFR-2 D731A:	(715)	LKDGNRNLT	RRVRKEAE	GLYTCQACSVL	(743)
VEGFR-2 RD/AA:	(715)	LKDGNRNLT	RAVRKEAE	GLYTCQACSVL	(743)
VEGFR-2 RRR/AAA:	(715)	LKDGNRNLT	AAVAKEDE	GLYTCQACSVL	(743)
VEGFR-2 RRRK/AAAS:	(715)	LKDGNRNLT	AAVASEDE	GLYTCQACSVL	(743)
VEGFR-2 ED/AA:	(715)	LKDGNRNLT	RRVRKAAE	GLYTCQACSVL	(743)
VEGFR-2 EDE/AAA:	(715)	LKDGNRNLT	RRVRKAAA	GLYTCQACSVL	(743)

Figure 3-1: Schematic representation of the β^E - β^F loop in VEGFR-2 D7 and sequences of generated mutants.

Mutated amino acids are indicated in red, wild type amino acids in blue.

We transiently expressed these mutant receptors in HEK293 cells and generated stably expressing retrovirus-infected PAE cell lines. To create amphitropic retroviruses, VEGFR-2 constructs were cloned into the pLIB retroviral expression vector providing a ψ^+ packaging signal. The packaging cell line HEK293 Ampho expressing the viral gag, pol, and env genes, was transfected with the retroviral expression vector. The viral genomic transcript containing the target gene and a selectable neomycin resistance marker was packaged into infectious virus and subsequently used to infect PAE cells.

Transiently or stably transfected cells were starved, stimulated with VEGF-A₁₆₅ for 10 min and lysed. Ligand-induced VEGFR-2 activation was determined by western blotting with anti-phosphotyrosine 1175 and anti-VEGFR-2 antibodies. All mutants except mutant xD7EF, whose phosphorylation was completely blocked, retained some autophosphorylation activity both in stable (Fig. 3-2) and in transiently transfected cells (Suppl. Fig. 3-12). The ratio of phosphorylation normalized to total VEGFR-2 compared to wt (wt value set to 1.0) was: RRRK: 0.51 ± 0.10 ; mutant RRR: 0.65 ± 0.36 ; mutant R: 0.43 ± 0.18 ; mutant EDE: 0.44 ± 0.26 ; mutant ED: 0.78 ± 0.34 ; mutant D: 0.68 ± 0.11 ; mutant xD7EF: 0.00 ± 0.08 .

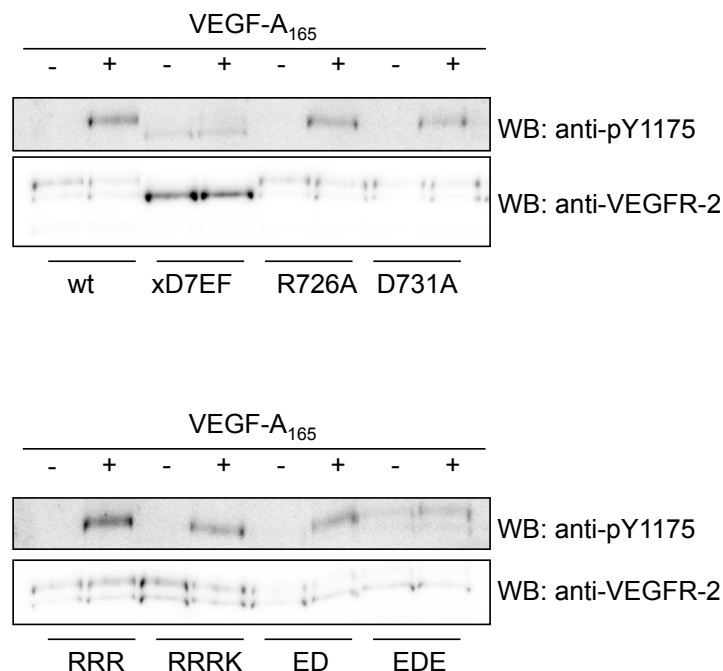


Figure 3-2: The conserved dimerization motif in D7 is crucial for ligand-induced activation of VEGFR-2.

Ligand-induced activation of VEGFR-2 is compromised by mutation of the EF-loop in D7. PAE cells stably expressing the indicated VEGFR-2 mutants were generated by retroviral transduction. Cells were stimulated with 1.5 nM VEGF-A₁₆₅ for 10 min at 37°C. Cell lysates were analysed on Western blots with phospho-specific antibody pY1175 and anti-VEGFR-2 antibody.

Therefore, the homotypic interactions that take place between D7 play an essential role in receptor activation. These data show that homotypic interaction between D7 revealed in the published VEGFR-2 D7 structure (Yang *et al.*, 2010) is required for receptor activation. Point mutation of these sites gave rise to partially defective receptors presumably due to compensatory interactions mediated by other charged amino acids in the EF loop. Mutation of all charged amino acids in the EF loop completely blocked receptor activation in both transiently and stably transfected cell lines and thus showed that D7 interaction plays an essential role in receptor activation.

For D4, which seems to be involved in receptor dimerization (Ruch *et al.*, 2007) but has not yet been as extensively studied as D7, we generated mutants where the entire domain was either replaced by D5 of VEGFR-1 (3/5) or deleted (Delta 4). Mutants were transiently or stably transfected into HEK293 and PAE cells respectively. Both mutants were completely inactive in the phosphorylation assay (Fig. 3-3 and Suppl. Figures 3-13 and 3-14). The ratio of phosphorylation normalized to total VEGFR-2 compared to wt (wt value set to 1.0) was: 3/5: 0.02 ± 0.03 ; mutant $\Delta 4$: 0.00 ± 0.12 , mutant $\Delta 5$ 0.93. This shows that D4 is required for correctly positioning receptor monomers in active dimers. In addition to D7, D4 plays a crucial role in VEGFR-2 activation.

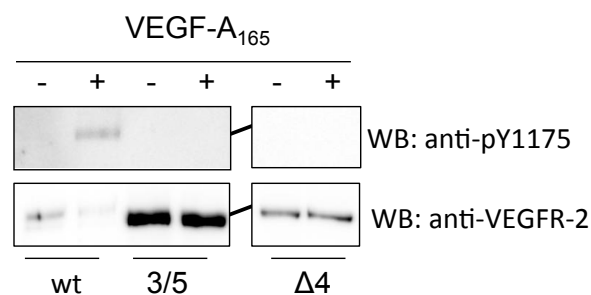


Figure 3-3: D4 is essential for ligand-induced VEGFR-2 activation.

Ligand-induced activation of VEGFR-2 is compromised by mutation of D4. PAE cells stably expressing VEGFR-2 3/5 or VEGFR-2 Delta 4 were stimulated with 1.5 nM VEGF-A₁₆₅ for 10 min at 37 °C. Cell lysates were analysed on Western blots with phospho-specific antibody pY1175 and anti-VEGFR-2 antibody.

3.4.2 Isolation and characterization of Ig-homology domain-specific DARPins

To test the possibility whether VEGFR-2 activation can be blocked with reagents specifically binding to D4 or D7, we selected Designed Ankyrin Repeat Proteins (DARPins, (Binz *et al.*, 2004)) binding to single Ig homology domains of VEGFR-2 ECD. Ribosome display was employed to select binders specific for the ECD of VEGFR-2. My colleague Edward Stutfeld cloned the expression plasmids, expressed and purified all proteins used for ribosome display. The selected DARPins were then verified on recombinant VEGFR-2 ECD protein. A total of 18 DARPins was isolated and their affinities determined by surface plasmon resonance (confidential data, Molecular Partners AG, Schlieren). All DARPins bound the receptor with high affinity with Kds below 10 nM. To determine the specificity of each DARPIn, an ELISA with distinct ECD proteins encompassing various Ig homology domains was performed. Proteins used were: ECD D1-7, D7, D2-3 and D2-4. DARPIn 6G9 bound to D1-7, D2-3, and D2-4. DARPIn 6C8 was shown to be specific for D1-7 and D2-4. DARPIn 7H4 bound to D1-7 and D7 (Fig. 3-4). In conclusion, DARPIn 6G9 is specific for D2-3, DARPIn 6C8 for D4, and DARPIn 7H4 for D7.

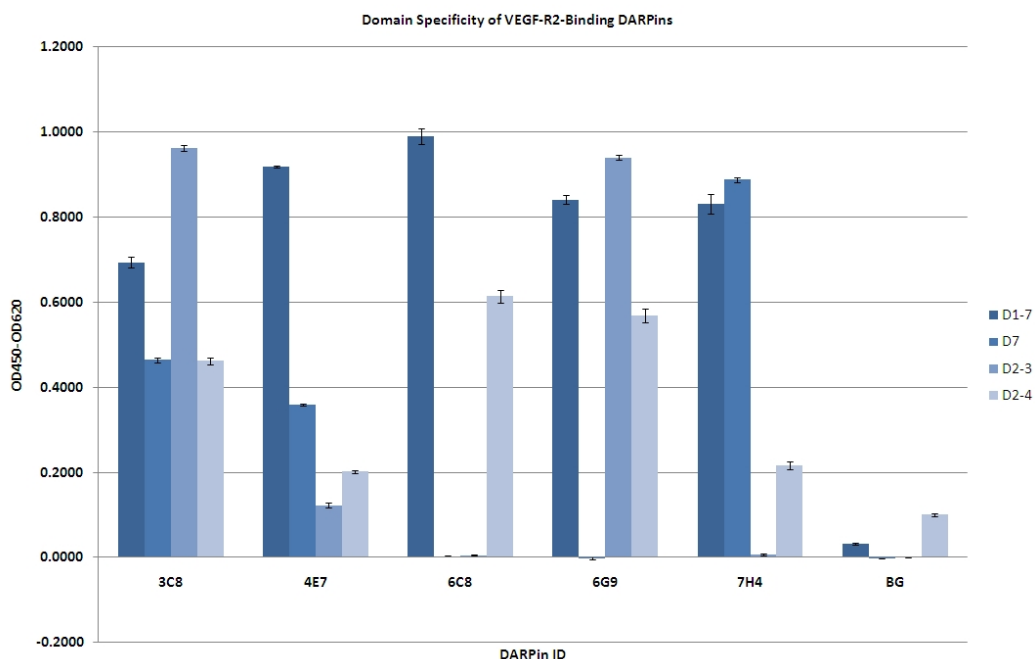


Figure 3-4: DARPIn specificity for VEGFR-2.

Specificity of DARPins 3C8, 4E7, 6C8, 6G9, and 7H4 against VEGFR-2 ECD was determined by ELISA. Proteins used were: D1-7, D7, D2-3, and D2-4. BG: background signal. Figure and data in collaboration with Molecular Partners AG, Schlieren.

To verify that these DARPins recognized VEGFR-2 also on cells, we analyzed receptor binding by fluorescence microscopy using a series of distinct receptor-expressing cells. HEK293 cells expressing wt or mutant VEGFR-2 (VEGFR-2 Delta4) were fixed, permeabilized and incubated with DARPins. DARPins were then labelled with anti-His and fluorescently labelled anti-mouse antibodies. DARPins 6C8 and 6G9 both recognized the receptor on the cell surface as well as in intracellular vesicles following ligand stimulation (Fig. 3-5). As expected, 6G9 bound both wt as well as D4 deleted VEGFR-2. In agreement with the epitope-mapping ELISA, 6C8 only recognized wt VEGFR-2, but not D4 deleted receptor. Control stainings can be found in suppl. Fig. 3-15.

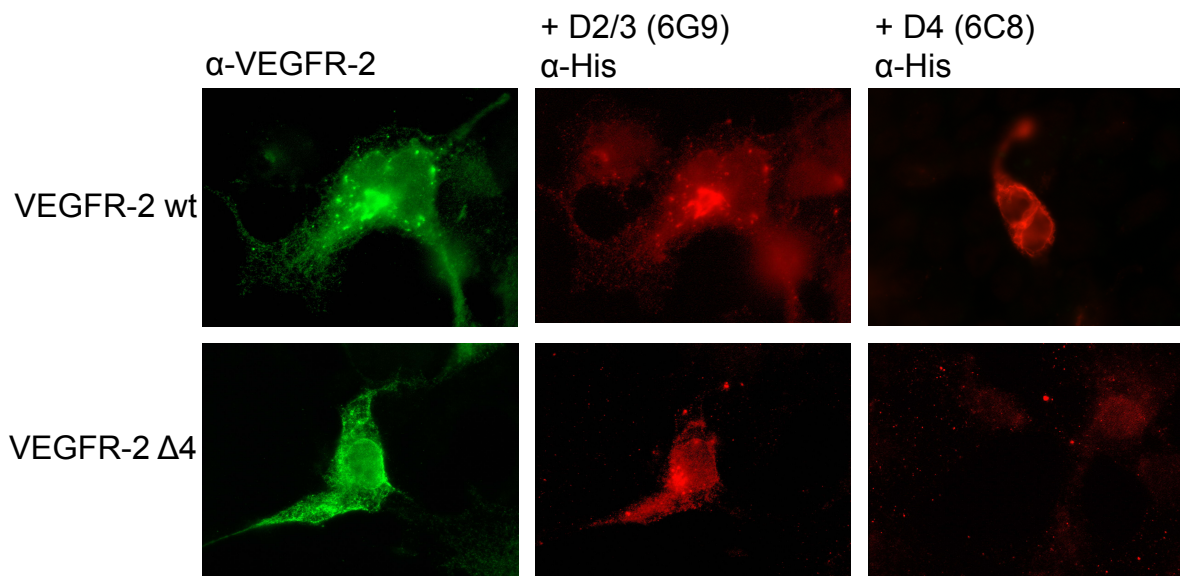


Figure 3-5: DARPIn 6C8 binds to D4 and DARPIn 6G9 to D2-3.

HEK293 cells were transiently transfected with VEGFR-2 wt (top) or $\Delta 4$ mutant (bottom), fixed and stained with DARPIn 6G9 or 6C8, anti-His, and anti-mouse Cy3 antibodies (red). As a control (left panels), cells were stained with a commercially available anti-VEGFR-2 antibody and an Alexa488 labeled secondary antibody (green). Figure K. Ballmer-Hofer.

3.4.3 Effect of DARPins on ligand-mediated receptor dimerization

Next, we analysed whether inhibitors of D4 affected ligand-mediated receptor dimerization. Multi-angle light scattering (MALS) experiments were carried out by my colleague Edward Stutfeld. We determined receptor dimerization using recombinant receptor ECD proteins incubated with ligand in the presence or absence of DARPins and analyzed by MALS. DARPin 6G9 specific for D2-3 completely blocked receptor dimerization (Fig. 3-6).

Incubation of VEGFR-2-ECD with the DARPin 6G9 showed three peaks with calculated M_w s of 110.6, 28.7, and 18.7 kDa, corresponding to one VEGFR-2-ECD molecule in complex with the DARPin 6G9, unbound VEGF- A_{121} , and excess of DARPin 6G9, respectively. On the other hand, the inhibitory DARPin 6C8 which is specific for D4 resulted in two peaks with apparent M_w of 217.2 and 20.4 kDa. While the peak with an apparent M_w of 20.4 kDa represents the excess of DARPin 6C8, the peak with the calculated M_w of 217.2 kDa consists of VEGFR-2-ECD bound to the DARPin as well as the VEGF- A_{121} . This is supported by the fact that the elution volume of VEGFR-2-ECD/6C8/VEGF- A_{121} shifts to a lower value compared to VEGFR-2-ECD/VEGF- A_{121} alone, suggesting that a bigger complex is present.

However, it is arguable whether the complex contains two DARPin molecules or only one DARPin molecule. The addition of the theoretical M_w s of the individual components gives values of 235 kDa for a 2:2:2 (VEGFR-2/VEGF/DARPin) complex and 217 kDa for a 2:2:1 complex, indicating that the latter is present. Nonetheless, these results suggest, that DARPin 6G9 inhibits VEGFR-2 signaling by blocking the ligand-binding site, whereas DARPin 6C8 affects the VEGFR-2 signaling in an “allosteric” like mechanism without preventing ligand-binding.

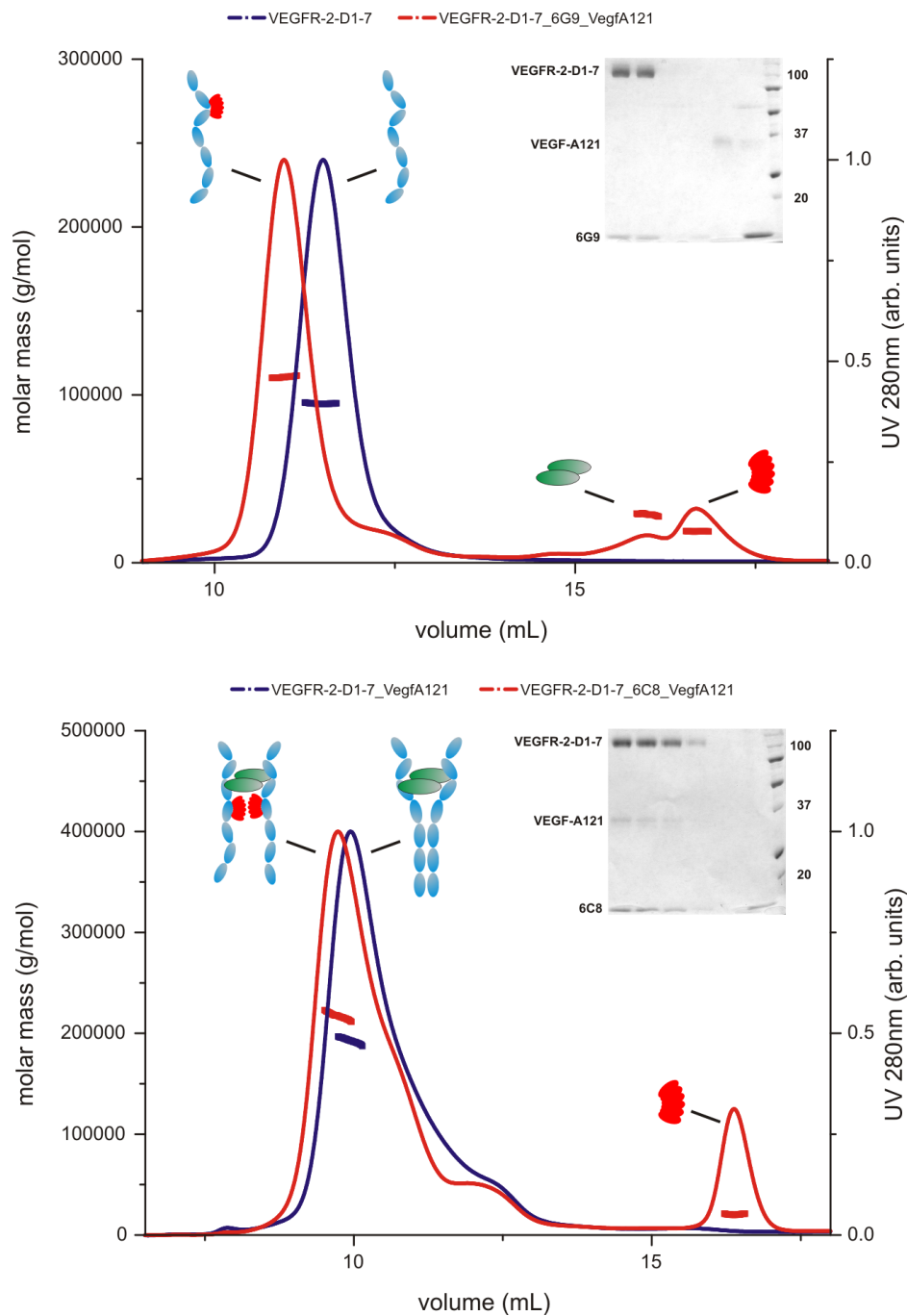


Figure 3-6: DARPin 6C8 does not interfere with dimerization of VEGFR-2 ECD whereas DARPin 6G9 prevents dimerization in the presence of VEGF.

Receptor ECD proteins were incubated with ligand in the presence of DARPin 6G9 (top panel) or 6C8 (bottom panel) and analyzed by MALS. After the MALS run, proteins were analyzed by Western blot to confirm their dimerization status. Figure E. Stuttgart.

3.4.4 Functional characterization of receptor-inhibitory DARPins

All 18 DARPins specifically binding to the ECD of VEGFR-2 were now tested for their ability to inhibit VEGFR-2 activation (suppl. Fig. 3-16). PAE cells expressing VEGFR-2 were incubated with DARPins for 30 min before stimulation with VEGF-A₁₆₅ (Fig. 3-7 top). DARPIn 6G9 completely blocked receptor kinase activation. Most interestingly, the D4-specific DARPIn 6C8 also reduced ligand-induced receptor phosphorylation. The two DARPins bind to different Ig homology domains and both inhibit activation. Furthermore, DARPIn 6G9 completely inhibited VEGF-A₁₆₅ induced PLC- γ 1 phosphorylation whereas 6C8 led to a decrease of PLC- γ 1 phosphorylation in PAE-VEGFR-2 cells (Fig. 3-7 bottom).

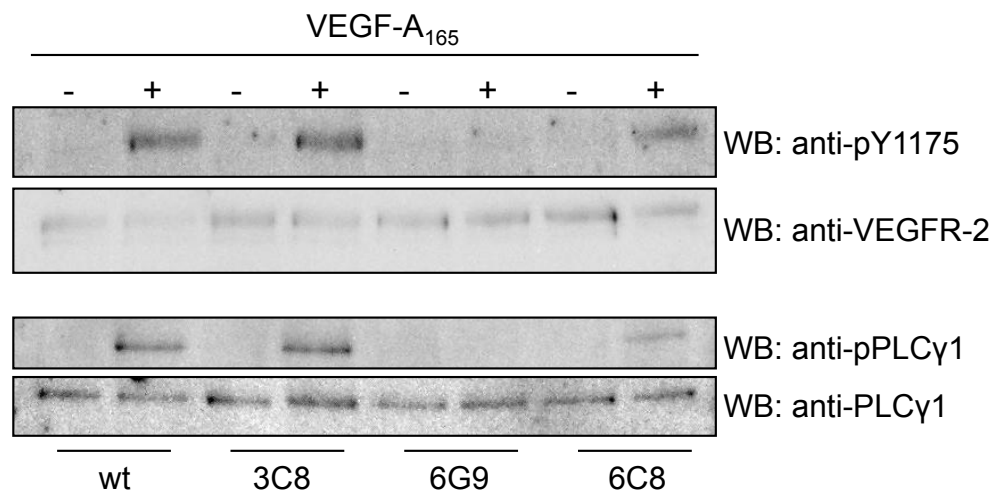


Figure 3-7: DARPins 6G9 and 6C8 inhibit VEGFR-2 activation and downstream signaling.

PAE-VEGFR-2 cells were incubated with 100 nM DARPins for 30 min at 37°C and stimulated with 1.5 nM VEGF-A₁₆₅ for 10 min at 37°C. Cell lysates were analysed on Western blots with phospho-specific antibody pY1175, anti-VEGFR-2 antibody (top) and phospho-PLG- γ 1, anti-PLC- γ 1 antibody (bottom).

Immunofluorescence of VEGFR-2 expressing PAE cells incubated with DARPins 30 min prior to stimulation showed that the receptor was retained on the cell surface (Fig. 3-8), while receptor was rapidly internalized in the absence of DARPins following ligand stimulation. Therefore both DARPins 6C8 and 6G9 blocked internalization of the receptor.

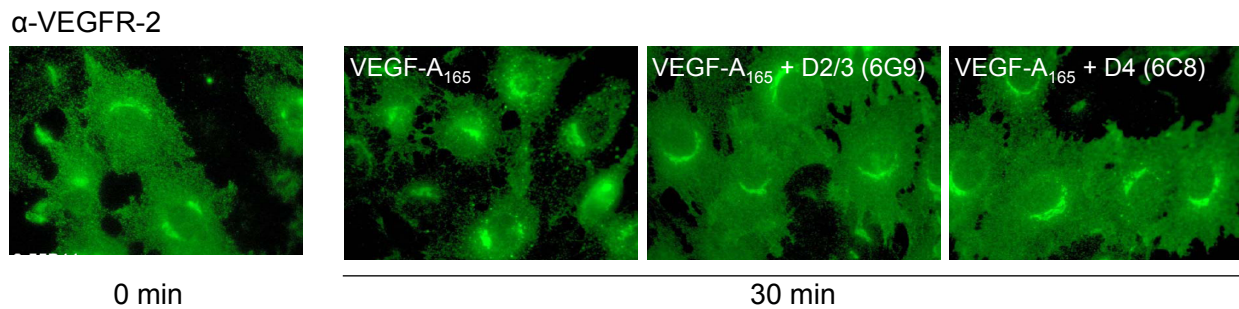


Figure 3-8: DARPins 6G9 and 6C8 inhibit VEGFR-2 internalization after stimulation.

PAE-VEGFR-2 cells were incubated with DARPins 6G9 or 6C8 30 min prior to ligand stimulation. Cells were fixed before stimulation (left panel) or 30 minutes after stimulation (three right panels). Membrane-bound and internalized VEGFR-2 was detected with an anti-VEGFR-2 antibody.

Figure K. Ballmer-Hofer.

To analyze the effect of the inhibitory DARPins on endothelial cell sprouting, we embedded BAEC spheroids in collagen gels containing 100 nM of DARPins. The incubation with DARPIn 6C8 led to significantly decreased relative sprouting compared to control (Fig. 3-9). The effect was more drastic than with the 6G9 DARPIn. Experiment was repeated and showed similar results.

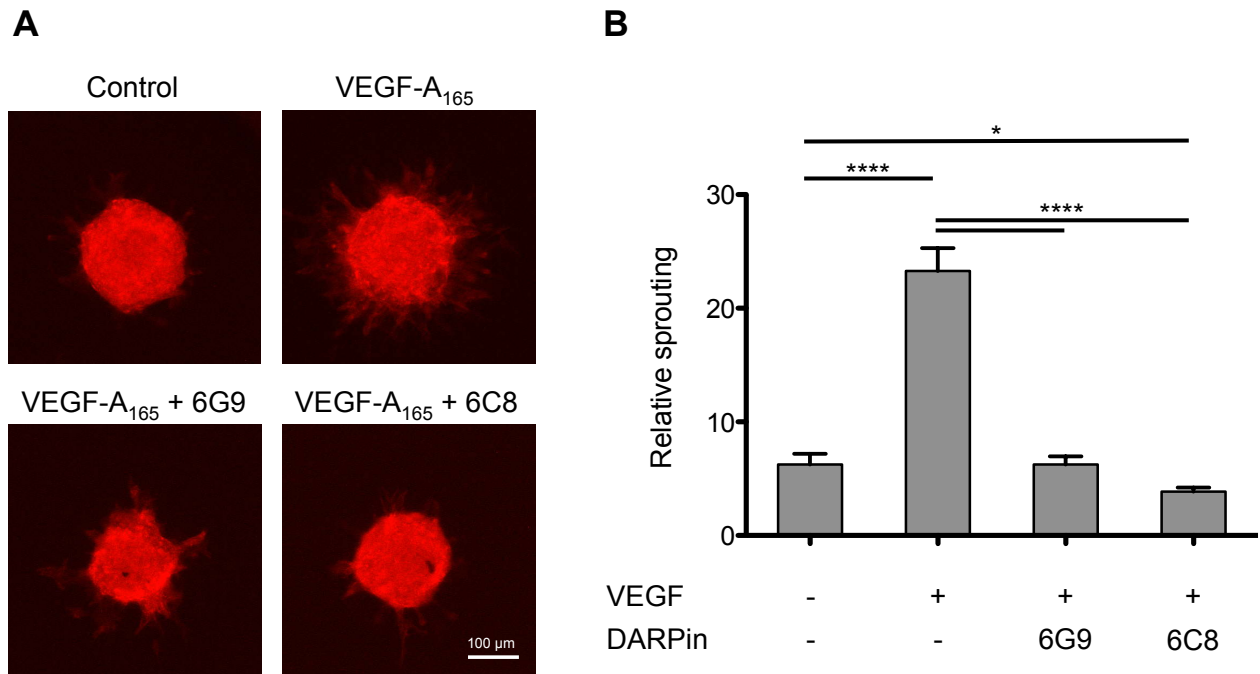


Figure 3-9: DARPins 6G9 and 6C8 inhibit sprouting of BAECs in the EC-spheroid assay.

(A) BAECs were embedded in collagen gels containing 100 nM DARPins. Collagen gels were overlaid with 1.5 nM VEGF-A₁₆₅ and sprouting was analysed after 24 h. Cells were fixed and visualized with a TRITC-labeled anti-phalloidin antibody. (B) Relative sprouting (number x average length of sprouts), * $p < 0.05$, **** $p < 0.0001$. Error bars represent \pm SEM.

We further monitored endothelial cell sprouting by live-cell imaging. Spheroids stimulated with VEGF-A₁₆₅ were incubated in the presence or absence of DARPin 6C8 and monitored for 16 h. Representative pictures are presented in Fig. 3-10 (without DARPin) and Fig. 3-11 (with DARPin 6C8) and confirmed inhibition of BAEC sprouting by DARPin 6C8.

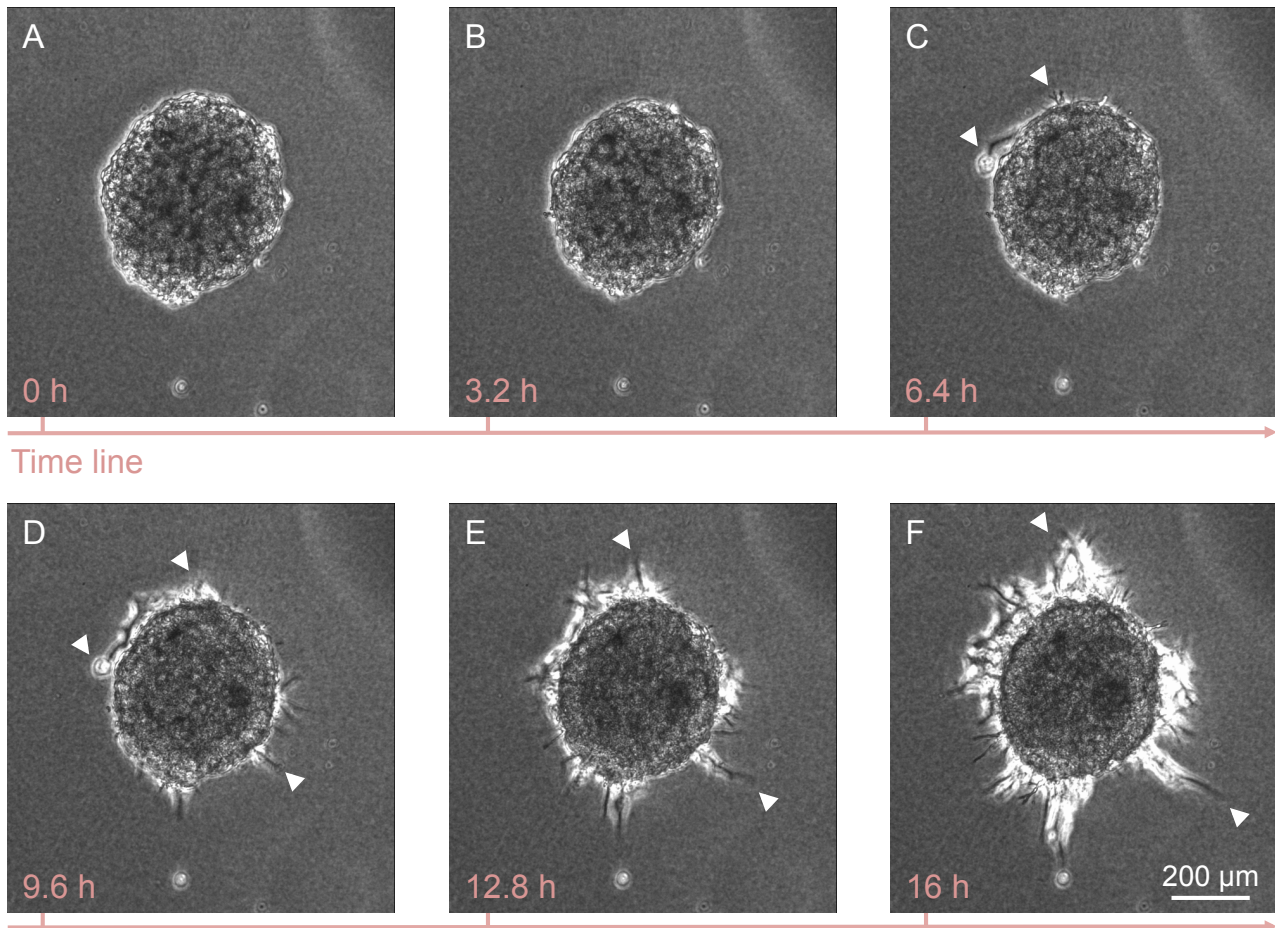


Figure 3-10: Endothelial cell sprouting over time.

Sprouting of BAEC spheroids was monitored over 16 h after VEGF-A₁₆₅ incubation. Figures show six representative time points (A: 0 h, B: 3.2 h, C: 6.4 h, D: 9.6 h, E: 12.8 h, F: 16 h). Arrowheads indicate emerging and growing sprouts.

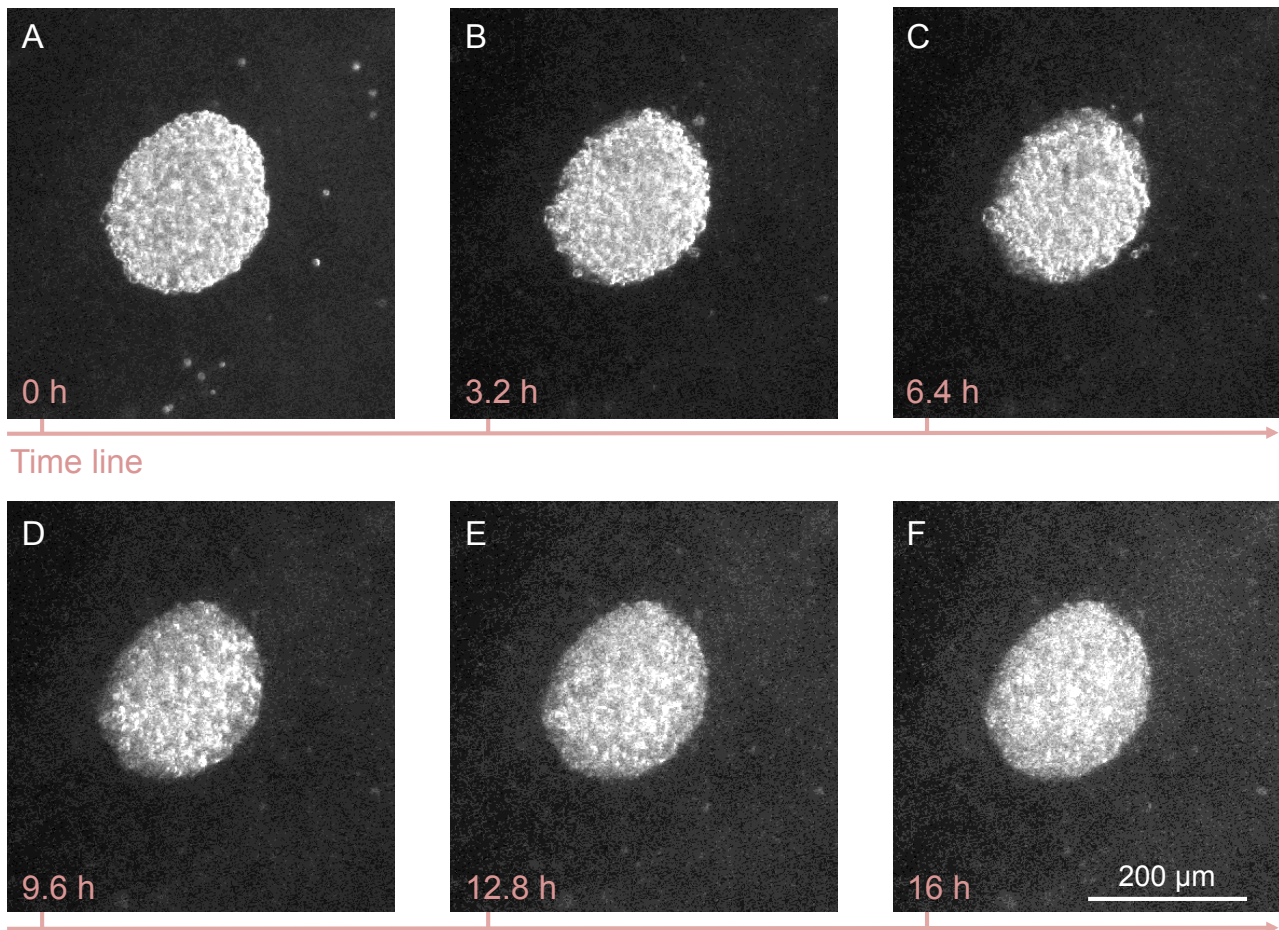


Figure 3-11: Inhibition of endothelial cell sprouting by DARPin 6C8.

Sprouting of BAEC spheroids was monitored over 16 h after VEGF-A₁₆₅ incubation in the presence of DARPin 6C8. Figures show six representative time points (A: 0 h, B: 3.2 h, C: 6.4 h, D: 9.6 h, E: 12.8 h, F: 16 h).

3.5 Discussion

We demonstrated that homotypic interactions between D7 previously indicated in the VEGFR-2 D7 structure (Yang *et al.*, 2010) are required for receptor activation. These interactions are mediated by conserved paired amino acids in the loop linking the β E and β F strands. Point mutation of these residues gave rise to only partially defective receptors presumably due to compensatory interactions mediated by other charged amino acids in the loop. Mutation of all charged amino acids in the EF loop completely blocked receptor activation in both transiently and stably transfected cell lines and thus confirmed that D7 interactions play an essential role in receptor activation.

Our results are partially contradictory to the recently published functional data (Yang *et al.*, 2010). Yang *et al.* showed that also point mutations in the EF loop are sufficient to strongly compromise the ligand-induced activation of VEGFR-2. Our data show that receptor kinase inhibition is only observed when the entire loop was mutated. There are various explanations for this observation: the cell line used by Yang *et al.* for the generation of stable lines are NIH-3T3 cells, a non-endothelial fibroblast cell line usually not involved in angiogenesis. We believe that our PAE cells are more representative of endothelial cells and thus better suited for functional analysis. In addition, some of the receptor mutants employed in the study were chimeric receptors composed of the VEGFR-2 ECD linked to the TM and cytoplasmic domain of PDGFR. The authors claim that this was done to overcome the relatively weak kinase activity of VEGFR-2. Again, such artificially engineered receptors might be problematic for mimicking the actual *in vivo* situation in developing vessels.

The EM structure of the ECD of VEGFR-2 published by our laboratory revealed that in addition to D7, D4 also seems to be involved in homotypic interactions between ligand-bound receptor dimers (Ruch *et al.*, 2007). In agreement with functional data published earlier on VEGFR-1 (Barleon *et al.*, 1997), D4 would be involved in stabilizing receptor dimers. To investigate the role of D4 in receptor activation and in intracellular signaling, we constructed VEGFR-2 mutants where D4 was either deleted (Δ 4) or replaced by D5 of VEGFR-1 (mutant 3/5), a domain which until now has not been shown to play a specific role in receptor activation. We performed phosphorylation assays with HEK293 cells transiently transfected with the D4 mutants and further generated stable PAE cells expressing this mutant. Compared to transiently transfected cells, stably transfected cell lines expressed physiologically relevant receptor levels. In contrast to the *wt* VEGFR-2, D4 mutants were not phosphorylated after VEGF-A stimulation showing that D4

is indeed indispensable for receptor activation. By manual sequence alignment, Yang *et al.* identified a conserved sequence motif of “D/E-x-G” amino acids in D4 similar to the dimerization motif in D4 of c-Kit and PDGFR. In their study, mutations of the conserved D392 to an A did not lead to receptor inactivation, neither did the mutations of residues E387 and R391 which they claimed to be the non-conserved pair of amino acids with opposite charges responsible for the generation of salt bridges in D4 (similar to R726 and D731 in D7). We propose that similar to the D7 mutants, compensatory interactions are mediated by other charged amino acids in the loop, such as for example E390. Another possibility could be that D4 interactions are mediated through a different interface, as proposed earlier (Yang *et al.*, 2010). This seems highly probable since the sequence identity between D4 of PDGFR- α and VEGFR-2 is only 20% which makes it rather difficult to draw conclusions based on sequence alignment.

We also demonstrated that activation of VEGFR-2 requires specific positioning of intracellular kinase domains relative to each other following conformational changes (Dell'Era Dosch *et al.*, 2009). Dimerization is hence necessary but not sufficient for receptor activation and downstream signaling, and requires exact positioning of the kinase domains relative to each other in receptor dimers. We now show that this orientation is mediated by the homotypic interactions between the membrane-proximal Ig-homology domains in the ECD in the full length receptor. As proposed for the c-Kit receptor (D4) (Lemmon and Ferguson, 2007), we suggest that the weak interactions between ECD domains (D4 and D7 for VEGFR-2) are important for proper alignment of receptor monomers. We assume that the specific orientation resulting from ECD mediated dimerization through the binding of the ligand leads to a conformational reorganization of the juxtamembrane domain and intracellular kinase domain and subsequent kinase activation.

In this study we provide functional evidence for the findings described in our EM structure of the VEGFR-2 ECD (Ruch *et al.*, 2007). We demonstrate the importance of ECD Ig-homology domains D4 and D7 in VEGFR-2 activation. Both domains are required for mediating weak interactions between receptor dimers that are essential for receptor activation.

In conclusion, homotypic contacts in the VEGFR-2 ECD seem to be ideal targets for therapeutic intervention in the treatment of diseases in which pathological RTK activation is observed. In a next step, we therefore developed specific binders for Ig-homology domains D4 and D7 of the VEGFR-2 ECD. The advantage of such VEGFR-2 inhibitors is that, in contrast to other less specific angiogenesis inhibitors, they specifically bind to the receptors and therefore interfere only with distinct signaling pathways. Since VEGF-A binds in an overlapping pattern to several VEGFRs, its inhibition interferes with a multitude of pathways (lymphangiogenesis). The clinically

most advanced VEGFR-2 inhibitor so far is Ramucirumab (IMC-1121) (Spratlin, 2011), a chimeric antibody against the ligand-binding domain of VEGFR-2. In early clinical trials many patients developed severe side-effects due to the chimeric antibodies, IMC-1121 was therefore fully humanized and is now being tested in several phase III clinical trials <http://clinicaltrials.gov/ct2/results?term=ramucirumab>. However, the disadvantage of inhibitors against ligand-binding domains is that they have to compete with the ligand and are less efficient at high ligand concentrations.

We screened DARPIn libraries against the entire ECD of VEGFR-2 and identified a number of inhibitors against the ligand-binding domain of VEGFR-2. As expected, these DARPins completely abolished ligand-induced VEGFR-2 activation and were a very good positive control for our experiments. In addition, and even more interestingly, we identified the 6C8 DARPIn that binds specifically to D4 of the ECD. Incubation of PAE cells with the inhibitor prior to stimulation led to decreased receptor activation. Downstream signaling to PLC- γ was also compromised and sprouting in BAE cells was significantly weaker. We have thus found a potent inhibitor of VEGFR-2 activation which has a different inhibition mechanism than inhibitors that interact with the ligand-binding domain.

To further characterize the mechanism of inhibition, we investigated the dimerization status of ECD-proteins incubated with DARPIn 6C8. The DARPIn still enabled ligand binding. More importantly, 6C8 did not interfere with receptor dimerization. This confirms the findings that the homotypic interactions in the ECD are dispensable for receptor dimerization as shown for RTKs such as Kit (Yuzawa *et al.*, 2007), PDGFR (Yang *et al.*, 2008), and VEGFR (Yang *et al.*, 2010). In addition, the receptor was still dimerized when the inhibitor was present and dimerization is thus not sufficient for activation of the VEGFR-2.

In summary, we have identified a high-affinity inhibitor specific for D4 of VEGFR-2 that has the advantage of binding specifically to VEGFR-2 and functions independently from ligand concentration. Our inhibitor suppresses VEGF-A mediated receptor activation and downstream signaling by interfering with the correct 3 dimensional organization of receptor monomers in active dimers. The only dimerization blocking inhibitor in clinical trials so far is pertuzumab, an antibody against ErbB2 (Franklin *et al.*, 2004) (Badache and Hynes, 2004). Pertuzumab blocks ErbB2 heterodimerization with other members of the ErbB family. At the time of writing, Tvorogov *et al.* reported a mAb against D5 of VEGFR-3 which by inhibiting VEGFR-2/VEGFR-3 heterodimerization suppresses signal transduction, migration, and sprouting of microvascular endothelial cells (Tvorogov *et al.*, 2010). Furthermore, Kendrew *et al.* generated a human Ab in a

Xenomouse which binds to D4-7 of VEGFR-2 and suppresses VEGFR-2 activation (Kendrew *et al.*, 2011). They speculate that the Ab interferes with receptor dimerization but could not decipher the mode of action.

Potent and high-affinity inhibitors like the identified DARPin could in the future be employed in clinical applications such as tumor vasculature imaging. Furthermore, one could consider using it as an angiogenesis inhibitor *in vivo*.

3.6 Supplementary Information

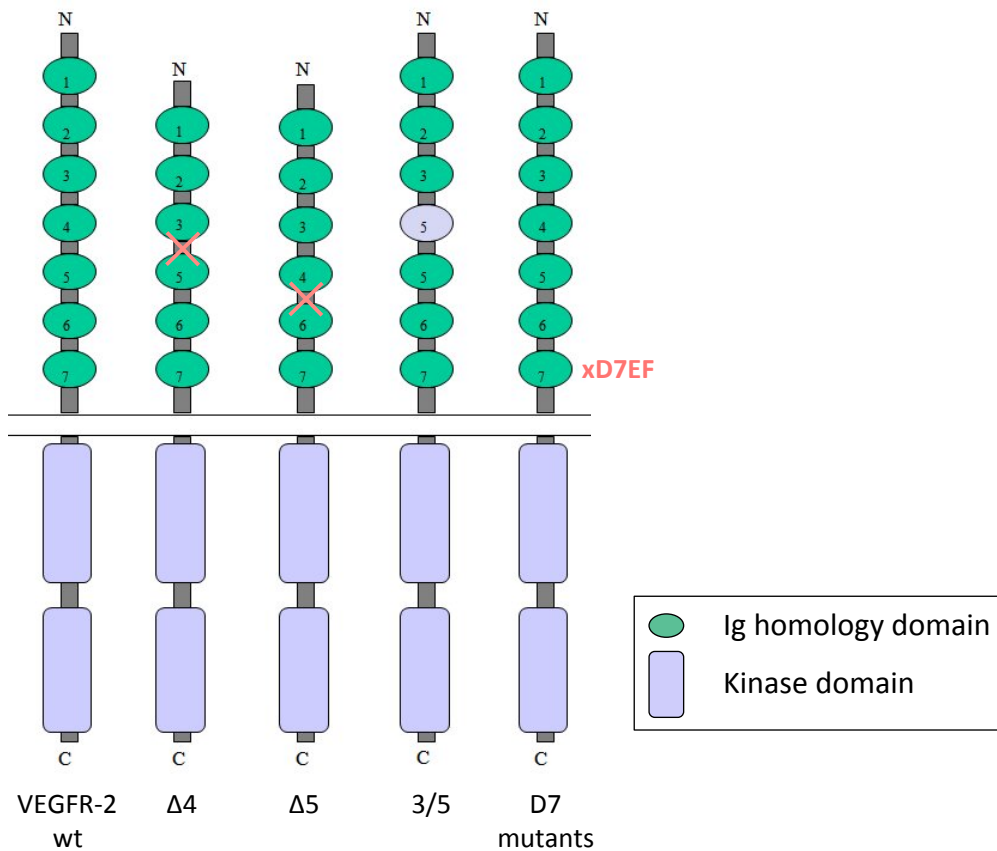


Figure 3-12: Schematic representation of VEGFR-2 mutants.

Green spheres represent the Ig homology domains in the ECD of VEGFR-2. Shown are VEGFR-2 wt, VEGFR-2 $\Delta 4$, VEGFR-2 $\Delta 5$, VEGFR-2 3/5, and VEGFR-2 D7 mutants.

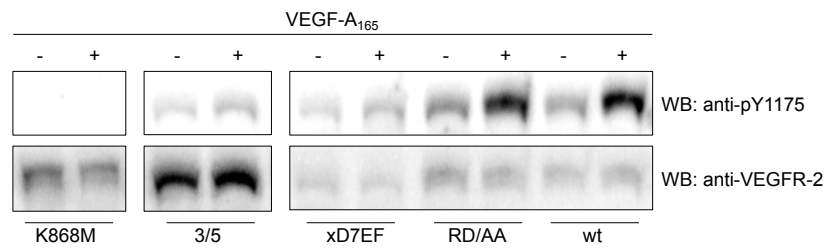


Figure 3-13: Ligand-induced activation of VEGFR-2 is compromised by mutation of D4 and D7.

HEK293 cells were transiently transfected with the indicated VEGFR-2 mutants and stimulated with 1.5 nM VEGF-A₁₆₅ for 10 min at 37°C. Cell lysates were analysed on Western blots with phospho-specific antibody pY1175 and anti-VEGFR-2 antibody.

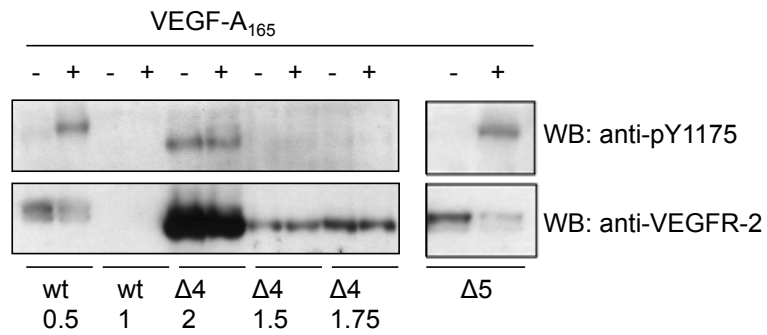


Figure 3-14: Ligand-induced activation of VEGFR-2 is compromised by mutation of D4.

We adjusted the expression level of the VEGFR-2 mutant constructs by titrating the amount of DNA used for transfection. HEK293 cells were transiently transfected with the indicated VEGFR-2 mutants. Amount of DNA used for transfection was varied to obtain a comparable expression level between the mutants. Amounts were 0.5 and 1 μ g for the wt construct and 2, 1.5, 1.75 μ g for Δ 4. Cells were stimulated with 1.5 nM VEGF-A₁₆₅ for 10 min at 37 °C. Cell lysates were analysed on Western blots with phospho-specific antibody pY1175 and anti-VEGFR-2 antibody.

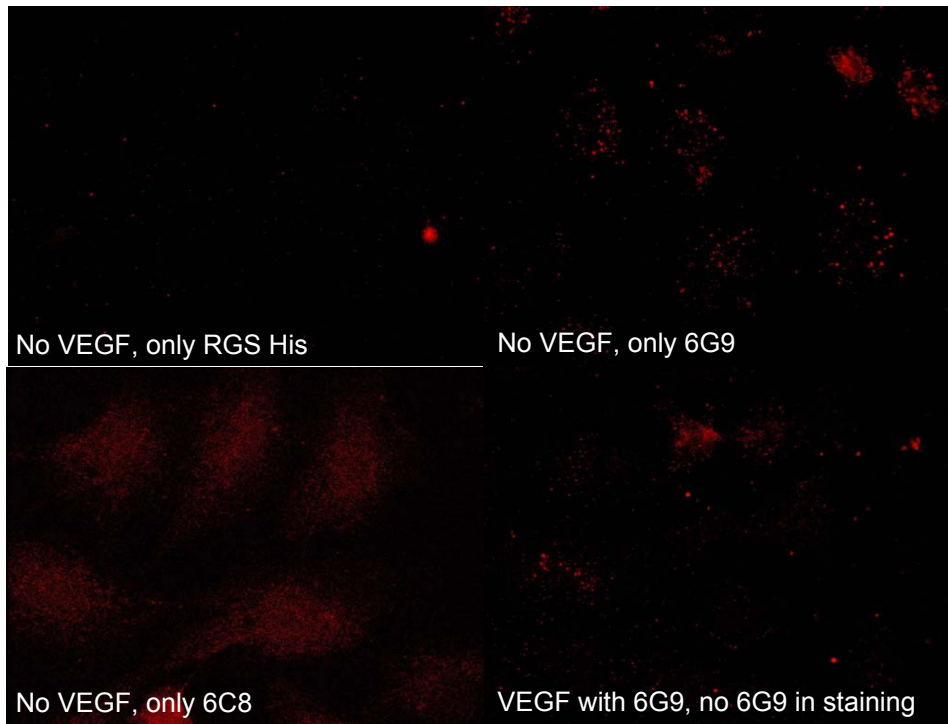


Figure 3-15: Stainings of VEGFR-2 on cells with DARPins are specific.

Control stainings were performed. DARPins and antibodies were used are indicated in white. HEK293 cells were transiently transfected with VEGFR-2 plasmids, fixed and stained with DARPin 6G9 or 6C8, anti-RGS His, and anti-mouse Cy3 antibodies (red).

Figure K. Ballmer-Hofer.

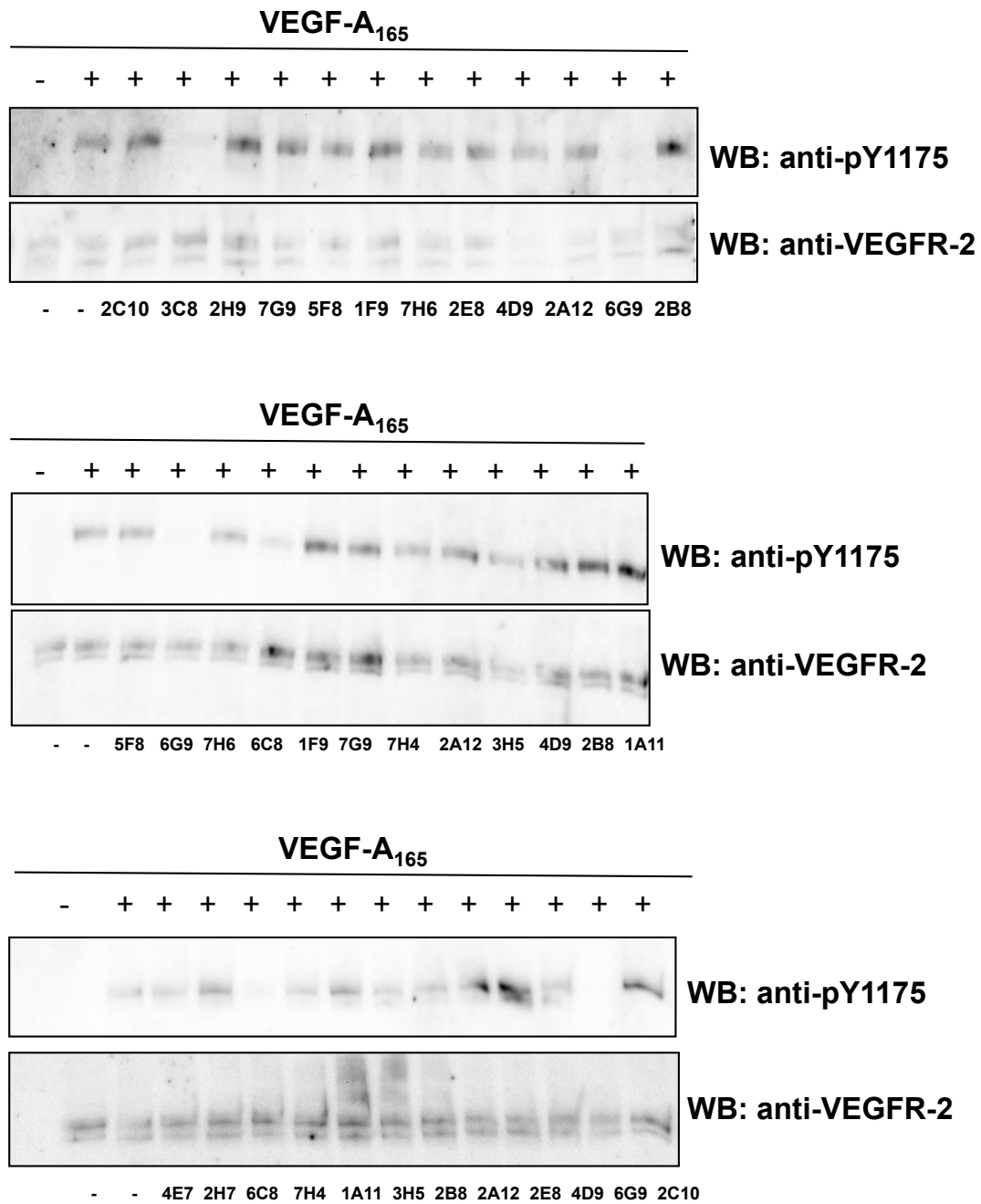


Figure 3-16: DARPins 3C8, 6G9, and 6C8 inhibit VEGFR-2 activation.

PAE-VEGFR-2 cells were incubated with 100 nM DARPins for 30 min at 37 °C and stimulated with 1.5 nM VEGF-A₁₆₅ for 10 min at 37 °C. Cell lysates were analysed by Western blot with phospho-specific antibody pY1175 and anti-VEGFR-2 antibody.

Table 3-1: Primers used for cloning VEGFR-2 3/5 mutant.

Construct	Orientation	5 – 3 sequence
pcDNA5 FRT VEGFR-2 3/5	forward 347	5'GCA CAT TTG TCA GGG TCC ATG AAA AAC CAG ACC CGG CTC TCT ACC 3'
	reverse 346	5'GAT TAG AGA TTT CTC ACC AAT CTG GGG TGG CAC ATC TGT GAT ATA AAA GC 3'

Table 3-2: Primers used for cloning VEGFR-2 domain 7 mutants.

The codons introducing the mutations are underlined.

Construct	Orientation	5 – 3 sequence
pcDNA5 FRT VR2 R	forward	5' CCG GAA CCT CAC TAT CCG CGC AGT GAG GAA GGA GGA CGA AGG 3'
pcDNA5 FRT VR2 D	forward	5' AGT GAG GAA GGA GGC CGA AGG CCT CTA CAC CTG CC 3'
pcDNA5 FRT VR2 xD7EF	forward	5' GGG AAC CGG AAC CTC ACT ATC GCC GCA GTG GCC TCA GCC GCC GAA GGC CTC TAC ACC TGC CAG 3'
pcDNA5 FRT VR2 RRR	forward 338	5' GGG AAC CGG AAC CTC ACT ATC <u>GCC</u> <u>GCA</u> GTG <u>GCC</u> AAG GAG GAC GAA GGC CTC TAC ACC TGC CAG 3'
pcDNA5 FRT VR2 RRRK	forward 339	5' GGG AAC CGG AAC CTC ACT ATC <u>GCC</u> <u>GCA</u> GTG <u>GCC</u> <u>TCA</u> GAG GAC GAA GGC CTC TAC ACC TGC CAG 3'
pcDNA5 FRT VR2 ED	forward 340	5' GGG AAC CGG AAC CTC ACT ATC CGC AGA GTG AGG AAG <u>GCC</u> <u>GCC</u> GAA GGC CTC TAC ACC TGC CAG 3'
pcDNA5 FRT VR2 EDE	forward 341	5' GGG AAC CGG AAC CTC ACT ATC CGC AGA GTG AGG AAG <u>GCC</u> <u>GCC</u> <u>GCC</u> GGC CTC TAC ACC TGC CAG 3'
Reverse primer (for all above)	reverse	5'ACA GGG ATT GCT CCA ACG TAG 3'

Table 3-3: Primers used for cloning pLIB constructs.

The codons introducing the restriction sites or the mutations are underlined.

Construct	Orientation	5 – 3 sequence
pLIB VEGFR-2 wt	forward (Sall restriction site underlined)	5' GAT <u>CGT CGA CAT</u> GGA GAG CAA GGT GCT GCT GGC CG 3'
	reverse (NotI restriction site underlined)	5' TAG ACT CGA <u>GCG GCC GCT</u> CAC AGA TCC TCT TC 3'
pLIB VEGFR-2 3/5	forward/reverse as first entry	
pLIB VEGFR-2 K868M	forward/reverse as first entry	
pLIB VEGFR-2 R	forward/reverse as first entry	
pLIB VEGFR-2 D	forward/reverse as first entry	
pLIB VEGFR-2 RD	forward/reverse as first entry	
pLIB VEGFR-2 RRR	forward 338	5' GGG AAC CGG AAC CTC ACT ATC <u>GCC GCA</u> GTG <u>GCC</u> AAG GAG GAC GAA GGC CTC TAC ACC TGC CAG 3'
pLIB VEGFR-2 RRRK	forward 339	5' GGG AAC CGG AAC CTC ACT ATC <u>GCC GCA</u> GTG <u>GCC TCA</u> GAG GAC GAA GGC CTC TAC ACC TGC CAG 3'
pLIB VEGFR-2 ED	forward 340	5' GGG AAC CGG AAC CTC ACT ATC CGC AGA GTG AGG AAG <u>GCC GCC</u> GAA GGC CTC TAC ACC TGC CAG 3'
pLIB VEGFR-2 EDE	forward 341	5' GGG AAC CGG AAC CTC ACT ATC CGC AGA GTG AGG AAG <u>GCC GCC GCC</u> GGC CTC TAC ACC TGC CAG 3'
Reverse primer (for the four constructs: RR, RRR, ED, EDE)	reverse	5' ACA GGG ATT GCT CCA ACG TAG 3'

4 Isolation of single chain variable fragment antibodies against Ig-homology domain 7 of the VEGFR-2 extracellular domain

4.1 Introduction

Monoclonal antibodies (mAbs) have proven to be effective therapeutic agents and are the major group of recombinant proteins currently used in the clinic (Reichert *et al.*, 2005). Originally, mAbs were generated by fusing mouse lymphocytes and myeloma cells to create antibody-secreting murine hybridomas (Kohler *et al.*, 1975). However, murine antibodies present several disadvantages such as immunogenicity and lack of efficacy when used in humans (Tjandra *et al.*, 1990). To circumvent these limitations, genetic engineering has been used to humanize the antibodies, replacing the murine antibody scaffold by human amino acid sequences (Riechmann *et al.*, 1988). Recently, the generation of antibodies in living organisms has been extended by the use of genetically engineered antibody libraries. Diversity in the libraries is obtained by performing polymerase chain reaction (PCR) on V-germline genes with degenerated primers against the Complementarity Determining Region (CDR3) of the variable regions of immunoglobulins (Winter *et al.*, 1994). Through the phage-display technology, antibodies against almost any antigen can be selected *in vitro* from such highly diverse libraries. Single chain variable fragments (scFvs) are expressed on the surface of a filamentous phage as fusion proteins with the phage minor coat protein (pIII). ScFvs with desired specificities are selected by repeated panning on the antigen of interest (Pini *et al.*, 1998). ScFvs of interest are then further amplified by infection of bacterial strains with the selected phages. Determination of the scFv DNA sequence is possible and subsequent reformatting into fully human immunoglobulins can be achieved. The advantage of these antibodies for the use in human therapy over non-human, chimeric or humanized antibodies is their reduced immunogenicity.

In this chapter I present the *in vitro* screening procedure of a scFv library against domain 7 (D7) of the VEGFR-2 extracellular domain (ECD). I performed the screen by phage display technology using the ETH-2 Gold antibody phage-display library (Silacci *et al.*, 2005). A promising scFv candidate was amplified in *E. coli* and purified. The D7 binding scFv was further tested for specificity and the ability to inhibit VEGFR-2 on endothelial cells.

4.2 Materials and Methods

4.2.1 Phage selection on immobilized antigen

The ETH-2 Gold antibody phage-display library was kindly provided by Prof. Neri (ETH Zürich, Switzerland) (Silacci *et al.*, 2005). A Maxisorp immunotube (Nunc GmbH, Wiesbaden, Germany) was coated with 50 µg/ml VEGFR-2 D7 (in 25 mM HEPES pH 7.5, 150 mM NaCl) o/n at RT using 4 ml of protein solution. The next day, the solution was discarded and the tube was rinsed three times with PBS. Blocking was performed on an orbital shaker for 2h with PBS containing 2.5% milk powder. The phage stock solution containing 5×10^{12} transducing units (tu) in PBS 2% milk powder was added to the immunotube. The tube was incubated at RT for 30 min in an orbital shaker and for 1.5 h standing upright. The immunotube was now thoroughly rinsed 10 times with PBS 0.1% Tween 20 and 10 times with PBS. In the following selection rounds, tubes were washed 20 times with each buffer. Bound phage was eluted by adding 1 ml 100 mM triethylamine (Sigma-Aldrich, Switzerland) to the tube and inverting at RT for 5 min. The eluate was added to an Eppendorf tube containing 500 µl 1 M Tris-HCl pH 7.4 to neutralize the triethylamine. The eluted phage was used to infect 10 ml of exponentially growing TG1 *E. coli*. TG1 at OD₆₀₀ = 0.5 were infected for 30-40 min at 37 °C. Infected TG1 bacteria were centrifuged at 3,300 g for 10 min. Pelleted bacteria were resuspended in 0.5 ml 2xTYE (yeast extract tryptone medium) and spread on two large 2xTYE plates (1.5% (w/v) agar) containing 100 µg/ml ampicillin and 1% glucose. Plates were incubated o/n at 30 °C. Three rounds of selection were performed.

4.2.2 Enzyme linked Immunosorbent Assay

Following three rounds of panning, individual bacterial colonies containing the phagemid were picked and grown in a 96-well plate in 2xTYE ampicillin 0.1% glucose for 3 h at 37 °C. The production of soluble scFv was induced by adding isopropyl-β-D-thiogalactopyranoside (IPTG) (Fermentas) to a final concentration of 1 mM. The bacteria were further incubated for 16 h at 30 °C. The plate was centrifuged for 15 min at 1800 g and 50 µl bacterial supernatant from each well were used for enzyme linked immunosorbent assay (ELISA). A 96-well maxisorp plate (Nunc) was coated with VEGFR-2 D7 (5 µg/ml) o/n at 4 °C. Wells were rinsed three times with PBS and blocked with 350 µl PBS containing 5% BSA for 2 h on a shaker at RT. The bacterial supernatants were added and the ELISA plate was incubated for 1 h at RT on a shaker. Wells were thoroughly

rinsed three times with PBS-0.1% Tween 20 and three times with PBS before they were incubated with the anti-myc tag antibody (9B11 2040 Cell Signaling Technology) (1:1000 in PBS 2.5% BSA). After rinsing, an anti-mouse HRP antibody (Southern Biotech) (1:10.000 in PBS 2.5% BSA) was added for 1h at RT. When ELISA was performed directly with phages, an anti-phage antibody was used (M13 antiphage HRP-linked, ab50370, Abcam) (1:5000). Wells were washed again before 100 μ l of ready-to-use 3,3',5,5'-tetramethylbenzidine (TMB) substrate solution (Thermo Scientific Pierce) were added to each well. The reaction was stopped after 10 min by adding 2 M H₂SO₄ and the OD₄₅₀ was recorded.

4.2.3 Expression and Purification of scFv

A single colony of phagemid bearing *E.coli* TG1 was grown o/n at 37 °C in 2xTYE ampicillin 1% glucose. The next day, 1 mL of TG1 was transferred to 1 L of 2xTYE ampicillin 0.1 % glucose and bacteria were grown for 3 h at 37 °C, 200 rpm. At an OD₆₀₀ = 0.9, cells were induced by addition of IPTG to a final concentration of 1 mM. Cultures were then grown for another 16 h at 30 °C, 200 rpm. The following steps were all performed at 4 °C to avoid proteolytic digestion. Supernatants were centrifuged for 30 min at 4000 g and filtered through a 0.45 μ m filter (Millipore). The supernatant was loaded onto a Protein A affinity column (Amersham Pharmacia Biotech). The column was washed first with Buffer A (100 mM NaCl, 0.1% Tween-20, 0.5 mM EDTA in PBS) then Buffer B (500 mM NaCl, 0.5 mM EDTA in PBS). The protein was eluted with 100 mM triethylamine into tubes containing Tris HCl pH 6.8 for neutralization. The eluate was dialyzed overnight against PBS and concentrated. Proteins were stored at -80°C until further use. Proteins were resolved on 12% gels.

4.2.4 Receptor kinase Inhibition Assay

The inhibition assay was performed as described with the DARPins in section 3.2. Concentrations of scFv 3B1 were 0.03; 0.1; 0.3; 0.6; 1.2; and 2.5 μ M. H9, a control scFv binding to VEGF-A and blocking its interaction with VEGFR-2 was used as a control for the inhibition of VEGFR-2 activation.

4.3 Results

4.3.1 Production and purification of VEGFR-2 D7

Purified VEGFR-2 ECD D7 was kindly provided by my colleague Edward Stutfeld. In brief, D7 was expressed in transiently transfected HEK293T cells. D7 was enriched by immobilized metal ion affinity chromatography (IMAC) and further purified by size exclusion chromatography (SEC). Purified D7 was frozen at -80°C until further use.

4.3.2 Phage display selection of scFvs against VEGFR-2 ECD D7

We used the human fully synthetic ETH-2 Gold antibody phage-display library (Silacci *et al.*, 2005) for the selection of binders specific for D7 of VEGFR-2. D7 protein was coated to an immunotube o/n before phage library was added. Phages displaying scFvs that bound to D7 were retained while non-binding phages were removed by repetitive washing. D7 binding phages were then eluted and used to infect *E. coli* cultures in repeating selection and infection rounds. In this way, specific binders were amplified and enriched. An enrichment factor (EF) is calculated and represents the ratio of output vs. input phage titer (in transducing units, tu). Final enrichment was calculated from the EF ratio of consecutive rounds ($\text{EF}_n/\text{EF}_{n-1}$). In total, three rounds of phage selection were performed which led to a 50-fold enrichment between selection rounds two and three (Table 4-1).

Table 4-1: Enrichment of binding phages during selection rounds.

Round	Input (tu)	Output (tu)	EF (output/input)	Enrichment ($\text{EF}_n/\text{EF}_{n-1}$)
1	0.1×10^{13}	6.5×10^4	6.5×10^{-8}	n/a
2	1.6×10^{13}	3.5×10^5	2.2×10^{-8}	0.34
3	5.5×10^{13}	6.0×10^7	1.1×10^{-6}	50

After three selection rounds, a total of 288 clones were picked to perform an initial enzyme linked immunosorbent assay (ELISA) for the identification of potential binder of VEGFR-2 D7. It has to be emphasized that we encountered unexpectedly low absorbance signals in the ELISA screen, probably due to low concentrations of scFvs in the 96-well plates. Binding of scFvs to both D7 and D1-7 was tested and, based on signal intensity in the ELISA screening, potential binders were selected as candidates for further rounds of verification. We focused on the two scFvs 3B1 and 6G2 which gave the strongest signal. ScFv 1A1 was used as a non-binding control selected from the library. The three scFvs were produced in larger amounts and used in a secondary verification ELISA at higher scFv concentration. ScFvs 3B1 and 6G2 bound specifically to D7 and D1-7 (Fig. 4-1). The 3E1 scFv showed unspecific binding to control protein and was therefore not considered for further detailed functional characterization.

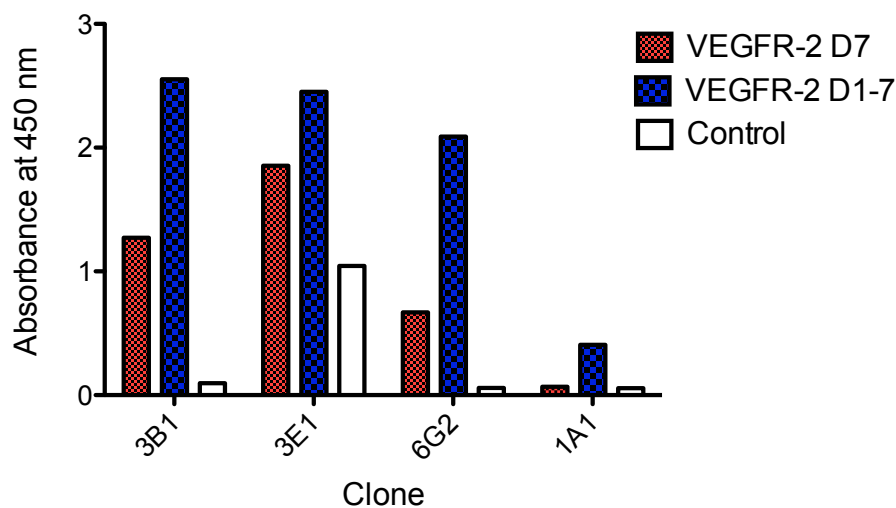


Figure 4-1: Binding specificities of anti-VEGFR-2 D7 scFv clones.

ELISA of scFvs 3B1, 3E1, 6G2, and negative control scFv 1A1. Maxisorp plates were coated with VEGFR-2 D7, VEGFR-2 D1-7, or control protein. Phage supernatant containing the scFvs was added. ELISA was developed after addition of antibodies.

Myc-tag containing scFv 3B1 was expressed in 1L cultures and purified from the supernatant on a Protein A Sepharose column. We obtained a yield of 2.8 mg per liter. The purified scFv was then analysed by SDS-PAGE (Fig. 4-2). The major band was the 30 kDa monomer band indicating the expected molecular weight of a scFv. Bands with higher molecular weight represent oligomers. The Coomassie-blue stained gel also showed two lower bands not containing the myc-tag.

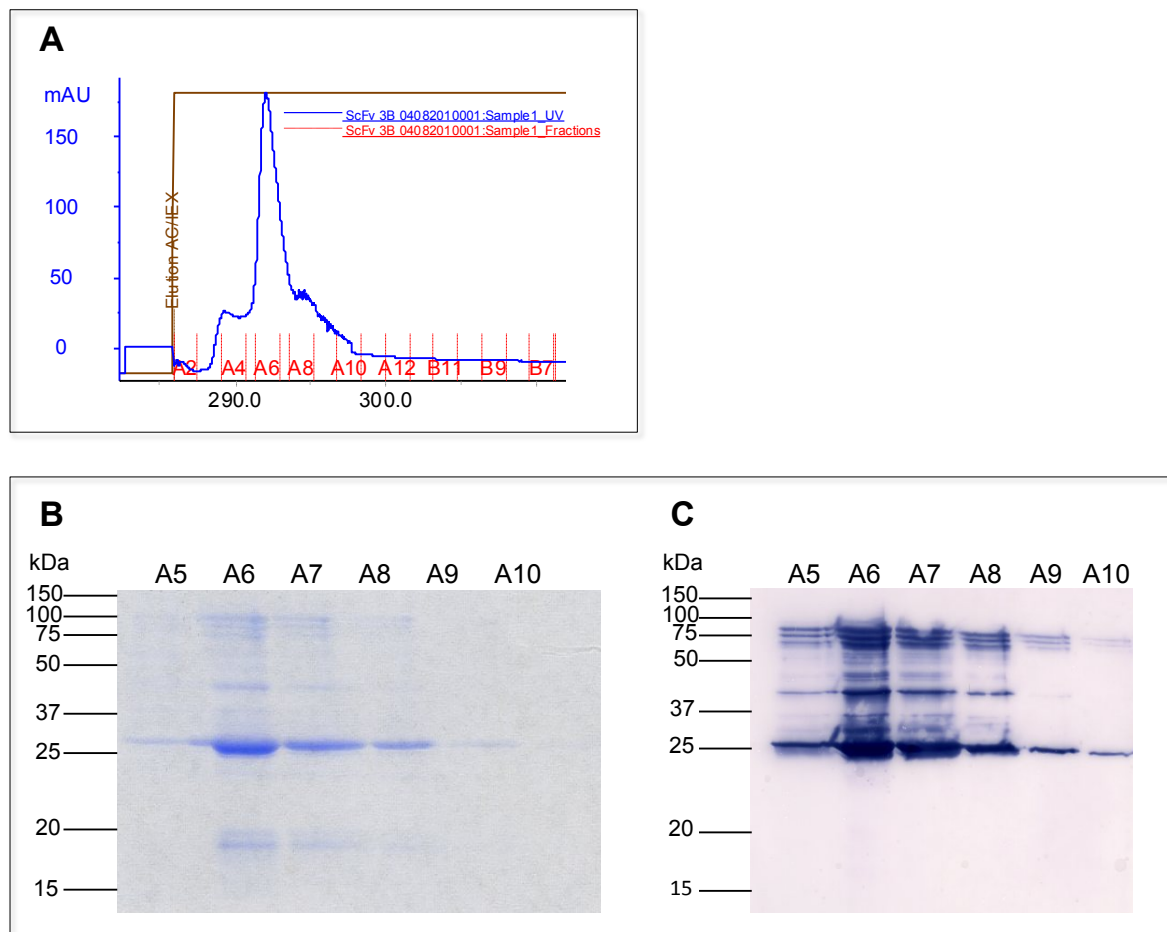


Figure 4-2: Purification of anti-VEGFR-2 D7 scFv 3B1.

(A) Elution profile on a Protein-A Sepharose column. Fractions were resolved on a 12% polyacrylamide gel.

(B) Coomassie-blue staining. (C) Anti-myc immunoblot.

To determine the sequence of scFv 3B1, DNA was sequenced and showed the following amino acid sequences in the V_H - and V_λ -segments (Table 4-2).

Table 4-2: Amino-acid sequences in the randomized CDR3s of anti-VEGFR2 D7 scFvs.

scFv	V_H (DP47)	V_λ (DPL16)
	95 96 97 98 99 100	91 92 93 94 95 96
3B1	K T L W K R	V P Y D P A

4.3.3 Functional characterization of anti-VEGFR-2 D7 scFv 3B1

Inhibition of VEGFR-2 activation by scFv 3B1 was now tested. The functional assay was similar to the one performed with the DARPin inhibitors (see section 3.4.4). PAE-VEGFR-2 cells were incubated with scFv prior to stimulation with 1.5 nM VEGF-A₁₆₅. Western blot analysis was performed with cell lysates to determine receptor activation. Even at concentrations as high as 2.5 μM, scFv 3B1 did not inhibit receptor activation (Fig. 4-4). The affinity of 3B1 to D7 will have to be determined in a competitive ELISA. Affinity maturation of the scFv could be performed to improve binding strength.

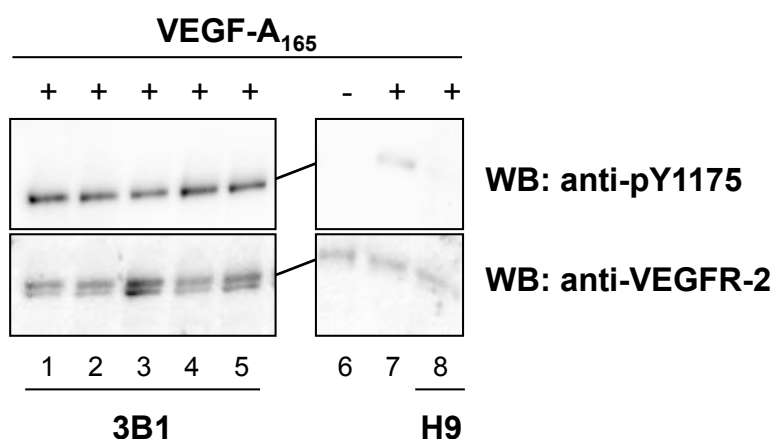


Figure 4-3: ScFvs 3B1 in its current form does not inhibit VEGFR-2 activation.

PAE-VEGFR-2 cells were incubated with increasing concentrations of scFv 3B1 (lane 1-5: 0.1; 0.3; 0.6; 1.2; and 2.5 μM) or H9, a control scFv binding to VEGF-A and blocking its interaction with VEGFR-2 (lane 8) at 37 °C for 30 min. Cells were stimulated with 1.5 nM VEGF-A₁₆₅ at 37 °C for 10 min. Lanes 6 and 7 represent unstimulated and stimulated cells, respectively. These cells were not incubated with any inhibitor. Cell lysates were analysed by Western blot with phospho-specific antibody pY1175 and anti-VEGFR-2 antibody protein.

4.4 Discussion

The fully human synthetic antibody library (ETH-2 Gold Library) (Silacci *et al.*, 2005) was used to select scFvs against the D7 of the VEGFR-2 ECD. I identified scFv (3B1) using phage display which showed specific binding to the VEGFR-2 ECD D7. Preliminary experiments demonstrated the ability of 3B1 to bind VEGFR-2 on PAE cells stably expressing VEGFR-2 but will need to be confirmed. In its current form, the scFv did not inhibit ligand-induced activation of VEGFR-2 in PAE cells. Future experiments could therefore consist in further modifying the successful binder by for example reformatting it into an IgG antibody. This could lead to an increased chance of inhibiting receptor activation caused by the more bulky structure of the IgG while preserving the binding specificity to VEGFR-2 D7 identified in my screen. All scFvs will need further characterization including the determination of their affinity against D7 e.g. in a competitive ELISA assay or by Isothermal Titration Calorimetry. The scFvs may further be tested for inhibition of VEGFR-2 downstream signaling and sprouting assays already discussed in section 3.5 for the DARPins.

5 Novel functional germline variations in the vascular endothelial growth factor receptor 2 gene and their effect on gene expression and microvessel density in lung cancer

The full manuscript can be found in appendix B.

My contribution to this manuscript consisted in performing receptor activation assays with the different VEGFR-2 Single Nucleotide Polymorphisms (SNPs). HEK293 cells were transiently transfected with VEGFR-2 variants, stimulated with VEGF-A₁₆₅, and lysed. Western blot analysis was performed with anti-pTyr1175 and anti-VEGFR-2 antibodies. Amount of VEGFR-2 phosphorylation was quantified and statistically analysed (Fig. 2 in manuscript). Q472H showed a 46% increase in VEGFR-2 phosphorylation after VEGF-A165 stimulation ($p=0.035$).

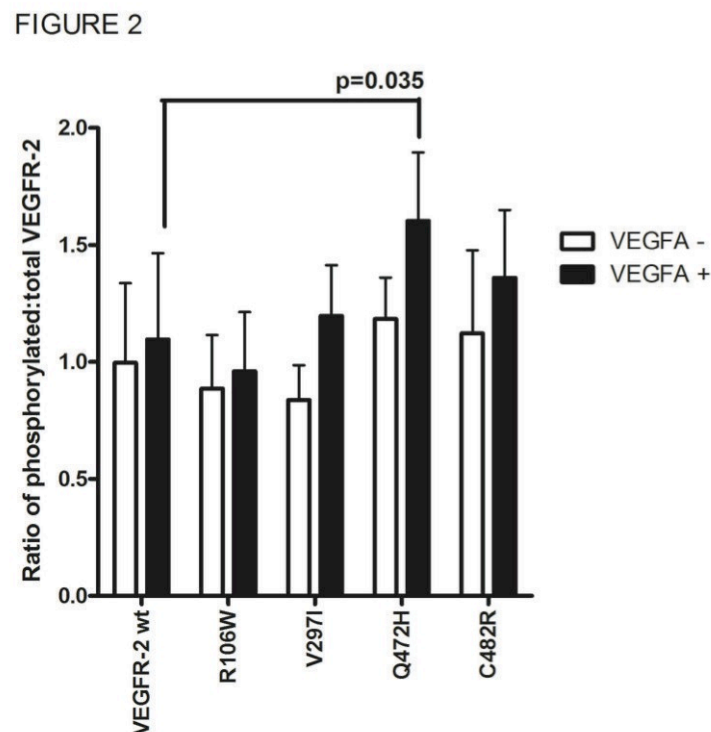


Figure 5-1: VEGFR-2 phosphorylation in HEK293 cells and effect of four non-synonymous variants.

The y axis corresponds to the ratio of phosphorylated VEGFR-2 to total VEGFR-2. Values are normalized to basal phosphorylation levels of reference sequence *KDR*. “-” refers to basal phosphorylation levels and “+” refers to VEGF-A stimulation. Wt = reference sequence cDNA. The mean \pm SEM of 3 experiments in triplicate is shown.

6 Monitoring Migration of Endothelial Cells on Micropatterned Biochips

6.1 Abstract

The vascular endothelial growth factor (VEGF) family consists of six polypeptides, VEGF-A, -B, -C, -D, -E, and PlGF. VEGFs exist as different isoforms which lead to distinct signal output. By specifically binding to type V receptor tyrosine kinases VEGFR-1, -2, and -3 and to coreceptors such as neuropilins, VEGFs regulate blood and lymphatic vessel development that play an important role in cancer development. However, the technologies to monitor these distinct outputs are currently limited. Here we present two methodologies to study VEGF-induced angiogenesis of endothelial cells on micropatterned coverslips that mimic the *in vivo* environment. Immunostaining demonstrates specific VEGF binding to coverslips patterned by “Molecular Assembly Patterning after Lift-Off” or by microfluidics. Immobilized VEGF was biologically active and endothelial cells expressing the receptor for the immobilized ligands migrated towards and adhered to the patterns. The chips present a robust and reproducible system that can be used to further characterize various cellular behaviors generated by multiple VEGF isoforms.

6.2 Introduction

Endothelial cell differentiation and sprouting is influenced by the extracellular matrix (ECM), neighboring cells and matrix-bound and soluble factors. Endothelial cells are capable of detecting slow increases in the local concentration of diffusible factors and are exposed to gradients of ECM-bound growth factors. Taken together, these factors generate the signals promoting cellular motility, proliferation, or differentiation and ultimately lead to the formation of new functional blood vessels.

The most prominent growth factors in angiogenesis are the Vascular Endothelial Growth Factors (VEGFs). VEGFs interact with their target cells through receptor tyrosine kinases (RTKs), the VEGF receptors (VEGFR-1, -2 and -3). Ligand-induced activation of VEGFR-2 leads to intracellular signaling which subsequently mediates proliferation, migration, survival, and permeability of cells. VEGFs exist as many different isoforms which differ in their binding affinity to ECM molecules (Robinson and Stringer, 2001). Heparan sulfate glycosaminoglycans (HSPGs), components of the ECM, are highly sulfated glycosaminoglycan which have the function of storing and protecting growth factors such as VEGF (Folkman and Shing, 1992). VEGF-A₁₆₅ binds to

HSPG via the heparin-binding domain located at the C-terminus whereas VEGF-A₁₂₁ lacks this domain and is therefore soluble. Our laboratory has previously shown that different VEGF isoforms trigger distinct cellular responses (Cébe-Suarez *et al.*, 2008; Cébe-Suarez *et al.*, 2006a). The activation kinetics of VEGFR-2 are prolonged when the receptor is stimulated with matrix-bound VEGF compared to soluble VEGF. Furthermore, it has been recently demonstrated that the pattern of tyrosine phosphorylation is different when cells are stimulated with VEGF-A₁₆₅ compared to VEGF-A₁₂₁ and that the p38 MAPK downstream signaling pathway is enhanced (Chen *et al.*, 2010). However, robust and reproducible techniques for the analysis of differences in cell behavior as a result of cells encountering soluble versus immobilized growth factors still need to be established. Existing technologies for protein immobilization include amine/carboxylic acid chemistry (Mann *et al.*, 2001) (Stefonek-Puccinelli and Masters, 2008), thiol chemistry (Park *et al.*, 2006), and biotin-avidin interactions (Gunawan *et al.*, 2007). However, these approaches often lead to proteins bound in different conformations and orientation which may result in reduced protein activity. A few groups have used the elegant technique of indirectly coupling VEGF via heparin to obtain more uniform immobilization. Maynard *et al.* utilized a heparin-mimicking polymer to nanopattern VEGF (Christman *et al.*, 2008) but did not test the surfaces for cell behavior in this study. Anderson *et al.* bound VEGF covalently as well as electrostatically to a heparin-modified surface (Anderson *et al.*, 2009). Electrostatically and covalently immobilized VEGFs both led to similar levels of receptor phosphorylation. The drawback in this approach is that the VEGF was not micropatterned but present on the entire surface.

Here, we present a study of micropatterned VEGF that can be used for cell studies. In a first approach, we made use of the natural affinity of VEGF-A₁₆₅ to heparin for the binding of VEGF to a patterned surface. This strategy assured the correct positioning and orientation of the growth factor on the surface. For this, we combined the two techniques of micropatterning and indirect coupling via heparin for the site-selective anchoring of VEGF-A₁₆₅. The surfaces allowed us to compare the behavior of cells encountering bound VEGF as opposed to soluble VEGF. To mimic the *in vivo* situation, a second approach consisted in generating a gradient of VEGF employing the technique of microfluidics.

6.3 Materials and Methods

6.3.1 Materials

The two polymers, poly(L-lysine)-graft-poly(ethylene glycol) (PLL-g-PEG) and PLL-g-PEG/PEG-biotin were purchased from SurfaceSolutionS GmbH, Zürich. PLL-g-PEG are composed of a poly-L-lysine backbone of 20 kDa grafted with PEG side chains of 2 kDa. The grafting ratio g indicates the number of lysine monomer units per PEG side chain. In the PLL-g-PEG biotin, 20% of the side chains consist of PEG-biotin (3.4 kDa). PLL-g-PEGs were dissolved in HEPES buffer (10 mM 4-(2-hydroxy-ethyl) piperazine-1-ethane-sulfonic acid and 150 mM NaCl, pH 7.4).

6.3.2 Molecular-Assembly Patterning after Lift-Off

The Molecular-Assembly Patterning after Lift-Off (MAPL) technique combines conventional photolithography and assembly of functional PEG-graft polycationic copolymers on a negatively charged oxide-coated wafer (Falconnet *et al.*, 2004). A 6 nm thick Nb₂O₅ layer was sputtered onto the 12 mm diameter glass coverslips. Photolithography was performed in a cleanroom in which coverslips were spin coated with photoresist, UV-illuminated through a mask containing the desired patterns and developed. After washing and O₂ plasma-treatment for 2 min, coverslips were coated with 100% PLL-g-PEG/PLL-g-PEG biotin (20% of PEG chains biotinylated) (1 mg/ml, for 40 min at RT). Here, adsorption from solution occurs via electrostatic interactions between the positively charged PLL backbone and the negatively charged metal oxide surface. Lift-off of the photoresist was performed using “Microposit Remover 1165”, an organic solvent. Coverslips were rinsed extensively with H₂O and backfilling was performed with non-functionalized PLL-g-PEGs (1 mg/ml, for 40 min at RT). For complex formation, Neutravidin (0.9 μM) was incubated with Heparin-biotin (1.2 μM) for 30 min at RT. The complex was exposed to the biotinylated pattern on the coverslips by incubating for 1h at RT. VEGF-A₁₆₅ or VEGF-A₁₂₁ (24 μg/ml in PBS with 1% BSA) were bound for 1h at RT. Coverslips were washed with PBS and used for immunostainings or for cell experiments.

6.3.3 Microfluidics

Microfluidic channels of 50 μm depth were etched into a silicon wafer using a patterned photoresist mask and anisotropic KOH etching protocols. The wafer was cut into individual microfluidic chips. Each chip had a total of 20 microfluidic channels with channel width ranging from 30 μm to 100 μm . Channel width could be chosen according to needs. Coverslips were overlaid with a thin film of PDMS (Sylgard 184, Down Corning, USA mixed 10:1 (w/w) with curing agent) which was cured for 3h at 70°C. Prior to each use, the chips with the microfluidic channels were cleaned in a UV-Ozone cleaner (Jelight Co. Inc., USA) for 45 minutes. Chips were then placed on the PDMS-coated coverslip with the channels facing downwards. The channels were filled with 4 μl of protein in PBS at a concentration of 100 $\mu\text{g/ml}$. To prevent uncontrolled evaporation of the protein solution within the channels, an excess of protein solution was pipetted to both ends of the channels and the chips were incubated o/n in a humidity chamber at 4°C. The channels were rinsed with PBS by simultaneously pipetting PBS on one side and using a clean room paper on the other side as a flow promoter. The coverslips were separated from the chips and 1% BSA was used to prevent unspecific binding on coverslips. After each use, the chips with the microfluidic channels were rinsed with PBS and ddH₂O and dried under a N₂-stream. Coverslips with the patterned proteins were then used for cell experiments.

6.3.4 Cell culture

Porcine Aortic Endothelial (PAE) cells expressing the Vascular Endothelial Growth Factor Receptor 2 (VEGFR-2) were grown on VEGF-A₁₆₅ patterns for 4h at 37°C. Cells were fixed with 3.7% formaldehyde in PBS for 10 min at RT followed by extensive washing with PBS. Cells were permeabilized with 1% NP40 in PBS for 10 min at RT. Primary antibodies (α -VR2 Sigma V9134 1:300, α -VEGF Sigma 1:100 in PBS) were added o/n at 4°C. Then, coverslips were washed with PBS and incubated with fluorescently-labeled secondary antibodies (α -m-Alexa488 1:250, α -g-Cy3 1:500) for 1h at RT. Samples were washed with PBS before they were embedded in gelvatol (15% gelvatol, 33% glycerol, 0.1% sodium azide). Images were acquired on an Olympus IX81 epifluorescence microscope.

6.4 Results

6.4.1 VEGF Immobilization through Molecular-Assembly Patterning by Lift-Off (MAPL)

The process of photolithography on our glass coverslips was carried out in a cleanroom. The desired pattern was generated on standard glass coverslips. The MAPL technique developed at ETH Zürich (Falconnet *et al.*, 2004) was successfully adapted to the immobilization of VEGF-A₁₆₅ (Fig 6-1).

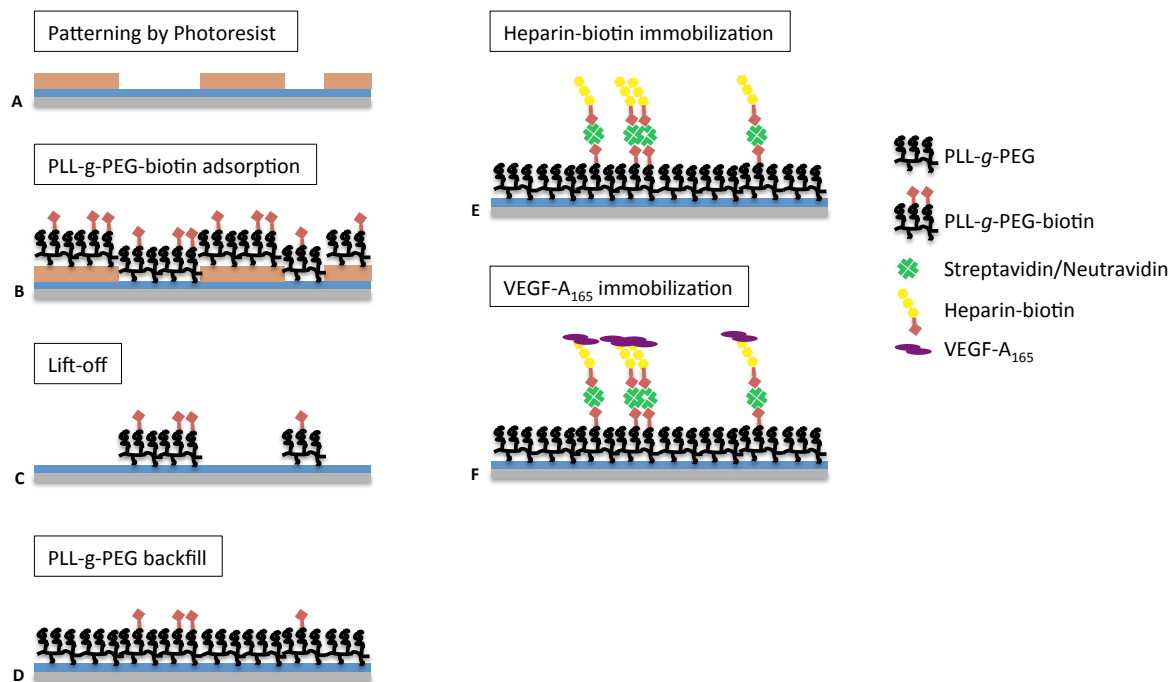


Figure 6-1: Molecular patterning after Lift-Off strategy for the immobilization of VEGF-A₁₆₅.

(A) Photoresist is patterned on niobium-coated coverslips by UV-illumination. (B) PLL-g-PEG-biotin are immobilized by spontaneous assembly. (C) Photoresist is lifted-off. (D) Non-functionalized PLL-g-PEGs are used for the backfill to prevent unspecific protein adsorption. (E) Heparin-biotin preincubated with Neutravidin is bound to the PLL-g-PEG-biotin pattern. F: VEGF-A₁₆₅ binds to Heparin via its heparin-binding domain. Original artwork (inspired by (Sala *et al.*, 2010)).

Using this technology, we created patterns of functionalized PLL-g-PEG-biotin in a nonfouling, protein-resistant PLL-g-PEG background. For backfilling, proteins such as BSA could also be used instead of PLL-g-PEGs to prevent unspecific binding (data not shown). PLL-g-PEG-based copolymers directly conjugated with biotin were used to immobilize Neutravidin. Correct patterning was checked by binding Alexa488-labeled Streptavidin instead of Neutravidin (Fig. 6-2). Patterns ranging from 100 μm thick lines down to 5 μm could be visualized.

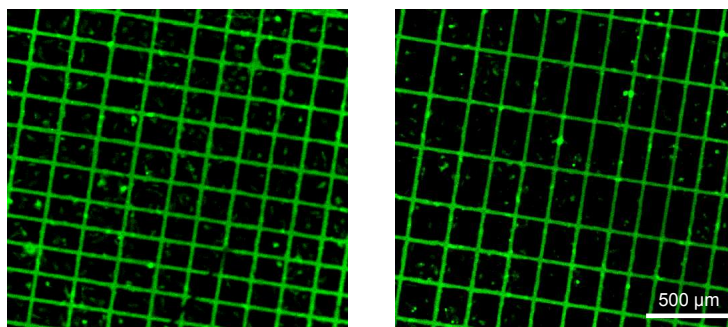


Figure 6-2: Immobilization of Streptavidin-Alexa488 on the PLL-g-PEG biotin pattern produced by MAPL.

Patterned chips were incubated with 50 $\mu\text{g}/\text{ml}$ Streptavidin-Alexa488 for 30 min at RT. The two figures show patterns with different dimensions. Depending on the mask used in the photolithographic process, various patterns could be generated.

Commercially available heparin-biotin was incubated at a predetermined ratio with Neutravidin and the complex was bound to the PLL-g-PEG biotin pattern on the coverslips. Next, we made use of the natural affinity of VEGF-A₁₆₅ to heparin to indirectly couple the protein to patterned surfaces. VEGF-A₁₂₁ which does not have a heparin binding site was used as a negative control. VEGF-A₁₆₅ was immobilized via its heparin-binding domain and the specific immobilization of VEGF to the surfaces was studied by immunostaining (Fig. 6-3). For this, VEGF was visualized with an anti-VEGF antibody specific for both VEGF isoforms, VEGF-A₁₆₅ and -A₁₂₁. The expected pattern could be seen with VEGF-A₁₆₅ showing a strong fluorescence staining whereas VEGF-A₁₂₁ gave a diffuse signal and therefore as expected had not bound specifically to the heparin.

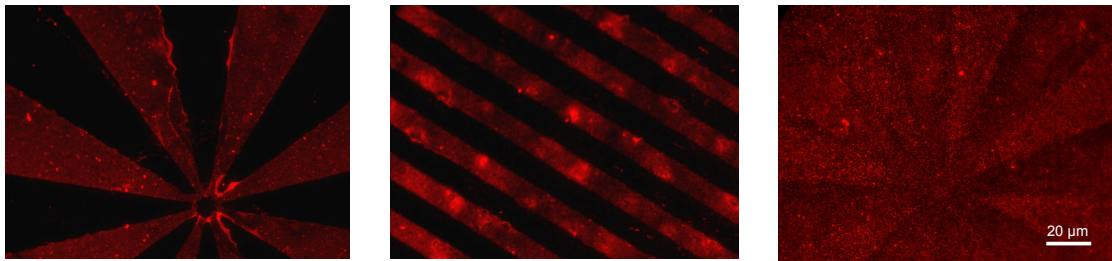


Figure 6-3: Immobilization of VEGF-A₁₆₅ via heparin on the PLL-g-PEG biotin pattern.

Patterned chips were incubated with Heparin-biotin (1.2 μM) preincubated with Neutravidin (0.9 μM). VEGF-A₁₆₅ (left and middle image) or VEGF-A₁₂₁ (right image) was added at a concentration of 24 μg/ml at RT for 1 h and detected with an anti-VEGF antibody. A Cy3-labeled secondary antibody was used.

6.4.2 Cell attachment to immobilized VEGF-A₁₆₅

After having successfully immobilized VEGF, the next step was to check whether VEGF-A₁₆₅ was still biologically active in this form and whether cells expressing VEGFR-2 were able to sense and bind the VEGF. Porcine aortic endothelial cells (PAE) expressing VEGFR-2 were grown on VEGF-A₁₆₅ patterns for 2 h, fixed and immunostained with an anti-VEGFR-2 antibody. PAE cells migrated and divided on the generated micropatterns. Cells preferably attached to the areas where VEGF-A₁₆₅ was immobilized (Fig. 6-4). Many cells that did not adhere directly to the VEGF-A₁₆₅ patterned lines but were found in between the pattern, did not show VEGFR-2 staining, further supporting our hypothesis that cells expressing the VEGFR-2 sense and bind to immobilized VEGF-A₁₆₅. Using live-cell imaging, cells migrating from one patterned line to another could be followed (Fig. 6-5). In a next step it will be important to confirm that PAE-VEGFR-2 cells specifically bind to immobilized VEGF-A₁₆₅ and that this effect is not due to different chemical or physical properties of patterned surfaces. Preliminary experiments have been performed where the surface was pre-incubated with an inhibitor against VEGF-A₁₆₅ blocking its binding to VEGFR-2. On these surfaces, PAE-VEGFR-2 cells should no longer bind the immobilized VEGF.

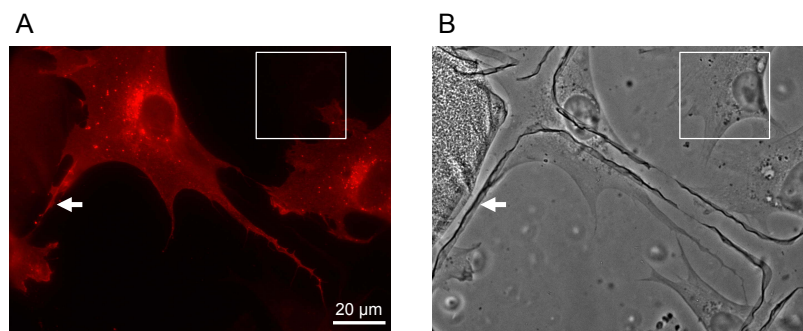


Figure 6-4: PAE-VEGFR-2 cells grown on VEGF-A₁₆₅ patterned coverslips.

Cells were grown on chips for 2h at 37°C, fixed, and (A) visualized with an anti-VEGFR-2 antibody (red) or (B) shown by phase-contrast. Arrows indicate filopodia of PAE-VEGFR-2 cell following patterned VEGF-A₁₆₅. White square highlights a cell not expressing VEGFR-2 which does not adhere to the VEGF derivatized substrate potentially indicating unspecific adherence.

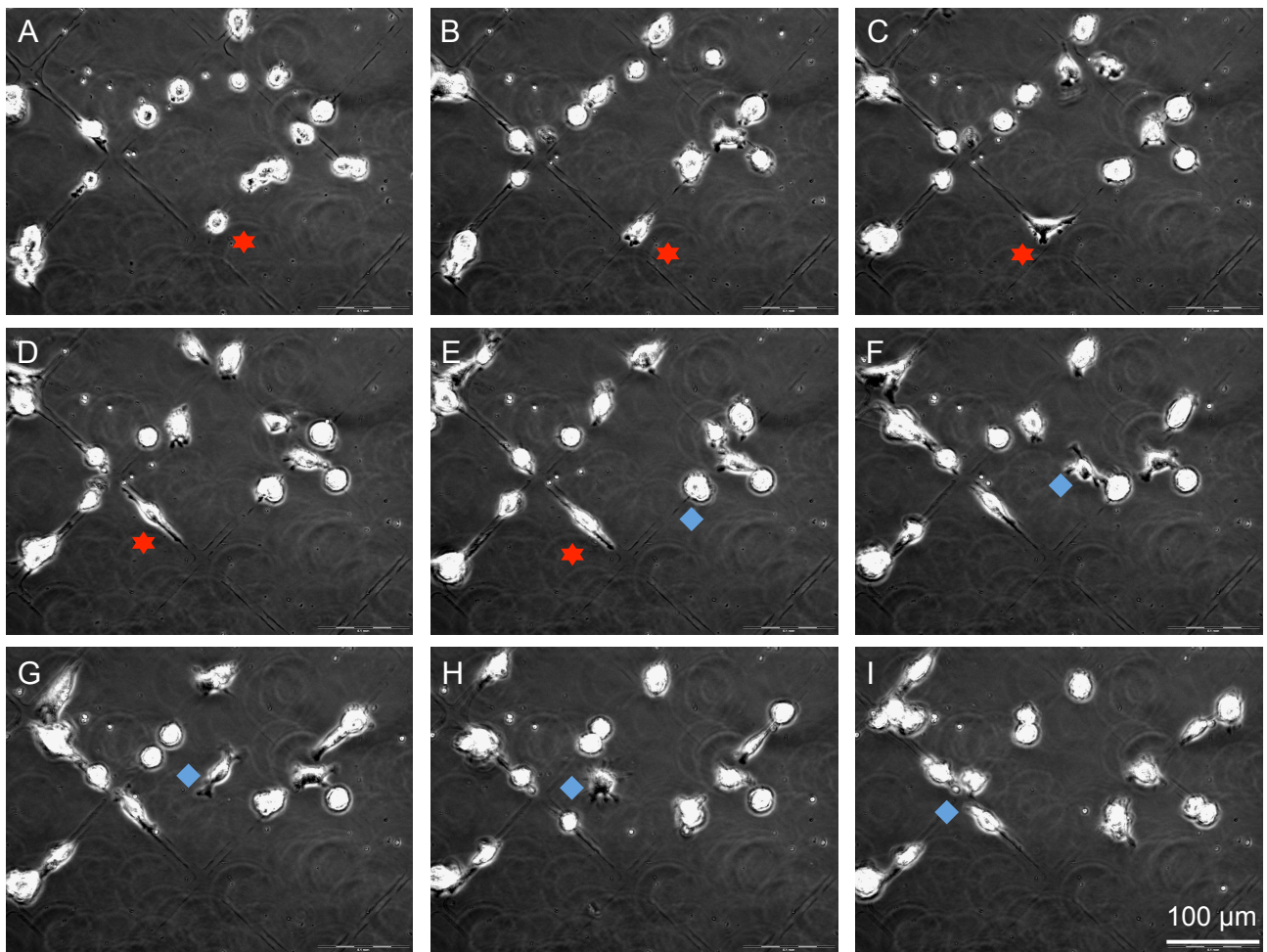


Figure 6-5: Migration of PAE-VEGFR-2 cells on VEGF-A₁₆₅ patterns

Migration of PAE-VEGFR-2 cells on VEGF-A₁₆₅ patterns was monitored over 1.5 h. Figures show nine representative time points (A: 0 min, B: 12 min, C: 24 min, D: 36 min, E: 48 min, F: 60 min, G: 72 min, H: 84 min, I: 96 min). The red star follows a cell spreading onto the pattern and the blue diamond a cell moving from one patterned line diagonally to another patterned line.

6.4.3 Generation of a protein gradient through microfluidics

Reproducing a protein gradient on coverslips would be an elegant way to imitate the gradients of growth factors encountered by endothelial cells *in vivo*. Microfluidics, a technique allowing the manipulation of small volumes of protein solution through channels, seemed the appropriate technique to generate such a gradient. The experiments of VEGF-patterning by microfluidics were performed by my colleague Jörg Ziegler from the Laboratory of Micro- and Nanotechnology at PSI. Polydimethylsiloxane (PDMS) was used as a substrate on the coverslips. It belongs to a group of polymeric organosilicon compounds commonly referred to as silicones. PDMS is used in many applications due to its stability, low surface tension and lack of toxicity. The glass coverslips were covered with a thin film of PDMS which acts as an adhesive substrate and allowed better positioning of the channel-containing silicon dioxide chip on the coverslips. The resulting layer of PDMS is very thin and optically clear and therefore allows imaging of cells through the coated coverslip. Cells showed normal growth behavior on PDMS-coated coverslips. The silicon dioxide chip was placed on the coverslip and protein solution added to both ends of the microfluidic channels (Fig. 6-5). The channels immediately filled with the protein solution due to the capillary pressure. This pressure results from the hydrophilic property of the silicon dioxide and the micrometer sized dimensions of the channels. Channels were rinsed before removal of the silicon dioxide chip from the glass coverslip. The coverslip was then incubated with bovine serum albumin (BSA) to prevent unspecific protein binding. Binding of VEGF-A₁₂₁ or -A₁₆₅ was confirmed by immunofluorescence staining (Fig. 6-6 bottom).

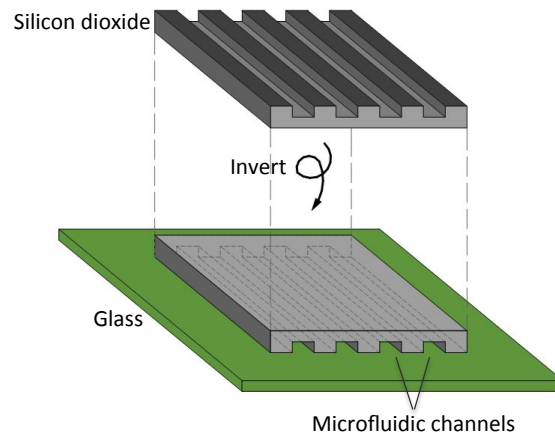


Figure 6-6: Microfluidics strategy for the generation of a VEGF-A gradient on coverslips.

Silicon dioxide chip containing the microfluidic channel was placed on a glass coverslip previously coated with a thin layer of PDMS. Protein solution (100 $\mu\text{g}/\text{ml}$ VEGF-A₁₂₁, -A₁₆₅, or BSA) was placed at the entry of the channels and immediately filled the channels. Channels were rinsed and silicon dioxide chip removed. Coverslips were used for immunofluorescence stainings and cell experiments. Original artwork.

6.4.4 Cell growth on VEGF-A gradients

PAE-VEGFR-2 cells were grown on the surfaces with immobilized VEGF-A₁₂₁, -₁₆₅, or BSA as a control. After 2 h of incubation at 37 °C, cells were fixed. Immobilized VEGF-A₁₂₁ or -₁₆₅ was detected with an anti-VEGF antibody and VEGFR-2 on the cells was visualized with an anti-VEGFR-2 antibody. As expected, cells exclusively attached to the immobilized VEGF-A₁₂₁ and -₁₆₅ and not to the albumin passivated surfaces. Furthermore, a weak gradient of VEGF-A₁₆₅ could be visualized. To enhance this gradient, lower concentrations of protein could be used. Preliminary experiments were carried out with such low amounts of VEGF-A₁₂₁ and -₁₆₅ but will need further investigation. Experiments with inhibitors blocking VEGF-A binding to VEGFR-2 will need to be performed here as described above to confirm that cells bind specifically to the immobilized VEGF-A.

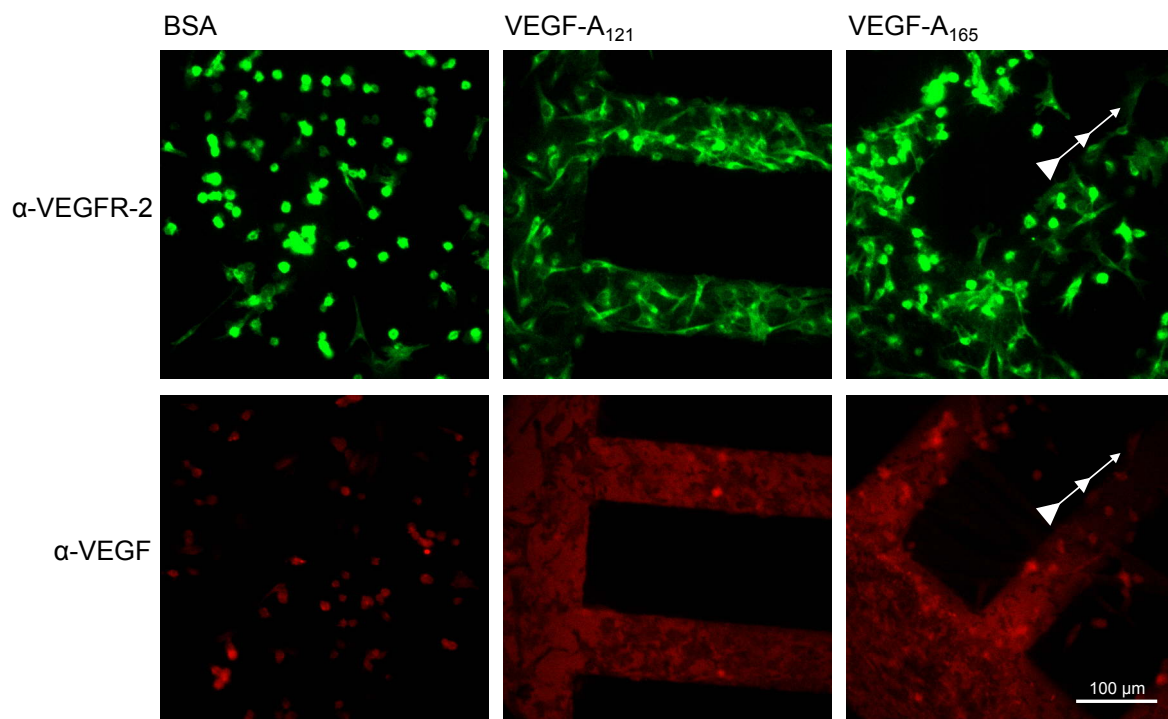


Figure 6-7: PAE-VEGFR-2 cells grown on VEGF-A₁₆₅ gradients.

Microfluidic channels of 80 μm width were used. BSA (left), VEGF-A₁₂₁ (middle), or VEGF-A₁₆₅ (right) was immobilized on the PDMS surface by capillary flow through microfluidic channels. PBS containing 1% BSA was used to block unspecific protein binding. Cells were grown on chips at 37 °C for 2 h, fixed, and stained with an anti-VEGFR-2 antibody. Immobilized VEGF was stained with an anti-VEGF antibody. Arrows indicate VEGF-gradient.

6.5 Discussion

In order to study VEGF signaling in a context reflecting the *in vivo* situation as closely as possible, we generated micropatterned surfaces of VEGF. Bound VEGF will allow us to gain insight into the differences in cell behavior arising from the various VEGF isoforms and elucidate in more details the process of angiogenesis.

Many techniques of protein immobilization result in the immobilized protein being bound through different conformations on the surface and lead to a reduction of protein activity. We made use of the natural affinity of VEGF-A₁₆₅ to HSPG to indirectly immobilize VEGF and in this way to obtain more uniform orientation of the molecules. This approach furthermore allowed us to circumvent the need of biotinylating VEGF, a process that generated an inactive protein (data not shown).

We were able to immobilize VEGF on patterned surfaces using two different techniques which both have their advantages and disadvantages. In the MAPL approach, the indirect coupling of VEGF through immobilization of heparin ensures the correct positioning and orientation of VEGF. This technique is therefore useful to study the different cell responses to bound VEGF-A₁₆₅ versus soluble VEGF-A₁₂₁.

Microfluidic chips on the other hand present the major advantage of allowing the generation of protein gradients. This is achieved by varying the concentration of proteins and/or the flow velocity. The mechanisms by which endothelial cells respond to graded distributions of growth factors are still poorly understood and our gradient-generating system would be well suited to study these. We tried to combine gradient-formation and indirect VEGF-immobilization but encountered problems with the immobilization of heparin on the PDMS-coated coverslips. The problems might be due to the chemical properties of PDMS. After polymerization and cross-linking, PDMS displays an external hydrophobic surface. Plasma oxidation is used to make the surface hydrophilic through the presence of silanol groups (SiOH). Without further modification, the oxidized surfaces have a greater resistance to adsorption of hydrophobic and negatively charged species than unmodified PDMS. This may explain why negatively charged heparin does not bind. Direct binding of VEGF-A₁₂₁ and -A₁₆₅ to PDMS has proven successful.

In both techniques, the growth factor retained its biological activity since cells expressing VEGFR-2 sensed and migrated towards the VEGF-A. We have preliminary indications that migration and attachment of cells is furthermore VEGF gradient-dependent since more cells

attached to areas where the concentration of micropatterned VEGF was higher as seen in double immunofluorescence staining (Fig. 6-6).

The 2 h incubation time for cell attachment did not allow for an extensive study of VEGFR-2 phosphorylation since this event takes place mostly in the first 15-30 min of receptor contact with the growth factor. In a next step, one could therefore consider growing cells on an extra surface before bringing them into contact with the VEGF-pattern (Anderson *et al.*, 2009). PAE cells stably transfected with fluorescently tagged VEGFR-2 could be grown on patterns and used for performing live-cell imaging. This would allow to monitor VEGFR-2 internalization after stimulation and show differences between the signal output and the uptake of soluble VEGF-A₁₂₁ versus bound VEGF-A₁₆₅.

To study VEGF signaling in a cellular model reflecting the situation *in vivo* as closely as possible we will use vessel sprouting assays performed with endothelial cell spheroids. We will investigate the mechanisms responsible for vessel formation by VEGF isoforms. Endothelial cells cultured in standard two-dimensional cell culture lose many of their differentiated phenotypic properties. To overcome these limitations, endothelial cells are cultured as spheroids.

In summary, we have developed microstructured biochips to better investigate the behavior of an endothelial cell encountering soluble or immobilized growth factors. These surfaces reproduce the *in vivo* situation where VEGF is bound to the ECM via HSPG and create a three-dimensional environment mimicking the natural environment of cells. Furthermore, the comparison of cells encountering soluble growth factor with cells being in contact with immobilized growth factor now becomes possible.

7 Conclusions and Outlook

The concept that tumors are dependent on blood vessels surrounding them and the idea that inhibiting the formation of new blood vasculature in cancer might weaken the tumor, arose almost forty years ago. Since then, a variety of angiogenic drugs have been developed and many of them have entered clinical trials. A promising target for anti-angiogenic therapies is VEGFR-2, the main mediator of angiogenic signaling in endothelial cells. VEGFR-2 was also the main object of investigation in my thesis. In a first project, we demonstrated the importance of VEGFR-2 ECD Immunoglobulin-homology domains 4 and 7 for receptor activation. With the help of these new insights into the molecular mechanisms underlying kinase activation, we were able to generate specific and high affinity binders to the ECD of VEGFR-2. We identified a DARPin that binds to D4 and inhibits VEGFR-2 in an allosteric fashion not interfering with ligand-binding.

Potent and high-affinity inhibitors like the identified DARPin 6C8 could have potential in clinical applications such as in tumor vasculature imaging. Imaging in live mice could be carried out with different technologies such as positron emission tomography (PET) or single-photon emission computed tomography (SPECT) using tagged variants of the DARPin. Furthermore, the potential of using the binders as angiogenesis inhibitors *in vivo* can be tested in chorioallantoic membrane (CAM) assays and later in mouse tumour models.

In its current form, our D7-binding scFv does not inhibit ligand-induced VEGFR-2 activation. Future experiments could consist in reformatting the scFv into an IgG antibody and therefore increasing the probability of it inhibiting VEGFR-2 activation. Another possibility would be the bioconjugation of the scFv to drugs for site-specific delivery of these drugs. One could furthermore consider performing a phage display scFv screen against D4 of VEGFR-2 to identify D4 binders. Similarly to our identified D4 DARPin, D4 scFv might lead to allosteric VEGFR-2 inhibition.

In a collaboration project with the Laboratory for Micro and Nanotechnology at PSI, we developed micropatterned biochips mimicking the *in vivo* environment of endothelial cells. Our microstructured biochips present useful tools to better investigate the behavior of an endothelial cell encountering a variety of soluble and matrix-bound growth factors. In a follow-up project, the *in vitro* findings will be supplemented by findings derived from *in silico* modeling of the angiogenesis process. The computational modeling will be performed by the group of Prof. Petros Koumoutsakos from the Department of Computer Science at ETH Zürich (Milde *et al.*, 2008).

8 Abbreviations

ALS	Amyotrophic lateral sclerosis
AMD	Age-related macular degeneration
ATP	Adenosine triphosphate
BSA	Bovine serum albumin
CDR	Complementarity determining region
c-Kit	Stem cell factor receptor
CRC	Colorectal cancer
CSF1	Colony stimulating factor-1
CSF1R	Colony stimulating factor-1 receptor
DARPin	Designed Ankyrin Repeat Protein
DMEM	Dulbecco's modified eagle's medium
<i>E.coli</i>	Escherichia coli
ECD	Extracellular domain
ECM	Extracellular matrix
EF	Enrichment factor
EGF	Epidermal growth factor
EGFR	Epidermal growth factor receptor
EM	Electron microscopy
eNOS	Endothelial nitric oxide synthase
Eph	Ephrin receptor
ELISA	Enzyme-linked immunosorbent assay
ER	Endoplasmic reticulum
ERK	Extracellular signal-regulated kinase
FAK	Focal adhesion kinase
FBS	Fetal bovine serum
FDA	Food and Drug Administration
FGF	Fibroblast growth factor
FGFR	Fibroblast growth factor receptor
Flk-1	Fetal liver kinase-1 = VEGFR-2

Flt-4	Fetal liver kinase-4 = VEGFR-3
HEK293	Human embryonic kidney cells 293
HEK293 Ampho	Human embryonic kidney cells 293 Amphotropic
HIF-1	Hypoxia inducible factor-1
HSPG	Heparan sulfate proteoglycan
IMAC	Immobilized metal ion affinity chromatography
KID	Kinase insert domain
MALS	Multi-angle light scattering
MAPK	Mitogen-activated protein kinase MAPK kinase
MAPL	Molecular-Assembly Patterning after Lift-Off
MEK	MAPK kinase
MWCO	Molecular weight cut off
NaPPi	Sodium pyrophosphate
NCS	Newborne calf serum
Ni-NTA	Nickel-nitrilotriacetic acid
NO	Nitric oxide
Nrp-1/-2	Neuropilin-1/-2
NSCLC	Non-small cell lung cancer
PAK2	p21-activated protein kinase-2
PAE	Porcine aortic endothelial cells
PAO	Phenyl arsine oxide
PBS	Phosphate buffered saline
PCR	Polymerase chain reaction
PDMS	Polydimethylsiloxane
PDGF	Platelet derived growth factor
PDGFR	Platelet derived growth factor receptor
PI3-K	Phosphoinositol-3 kinase
PKC	Protein kinase C
PLC- γ 1	Phospholipase C gamma 1
PIGF	Placenta growth factor
PMSF	Phenylmethylsulfonyl fluoride
pNPP	Para-nitrophenyl phosphate
PTB	Phosphotyrosine binding domain

PVDF	Polyvinylidene fluoride
rpm	Rounds per minute
RTK	Receptor tyrosine kinase
SAPK	Stress activated protein kinase
SCF	Stem cell factor
ScFv	Single-chain variable fragment
SDS-PAGE	Sodium dodecylsulfate polyacryl gel electrophoresis
SH2	Src homology-2 domain
Shb	Src homology-2 protein in beta-cells
SHP1/2	Src homology phosphatase-1/-2
SNP	Single nucleotide polymorphism
sVEGFR	Soluble VEGFR
TK	Tyrosine kinase
TMB	3,3',5,5'-tetramethylbenzidine substrate solution
TMD	Transmembrane domain
TSAD	T cell-specific adaptor
UDM	n-Undecyl- β -D-maltopyranoside
VEGF	Vascular endothelial growth factor
VEGFR	Vascular endothelial growth factor receptor
VPF	Vascular permeability factor / VEGF

9 References

1. Alitalo K, Tammela T, and Petrova TV (2005) Lymphangiogenesis in development and human disease. *Nature*, **438**, 946-953.
2. Anderson SM, Chen TT, Iruela-Arispe ML, and Segura T (2009) The phosphorylation of vascular endothelial growth factor receptor-2 (VEGFR-2) by engineered surfaces with electrostatically or covalently immobilized VEGF. *Biomaterials*.
3. Badache A and Hynes NE (2004) A new therapeutic antibody masks ErbB2 to its partners. *Cancer Cell*, **5**, 299-301.
4. Barleon B, Totzke F, Herzog C, Blanke S, Kremmer E, Siemeister G, Marmé D, and Martiny-Baron G (1997) Mapping of the sites for ligand binding and receptor dimerization at the extracellular domain of the vascular endothelial growth factor receptor FLT-1. *J Biol Chem*, **272**, 10382-10388.
5. Bergers G and Hanahan D (2008) Modes of resistance to anti-angiogenic therapy. *Nat Rev Cancer*, **8**, 592-603.
6. Binz HK, Amstutz P, Kohl A, Stumpp MT, Briand C, Forrer P, Grutter MG, and Pluckthun A (2004) High-affinity binders selected from designed ankyrin repeat protein libraries. *Nat Biotechnol*, **22**, 575-582.
7. Binz HK, Stumpp MT, Forrer P, Amstutz P, and Pluckthun A (2003) Designing repeat proteins: well-expressed, soluble and stable proteins from combinatorial libraries of consensus ankyrin repeat proteins. *J Mol Biol*, **332**, 489-503.
8. Brahimi-Horn C, Berra E, and Pouyssegur J (2001) Hypoxia: the tumor's gateway to progression along the angiogenic pathway. *Trends Cell Biol*, **11**, S32-S36.
9. Brockington A, Lewis C, Wharton S, and Shaw PJ (2004) Vascular endothelial growth factor and the nervous system. *Neuropathol Appl Neurobiol*, **30**, 427-446.
10. Carmeliet P, Dor Y, Herbert JM, Fukumura D, Brusselmans K, Dewerchin M, Neeman M, Bono F, Abramovitch R, Maxwell P, Koch CJ, Ratcliffe P, Moons L, Jain RK, Collen D, and Keshet E (1998) Role of HIF-1alpha in hypoxia-mediated apoptosis, cell proliferation and tumour angiogenesis. *Nature*, **394**, 485-490.

11. Carmeliet P and Jain RK (2000) Angiogenesis in cancer and other diseases. *Nature*, **407**, 249-257.
12. Cébe-Suarez S, Grünewald FS, Jaussi R, Li X, Claesson-Welsh L, Spillmann D, Mercer AA, Prota AE, and Ballmer-Hofer K (2008) Orf virus VEGF-E NZ2 promotes paracellular NRP-1/VEGFR-2 coreceptor assembly via the peptide RPPR. *FASEB J*, **22**, 3078-3086.
13. Cébe-Suarez S, Pieren M, Cariolato L, Arn S, Hoffmann U, Bogucki A, Manlius C, Wood J, and Ballmer-Hofer K (2006a) A VEGF-A splice variant defective for heparan sulfate and neuropilin-1 binding shows attenuated signaling through VEGFR-2. *Cell Mol Life Sci*, **63**, 2067-2077.
14. Cébe-Suarez S, Zehnder-Fjällman AH, and Ballmer-Hofer K (2006b) The role of VEGF receptors in angiogenesis; complex partnerships. *Cell Mol Life Sci*, **63**, 601-615.
15. Celletti FL, Waugh JM, Amabile PG, Brendolan A, Hilfiker PR, and Dake MD (2001) Vascular endothelial growth factor enhances atherosclerotic plaque progression. *Nat Med*, **7**, 425-429.
16. Chen TT, Luque A, Lee S, Anderson SM, Segura T, and Iruela-Arispe ML (2010) Anchorage of VEGF to the extracellular matrix conveys differential signaling responses to endothelial cells. *J Cell Biol*, **188**, 595-609.
17. Christinger HW, Fuh G, de Vos AM, and Wiesmann C (2004) The crystal structure of PlGF in complex with domain 2 of VEGFR1. *J Biol Chem*, **279**, 10382-10388.
18. Christman KL, Vazquez-Dorbatt V, Schopf E, Kolodziej CM, Li RC, Broyer RM, Chen Y, and Maynard HD (2008) Nanoscale growth factor patterns by immobilization on a heparin-mimicking polymer. *J Am Chem Soc*, **130**, 16585-16591.
19. Chung AS, Lee J, and Ferrara N (2010) Targeting the tumour vasculature: insights from physiological angiogenesis. *Nat Rev Cancer*, **10**, 505-514.
20. Ciulla TA and Rosenfeld PJ (2009) Antivascular endothelial growth factor therapy for neovascular age-related macular degeneration. *Curr Opin Ophthalmol*, **20**, 158-165.
21. Cole SP, Campling BG, Atlaw T, Kozbor D, and Roder JC (1984) Human monoclonal antibodies. *Mol Cell Biochem*, **62**, 109-120.
22. Cunningham SA, Arrate MP, Brock TA, and Waxham MN (1997) Interactions of FLT-1 and KDR with phospholipase C α : identification of the phosphotyrosine binding sites. *Biochem Biophys Res Commun*, **240**, 635-639.
23. Dance M, Montagner A, Yart A, Masri B, Audigier Y, Perret B, Salles JP, and Raynal P (2006) The adaptor protein Gab1 couples the stimulation of vascular endothelial growth

- factor receptor-2 to the activation of phosphoinositide 3-kinase. *J Biol Chem*, **281**, 23285-23295.
24. Dell'Era Dosch D and Ballmer-Hofer K (2009) Transmembrane domain-mediated orientation of receptor monomers in active VEGFR-2 dimers. *FASEB J*, **24**, 32-38.
 25. Detmar M (2004) Evidence for vascular endothelial growth factor (VEGF) as a modifier gene in psoriasis. *J Invest Dermatol*, **122**, xiv-xxv.
 26. Doanes AM, Hegland DD, Sethi R, Kovesdi I, Bruder JT, and Finkel T (1999) VEGF stimulates MAPK through a pathway that is unique for receptor tyrosine kinases. *Biochem Biophys Res Commun*, **255**, 545-548.
 27. Ebos JM, Lee CR, Cruz-Munoz W, Bjarnason GA, Christensen JG, and Kerbel RS (2009) Accelerated metastasis after short-term treatment with a potent inhibitor of tumor angiogenesis. *Cancer Cell*, **15**, 232-239.
 28. Falconnet D, Koenig A, Assi T, and Textor M (2004) A combined photolithographic and molecular-assembly approach to produce functional micropatterns for applications in the biosciences. *Advanced Functional Materials*, **14**, 749-756.
 29. Ferrara N, Chen H, Davis ST, Gerber HP, Nguyen TN, Peers D, Chisholm V, Hillan KJ, and Schwall RH (1998) Vascular endothelial growth factor is essential for corpus luteum angiogenesis. *Nat Med*, **4**, 336-340.
 30. Fidler IJ (2000) Angiogenesis and cancer metastasis. *The cancer journal from Scientific American*, **6 Suppl 2**, S134-S141.
 31. Folkman J (1971) Tumor angiogenesis: therapeutic implications. *N Engl J Med*, **285**, 1182-1186.
 32. Folkman J and Shing Y (1992) Control of angiogenesis by heparin and other sulfated polysaccharides. *Adv Exp Med Biol*, **313**, 355-364.
 33. Franklin MC, Carey KD, Vajdos FF, Leahy DJ, de Vos AM, and Sliwkowski MX (2004) Insights into ErbB signaling from the structure of the ErbB2-pertuzumab complex. *Cancer Cell*, **5**, 317-328.
 34. Friedman HS, Prados MD, Wen PY, Mikkelsen T, Schiff D, Abrey LE, Yung WK, Paleologos N, Nicholas MK, Jensen R, Vredenburgh J, Huang J, Zheng M, and Cloughesy T (2009) Bevacizumab alone and in combination with irinotecan in recurrent glioblastoma. *J Clin Oncol*, **27**, 4733-4740.
 35. Geiser M, Cébe R, Drewello D, and Schmitz R (2001) Integration of PCR fragments at any specific site within cloning vectors without the use of restriction enzymes and DNA ligase. *Biotechniques*, **31**, 88-90, 92.

36. Gerber HP, McMurtry A, Kowalski J, Yan M, Keyt BA, Dixit V, and Ferrara N (1998) Vascular endothelial growth factor regulates endothelial cell survival through the phosphatidylinositol 3'-kinase/Akt signal transduction pathway. Requirement for Flk-1/KDR activation. *J Biol Chem*, **273**, 30336-30343.
37. Gerhardt H, Golding M, Fruttiger M, Ruhrberg C, Lundkvist A, Abramsson A, Jeltsch M, Mitchell C, Alitalo K, Shima D, and Betsholtz C (2003) VEGF guides angiogenic sprouting utilizing endothelial tip cell filopodia. *J Cell Biol*, **161**, 1163-1177.
38. Green LL (1999) Antibody engineering via genetic engineering of the mouse: XenoMouse strains are a vehicle for the facile generation of therapeutic human monoclonal antibodies. *J Immunol Methods*, **231**, 11-23.
39. Grünewald FS, Prota AE, Giese A, and Ballmer-Hofer K (2010) Structure-function analysis of VEGF receptor activation and the role of coreceptors in angiogenic signaling. *Biochim Biophys Acta*, **1804**, 567-580.
40. Gunawan RC, King JA, Lee BP, Messersmith PB, and Miller WM (2007) Surface presentation of bioactive ligands in a nonadhesive background using DOPA-tethered biotinylated poly(ethylene glycol). *Langmuir*, **23**, 10635-10643.
41. Hanes J and Pluckthun A (1997) In vitro selection and evolution of functional proteins by using ribosome display. *Proc Natl Acad Sci U S A*, **94**, 4937-4942.
42. Hirakawa S, Brown LF, Kodama S, Paavonen K, Alitalo K, and Detmar M (2007) VEGF-C-induced lymphangiogenesis in sentinel lymph nodes promotes tumor metastasis to distant sites. *Blood*, **109**, 1010-1017.
43. Holmqvist K, Cross MJ, Rolny C, Hägerkvist R, Rahimi N, Matsumoto T, Claesson-Welsh L, and Welsh M (2004) The adaptor protein Shb binds to tyrosine 1175 in the Vascular Endothelial Growth Factor (VEGF) Receptor-2 and regulates VEGF-dependent cellular migration. *J Biol Chem*, **279**, 22267-22275.
44. Hoogenboom HR (1991) Multi-subunit proteins on the surface of filamentous phage: methodologies for displaying antibody (Fab) heavy and light chains. *Nucleic Acids Res*.
45. Hurwitz H (2004) Integrating the Anti-VEGF-A Humanized Monoclonal Antibody Bevacizumab with Chemotherapy in Advanced Colorectal Cancer. *Clin Colorectal Cancer*, **4 Suppl 2**, S62-S68.
46. Huston JS, Levinson D, Mudgett-Hunter M, Tai MS, Novotny J, Margolies MN, Ridge RJ, Bruccoleri RE, Haber E, Crea R, and . (1988) Protein engineering of antibody binding sites: recovery of specific activity in an anti-digoxin single-chain Fv analogue produced in *Escherichia coli*. *Proc Natl Acad Sci U S A*, **85**, 5879-5883.

47. Hyder SM and Stancel GM (1999) Regulation of angiogenic growth factors in the female reproductive tract by estrogens and progestins. *Molecular Endocrinology*, **13**, 806-811.
48. Jain RK (2005) Normalization of tumor vasculature: an emerging concept in antiangiogenic therapy. *Science*, **307**, 58-62.
49. Jain RK, Duda DG, Clark JW, and Loeffler JS (2006) Lessons from phase III clinical trials on anti-VEGF therapy for cancer. *Nat Clin Pract Oncol*, **3**, 24-40.
50. Jurisic G and Detmar M (2009) Lymphatic endothelium in health and disease. *Cell Tissue Res*, **335**, 97-108.
51. Kawasaki K, Watabe T, Sase H, Hirashima M, Koide H, Morishita Y, Yuki K, Sasaoka T, Suda T, Katsuki M, Miyazono K, and Miyazawa K (2008) Ras signaling directs endothelial specification of VEGFR2⁺ vascular progenitor cells. *J Cell Biol*, **181**, 131-141.
52. Kendall RL, Rutledge RZ, Mao X, Tebben AJ, Hungate RW, and Thomas K (1999) Vascular endothelial growth factor receptor KDR tyrosine kinase activity is increased by autophosphorylation of two activation loop tyrosine residues. *J Biol Chem*, **274**, 6453-6460.
53. Kendrew J, Eberlein C, Hedberg B, McDaid K, Smith NR, Weir HM, Wedge SR, Blakey DC, Foltz IN, Zhou J, Kang JS, and Barry ST (2011) An antibody targeted to VEGFR-2 Ig domains 4-7 inhibits VEGFR-2 activation and VEGFR-2 dependent angiogenesis without affecting ligand binding. *Mol Cancer Ther*.
54. Kohler G and Milstein C (1975) Continuous cultures of fused cells secreting antibody of predefined specificity. *Nature*, **256**, 495-497.
55. Krupinski J, Kaluza J, Kumar P, Kumar S, and Wang JM (1994) Role of angiogenesis in patients with cerebral ischemic stroke. *Stroke*, **25**, 1794-1798.
56. Lamalice L, Houle F, and Huot J (2006) Phosphorylation of Tyr1214 within VEGFR-2 triggers the recruitment of Nck and activation of Fyn leading to SAPK2/p38 activation and endothelial cell migration in response to VEGF. *J Biol Chem*.
57. Lamalice L, Houle F, Jourdan G, and Huot J (2004) Phosphorylation of tyrosine 1214 on VEGFR2 is required for VEGF-induced activation of Cdc42 upstream of SAPK2/p38. *Oncogene*, **23**, 434-445.
58. Laramee M, Chabot C, Cloutier M, Stenne R, Holgado-Madruga M, Wong AJ, and Royal I (2007) The scaffolding adapter Gab1 mediates VEGF signaling and is required for endothelial cell migration and capillary formation. *J Biol Chem*, **282**, 7785-7769.
59. Lemmon MA and Ferguson KM (2007) A new twist in the transmembrane signaling toolkit. *Cell*, **130**, 213-215.

60. Leppanen VM, Prota AE, Jeltsch M, Anisimov A, Kalkkinen N, Strandin T, Lankinen H, Goldman A, Ballmer-Hofer K, and Alitalo K (2010) Structural determinants of growth factor binding and specificity by VEGF receptor 2. *Proc Natl Acad Sci USA*, **107**, 2425-2430.
61. Li J, Zhang YP, and Kirsner RS (2003) Angiogenesis in wound repair: angiogenic growth factors and the extracellular matrix. *Microsc Res Tech*, **60**, 107-114.
62. Liekens S, De CE, and Neyts J (2001) Angiogenesis: regulators and clinical applications. *Biochem Pharmacol*, **61**, 253-270.
63. Loges S, Mazzone M, Hohensinner P, and Carmeliet P (2009) Silencing or fueling metastasis with VEGF inhibitors: antiangiogenesis revisited. *Cancer Cell*, **15**, 167-170.
64. Luttun A and Carmeliet P (2003) Soluble VEGF receptor Flt1: the elusive preeclampsia factor discovered? *J Clin Invest*, **111**, 600-602.
65. Mann BK, Schmedlen RH, and West JL (2001) Tethered-TGF-beta increases extracellular matrix production of vascular smooth muscle cells. *Biomaterials*, **22**, 439-444.
66. Marasco WA and Sui J (2007) The growth and potential of human antiviral monoclonal antibody therapeutics. *Nat Biotechnol*, **25**, 1421-1434.
67. Matsumoto T, Bohman S, Dixelius J, Berge T, Dimberg A, Magnusson P, Wang L, Wikner C, Qi JH, Wernstedt C, Wu J, Bruheim S, Mugishima H, Mukhopadhyay D, Spurkland A, and Claesson-Welsh L (2005) VEGF receptor-2 Y951 signaling and a role for the adapter molecule TSA1 in tumor angiogenesis. *EMBO J*, **24**, 2342-2353.
68. Mattheakis LC, Bhatt RR, and Dower WJ (1994) An in vitro polysome display system for identifying ligands from very large peptide libraries. *Proc Natl Acad Sci U S A*, **91**, 9022-9026.
69. McCafferty J, Griffiths AD, Winter G, and Chiswell DJ (1990) Phage antibodies: filamentous phage displaying antibody variable domains. *Nature*, **348**, 552-554.
70. Milde F, Bergdorf M, and Koumoutsakos P (2008) A hybrid model for three-dimensional simulations of sprouting angiogenesis. *Biophys J*, **95**, 3146-3160.
71. Miller K, Wang M, Gralow J, Dickler M, Cobleigh M, Perez EA, Shenkier T, Cella D, and Davidson NE (2007) Paclitaxel plus bevacizumab versus paclitaxel alone for metastatic breast cancer. *N Engl J Med*, **357**, 2666-2676.
72. Nishizuka Y (1984) The role of protein kinase C in cell surface signal transduction and tumour promotion. *Nature*, **308**, 693-698.

73. Nissen NN, Polverini PJ, Koch AE, Volin MV, Gamelli RL, and Di P (1998) Vascular endothelial growth factor mediates angiogenic activity during the proliferative phase of wound healing. *Am J Pathol*, **152**, 1445-1452.
74. Olsson AK, Dimberg A, Kreuger J, and Claesson-Welsh L (2006) VEGF receptor signalling - in control of vascular function. *Nat Rev Mol Cell Biol*, **7**, 359-371.
75. Ortega S, Ittmann M, Tsang SH, Ehrlich M, and Basilico C (1998) Neuronal defects and delayed wound healing in mice lacking fibroblast growth factor 2. *Proc Natl Acad Sci U S A*, **95**, 5672-5677.
76. Paez-Ribes M, Allen E, Hudock J, Takeda T, Okuyama H, Vinals F, Inoue M, Bergers G, Hanahan D, and Casanovas O (2009) Antiangiogenic therapy elicits malignant progression of tumors to increased local invasion and distant metastasis. *Cancer Cell*, **15**, 220-231.
77. Pajusola K, Aprelikova O, Korhonen J, Kaipainen A, Pertovaara L, Alitalo R, and Alitalo K (1992) FLT4 receptor tyrosine kinase contains seven immunoglobulin-like loops and is expressed in multiple human tissues and cell lines. *Cancer Res*, **52**, 5738-5743.
78. Paleolog EM (2002) Angiogenesis in rheumatoid arthritis. *Arthritis Res*, **4 Suppl 3**, S81-S90.
79. Park TJ, Lee SY, Lee SJ, Park JP, Yang KS, Lee KB, Ko S, Park JB, Kim T, Kim SK, Shin YB, Chung BH, Ku SJ, Kim dH, and Choi IS (2006) Protein nanopatterns and biosensors using gold binding polypeptide as a fusion partner. *Anal Chem*, **78**, 7197-7205.
80. Pasqualini R and Arap W (2004) Hybridoma-free generation of monoclonal antibodies. *Proc Natl Acad Sci U S A*, **101**, 257-259.
81. Pini A, Viti F, Santucci A, Carnemolla B, Zardi L, Neri P, and Neri D (1998) Design and use of a phage display library. Human antibodies with subnanomolar affinity against a marker of angiogenesis eluted from a two-dimensional gel. *J Biol Chem*, **273**, 21769-21776.
82. Presta LG, Chen H, Connor SJ, Chisholm V, Meng YG, Krummen L, Winkler M, and Ferrara N (1997) Humanization of an anti-vascular endothelial growth factor monoclonal antibody for the therapy of solid tumors and other disorders. *Cancer Res*, **57**, 4593-4599.
83. Reichert JM, Rosensweig CJ, Faden LB, and Dewitz MC (2005) Monoclonal antibody successes in the clinic. *Nat Biotechnol*, **23**, 1073-1078.
84. Riechmann L, Clark M, Waldmann H, and Winter G (1988) Reshaping human antibodies for therapy. *Nature*, **332**, 323-327.
85. Robinson CJ and Stringer SE (2001) The splice variants of vascular endothelial growth factor (VEGF) and their receptors. *J Cell Sci*, **114**, 853-865.

86. Ruch C, Skiniotis G, Steinmetz MO, Walz T, and Ballmer-Hofer K (2007) Structure of a VEGF-VEGF receptor complex determined by electron microscopy. *Nat Struct Mol Biol*, **14**, 249-250.
87. Sala A, Ehrbar M, Trentin D, Schoenmakers RG, Voros J, and Weber FE (2010) Enzyme mediated site-specific surface modification. *Langmuir*, **26**, 11127-11134.
88. Sandler A (2007) Bevacizumab in non small cell lung cancer. *Clin Cancer Res*, **13**, s4613-s4616.
89. Schlessinger J and Lemmon MA (2003) SH2 and PTB domains in tyrosine kinase signaling. *Sci STKE*, **2003**, RE12.
90. Schmidt A, Brixius K, and Bloch W (2007) Endothelial precursor cell migration during vasculogenesis. *Circ Res*, **101**, 125-136.
91. Shalaby F, Rossant J, Yamaguchi TP, Gertsenstein M, Wu XF, Breitman ML, and Schuh AC (1995) Failure of blood-island formation and vasculogenesis in Flk-1- deficient mice. *Nature*, **376**, 62-66.
92. Shams N and Ianchulev T (2006) Role of vascular endothelial growth factor in ocular angiogenesis. *Ophthalmol Clin North Am*, **19**, 335-344.
93. Shepard DR and Garcia JA (2009) Toxicity associated with the long-term use of targeted therapies in patients with advanced renal cell carcinoma. *Expert Rev Anticancer Ther*, **9**, 795-805.
94. Shibuya M and Claesson-Welsh L (2005) Signal transduction by VEGF receptors in regulation of angiogenesis and lymphangiogenesis. *Exp Cell Res*, **312**, 549-560.
95. Shibuya M, Yamaguchi S, Yamane A, Ikeda T, Tojo A, Matsushime H, and Sato M (1990) Nucleotide sequence and expression of a novel human receptor- type tyrosine kinase gene (flt) closely related to the fms family. *Oncogene*, **5**, 519-524.
96. Shinkai A, Ito M, Anazawa H, Yamaguchi S, Shitara K, and Shibuya M (1998) Mapping of the sites involved in ligand association and dissociation at the extracellular domain of the kinase insert domain-containing receptor for vascular endothelial growth factor. *J Biol Chem*, **273**, 31283-31288.
97. Shiojima I, Sato K, Izumiya Y, Schiekofer S, Ito M, Liao R, Colucci WS, and Walsh K (2005) Disruption of coordinated cardiac hypertrophy and angiogenesis contributes to the transition to heart failure. *J Clin Invest*, **115**, 2108-2118.
98. Silacci M, Brack S, Schirru G, Marlind J, Ettore A, Merlo A, Viti F, and Neri D (2005) Design, construction, and characterization of a large synthetic human antibody phage display library. *Proteomics*, **5**, 2340-2350.

99. Spratlin J (2011) Ramucirumab (IMC-1121B): Monoclonal Antibody Inhibition of Vascular Endothelial Growth Factor Receptor-2. *Curr Oncol Rep*, **13**, 97-102.
100. Starovasnik MA, Christinger HW, Wiesmann C, Champe MA, de Vos AM, and Skelton NJ (1999) Solution structure of the VEGF-binding domain of Flt-1: comparison of its free and bound states. *J Mol Biol*, **293**, 531-544.
101. Stefonek-Puccinelli TJ and Masters KS (2008) Co-immobilization of gradient-patterned growth factors for directed cell migration. *Ann Biomed Eng*, **36**, 2121-2133.
102. Stumpp MT and Amstutz P (2007) DARPins: a true alternative to antibodies. *Curr Opin Drug Discov Devel*, **10**, 153-159.
103. Stumpp MT, Binz HK, and Amstutz P (2008) DARPins: a new generation of protein therapeutics. *Drug Discov Today*, **13**, 695-701.
104. Takahashi T, Ueno H, and Shibuya M (1999) VEGF activates protein kinase C-dependent, but Ras-independent Raf-MEK-MAP kinase pathway for DNA synthesis in primary endothelial cells. *Oncogene*, **18**, 2221-2230.
105. Tao Q, Backer MV, Backer JM, and Terman BI (2001) Kinase insert domain receptor (kdr) extracellular immunoglobulin-like domains 4-7 contain structural features that block receptor dimerization and vascular endothelial growth factor-induced signaling. *J Biol Chem*, **276**, 21916-21923.
106. Terman BI, Carrion ME, Kovacs E, Rasmussen BA, Eddy RL, and Shows TB (1991) Identification of a new endothelial cell growth factor receptor tyrosine kinase. *Oncogene*, **6**, 1677-1683.
107. Tjandra JJ, Ramadi L, and McKenzie IF (1990) Development of human anti-murine antibody (HAMA) response in patients. *Immunol Cell Biol*, **68 (Pt 6)**, 367-376.
108. Traxler P (2003) Tyrosine kinases as targets in cancer therapy - successes and failures. *Expert Opin Ther Targets*, **7**, 215-234.
109. Tvorogov D, Anisimov A, Zheng W, Leppanen VM, Tammela T, Laurinavicius S, Holnthoner W, Helotera H, Holopainen T, Jeltsch M, Kalkkinen N, Lankinen H, Ojala PM, and Alitalo K (2010) Effective Suppression of Vascular Network Formation by Combination of Antibodies Blocking VEGFR Ligand Binding and Receptor Dimerization. *Cancer Cell*, **18**, 630-640.
110. Wiesmann C, Fuh G, Christinger HW, Eigenbrot C, Wells JA, and de Vos AM (1997) Crystal structure at 1.7 Å resolution of VEGF in complex with domain 2 of the Flt-1 receptor. *Cell*, **91**, 695-704.

111. Willett CG, Boucher Y, di TE, Duda DG, Munn LL, Tong RT, Chung DC, Sahani DV, Kalva SP, Kozin SV, Mino M, Cohen KS, Scadden DT, Hartford AC, Fischman AJ, Clark JW, Ryan DP, Zhu AX, Blaszkowsky LS, Chen HX, Shellito PC, Lauwers GY, and Jain RK (2004) Direct evidence that the VEGF-specific antibody bevacizumab has antivascular effects in human rectal cancer. *Nat Med*, **10**, 145-147.
112. Winter G, Griffiths AD, Hawkins RE, and Hoogenboom HR (1994) Making antibodies by phage display technology. *Annu Rev Immunol*, **12**, 433-455.
113. Wu LW, Mayo LD, Dunbar JD, Kessler KM, Baerwald MR, Jaffe EA, Wang D, Warren RS, and Donner DB (2000a) Utilization of distinct signaling pathways by receptors for vascular endothelial cell growth factor and other mitogens in the induction of endothelial cell proliferation. *J Biol Chem*, **275**, 5096-5103.
114. Wu LW, Mayo LD, Dunbar JD, Kessler KM, Ozes ON, Warren RS, and Donner DB (2000b) VRAP is an adaptor protein that binds KDR, a receptor for vascular endothelial cell growth factor. *J Biol Chem*, **275**, 6059-6062.
115. Yang AD, Bauer TW, Camp ER, Somcio R, Liu W, Fan F, and Ellis LM (2005) Improving delivery of antineoplastic agents with anti-vascular endothelial growth factor therapy. *Cancer*.
116. Yang Y, Xie P, Opatowsky Y, and Schlessinger J (2010) Direct contacts between extracellular membrane-proximal domains are required for VEGF receptor activation and cell signaling. *Proc Natl Acad Sci USA*, **107**, 1906-1911.
117. Yang Y, Yuzawa S, and Schlessinger J (2008) Contacts between membrane proximal regions of the PDGF receptor ectodomain are required for receptor activation but not for receptor dimerization. *Proc Natl Acad Sci USA*, **105**, 7681-7686.
118. Yuzawa S, Opatowsky Y, Zhang Z, Mandiyan V, Lax I, and Schlessinger J (2007) Structural Basis for Activation of the Receptor Tyrosine Kinase KIT by Stem Cell Factor. *Cell*, **130**, 323-334.
119. Zahnd C, Amstutz P, and Pluckthun A (2007) Ribosome display: selecting and evolving proteins in vitro that specifically bind to a target. *Nat Methods*, **4**, 269-279.
120. Zahnd C, Spinelli S, Luginbuhl B, Amstutz P, Cambillau C, and Pluckthun A (2004) Directed in vitro evolution and crystallographic analysis of a peptide-binding single chain antibody fragment (scFv) with low picomolar affinity. *J Biol Chem*, **279**, 18870-18877.

10 Acknowledgements

First of all I would like to thank Kurt Ballmer-Hofer for giving me the great opportunity to do my PhD in his group on this very interesting topic. I am grateful for his constant support and the valuable advices and I very much admire his positive and motivating attitude.

I would like to express my thanks to Thérèse Resink for being part of my PhD committee and for her helpful advices as well as the pleasant atmosphere during our annual committee meetings.

Special thanks go to Celestino Padeste for introducing me to the fascinating world of microtechnology. Celestino gave me the possibility to work in a cleanroom, a very special and unique experience for me.

A big thank you to all my colleagues at BMR and especially to all the present and former members of Kurt's group: Anja, Sandro, Eddi, Kathi, Thomas, Kaisa, Philipp, Nathalie, Sandra, Caroline, Pascale, Debbi, Maurice, Andreas, Nadia, Petra, Bea. You all created such a pleasant working atmosphere which I enjoyed very much. I also like to think back to the very pleasant afternoons we PhDs spent in Basel during and after our Signaling lecture. And I am really happy that so many of my colleagues have now become very good friends of mine.

I would like to thank Eddi for our great collaboration on the DARPin project. I really enjoyed working with you. Sandro, you were the greatest lab colleague ever, I will always keep our lab atmosphere in very good memory. Kaisa, thanks for being the most reliable coffee-break colleague and Kathi thanks for the great laughs in the cell culture.

Thanks a lot to Ulla, Antonietta, and Nathalie for amongst other things keeping the labs running.

Thomas Schleier and the students Beata Biri and Natalie Fahrer helped me a lot in all the experimental work, thank you for that. Bea, I really enjoyed the time you spent with us at PSI.

Many thanks go to Jörg Ziegler, Bianca Haas, and Christine Scossa from the Laboratory for Nano and Microtechnology for all the micropatterned chips and experimental support.

I thank Kaspar Binz and Johan Abram from Molecular Partners AG Schlieren for the very fruitful collaboration on the DARPin project.

I would like to thank Eliane Fischer and Evelyne Furger from the Center for Radiopharmaceutical Sciences for introducing me to the field of phage display. Evelyne, I would have been really lost without your great protocols.

Meiner lieben Elena möchte ich für die ganze Unterstützung, die vielen Gespräche, die lustigen Zugfahrten, die tollen Kaffeepausen danken. Ich bin so froh, dass ich dich kennenlernen durfte.

Anja, vielen Dank für unsere tolle Freundschaft die mir sehr viel bedeutet. Ich bin wirklich begeistert von deiner offenen und positiven Art.

J'aimerais remercier Sophie pour notre superbe amitié, merci pour tout ton soutien, ton énergie, ton humour...

And I owe my greatest thanks to my family and Tom, thank you so much for your endless support, your patience, and your great help in so many different ways. And thank you for always being there for me...

11 List of Publications

- I. Grünewald FS, Prota AE, **Giese A**, and Ballmer-Hofer K (2010) Structure-function analysis of VEGF receptor activation and the role of coreceptors in angiogenic signaling. *Biochim Biophys Acta*, **1804**, 567-580. See appendix A.
- II. Glubb DM, Cerri E, **Giese A**, Zhang W, Mirza O, Thompson EE, Chen P, Das S, Jassem J, Rzyman W, Lingen MW, Salgia R, Hirsch FR, Dziadziuszko R, Ballmer-Hofer K, Innocenti F (2011) Novel functional germline variants in the vascular endothelial growth factor receptor 2 gene (KDR) and their effect on gene expression and microvessel density in lung cancer. *Clinical Cancer Research* (2011). doi:10.1158/1078-0432.CCR-11-0379
See appendix B.
- III. **Giese A**, Padeste C, and Ballmer-Hofer K (2010) Monitoring Vessel Formation of Endothelial Cells on Micropatterned Biochips. *European Cells and Materials*, **20**, Suppl. 3, 90, ISSN 1474-2262. See appendix C.
- IV. **Giese A**, Stuttfeld E, Binz K, and Ballmer-Hofer K (2011) Inhibition of receptor activation by Designed Ankyrin Repeat Proteins specific for the Ig-homology domain 4 of VEGFR-2 extracellular domain. *Manuscript in preparation*.

12 Curriculum Vitae

13 APPENDIX A



Review

Structure–function analysis of VEGF receptor activation and the role of coreceptors in angiogenic signaling

Felix S. Grünewald, Andrea E. Prota, Alexandra Giese, Kurt Ballmer-Hofer*

Paul Scherrer Institut, Biomolecular Research, 5232 Villigen PSI, Switzerland

ARTICLE INFO

Article history:

Received 25 June 2009

Received in revised form 22 August 2009

Accepted 4 September 2009

Available online 15 September 2009

Keywords:

VEGF

Angiogenesis

Neuropilin

Receptor tyrosine kinase

ABSTRACT

Vascular endothelial growth factors (VEGFs) constitute a family of six polypeptides, VEGF-A, -B, -C, -D, -E and PlGF, that regulate blood and lymphatic vessel development. VEGFs specifically bind to three type V receptor tyrosine kinases (RTKs), VEGFR-1, -2 and -3, and to coreceptors such as neuropilins and heparan sulfate proteoglycans (HSPG). VEGFRs are activated upon ligand-induced dimerization mediated by the extracellular domain (ECD). A study using receptor constructs carrying artificial dimerization-promoting transmembrane domains (TMDs) showed that receptor dimerization is necessary, but not sufficient, for receptor activation and demonstrates that distinct orientation of receptor monomers is required to instigate transmembrane signaling. Angiogenic signaling by VEGF receptors also depends on cooperation with specific coreceptors such as neuropilins and HSPG. A number of VEGF isoforms differ in binding to coreceptors, and ligand-specific signal output is apparently the result of the specific coreceptor complex assembled by a particular VEGF isoform. Here we discuss the structural features of VEGF family ligands and their receptors in relation to their distinct signal output and angiogenic potential.

© 2009 Elsevier B.V. All rights reserved.

1. Biology of VEGF family growth factors and their receptors

1.1. Introduction to VEGF

Vascular endothelial growth factors, VEGFs, were originally discovered as vascular permeability factor, VPF, an activity released by tumor cells that promotes vascular leakage [1]. It is now clear that VPF represented a biological activity attributable to a family of polypeptide growth factors that are encoded by several genes regulating blood and lymph vessel formation during embryonic development, in wound healing, and in maintaining vessel homeostasis in adult organisms. Excess or reduced production of VEGF results in imbalanced formation of blood or lymphatic vessels and causes many human diseases. VEGFs specifically interact with hematopoietic and endothelial precursor cells such as angioblasts, and with differentiating and mature endothelial cells.

Mammalian VEGF-A, -B, -C and placenta growth factor (PlGF) are required for blood vessel formation while VEGF-C and -D regulate the formation of lymphatic vessels [2,3]. In addition, orf family parapoxviruses encode VEGF-A homologues called VEGF-E, which show a high degree of structural identity with VEGF-A [4–6]. Despite only 25–35% amino acid sequence identity with VEGF-A they bind with comparable affinity to VEGFR-2 [7–9]. Moreover, VEGF-E family members lack a heparin binding domain and vary in their abilities

to bind neuropilins [7,8]. Several VEGF-like proteins, now called VEGF-F, have also been isolated from snake venoms and reported to have biological activity similar to VEGF-A₁₆₅ [10,11]. Vammin and VR-1 from the venoms of *Vipera ammodytes ammodytes* (Western sand viper) and *Daboia russelli russelli* (Russell's viper), which share ~50% amino acid sequence identity with VEGF-A₁₆₅, strongly stimulate proliferation of vascular endothelial cells *in vitro* and induce arterial hypotension in rats. Another VEGF-F variant from *Trimeresurus flavoviridis* snake venom, Tj_{sv}-VEGF, efficiently promotes vascular permeability similar to VEGF-A₁₆₅, while stimulation of endothelial cell proliferation by Tj_{sv}-VEGF is negligible [12].

Proteolytic processing and alternative splicing give rise to a wide variety of VEGF isoforms with distinct biological activities [13,14]. Fig. 1 shows a schematic representation of the most common splice variants of VEGF-A. All isoforms contain exons 1–5 and either exon 8a or 8b. A 26 amino acid signal sequence (exon 1 plus 4 amino acids of exon 2) is cleaved off during secretion. The VEGFR-1 and -2 binding domain consists of amino acids 1–109 and the VEGFR interaction sites are located at opposite poles of the dimeric molecule [15,16].

Variable combinations of exons 6–8 encode additional basic sequences that mediate binding to heparan sulfate (HS) and which can be released from full length VEGFs by plasmin cleavage [17]. Exon 6a, present only in VEGF-A₂₀₆, 189, 162, 145 and partially in VEGF-A₁₈₃, is a highly basic stretch of 24 amino acids that confers binding to HS and, as shown for VEGF-A₁₄₅, to components of the extracellular matrix of corneal endothelial cells distinct from HS [18]. Exon 6b has so far only been identified in the less well characterized VEGF-A₁₆₂ and in the longest isoform, VEGF-A₂₀₆. VEGF-A₁₆₅, 183, 189 and 206

* Corresponding author. Tel.: +41 56 310 4165.

E-mail address: kurt.ballmer@psi.ch (K. Ballmer-Hofer).URL: <http://mcb.web.psi.ch> (K. Ballmer-Hofer).

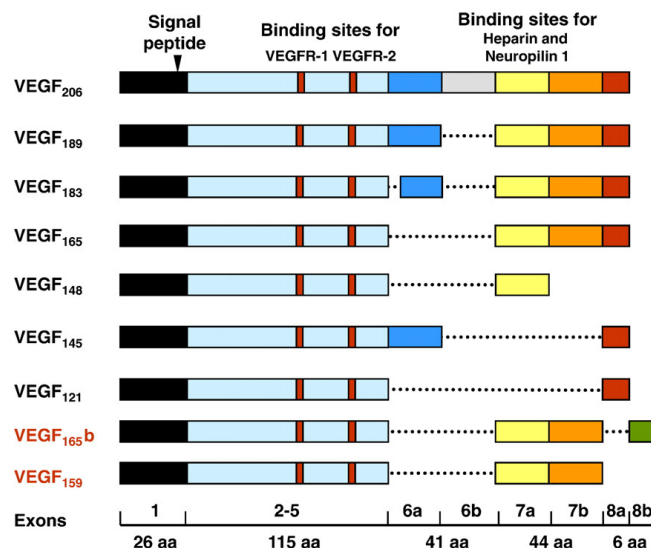


Fig. 1. Schematic representation of selected VEGF-A variants as discussed in the text.

contain an additional sequence encoded by exon 7 that also confers HS binding due to its basic properties and thus limits ligand diffusibility in tissues. The different HS binding affinities conferred by exons 6 and 7 result in specific spatial distribution of the different isoforms. VEGF-A₁₈₉ and VEGF-A₂₀₆ bind HS with high affinity through their exon 6a and 7 encoded basic stretches. Consequently, they remain tightly bound to the ECM, but can be released by cleavage with plasmin, urokinase or matrix metalloproteases [14,19–21] or by disruption of the HS matrix with heparinase [19]. VEGF-A₁₄₅ [18] and VEGF-A₁₆₅ have intermediary affinity to the ECM, while VEGF-A₁₂₁, lacking exons 6 and 7, is freely diffusible [19].

All VEGF-As, except VEGF-A₁₄₈, end with either exon 8a or 8b. Alternative splicing of exon 8 results in the formation of two families of proteins of identical length but differing in the carboxyterminal six amino acids. Exon 8a encodes the amino acids SLTRKD-COOH in place of the exon 8a sequence CDKPRR-COOH [22]. VEGF-A_{165b}, the first member of the VEGF_{xxx}b family to be described, was found to be present in normal tissue from kidney, but was not expressed by malignant tumor cells [22]. Additional members of the VEGF_{xxx}b family identified so far include VEGF-A_{121b}, VEGF_{145b}, VEGF-A_{189b} and unspecified larger isoforms [23] as well as VEGF-A_{183b} [24]. It is now clear that proteins of the VEGF_{xxx}b family make up a major fraction of VEGF-A in most normal tissues [22,24–26], whereas their expression is negligible in cancer cells [23,27,28]. At the molecular level, the anti-angiogenic effects of the VEGF_{xxx}b proteins can to a large extent be ascribed to reduced signaling via VEGFR-2 [23]. These isoforms are partial receptor agonists and, when coexpressed with exon 8a proteins, may exert an inhibitory function by competition for receptor binding. Interestingly, neither exon 8a nor 8b is required for binding to VEGFR-1 or -2 [23,29] and both isoforms bind to VEGF receptors with similar affinities and compete for binding to endothelial cells and to immobilized VEGFR-2 *in vitro* [23]. VEGF-A₁₅₉, an artificially created truncated mutant of VEGF-A₁₆₅ lacking exon 8, retains VEGFR-1 and -2 binding. In contrast to VEGF-A_{165b}, this mutant does not inhibit angiogenesis in matrigel [29] suggesting that competitive inhibition of VEGFR-2 binding does not fully account for the anti-angiogenic effect mediated by VEGF-A_{165b}. Taken together, we propose that the exon 8b isoforms of VEGF-A are partial

receptor agonists capable to elicit some of the signal output of VEGFRs such as for instance anti-apoptotic signaling or vessel permeabilization (for details see also section 2.4.) [26,30].

The complex interplay of VEGF family proteins with VEGF receptors and coreceptors is strictly required for shaping and maintaining the functionality of blood vessels. Correct spatial distribution of specific VEGF isoforms by differential ECM adherence [31] and the coordinated signal output initiated by distinct VEGFs are central for proper vessel organization.

1.2. Receptor specificity of VEGF

The biological functions of VEGF polypeptides result from binding to several cellular receptors: type V receptor tyrosine kinases (RTKs) such as VEGFR-1 (Flt-1), VEGFR-2 (KDR/Flk-1) and VEGFR-3 (Flt-4) [32–34], neuropilin-1 and -2 (NRP-1, -2) [35] and heparan sulfate proteoglycans (HSPG) [36]. Some VEGFs interact with multiple receptors while others show very specific receptor binding properties. PlGF and VEGF-B are specific for VEGFR-1 [37,38], VEGF-Es bind VEGFR-2 [4–6], and VEGF-C and -D bind VEGFR-2 and -3 [2,3]. Additional VEGF homologues were found in snake venoms collectively designated VEGF-F, the seventh member of the VEGF family [10]. VEGF-Fs bind to VEGFR-2 with dissociation constants similar to VEGF-A₁₆₅, but not to VEGFR-1, VEGFR-3 or NRP-1. More recently, a novel VEGF-like protein from the *Trimeresurus flavoviridis* snake venom (*Tfsv*-VEGF) with significantly different characteristics was described. *Tfsv*-VEGF strongly binds to VEGFR-1, but only weakly associates with VEGFR-2 [12].

In addition, VEGF-A splice variants show distinct binding patterns to coreceptors such as HSPG and neuropilins. In all VEGF-A variants exons 2–5 determine the specificity for VEGF RTKs 1–3 while exons 6 and/or 7 and 8 determine coreceptor binding. VEGFs can simultaneously bind two distinct receptors such as VEGFR-2 and neuropilin even when these receptors are expressed separately on adjacent cells [39]. This might be required for promoting endothelial cell migration and cell guidance, for instance, when vessels form along tracks defined by neural cells [40,41] or during endothelial tip cell guidance [42,43].

1.3. VEGF receptor activation and signaling

Similar to other RTKs, signaling by VEGFRs is initiated upon binding of a covalently linked ligand dimer to the extracellular receptor domain. This interaction promotes receptor homo- and heterodimerization followed by activation of the intracellular kinase domain. We have recently shown how VEGF induces dimerization of the extracellular receptor domain (ECD) [44]. VEGFR-2 monomers are dimerized upon ligand binding to Ig-like domains 2 and 3 and dimers are further stabilized by receptor–receptor contacts mediated by Ig-like domains 4 and 7. Similar results were published by Schlessinger's lab for the related Kit and PDGF receptors [45,46]. We recently showed that distinct dimerization-promoting transmembrane domains (TMDs) derived from oncogenic variants of ErbB receptors activate VEGFR-2. Such TMD constructs orient receptor monomers by intramembrane interactions mediated by charged amino acids [173]. RTK activation thus requires specific orientation of receptor monomers in an active dimer which results from ligand-induced ECD rearrangement.

Activation of RTKs leads to phosphorylation of specific tyrosine residues located in the intracellular juxtamembrane domain, the kinase domain, the kinase insert domain and the carboxyterminal tail of the receptor. The subsequent interaction between VEGFRs and downstream signaling effectors is mediated through Src homology-2 (SH-2) and phosphotyrosine-binding (PTB) domains (reviewed in [47]). Signaling by VEGF receptors has been reviewed comprehensively in recent review articles [48,49]; here we therefore refer only to some of the hallmarks of VEGFR-2 activation.

Y951, Y1054, Y1059, Y1175 and Y1214 were identified as the most prominent phosphorylation sites of hVEGFR-2 [50]. Y1054 and Y1059 located in the activation loop were classified as autophosphorylation sites important for the catalytic activity of the receptor kinase [51]. Site-directed mutagenesis led to the identification of Y801 and Y1175 as binding sites of phospholipase C- γ (PLC- γ) [52]. Phosphorylation and activation of PLC- γ give rise to diacylglycerol and inositol trisphosphate which stimulate protein kinase C (PKC) [53]. Mitogenic signaling by VEGFR-2 is Ras independent and mediated by PKC via Erk kinases [54–56].

VEGF-induced endothelial cell migration is mediated by the adaptor protein VRAP, also known as T cell-specific adaptor (TSAD) [57]. VRAP binding to Y951 leads to its phosphorylation and recruitment of Src kinase which promotes actin reorganization and cell migration [50]. Additionally, the adapter protein Shb binds to phosphorylated Y1175 and leads to phosphoinositide-3-kinase (PI 3-kinase)-mediated cytoskeleton reorganization as well as activation of focal adhesion kinase (FAK) [58]. Cell migration and capillary formation are regulated by VEGF through Gab1, which acts as an adaptor for Grb2, PI 3-kinase and the tyrosine phosphatase SHP2 [59,60]. VEGF-induced actin remodeling is also triggered through the sequential activation of the small GTPase Cdc42 and stress activated protein kinase (SAPK/p38) following phosphorylation of Y1214 [61]. This leads to phosphorylation and release of heat-shock protein 27 (HSP27) [27]. Early molecular events in cytoskeleton reorganization include recruitment of the adaptor protein Nck and the Src family kinase Fyn to VEGFR-2 and triggers phosphorylation of p21-activated protein kinase-2 (PAK2) and activation of Cdc42 and p38 MAPK [62]. An additional important function of VEGF is survival signaling via activation of PI 3-kinase and phosphorylation of Akt [63]. Finally, signaling by VEGFR-2 is important for endothelial cell specification, a process that might require activation of the Ras-Erk pathway [64].

2. The role of coreceptors in VEGF signaling

Signaling by VEGFs depends on activation of three RTKs: VEGFR-1, -2 and -3. In addition VEGF-A function is mediated by two types of coreceptors: heparan sulfate proteoglycans and neuropilins.

2.1. Neuropilins

NRP-1 is a type I transmembrane glycoprotein originally identified as the antigen of a specific monoclonal antibody raised against a neuronal cell surface protein of *Xenopus laevis* involved in target recognition of optic nerve fibres [69]. Later, it has been identified as a receptor for class 3 semaphorins, playing a crucial role in growth cone collapse during neural development [70–72]. A closely related protein, NRP-2, has been identified a decade later as an additional receptor for semaphorins [73,74]. Both proteins share a sequence homology of 44% and show distinct, but overlapping patterns of tissue distribution [74]. Independent of their function in neuronal guidance, neuropilins play key roles in the development of the cardiovascular system, cooperating with the function of the structurally unrelated ligands of the VEGF family [75–77].

A plethora of interaction partners of neuropilins has been identified, including VEGFR-1, VEGFR-2 [78], VEGFR-3 [79], FGF receptor 1 [80], plexins [81], the cell adhesion molecule L1-CAM [82], integrins [83], NIP/synectin/GIPC [84], galectin [85], fibroblast growth factor (FGF) 1, 2, 4 and 7, hepatocyte growth factor/scatter factor (HGF/SF), FGF-binding protein, prion protein and antithrombin III [80]. Furthermore, heparin and heparan sulfate proteoglycans bind to the extracellular domain of neuropilins and regulate their signaling [86]. Neuropilins lack a sequence encoding an intracellular enzymatic activity and are supposed to serve solely as coreceptors, thereby modulating receptor output by VEGF RTKs. The observation that VEGF-A₁₆₅ is able to induce VEGFR-2/NRP-1 complex formation led to the idea of VEGF-A₁₆₅ bridging the two receptors [39,77,87,88]. In the meantime it became clear that NRP-1 is also able to convey VEGF autocrine signaling via the PI 3-kinase pathway in breast cancer cells [89] and regulates endothelial cell attachment by acting on F-actin organization independent of VEGFR-2 [90].

An elegant experiment by Wang et al. using a chimera of the extracellular domain of EGF receptor fused to the transmembrane and the intracellular domain of NRP-1 revealed that endothelial cell migration, but not proliferation, is induced by the intracellular domain of NRP-1 independently of VEGFR-2 [91]. The carboxy-terminal three amino acids (SEA-COOH) are crucial for this process. These amino acids are known to interact with the PDZ domain of RGS-GAIP-interacting protein (GIPC, also termed neuropilin interacting protein, NIP, or synectin) and are highly conserved among neuropilins [84,92]. Ligand induced NRP-1/GIPC interaction is required for angiogenesis, but not for vasculogenesis, in zebrafish and for migration of endothelial cells [93]. GIPC interaction with GAIP, which shares the same carboxyterminal three amino acids, is implicated in the regulation of trafficking by clathrin coated vesicles [92]. In the absence of experimental evidence, it is tempting to speculate that this interaction is connected to the observed internalization of NRP-1 after stimulation with VEGF-A₁₆₅, but not VEGF-A₁₁₂ (originally presumed to represent VEGF-A₁₂₁, see below) which does not bind NRP-1 [94]. In fact, trafficking of NRP-1 and VEGFR-2 seems to play a key role in VEGF-A₁₆₅ induced signaling. Clathrin dependent endocytosis of the VEGFR-2/NRP-1 complex was observed upon VEGF-A₁₆₅ stimulation [95]. This process requires the presence of intracellular GIPC. Recently, it was reported that VEGF and semaphorin-independent binding of NRP-1 to GIPC controls internalization of $\alpha 5\beta 1$ integrin to Rab5 positive endosomes [96]. By interaction of GIPC with the motor protein Myo6, cointernalization of $\alpha 5\beta 1$ integrin and neuropilin at cell adhesion sites leads to endothelial cell attachment to fibronectin. Another line of evidence suggests that interaction with GIPC via the carboxyterminal SEA motif is required for formation of a trimeric VEGF-A/VEGFR-2/NRP-1 complex [97]. A careful analysis of all processes associated with receptor internalization following ligand stimulation is required to fully understand the role of neuropilins in receptor trafficking.

2.2. VEGF binding to neuropilins and its impact on VEGFR-2 signaling

The best characterized member of the VEGF-A family is VEGF-A₁₆₅ (VEGF-A₁₆₄ in mouse). Binding of VEGF-A₁₆₅ to NRP-1 has been discovered first by crosslinking of radiolabeled VEGF-A to the surfaces of tumor cells and HUVECs [76]. NRP-1 was characterized as a low affinity cell surface receptor that enhances chemotaxis upon stimulation with VEGF-A₁₆₅ when coexpressed with VEGFR-2 and enhanced VEGF-A/VEGFR-2 complex formation on porcine aortic endothelial (PAE) cells [76].

The molecular mechanism of VEGF-A signaling via NRP-1 has long remained elusive, given the lack of intracellular enzymatic activity of NRP-1 and the rather low affinity of VEGF-A₁₆₅ for NRP-1 compared to VEGFR-2 [76,78]. It is now becoming clear that trimeric coreceptor formation of VEGF-A, VEGFR-2 and NRP-1 is essential, but not sufficient, for induction of angiogenesis.

Experiments using antibodies selectively blocking VEGF-A₁₆₅/NRP-1 interaction show that VEGF-induced phosphorylation of VEGFR-2 and the downstream signaling kinases of the Erk and Akt families is not affected by VEGF-A/NRP-1 binding [125]. Similarly, it was shown that formation of the trimeric coreceptor complex is not required for activation of VEGFR-2, PLC- γ , Erk1 and Akt [121]. Signaling by VEGF-A variants defective for NRP-1 binding is, however, more transient [29]. A comprehensive screening approach investigating VEGFR-2 activated kinases showed that stable coreceptor complex formation is required for activation of p38 MAPK, for angiogenic sprouting and for vascular plexus formation in embryoid bodies [121]. Thus, rather than affecting VEGFR-2 activity directly, NRP-1 is likely to modulate signaling kinetics and the activation of specific signal output via VEGFR-2. A possible mechanism explaining NRP-1 function may be that coreceptor complexes are processed differently than VEGFR-2 alone. So for instance receptor turnover and localization in endocytic vesicles might be altered resulting in different signal output. Finally, VEGF-A₁₆₅ mediates VEGFR-2/NRP-1 complex formation also in *trans* when the receptors are expressed on separate cells [39], or when the NRP-1 extracellular domain is administered as a soluble protein suggesting a role in juxtacrine signaling [88].

The NRP-1 binding epitope of VEGF-A was attributed to exons 7 and 8 [77], consistent with the observation that VEGF-A₁₂₁ did not bind to NRP-1 [76]. More recent results show that the short carboxyterminal sequence encoded by exon 8a confers specificity towards NRP-1. Tuftsin, an immunostimulatory peptide homologous to the VEGF-A₁₆₅ carboxyterminus, specifically binds to NRP-1 and inhibits VEGF-A₁₆₅ induced autophosphorylation of VEGFR-2 [112]. Alanine scanning mutations of the peptide ATWLPPR, a VEGF-A exon 8a homologue shown to inhibit VEGF-A₁₆₅/NRP-1 binding and VEGF mediated angiogenesis [113,114], confirms the importance of the terminal arginine residue in NRP-1 binding. Interestingly, in the free peptide, the prolines are in the *trans* conformation [115].

VEGF-A₁₂₁ binding to VEGFR-2 is similar to that of the longer isoforms. However, autophosphorylation of VEGFR-2 elicited by VEGF-A₁₂₁ is attenuated and this may be due to altered binding to coreceptors [87]. There has been some confusion on binding to neuropilins as a result of the fact that a commercially available source of VEGF-A₁₂₁ used by several laboratories was actually truncated and represented VEGF-A₁₁₂ [116,117]. This variant lacks part of exon 5 and the entire exon 8 sequence that is now recognized to mediate NRP-1 binding [29,39,117]. VEGF-A₁₂₁ is indeed able to bind NRP-1, though more weakly than the longer VEGF-A isoforms, confirming that exon 8a confers specificity towards NRP-1.

The two most remarkable features of the exon 8a encoded sequence are a highly basic stretch at the carboxyterminus, apparently important for binding to HS [118] and NRP-1 [39] and a cysteine residue in position 160. In VEGF-A₁₆₅, C160 and the exon 7 encoded C146 form a disulfide bridge [119], resulting in a restrained conformation of the carboxyterminal tail [118]. By this arrangement,

the exon 7 and 8 encoded sequence is held in close proximity to the VEGF receptor binding site. Mutation of C146 prevents this disulfide bridge from forming and has been shown to reduce VEGF-A activity such as induction of vascular permeability [120]. This disulfide bridge apparently maintains the functionality of the HS binding epitope by properly positioning the carboxyterminal basic residues. Recent work in our laboratory showed that a mutant VEGF-A₁₆₅, in which C160 was mutated to serine, is indeed unable to bind heparin [39]. Remarkably, this mutant was also unable to bind to NRP-1, showing that binding to NRP-1 and HS is interdependent. The inability of exon 8b VEGF-As to promote the formation of the trimeric VEGF-A/NRP-1/VEGFR-2 complex has been drawn on to explain its reduced angiogenic potential. NRP-1 binding gain and loss of function mutants indeed show a strong correlation between neuropilin binding, coreceptor complex formation and angiogenesis in embryoid body assays [39,121].

The failure of VEGF-A_{165b} to induce vasculogenesis has recently been related to the fact that phosphorylation of mVEGFR-2 at Y1052 and Y1057 (Y1054/Y1059 in hVEGFR-2), located in the activation loop of the tyrosine kinase domain [122], is substantially lower after stimulation with VEGF-A_{165b}, compared to VEGF-A₁₆₅, VEGF₁₄₅ or VEGF-A₁₂₁ in cells expressing VEGFR-2 and NRP-1, whereas Y949 and Y1212 (Y941/Y1214 in hVEGFR-2) phosphorylation levels were comparable [123]. Earlier work by our group had already established that phosphorylation of Y1175 in human and bovine VEGFR-2 upon stimulation with VEGF-A_{165b} is delayed and more transient compared to VEGF-A₁₆₅, resulting in reduced signaling through the MAP kinases Erk-1 and -2 [29]. Kawamura et al. suggested that VEGF-A_{165b} fails to rotate the VEGFR-2 monomers into a position that allows for efficient phosphorylation of Y1052 and Y1057 in receptor dimers [123]. In fact, it has been shown that VEGFR-2 activation depends on specific rotational restraints of receptor monomers in ligand-induced dimers (Dell'Era Dosch and Ballmer-Hofer, unpublished). Whether VEGF-A exon 8a is indeed required to correctly position the tyrosine kinase domain of VEGFR-2 in coreceptor complexes remains to be established. Taken together, we propose that exon 8b isoforms activate VEGFRs and coreceptor complexes in specific ways eliciting distinct signal output required for vessel homeostasis, but not for angiogenesis.

Important insights into neuropilin binding and coreceptor complex formation were also gained by analysis of parapoxvirus-encoded VEGF-E homologues. Distinct VEGF-E variants isolated from numerous virus strains differ in their ability to interact with NRP-1 and HS [7,9]. VEGF-E NZZ, for instance, binds NRP-1, but not HS. Whereas VEGF-A requires interaction with HS to form a stable VEGF-A/VEGFR-2/NRP-1 complex, VEGF-E NZZ does so in the absence of an HS binding site due to the presence of a high affinity NRP-1 binding epitope (RPPR) located near the carboxyterminus [39,121]. Interestingly, coreceptor complex formation involving VEGFR-2 and NRP-1 and the corresponding biological response are restored by replacing exon 8a in VEGF-A₁₂₁ by the peptide RPPR derived from VEGF-E NZZ. Based on these data we propose that the structural context of the carboxyterminal exon 8a encoded motif is crucial for the formation of trimeric VEGF-A/VEGFR-2/NRP-1 complexes. HS binding conferred by exon 7 is required to stabilize the interaction of VEGF-A with NRP-1 and presumably to alleviate electrostatic repulsion between the HS binding domains of VEGF-A and its receptors. On the other hand, despite the presence of exon 8a, VEGF-A₁₄₅ was shown not to bind to NRP-1, yet showed affinity for NRP-2 [124]. These findings suggest that exons 7 and 8a are required for binding to NRP-1, while exon 6 and 8a sequences cooperate in NRP-2 binding.

2.3. Heparan sulfate proteoglycans

Heparan sulfate proteoglycans are ubiquitous components of the cell surface and of the extracellular matrix (ECM), consisting of a protein core, to which one or more glycosaminoglycan (GAG) chains

are covalently attached. Heparan sulfate is an anionic GAG built from repeating disaccharides composed of an uronic acid (either D-glucuronic acid or its C5 epimer L-iduronic acid) and a derivative of D-glucosamine that can be either N-sulfated or N-acetylated. Clusters of N-sulfated disaccharides, referred to as S-domains, are flanked by transition domains of alternating N-acetylated and N-sulfated units, the T-domains. These sulfated regions are separated by stretches rich in N-acetylation, the NA domains. Considerable heterogeneity is further introduced by variable degrees of O-sulfation at C2 of the uronic acid unit, as well as C3 and C6 of D-glucosamine in the NS and alternating domains. Typically, HS chains reach lengths of 40–200 monosaccharide units. The fine structure and disaccharide distribution of HS chains is dependent on the tissue origin and therefore contributes to tissue specific signaling [65]. Heparin is an unusual HS in that it is composed primarily of extended NS domains with a 2-O-sulfated iduronic acid and 6-O-sulfated, N-sulfated glucosamine containing disaccharide as major constituent. It is usually not presented on the cell surface but stored in cytoplasmic granules of mast cells. Binding of protein ligands to the highly negative heparin chains depends predominantly on electrostatic interactions mediated by the sulfate substituents (for reviews on the function of heparin see [66–68]).

2.4. The role of heparan sulfate proteoglycans in VEGF function

The interaction of VEGF-A₁₆₅ with HS has been located to the carboxyterminal heparin binding domain (HBD) and was shown to depend on basic residues in exons 6 and 7. Site-directed mutagenesis experiments identified arginine residues R123, R124 and R159 of VEGF-A₁₆₅ as crucial residues for the interaction with HS [98]. This finding is supported by the refined NMR structure of the HBD [99], where these residues are localized on a contiguous binding surface on one face of the domain. Together with K125, K140, R145, R149 and R156 they form an electropositive patch positioned to interact with negatively charged HS (Fig. 4). Surprisingly, both VEGF-A_{165b} and the C160S VEGF-A₁₆₅ mutant, which is unable to form the disulfide bridge between C146 and C160, have lost their HS binding potential, suggesting that the exon 8a encoded sequence is required to maintain proper folding of the HBD. Instead of or in addition to the described interactions, VEGF-A isoforms containing exon 6a (VEGF-A₁₄₅, VEGF-A₁₆₂, VEGF-A₁₈₃, VEGF-A₁₈₉ and VEGF-A₂₀₆) strongly bind HS through this highly basic stretch. No structural information is available on this interaction, but the abundance of positively charged residues (13 of 25 amino acids) suggests strong ionic interactions. Exon 6b, in contrast, does not confer binding to HS due to the lack of basic residues, and the combination of exons 6a and 6b present in VEGF-A₁₆₂ leads to only weak binding [100]. VEGF-A₁₄₅ is an isoform initially identified in tumor cells from the female reproductive system that contains exon 6a and 8a, but not 7. As expected by the presence of exon 6a, VEGF-A₁₄₅ strongly binds to the extracellular matrix. Surprisingly, this protein cannot be released from the ECM by heparinase [18].

Robinson et al. performed an extensive analysis on the domain structure within HS chains required to bind to VEGF-A₁₆₅ [101]. They found no correlation between binding and the presence of specific disaccharides or the overall level of sulfation. Rather, the minimal requirement for VEGF-A₁₆₅ binding is a fragment containing at least one S-domain and the flanking T-domains. In contrast to members of the FGF family, VEGF-A failed to bind to isolated S-domains. Both N-sulfation and 6-O-sulfation in the HS S-domains are crucial for VEGF-A₁₆₅ binding, whereas 2-O-sulfate groups and carboxylate groups contribute to a lesser extent [101], a finding in agreement with previous results obtained with heparin [102]. VEGF-A binding to HS therefore differs from HGF and FGF-2 which strictly require 2-O-sulfation. Different patterns of HS chains could thus contribute to the tissue specificity of growth factor signaling.

Docking studies predict numerous contacts between the electropositive patch of the VEGF-A₁₆₅ HBD on the one hand and carboxylate and sulfate groups of six HS monosaccharides on the other hand, with a high degree of flexibility regarding the orientation and positioning of the GAG in the binding groove. Indeed, under nonphysiological low salt conditions, oligomers as short as 8 monosaccharide units bind to VEGF-A, whereas longer oligomers of 22–26 are preferentially bound from mixtures of K5 lyase treated HS. This suggests the engagement of both HBDs of a VEGF-A₁₆₅ dimer in the complex [101].

Theoretically, binding of growth factors to HSPG can serve four basic functions: (i) concentration of the growth factor at the cell surface and presentation to cell surface receptors, (ii) engagement of the HSPG in a coreceptor complex with altered binding or signaling properties compared to a minimal growth factor/receptor complex, (iii) restriction of growth factor diffusion to provide spatially restricted signaling cues and (iv) creation of a growth factor reservoir that can be released by hydrolytic processing of either the HS chain or the growth factor [103]. A conclusive interpretation of HS function in the context of the VEGF-A/VEGFR-2/NRP-1 complex proves difficult since each of the components is on its own capable to engage in HS binding and because NRP-1 itself is also subject to GAG modification.

Gitay-Goren et al. [104] showed that VEGF-A₁₆₅ binding to adult bovine aortic endothelial cells (ABAE) and human vascular endothelial cells (HUVEC) is increased by low concentrations (0.1–10 µg/ml) of heparin. The effect of heparin was attributed to the presence of VEGFR-2, since binding was not increased in cells expressing only VEGFR-1 [105]. A contribution of VEGFR-2 is further suggested by the enhancement of VEGF-A₁₆₅ binding to a soluble VEGFR-2-Fc fusion protein by the addition of heparin *in vitro* [106]. Heparin fragments of 22–24 monosaccharides constitute the minimal size for binding enhancement, while shorter heparin fragments are inhibitors [107]. An important role of cell surface HSPG was suggested by the observation that VEGF-A₁₆₅/VEGFR-2 binding is reduced in cell lines defective for HS synthesis [108] or following treatment of cells with heparinase [104], yet is restored by the addition of exogenous heparin. Interestingly, while the VEGF-A₁₂₁/VEGFR-2 interaction is not altered by heparin *in vitro* [109], a VEGF-A₁₆₅ variant that has been rendered incapable of binding to heparin by site-directed mutagenesis is unaffected in VEGFR-2 binding and is biologically active as judged by its ability to activate VEGFR-2 downstream signaling via tissue factor promoting microvessel outgrowth from aortic rings [98].

Chiang and Flanagan showed that the soluble extracellular domain of VEGFR-2 isolated from conditioned medium is retained by heparin sepharose, suggesting direct binding to HSPG [110]. Although the involvement of other factors present in the medium could not be excluded, this interaction was attributed to a short basic stretch between Ig-like domains 6 and 7 [108]. A highly basic decapeptide derived from that stretch binds heparin and inhibits VEGF-A₁₆₅ binding to VEGFR-2 in the presence of heparin, suggesting a specific interaction, rather than competition for VEGF. Only recently, a dose-dependent direct interaction of VEGFR-2 with heparin was reported [111].

2.5. Interaction of heparan sulfate with neuropilins

NRP-1 binds HS fragments of at least eight monosaccharides via its combined b1b2 domains. Consistent with the observation that either b1 or b2 alone fail to bind heparin [86], R359 and K373 in the b1 domain and R513, K514 and K516 in the b2 domain were determined to be key mediators of HS dependent dimerization [126]. These residues form a contiguous electropositive stretch on the NRP-1 surface that could conceivably accommodate 12 monosaccharide units. HS binding to this groove located close to the observed tuftsin

binding site might serve to properly align the b1 and b2 domains. Interestingly, a HS tetradecasaccharide, but not shorter oligosaccharides, triggers NRP-1 and NRP-2 b1b2 domains to form dimers. Although neuropilin homo- and heterodimerization via their MAM domains and TMDs have been implicated in semaphorin signaling by several groups, the role of dimerization in VEGF signaling is less well defined [71,127–130]. Yamada et al. showed that soluble dimeric NRP-1 rescues VEGF-A₁₆₅ mediated VEGFR-2 signaling in endothelial cells from NRP-1 knockout mice *in vitro* [131]. Dimeric NRP-1 ECD compensates vascular defects in mesoderm explants and embryos, whereas monomeric NRP-1 inhibits angiogenesis. It was proposed that VEGF is presented to VEGFR-2 by dimeric NRP-1, while monomeric coreceptor acts as a decoy, competing for VEGF.

Besides influencing the VEGF-A/VEGFR-2 interaction directly, HS modulates also VEGF-A/NRP-1 interaction and thereby the formation of coreceptor complexes. Fuh et al. reported that the affinity of VEGF-A₁₆₅ to NRP-1 is greatly enhanced by the presence of heparin [78]. While an octasaccharide suffices to bind NRP-1, 20–24 monosaccharide units are minimally required to enhance its interaction with VEGF-A₁₆₅ consistent with the idea that the protein ligands occupy different binding sites on a single heparin oligosaccharide chain [86]. The optimal concentration was found to be 100 nM to 1 μM heparin [78]. *In vitro*, the ability of NRP-1 to increase the affinity of VEGF-A₁₆₅ to soluble VEGFR-2 is strictly dependent on the addition of HS [78] suggesting that HS is required to stabilize a trimeric receptor/ligand complex. We showed that a stable coreceptor complex can only be induced by VEGF-A variants capable to bind both HS and NRP-1 and concluded that HS is required to stabilize the VEGF-A/NRP-1 interaction [30].

NRP-1 itself is also modified by GAG in a cell type-specific manner at the highly conserved S612 residue. A substantial fraction of NRP-1 from coronary artery smooth muscle cells is modified by chondroitinsulfate (CS), whereas in HUVEC a smaller fraction is modified by HS or CS. VEGF-A binding to the NRP-1 core protein is markedly increased by the GAG modifications. Furthermore, VEGFR-2 degradation after ligand stimulation is accelerated in endothelial cells expressing NRP-1 lacking GAG modification, resulting in more transient signaling. In contrast, CS modified NRP-1 in smooth muscle cells reduces VEGFR-2 expression levels posttranslationally [132]. As VEGF-A forms complexes with NRP-1 and VEGFR-2 expressed on separate cells [39], and GAG modifications have been shown to potentiate VEGFR-2 signaling *in trans* [133], the observed reduction of VEGFR-2 internalization might be explained by VEGFR-2 being trapped in a stable trimeric complex with NRP-1 expressed on adjacent cells.

2.6. Heparan sulfate proteoglycans are essential for cell proliferation and embryonic development

The importance of correctly modified HS for cellular responses to VEGF-A₁₆₅ has been demonstrated by several groups. HUVEC cells treated with sodium chlorate, an inhibitor of HS sulfation, fail to proliferate in response to VEGF-A₁₆₅ unless heparin or sulfate is added to the medium. Importantly, desulfated heparins, including 2-*O*-desulfated heparin, were not able to restore HUVEC proliferation. In zebrafish, depletion of 6-*O*-sulfation by specific inactivation of the sulfotransferase HS6TS-2 results in abnormalities in branching morphogenesis of the caudal vein during embryonic development [102]. Analysis of the endothelial markers revealed that primary formation of axial vessels and sprouting of intersegmental vessels are not dependent on the native sulfation pattern, but vascular remodeling is impaired. Simultaneous reduction of HS6ST-2 and VEGF-A expression had a synergistic effect and increased the frequency of abnormalities, but an effect on additional HS binding growth factors cannot be excluded [134].

Mammalian embryoid bodies derived from *Ndst1/2*^{-/-} stem cells defective in a sulfotransferase, which is essential for HS biosynthesis,

fail to respond to VEGF-A₁₆₅ [133]. The addition of exogenous HS could not substitute for the lack of correctly modified HSPG in this system. Notably, coculture with cells expressing wild-type HSPG, but not VEGFR-2, resulted in rescue of VEGF-A₁₆₅ induced vascular development. The response was accompanied by potentiated and less transient activation of VEGFR-2 and could not be elicited by binding of VEGF-A₁₂₁. The authors propose that trapping of the activated receptor complex by HSPG *in trans* prevents internalization and degradation and thus accounts for prolonged signaling. This could indicate a role for HSPG in juxtacrine signaling.

Heparin binding has also been shown to be important in determining the spatial distribution of VEGF-A isoforms. Several laboratories examined vascular development in mouse embryos expressing specific splice isoforms of VEGF-A [31,135–137]. Taken together, these data show that VEGF-A_{164/164} mice were healthy while all the other mutants showed serious vascular defects. So for instance endothelial cells at the tip of branching vessels develop polarized filopodial extensions directed towards extracellular VEGF deposits that guide the growing vessel [42]. In wild-type mouse embryos secreted VEGF accumulates in patches close to its expression sites and forms a steep concentration gradient. In mice expressing exclusively VEGF-A₁₂₀, however, the spatial distribution is much less restricted due to the lack of attachment to the ECM via HS. Failure of VEGF-A₁₂₀ to attach to the ECM has severe repercussions on vessel branching. Endothelial cells are preferentially integrated into the lumen of existing vessels instead of forming new branch points, resulting in thicker, less complex vasculature. In contrast, the vasculature of mice expressing exclusively VEGF-A₁₈₈ is excessively branched with reduced vessel diameter. These defects are a consequence of impaired polarization of the filopodial extensions of endothelial cells in response to immobilized VEGF rather than impaired cell proliferation [31]. Likewise, tumors expressing VEGF-A₁₈₈ develop a dense network of vessels, but are unable of recruiting supplying vessels from their neighborhood, because tightly stroma-bound VEGF-A₁₈₈ cannot diffuse into the surrounding tissue [138]. In contrast, VEGF-A₁₂₀ is readily diffusible from the expressing tumor and consequently large vessels are recruited from surrounding tissues, which fail to develop a branched microvasculature.

Two HSPGs, perlecan and glypican, have been implicated in VEGF signaling.

The extracellular matrix protein perlecan modulates processes as diverse as cell adhesion, proliferation and apoptosis (reviewed in [139]). Perlecan was shown to bind to VEGF-A via its HS side chains and combined administration to HUVEC cells increases VEGFR-2 activation [140]. Perlecan knock-down in tumor cells results in reduced proliferative response to VEGF-A₁₆₅ and FGF [141]. Similarly, perlecan knockdown in zebrafish leads to abnormal VEGF deposition defects in intersegmental vessel formation. The phenotype can be partially rescued by injection of VEGF-A₁₆₅ suggesting a dual role for perlecan as a regulator of VEGF localization and mediator of signaling via VEGFR-2 [140]. Glypican, a glycosylphosphatidylinositol anchored cell surface protein expressed in the vascular system, was also shown to bind to VEGF-A₁₆₅, but not to VEGF-A₁₂₁. Glypican potentiates VEGF-A₁₆₅ binding to soluble VEGFR-2 and to HUVEC cells and restores VEGFR-2 binding of VEGF-A₁₆₅ following damage by oxidizing agents [142]. However, this effect does not need to be specific for glypican, since heparin or HS could recover damaged VEGF-A₁₆₅ activity as well.

3. Structure of VEGF and its receptors

The structure of VEGF family proteins and their receptors is the subject of intense research and several high resolution structures for VEGF proteins are available. Here we review these structural data and discuss the functional implications derived from this extensive data set.

3.1. The structure of VEGF-A

The crystal structure of the VEGF receptor binding domain of VEGF-A was first reported by Muller and co-workers [15]. The VEGF-A structure consists of a homodimer that is covalently linked by two intermolecular disulfide bonds between C51 and C60 (Fig. 2A). It contains a cysteine knot motif, which has also been described for other VEGF family members and related growth factors, such as PDGF and TGF- β 2 [143–149]. The knot consists of an eight residue ring formed by the backbone atoms of residues 57–61 and 102–104 and two intramolecular disulfide bridges, C57–C102 and C61–C104, with a third disulfide bridge (C26–C68) that passes almost perpendicularly through the center of the ring. A central four-stranded antiparallel β -sheet formed by two pairs of twisted antiparallel β -strands, referred to as β 1, β 3, β 5 and β 6, extends from the cysteine knot motif. A single hydrogen bond connects β 3 and β 5, which makes the β -sheet highly irregular. Loop 1 connecting β 1 and β 3 contains a single turn of an α -helix as well as a short β -strand. This strand, together with the end of β 5 and the beginning of β 6, forms a short three-stranded β -sheet at the opposite end of the molecule from the cysteine knot. Residues from this sheet, helix α 2, and the loops L1 and L3 (β 5– β 6), together with residues from the aminoterminal α -helix of the opposite monomer, form a small hydrophobic core, which has been proposed to provide additional stabilization to the four-stranded central sheet [146]. The two monomers adopt an antiparallel orientation related by a 2-fold axis perpendicular to the plane of the β -sheets.

Based on a comprehensive mutagenesis study eight VEGFR-2 binding determinants have been identified that cluster into two symmetrical binding surfaces at either pole of the VEGF-A homodimer [15]. Within each of these surfaces the side chains of the eight residues cluster into two solvent accessible ‘hot spots,’ which are exposed on

the same pole of the molecule. The larger hot spot comprises residues I43, I46, I83, K84, P85 and E64 (Fig. 3, red). The smaller hot spot contains residues F17 and Q79 (Fig. 3, orange). The hypothesis of VEGF-induced dimerization of VEGFRs by binding a receptor molecule at either pole of VEGF-A has later been corroborated by the crystal structure of a complex between the receptor-binding domain of VEGF-A and VEGFR-1 domain 2 (Fig. 2B) [16] and by mutational and biophysical studies by Fuh and coworkers [150]. These studies showed that two molecules of VEGFR-2 are dimerized across the VEGF subunit interface and induce signaling. The crystal structure of the complex revealed predominantly hydrophobic interactions of VEGFR-1 domain 2 with the poles of the VEGF-A dimer [16]. No major conformational changes were observed in the overall structure of the receptor domain-bound VEGF-A compared to the structure of the free form. The largest differences were observed in the loop regions L1 and L3, which also show a high degree of flexibility in the free VEGF-A structure [15]. Moreover, deletion experiments showed that Ig-like domains 2–3 are sufficient for tight binding to VEGF-A. However, in the absence of X-ray crystallographic data for such a receptor–ligand complex, the orientation of receptor monomers in ligand complexes remains unknown. High resolution structural information is urgently needed to understand receptor activation and specificity of VEGF family ligands in molecular terms.

In the VEGFR-1 domain 2 complex structure the carboxyterminus of VEGFR-1 domain 2 points towards a 6.5 Å wide groove that extends from the pole to the membrane-facing side of the two VEGF-monomers (Fig. 3). Three side chains of the six large hot spot residues are located in the walls of this groove, while the remaining hot spot residues are at the membrane-facing side. According to these structural features and the experimental evidence that a receptor fragment of domains 2–3 binds 20-fold tighter to VEGF compared to

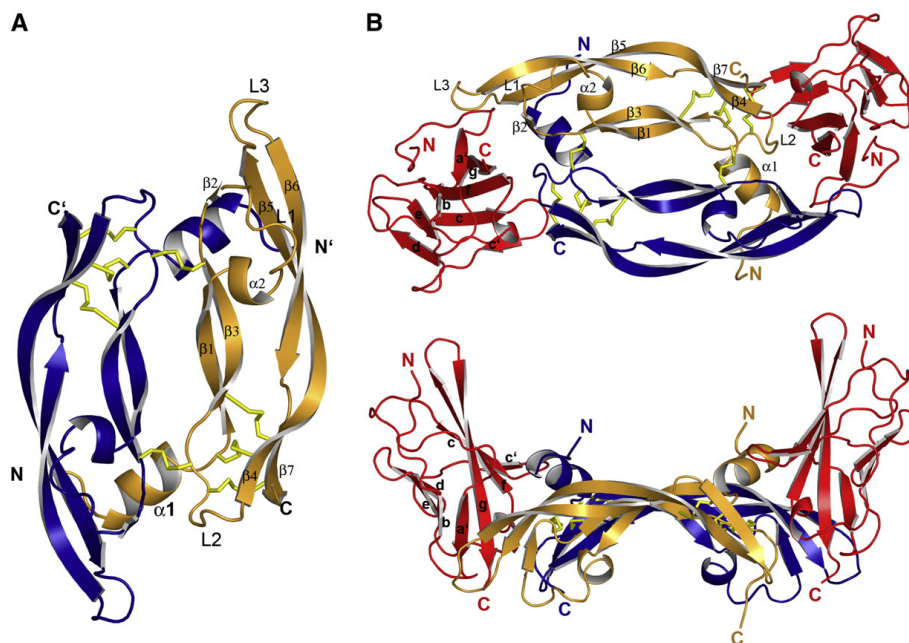


Fig. 2. Structures of VEGF-A and VEGFR-1 domain 2. Ribbon representations of (A) the nonliganded VEGF-A₁₀₉ ('bottom' view looking up from the cell membrane; PDB code 1VVF) and (B) the complex between VEGF-A₁₀₉ and VEGFR-1 domain 2 (top panel; bottom view; bottom panel; side view; PDB code 1FLT). The two VEGF monomers are shown in blue and light orange, respectively; the VEGFR-1 domain 2 in red. Disulfide bonds are shown as yellow sticks. The secondary structure elements are labeled according to the original references. The figure was prepared using PyMOL [170].

574

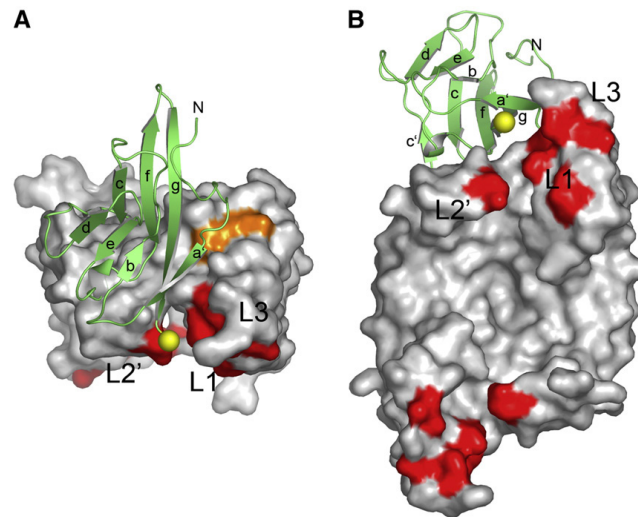
F.S. Grunewald et al. / *Biochimica et Biophysica Acta* 1804 (2010) 567–580

Fig. 3. Hotspots for VEGFR-2 binding. Surface representation of VEGF-A₁₀₉ in complex with domain 2 of VEGFR-1 (lime ribbon representation; PDB code 1FLT). Both critical hotspots for VEGFR-2 binding that were identified by mutational analysis are mapped onto the surface in red ('large') and orange ('small'), respectively. The carboxyterminus of domain 2 (yellow sphere) points towards the groove. Positioning of the D2–D3 linker in the groove would place the domain 3 in a favorable orientation for the interaction with the remaining hotspot residues.

domain 2 alone, it was proposed that in the native complex the linker between the domains 2 and 3 may occupy the groove, positioning the third domain in contact with the bottom face of VEGF [16]. Based on these assumptions and on the available crystal structure of the complex, a dimeric model of the receptor-binding domain of VEGF in complex with domains 1–4 of VEGFR-1 was constructed, in which the

domain 2–3 linker occupies the groove, and domain 3 is in contact with the bottom face of VEGF. In the proposed orientation the carboxytermini of the domains 3 are in close proximity to allow direct contacts between the domains 4 [16]. To date, no crystal structure of a multidomain VEGF receptor complex is available to confirm this model.

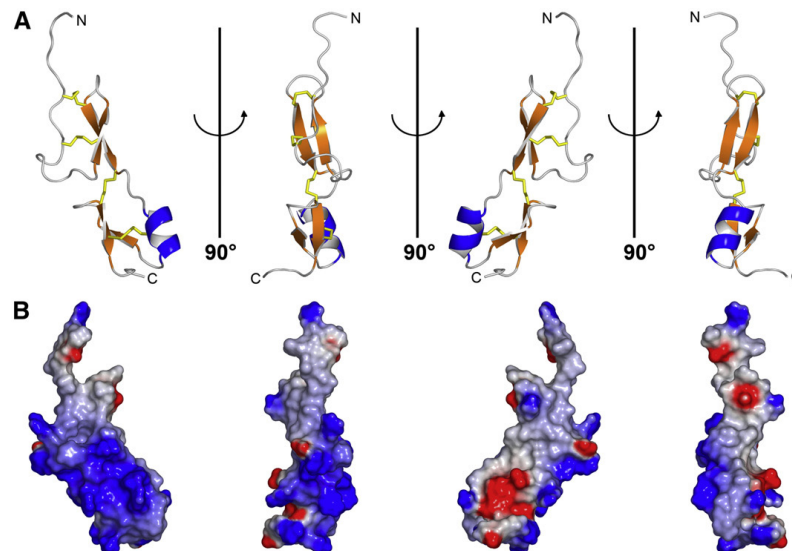


Fig. 4. Solution structure of the HBD of VEGF-A. (A) Cartoon representation of the HBD in four different orientations (PDB code 1VGH, model 1; 90° rotations about the vertical axis in the plane). The secondary structure elements are colored in orange and blue. The disulfide bonds are represented as yellow sticks. The amino- and carboxytermini are labeled. (B) Electrostatic surface potential (calculated with the program DelPhi [171,172]) mapped onto the surface of the HBD (same model and orientations as in (A)). The negative (red) and the positive (blue) electrostatic surface potentials are contoured at ± 8 kT.

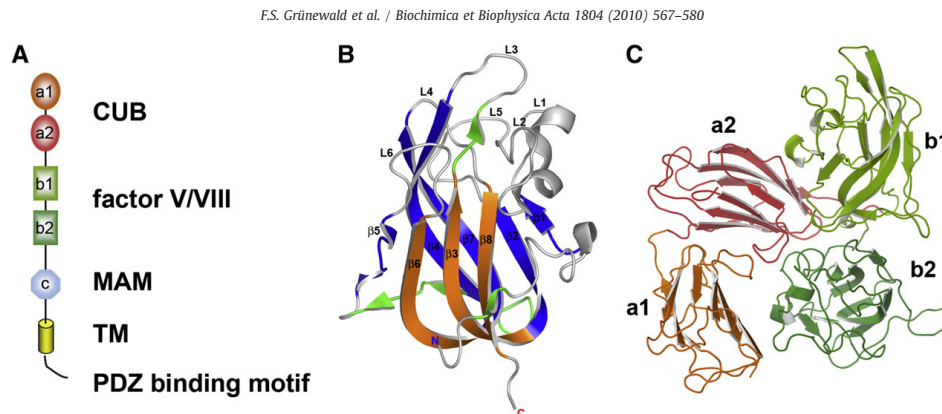


Fig. 5. Domain organization and structure of neuropilins. (A) Schematic drawing of the overall domain architecture of neuropilins. Neuropilins possess a ligand binding ectodomain consisting of CUB (a1/a2) and F5/8 (b1/b2) domains, followed by a membrane proximal MAM (C) domain. A short membrane-spanning domain (TM) and cytoplasmic tail with a PDZ binding motif comprise the remainder of the protein. CUB domains, orange/red; F5/8 domains, olive/dark green; MAM, light blue; TM, yellow. (B) Ribbon diagram of the NRP-1 b1 domain (PDB code 1KEX). The core of the β -barrel is formed by a three-stranded (orange) and a five-stranded (blue) antiparallel β -sheet. The six loops (L1–L6) extend at the top of the β -barrel. (C) Ribbon diagram of the NRP-2 a1a2b1b2 structure (PDB code 1QQL). The domains are colored using the same color code as in (A).

3.2. The VEGF-A heparin binding domain

The carboxyterminal domain of VEGF-A₁₆₅ comprises 55 residues with no significant sequence homology to known proteins and represents a unique heparin-binding domain [119]. It is highly basic and contains eight cysteine residues that form four disulfide bonds. The solution structure of the heparin-binding domain of VEGF-A₁₆₅ was determined by homo- and heteronuclear NMR spectroscopy [99,118]. The structure consists of two subdomains: the aminoterminal subdomain (residues 110–139) contains a disordered region and a single two-stranded β -sheet. The carboxyterminal subdomain (residues 139–165) is well ordered and contains a short α -helix packed against a two-stranded antiparallel β -sheet (Fig. 4). A cluster of charged residues (R123, R124, K125, K140, R145, R149 and R156) on one side of the carboxyterminal domain and an adjacent disordered loop from the aminoterminal domain has been proposed as putative HS binding site based on electrostatic surface potential calculations [118]. However, no structural study of a complex between the VEGF heparin-binding domain with a heparin fragment has been reported to date to reveal the details of this interaction.

3.3. The structure of VEGF-B

Two VEGF-B isoforms, VEGF-B₁₆₇ and VEGF-B₁₈₆, are generated by alternative splicing [151]. They exclusively interact with VEGFR-1, and not with VEGFR-2 or -3 [38]. Moreover, both isoforms bind NRP-1. Binding of VEGF-B₁₆₇ to NRP-1 is mediated by the heparin-binding domain, whereas binding of VEGF-B₁₈₆ is regulated by exposure of a short carboxyterminal proline-rich peptide upon proteolytic processing [152].

The crystal structures of VEGF-B [144] and of a complex with a neutralizing antibody Fab fragment were recently reported [153]. The overall structure of VEGF-B is similar to the known structures of other cysteine knot proteins. Human VEGF-B (residues 10–108) shares 46% sequence identity with human VEGF-A (residues 11–109) and 37% sequence identity with human PlGF (residues 19–118) and superimposes onto the dimers of VEGF-A and PlGF with r.m.s. deviations of 1.3 Å and 1.6 Å, respectively [144]. Major conformational differences have been observed in loops L1 and L3, which are important regions for receptor binding. Based on a predicted model for the association of VEGF-B with the second domain of VEGFR-1 and the structural data of the native protein, N46, P62, V48, D63 and I83 of VEGF-B were

proposed to form hydrogen-bonding and van der Waals interactions to H223 of VEGFR-1, contributing to VEGF-B/VEGFR-1 complex formation. Six out of the eight hot spot residues of VEGF-A that have been implicated in VEGFR-2 binding are conserved in VEGF-B [15]. Moreover, different positioning of P86 in loop L3 has been proposed to induce conformational differences in loop L3 that likely prevent VEGF-B from binding to VEGFR-2. The interaction of a neutralizing antibody with VEGF-B involves essential residues at each pole of the VEGF-B homodimer. The interface is rather flat and largely hydrophobic and lacks typical 'knob-into-hole' interactions as observed in the receptor complexes of VEGF-A [16] and PlGF [154]. Substantial overlap was observed between the buried surfaces in the VEGF-B/Fab complex and in the predicted model of VEGF-B/VEGFR-1, which share 11 conserved residues. Accordingly, the neutralizing effect of the antibody was proposed to occur by steric hindrance of the receptor binding interface and not as a consequence of induced conformational changes in the ligand [153].

3.4. The structures of VEGF-C and -D

VEGF-C and VEGF-D share a similar architecture with other VEGFs, including the cysteine knot motif. They are synthesized as precursor proteins with long amino- and carboxyterminal propeptides flanking the VEGFR-binding domain. Upon secretion, proteolytic cleavage of the propeptides releases the mature VEGF homology domain with increased affinity to both VEGFR-2 and VEGFR-3 [155,156]. Mature VEGF-C and VEGF-D have been described as a mixture of covalent and noncovalent dimers [155–158]. To date, no crystal structure has been reported for any of these two growth factors. Besides the conserved cysteine pattern typical for cysteine knot proteins, an additional cysteine residue is most likely located at the dimer interface of both VEGF-C and VEGF-D and might interfere with dimer formation by engagement to an intramolecular disulfide bridge. Recently, a model of VEGF-D was designed and the cysteines located at the subunit interface were mutated to study the effect of these residues on the structural and functional properties of VEGF-D [159]. The two conserved cysteines C44 and C53 were found to be essential for VEGF-D activity. In contrast, the replacement of the additional cysteine C25 by isoleucine, leucine or valine yielded novel VEGF-D variants with increased biological activity [159]. In the proposed model, cysteine C25 is located close to the conserved cysteines C44 and C53. Accordingly, a regulatory function was

assigned to cysteine C25 that limits and modulates the activity of the mature protein *in vivo*. Modulation of the exchange rate between intra- and intermolecular disulfide bond formation, in response to changes in the extracellular redox environment thereby enhancing the dimeric stability of VEGF-D, was proposed as a potential regulatory mechanism inherent to VEGF family members that have such an additional cysteine residue at the dimer interface [159]. Structural data on VEGF-C or VEGF-D will be required to prove this hypothesis.

3.5. The structure of VEGF-E

The crystal structure of the core region of VEGF-E N22 is very similar to the structural homologs VEGF-A, VEGF-B, PlGF, and the two snake venoms Vammin and VR-1 which superimpose with an r.m.s. deviation of ~1.0 Å [160]. Significant conformational differences are observed only in loops L1 and L3. The exchange of individual segments in loops L1 and L3 by the corresponding sequences from PlGF abolished binding to VEGFR-2, whereas a simultaneous exchange of both loops reduced binding and conferred the ability to VEGF-E to interact with VEGFR-1. Moreover, the exchange of R46 to I in loop L1 significantly increased the affinity of VEGF-E for both VEGF receptors. According to these observations, Pieren and coworkers suggested that loop L2 with D63, E64 and E67 is essential for binding to VEGF receptors, whereas the distinct orientation of loops L1 and L3 determines VEGF receptor specificity.

3.6. The structure of VEGF-F

The recently reported crystal structures of Vammin and VR-1 revealed high homology to VEGF-A (r.m.s.d. 1.2 Å for vamin and 1.6 Å for VR-1), but three distinct structural features differ from other known VEGF structures [149]. First, the insertion of T86 causes a different conformation in loop L3. Secondly, substantial differences in electrostatic surface potential are observed. Vammin and VR-1 feature a positive electrostatic surface potential in contrast to VEGF-A and PlGF, which are negative. Thirdly, R82 and R86 form a tight framework of salt bridges with E42, D45 and E93 that stabilizes the relative orientation of the loops L1 and L3.

3.7. VEGF receptor and neuropilin structures

Structural information on VEGF receptor ectodomains is limited to the solution structure of VEGFR-1 domain 2 in its nonliganded form [161], and to the crystal structures of VEGFR-1 domain 2 in complex with VEGF-A [16,161] and PlGF [154]. The crystal structures revealed

that this domain is a member of the I-set of the immunoglobulin superfamily [162]. VEGFR-1 domain 2 consists of a sandwich formed by two β -sheets, one consisting of five strands, the other of three. The strands in the three-stranded sheet are rather short and consist of only three or four residues. The hydrophobic core buries a disulfide bridge between C158 and C207 that connects the two β -sheets [16]. An unusual feature is a region near the aminoterminal that bulges away from the domain rather than pairing with the neighboring β -strand. Several of the residues in the bulge are in contact with VEGF. NMR analysis of VEGFR-1 domain D2 in the nonliganded state revealed a structure almost identical with that observed in the complex crystal structures. Therefore, the different conformations observed in the aminoterminal bulge have been proposed to arise from the inherent flexibility of this region, independent of ligand binding. In addition, an electron microscopy structure of the ligand-bound ECD of VEGFR-2 was published by our lab. These data show that receptor dimers are intertwined and form a rigid structure apparently required to instigate transmembrane signaling [44].

The ectodomains of neuropilins contain two aminoterminal CUB domains (a1 and a2), two coagulation factor V/VIII homology domains (b1 and b2) and a single MAM domain (meprin, A5, μ -phosphatase; also known as c) (Fig. 6A) [163,164]. Recently, several crystal structures of NRP-1 and -2 ectodomain fragments have been reported in their nonliganded state, in complex with the tuftsin tetrapeptide, and in complex with antibodies that selectively block either semaphorin or VEGF-A binding [126,165,166]. These structures have provided a first picture of the interactions of NRP-1 with its ligands and allowed to propose models for VEGF, semaphorin and heparin binding.

The NRP-1 b1 and b2 domains are characterized by the typical discoidin family β -barrel fold [167–169], which consists of a distorted jellyroll formed by a five- and a three-stranded antiparallel β -sheet and six loops or spikes (L1–L6) that extend at one end of the β -barrel (Fig. 6B). In the first reported structure of the NRP-1 b1 domain Lee and coworkers identified a polar cleft formed by these loops as the putative binding groove for the positively charged tails of VEGF-A₁₆₅ and semaphorins [165]. This hypothesis was later confirmed by Vander Kooi and coworkers with the crystal structures of both the NRP-1 b1b2 domains in the nonliganded state and in complex with tuftsin [126]. These structures revealed that the b1b2 domains form a single structural unit with an unexpected extensive interdomain interface and provided the first structural details on the interaction of NRP-1 with VEGF-A [126]. The carboxyterminal arginine (R4) of tuftsin occupies the acidic cleft and accounts for the majority of the interactions with NRP-1 b1b2. The side chain of R4 is stacked between the aromatic rings of Y297 (L1) and Y353 (L3) and forms a salt bridge

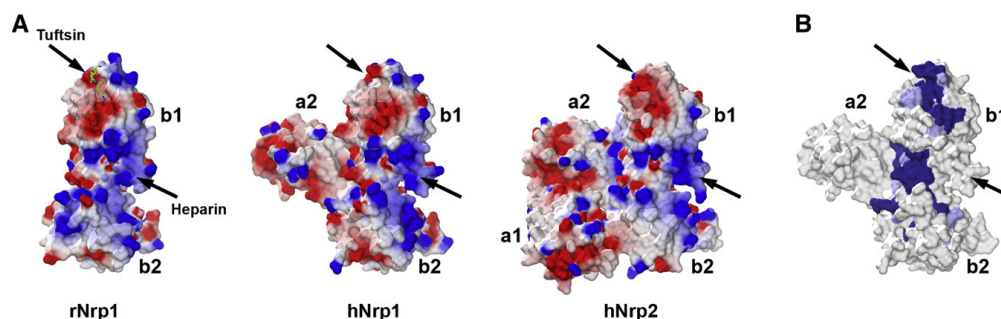


Fig. 6. The putative VEGF binding sites on neuropilins. (A) Electrostatic surface potential (calculated with the program DelPhi [171,172]) mapped onto the surfaces of the rat NRP-1 b1b2 (PDB code 2ORZ) and the human NRP-1 a2b1b2 (PDB code 2QQM) and NRP-2 a1a2b1b2 (PDB code 2QQL) domains. The tuftsin binding site and the putative heparin-binding patch are indicated by black arrows. The tuftsin molecule bound to rat NRP-1 is in green stick representation. The negative (red) and positive (blue) electrostatic surface potentials are contoured at ± 6 kT. (B) Surface representation of hNRP-1 (PDB code 2QQM). The two clusters of residues conserved among neuropilins are highlighted in dark (100% conserved) and light blue ($\geq 75\%$ conserved), respectively, according to Appleton and coworkers [166].

to the side chain of D320 (L2). Moreover, the carboxyterminus is tucked into the pocket and participates in specific interactions with S346, T349 and Y353 on loop L3.

In all crystal structures that contain both the a and the b domains a rigid structural unit is formed by the three domains a2, b1 and b2, which adopt the same arrangement around a pseudo 3-fold axis. The interdomain interfaces of this tightly packed core are highly conserved among both neuropilins. In contrast, the domain arrangement between a1 and the a2b1b2 core is not conserved in the two crystal forms and reveals a high degree of flexibility (Fig. 5C) [166]. The b1 domains of NRP-1 and -2 superimpose with an r.m.s. deviation of 0.6 Å with the most prominent difference in loop L1 of NRP-2, which contains an additional aspartic acid residue (D301) compared to NRP-1. The b2 domains superimpose less well (r.m.s.d. 2.7 Å) due to larger conformational differences observed in the spikes [166]. These variations have been implicated in the recognition of multiple binding partners, as these spikes generally define the binding sites within the discoidin family. The domains b1 and b2 are tightly packed against each other with an extensive interdomain interface that contains predominantly hydrophobic residues, which are highly conserved among all neuropilins. The interdomain junction forms a deep cleft that runs approximately perpendicular to the long axis of the two b domains. This cleft is surrounded by a set of positively charged residues (R359, K373, R513, K514 and K516), which have been identified as important for heparin binding based on site-directed mutagenesis experiments on rat NRP-1 [126]. This electropositive patch is also conserved in the structures of both human neuropilins (Fig. 6A). Accordingly, it has been proposed as a putative heparin binding site [126,166]. Based on sequence conservation analysis among 12 NRP-1 and -2 proteins Appleton and coworkers identified two clusters of conserved residues on the b1b2 domains, which map on the tuftsin binding site and on the edge of the proposed heparin binding region, suggesting an additional area of interaction between neuropilin and VEGF-A (Fig. 6B) [166]. The a1a2b1b2 domains of NRP-2 in complex with antibodies that selectively block either semaphorin or VEGF-A binding have been crystallized in two different crystal forms. Both crystal forms contain a conserved crystallographic interface that is mediated by the a1 domain. Based on the a1-mediated crystallographic dimers potential models have been proposed that could accommodate both the dimeric VEGFs or class 3 semaphorins [166].

Several structural studies provide a first detailed picture of both the VEGF-A and semaphorin binding domains of neuropilins. The reported structures offer a basis for the design of future crystallographic approaches to explore the molecular interactions underlying receptor activation and signaling mediated by VEGFs and semaphorins through both neuropilins. Additional structural information on complexes of both NRP-1 and -2 bound to different ligands and peptides will be required for a comprehensive understanding of the molecular details that define affinities and specificities of the various neuropilin ligands.

4. Outlook

In the absence of detailed structural information on the interactions of VEGFs with their multidomain receptors it remains unclear how the observed structural features determine receptor selectivity. Structural data on receptor–ligand complexes with various VEGF isoforms are therefore needed to assess the receptor specificity of VEGF family proteins. We also need more structural information to clarify the mechanism of VEGFR activation. A promising approach will be to investigate the extracellular and the intracellular receptor domains separately as these proteins require different milieus for proper folding. After assignment of the functions of individual domains, a comprehensive model for receptor signaling will be elaborated.

An aspect we did not cover in this article is the question where ligand-stimulated receptors are located in a cell when relaying their signals to downstream molecules such as cytoplasmic serine, threonine or tyrosine kinases of the various subfamilies, to lipid kinases, phospholipases, or G protein family signaling molecules. It is this remarkably complex interplay among the diverse signaling pathways activated by VEGF family proteins that determines signal specificity and biological output.

Acknowledgements

The authors thank Swiss National Science Foundation (grants 3100A-116507 and 31003A-112455) and Oncosuisse (grant OC2 01200-08-2007) for continuous support of their work.

References

- [1] D.R. Senger, S.J. Galli, A.M. Dvorak, C.A. Perruzzi, V.S. Harvey, H.F. Dvorak, Tumor cells secrete a vascular permeability factor that promotes accumulation of ascites fluid, *Science* 219 (1983) 983–985.
- [2] L. Jussila, K. Alitalo, Vascular growth factors and lymphangiogenesis, *Physiol. Rev.* 82 (2002) 673–700.
- [3] H. Takahashi, M. Shibuya, The vascular endothelial growth factor (VEGF)/VEGF receptor system and its role under physiological and pathological conditions, *Clin. Sci. (Lond.)* 109 (2005) 227–241.
- [4] D.J. Lyttle, K.M. Fraser, S.B. Fleming, A.A. Mercer, A.J. Robinson, Homologs of vascular endothelial growth factor are encoded by the poxvirus orf virus, *J. Virol.* 68 (1994) 84–92.
- [5] L.M. Wise, N. Ueda, N.H. Dryden, S.B. Fleming, C. Caesar, S. Roufai, M.G. Achen, S.A. Stacker, A.A. Mercer, Viral vascular endothelial growth factors vary extensively in amino acid sequence, receptor-binding specificities, and the ability to induce vascular permeability yet are uniformly active mitogens, *J. Biol. Chem.* 278 (2003) 38004–38014.
- [6] A.A. Mercer, L.M. Wise, A. Scagliarini, C.J. McInnes, M. Buttner, H.J. Rziha, C.A. McCaughan, S.B. Fleming, N. Ueda, P.F. Nettleton, Vascular endothelial growth factors encoded by Orf virus show surprising sequence variation but have a conserved, functionally relevant structure, *J. Gen. Virol.* 83 (2002) 2845–2855.
- [7] L.M. Wise, T. Veikkola, A.A. Mercer, L.J. Savory, S.B. Fleming, C. Caesar, A. Vitali, T. Mäkinen, K. Alitalo, S.A. Stacker, Vascular endothelial growth factor (VEGF)-like protein from orf virus N22 binds to VEGFR2 and neuropilin-1, *Proc. Natl. Acad. Sci. U. S. A.* 96 (1999) 3071–3076.
- [8] S. Ogawa, A. Oku, A. Sawano, S. Yamaguchi, Y. Yazaki, M. Shibuya, A novel type of vascular endothelial growth factor, VEGF-E (N2-7 VEGF), preferentially utilizes KDR/Flk-1 receptor and carries a potent mitotic activity without heparin-binding domain, *J. Biol. Chem.* 273 (1998) 31273–31282.
- [9] M. Meyer, M. Clauss, W.A. Lepple, J. Waltenberger, H.G. Augustin, M. Ziche, C. Lanz, M. Buttner, H.J. Rziha, C. Dehio, A novel vascular endothelial growth factor encoded by Orf virus, VEGF-E, mediates angiogenesis via signalling through VEGFR-2 (KDR) but not VEGFR-1 (Flt-1) receptor tyrosine kinases, *EMBO J.* 18 (1999) 363–374.
- [10] Y. Yamazaki, K. Takani, H. Atoda, T. Morita, Snake venom vascular endothelial growth factors (VEGFs) exhibit potent activity through their specific recognition of KDR (VEGF receptor 2), *J. Biol. Chem.* 278 (2003) 51985–51988.
- [11] Y. Komori, T. Nikai, K. Taniguchi, K. Masuda, H. Sugihara, Vascular endothelial growth factor VEGF-like heparin-binding protein from the venom of *Vipera aspis aspis* (Aspic viper), *Biochemistry* 38 (1999) 11796–11803.
- [12] H. Takahashi, S. Hattori, A. Iwamatsu, H. Takizawa, M. Shibuya, A novel snake venom vascular endothelial growth factor (VEGF) predominantly induces vascular permeability through preferential signaling via VEGF receptor-1, *J. Biol. Chem.* 279 (2004) 46304–46314.
- [13] M.R. Ladomery, S.J. Harper, D.O. Bates, Alternative splicing in angiogenesis: the vascular endothelial growth factor paradigm, *Cancer Lett.* 249 (2007) 133–142.
- [14] S. Lee, S.M. Jilani, G.V. Nikolova, D. Carpizo, M.L. Iruela-Arispe, Processing of VEGF-A by matrix metalloproteinases regulates bioavailability and vascular patterning in tumors, *J. Cell Biol.* 169 (2005) 681–691.
- [15] Y.A. Muller, B. Li, H.W. Christinger, J.A. Wells, B.C. Cunningham, A.M. de Vos, Vascular endothelial growth factor: crystal structure and functional mapping of the kinase domain receptor binding site, *Proc. Natl. Acad. Sci. U. S. A.* 94 (1997) 7192–7197.
- [16] C. Wiesmann, G. Fuh, H.W. Christinger, C. Eigenbrot, J.A. Wells, A.M. de Vos, Crystal structure at 1.7 Å resolution of VEGF in complex with domain 2 of the Flt-1 receptor, *Cell* 91 (1997) 695–704.
- [17] B.A. Keyt, L.T. Berleau, H.V. Nguyen, H. Chen, H. Heinsohn, R. Vandlen, N. Ferrara, The carboxyl-terminal domain (111–165) of vascular endothelial growth factor is critical for its mitogenic potency, *J. Biol. Chem.* 271 (1996) 7788–7795.
- [18] Z. Poltorak, T. Cohen, R. Sivan, Y. Kandellis, G. Spira, I. Vlodyavsky, E. Keshet, G. Neufeld, VEGF145, a secreted vascular endothelial growth factor isoform that binds to extracellular matrix, *J. Biol. Chem.* 272 (1997) 7151–7158.
- [19] K.A. Houck, D.W. Leung, A.M. Rowland, J. Winer, N. Ferrara, Dual regulation of vascular endothelial growth factor bioavailability by genetic and proteolytic mechanisms, *J. Biol. Chem.* 267 (1992) 26031–26037.

- [20] J.E. Park, G.A. Keller, N. Ferrara, The vascular endothelial growth factor (VEGF) isoforms: differential deposition into the subepithelial extracellular matrix and bioactivity of extracellular matrix-bound VEGF, *Mol. Biol. Cell* 4 (1993) 1317–1326.
- [21] J. Plouët, F. Moro, S. Bertagnoli, N. Coldeboeuf, H. Mazarguil, S. Clamens, F. Bayard, Extracellular cleavage of the vascular endothelial growth factor 189-amino acid form by urokinase is required for its mitogenic effect, *J. Biol. Chem.* 272 (1997) 13390–13396.
- [22] D.O. Bates, T.G. Cui, J.M. Doughty, M. Winkler, M. Sugiono, J.D. Shields, D. Peat, D. Gillatt, S.J. Harper, VEGF165b, an inhibitory splice variant of vascular endothelial growth factor, is down-regulated in renal cell carcinoma, *Cancer Res.* 62 (2002) 4123–4131.
- [23] J. Woolard, W.Y. Wang, H.S. Bevan, Y. Qiu, L. Morbidelli, R.O. Pritchard-Jones, T.G. Cui, M. Sugiono, E. Waite, R. Perrin, R. Foster, J. Digby-Bell, J.D. Shields, C.E. Whittles, R.E. Mushens, D.A. Gillatt, M. Ziche, S.J. Harper, D.O. Bates, VEGF165b, an inhibitory vascular endothelial growth factor splice variant: mechanism of action, *in vivo* effect on angiogenesis and endogenous protein expression, *Cancer Res.* 64 (2004) 7822–7835.
- [24] R. Perrin, O. Konopatskaya, Y. Qiu, S. Harper, D. Bates, A. Churchill, Diabetic retinopathy is associated with a switch in splicing from anti- to pro-angiogenic isoforms of vascular endothelial growth factor, *Diabetologia* 48 (2005) 2422–2427.
- [25] D.G. Nowak, J. Woolard, E.M. Amin, O. Konopatskaya, M.A. Saleem, A.J. Churchill, M.R. Ladomery, S.J. Harper, D.O. Bates, Expression of pro- and anti-angiogenic isoforms of VEGF is differentially regulated by splicing and growth factors, *J. Cell. Sci.* 121 (2008) 3487–3495.
- [26] H.S. Bevan, N.M. van den Akker, Y. Qiu, J.A. Polman, R.R. Foster, J. Yem, A. Nishikawa, S.C. Satchell, S.J. Harper, A.C. Gittenberger-de Groot, D.O. Bates, The alternatively spliced anti-angiogenic family of VEGF isoforms VEGFxxx in human kidney development, *Nephron, Physiol.* 110 (2008) 57–67.
- [27] R.O. Pritchard-Jones, D.B. Dunn, Y. Qiu, A.H. Varey, A. Orlando, H. Rigby, S.J. Harper, D.O. Bates, Expression of VEGFxxx, the inhibitory isoforms of VEGF, in malignant melanoma, *Br. J. Cancer* 97 (2007) 223–230.
- [28] A.H. Varey, E.S. Renne, Y. Qiu, H.S. Bevan, R.M. Perrin, S. Raffy, A.R. Dixon, C. Paraskeva, O. Zacheo, A.B. Hassan, S.J. Harper, D.O. Bates, VEGF165b, an antiangiogenic VEGF-A isoform, binds and inhibits bevacizumab treatment in experimental colorectal carcinoma: balance of pro- and antiangiogenic VEGF-A isoforms has implications for therapy, *Br. J. Cancer* 98 (2008) 1366–1379.
- [29] S. Cêbe-Suarez, M. Pieren, L. Cariolato, S. Arn, U. Hoffmann, A. Bogucki, C. Manlius, J. Wood, K. Ballmer-Hofer, A VEGF-A splice variant defective for heparan sulfate and neuropilin-1 binding shows attenuated signaling through VEGFR-2, *Cell. Mol. Life Sci.* 63 (2006) 2067–2077.
- [30] C.A. Glass, S.J. Harper, D.O. Bates, The anti-angiogenic vascular endothelial growth factor isoform, VEGF165b transiently increases hydraulic conductivity, probably through VEGF receptor 1 *in vivo*, *J. Physiol.* 572 (2006) 243–257.
- [31] C. Ruhrberg, G. Gerhardt, M. Golding, R. Watson, S. Ioannidou, H. Fujisawa, C. Betsholtz, D.T. Shima, Spatially restricted patterning cues provided by heparin-binding VEGF-A control blood vessel branching morphogenesis, *Genes Dev.* 16 (2002) 2684–2698.
- [32] M. Shibuya, S. Yamaguchi, A. Yamane, T. Ikeda, A. Tojo, H. Matsushime, M. Sato, Nucleotide sequence and expression of a novel human receptor- type tyrosine kinase gene (flt) closely related to the fms family, *Oncogene* 5 (1990) 519–524.
- [33] B.I. Terman, M.E. Carrion, E. Kovacs, B.A. Rasmussen, R.L. Eddy, T.B. Shows, Identification of a new endothelial cell growth factor receptor tyrosine kinase, *Oncogene* 6 (1991) 1677–1683.
- [34] K. Pajusola, O. Aprelikova, J. Korhonen, A. Kaipainen, L. Pertovaara, R. Alitalo, K. Alitalo, FLT4 receptor tyrosine kinase contains seven immunoglobulin-like loops and is expressed in multiple human tissues and cell lines, *Cancer Res.* 52 (1992) 5738–5743.
- [35] G. Neufeld, O. Kessler, Y. Herzog, The interaction of Neuropilin-1 and Neuropilin-2 with tyrosine-kinase receptors for VEGF, *Adv. Exp. Med. Biol.* 515 (2002) 81–90.
- [36] S. Tessier, P. Rockwell, D. Hicklin, T. Cohen, B.Z. Levi, L. Witte, L.R. Lemischka, G. Neufeld, Heparin modulates the interaction of VEGF165 with soluble and cell associated flk-1 receptors, *J. Biol. Chem.* 269 (1994) 12456–12461.
- [37] M. Errico, T. Riccioni, S. Iyer, C. Pisano, K.R. Acharya, G.M. Persico, F.S. De, Identification of placental growth factor determinants for binding and activation of Flt-1 receptor, *J. Biol. Chem.* 279 (2004) 43929–43939.
- [38] B. Olofsson, E. Korpelainen, M.S. Pepper, S.J. Mandriota, K. Aase, V. Kumar, Y. Gunji, M.M. Jeltsch, M. Shibuya, K. Alitalo, U. Eriksson, Vascular endothelial growth factor B (VEGF-B) binds to VEGF receptor-1 and regulates plasminogen activator activity in endothelial cells, *Proc. Natl. Acad. Sci. U. S. A.* 95 (1998) 11709–11714.
- [39] S. Cêbe-Suarez, F.S. Grinewald, R. Jaussi, X. Li, L. Claesson-Welsh, D. Spillmann, A.A. Mercer, A.E. Prota, K. Ballmer-Hofer, Orf virus VEGF-E N22 promotes paracellular NRP-1/VEGFR-2 coreceptor assembly via the peptide RPPR, *FASEB J.* 22 (2008) 3078–3086.
- [40] T. Kawasaki, T. Kitsuikawa, Y. Bekku, Y. Matsuda, M. Sanbo, T. Yagi, H. Fujisawa, A requirement for neuropilin-1 in embryonic vessel formation, *Development* 126 (1999) 4895–4902.
- [41] G. Neufeld, T. Cohen, N. Shraga, T. Lange, O. Kessler, Y. Herzog, The neuropilins: multifunctional semaphorin and VEGF receptors that modulate axon guidance and angiogenesis, *Trends Cardiovasc. Med.* 12 (2002) 13–19.
- [42] H. Gerhardt, M. Golding, M. Fruttiger, C. Ruhrberg, A. Lundkvist, A. Abramsson, M. Jeltsch, C. Mitchell, K. Alitalo, D. Shima, C. Betsholtz, VEGF guides angiogenic sprouting utilizing endothelial tip cell filopodia, *J. Cell Biol.* 161 (2003) 1163–1177.
- [43] H. Gerhardt, C. Ruhrberg, A. Abramsson, H. Fujisawa, D. Shima, C. Betsholtz, Neuropilin-1 is required for endothelial tip cell guidance in the developing central nervous system, *Dev. Dyn.* 231 (2004) 503–509.
- [44] C. Ruch, G. Skiniotis, M.O. Steinmetz, T. Walz, K. Ballmer-Hofer, Structure of a VEGF-VEGF receptor complex determined by electron microscopy, *Nat. Struct. Mol. Biol.* 14 (2007) 249–250.
- [45] S. Yuzawa, Y. Opatowsky, Z. Zhang, V. Mandiyan, I. Lax, J. Schlessinger, Structural basis for activation of the receptor tyrosine kinase KIT by stem cell factor, *Cell* 130 (2007) 323–334.
- [46] Y. Yang, S. Yuzawa, J. Schlessinger, Contacts between membrane proximal regions of the PDGF receptor ectodomain are required for receptor activation but not for receptor dimerization, *Proc. Natl. Acad. Sci. U. S. A.* 105 (2008) 7681–7686.
- [47] J. Schlessinger, M.A. Lemmon, SH2 and PTB domains in tyrosine kinase signaling, *Sci. STKE* 2003 (2003) RE12.
- [48] S. Cêbe-Suarez, A.H. Zehnder-Fjällman, K. Ballmer-Hofer, The role of VEGF receptors in angiogenesis: complex partnerships, *Cell. Mol. Life Sci.* 63 (2006) 601–615.
- [49] M. Shibuya, L. Claesson-Welsh, Signal transduction by VEGF receptors in regulation of angiogenesis and lymphangiogenesis, *Exp. Cell Res.* 312 (2005) 549–560.
- [50] T. Matsumoto, S. Bohman, J. Dixelius, T. Berge, A. Dimberg, P. Magnusson, L. Wang, C. Wikner, J.H. Qi, C. Wernstedt, J. Wu, S. Brubeim, H. Mugishima, D. Mukhopadhyay, A. Spurkland, L. Claesson-Welsh, VEGF receptor-2 Y951 signaling and a role for the adapter molecule TSAd in tumor angiogenesis, *EMBO J.* 24 (2005) 2342–2353.
- [51] R.L. Kendall, R.Z. Rutledge, X. Mao, A.J. Tebben, R.W. Hungate, K. Thomas, Vascular endothelial growth factor receptor KDR tyrosine kinase activity is increased by autophosphorylation of two activation loop tyrosine residues, *J. Biol. Chem.* 274 (1999) 6453–6460.
- [52] S.A. Cunningham, M.P. Arrate, T.A. Brock, M.N. Waxham, Interactions of FLT-1 and KDR with phospholipase C-γ: identification of the phosphotyrosine binding sites, *Biochem. Biophys. Res. Commun.* 240 (1997) 635–639.
- [53] Y. Nishizuka, The role of protein kinase C in cell surface signal transduction and tumour promotion, *Nature* 308 (1984) 693–698.
- [54] T. Takahashi, H. Ueno, M. Shibuya, VEGF activates protein kinase C-dependent, but Ras-independent Raf-MEK-MAP kinase pathway for DNA synthesis in primary endothelial cells, *Oncogene* 18 (1999) 2221–2230.
- [55] A.M. Doanes, D.D. Hegland, R. Sethi, I. Kovetski, J.T. Bruder, T. Finkel, VEGF stimulates MAPK through a pathway that is unique for receptor tyrosine kinases, *Biochem. Biophys. Res. Commun.* 255 (1999) 545–548.
- [56] L.W. Wu, L.D. Mayo, J.D. Dunbar, K.M. Kessler, M.R. Baerwald, E.A. Jaffe, D. Wang, R.S. Warren, D.B. Donner, Utilization of distinct signaling pathways by receptors for vascular endothelial cell growth factor and other mitogens in the induction of endothelial cell proliferation, *J. Biol. Chem.* 275 (2000) 5096–5103.
- [57] L.W. Wu, L.D. Mayo, J.D. Dunbar, K.M. Kessler, O.N. Ozes, R.S. Warren, D.B. Donner, VRAP is an adaptor protein that binds KDR, a receptor for vascular endothelial cell growth factor, *J. Biol. Chem.* 275 (2000) 6059–6062.
- [58] K. Holmqvist, M.J. Cross, C. Rolny, R. Hägerkvist, N. Rahimi, T. Matsumoto, L. Claesson-Welsh, M. Welsh, The adaptor protein Shb binds to tyrosine 1175 in the vascular endothelial growth factor (VEGF) receptor-2 and regulates VEGF-dependent cellular migration, *J. Biol. Chem.* 279 (2004) 22267–22275.
- [59] M. Laramée, C. Chabot, M. Cloutier, R. Stenne, M. Holgado-Madruga, A.J. Wong, I. Royal, The scaffolding adapter Gab1 mediates VEGF signaling and is required for endothelial cell migration and capillary formation, *J. Biol. Chem.* 282 (2007) 7785–7789.
- [60] M. Dance, A. Montagner, A. Yart, B. Masri, Y. Audigier, B. Perret, J.P. Salles, P. Raynal, The adaptor protein Gab1 couples the stimulation of vascular endothelial growth factor receptor-2 to the activation of phosphoinositide 3-kinase, *J. Biol. Chem.* 281 (2006) 23285–23295.
- [61] L. Lamalice, F. Houle, G. Jourdan, J. Huot, Phosphorylation of tyrosine 1214 on VEGFR2 is required for VEGF-induced activation of Cdc42 upstream of SAPK2/p38, *Oncogene* 23 (2004) 434–445.
- [62] L. Lamalice, F. Houle, J. Huot, Phosphorylation of Tyr1214 within VEGFR-2 triggers the recruitment of Nck and activation of Fyn leading to SAPK2/p38 activation and endothelial cell migration in response to VEGF, *J. Biol. Chem.* 281 (2006) 34009–34020.
- [63] H.P. Gerber, A. McMurtrey, J. Kowalski, M. Yan, B.A. Keyt, V. Dixit, N. Ferrara, Vascular endothelial growth factor regulates endothelial cell survival through the phosphatidylinositol 3'-kinase/Akt signal transduction pathway. Requirement for Flk-1/KDR activation, *J. Biol. Chem.* 273 (1998) 30336–30343.
- [64] K. Kawasaki, T. Watabe, H. Sase, M. Hirasawa, H. Koide, Y. Morishita, K. Yuki, T. Sasaoka, T. Suda, M. Katsuki, K. Miyazono, K. Miyazawa, Ras signaling directs endothelial specification of VEGFR2⁺ vascular progenitor cells, *J. Cell Biol.* 181 (2008) 131–141.
- [65] M.A.B.A. Dennissen, G.J. Jenniskens, M. Pieffers, E.M.M. Versteeg, M. Petitou, J.H. Veerkamp, T.H. Van Kuppevelt, Large, tissue-regulated domain diversity of heparan sulfates demonstrated by phage display antibodies, *J. Biol. Chem.* 277 (2002) 10982–10986.
- [66] M. Salmivirta, K. Lidholt, U. Lindahl, Heparan sulfate: a piece of information, *FASEB J.* 10 (1996) 1270–1279.
- [67] S.E. Stringer, J.T. Gallagher, Heparan sulphate, *Int. J. Biochem. Cell Biol.* 29 (1997) 709–714.
- [68] J.D. Esko, S.B. Selleck, Order out of chaos: assembly of ligand binding sites in heparan sulfate, *Annu. Rev. Biochem.* 71 (2002) 435–471.
- [69] S. Takagi, T. Tsuji, T. Amagai, T. Takamatsu, H. Fujisawa, Specific cell surface labels in the visual centers of *Xenopus laevis* tadpole identified using monoclonal antibodies, *Dev. Biol.* 122 (1987) 90–100.
- [70] Z. He, M. Tessier-Lavigne, Neuropilin is a receptor for the axonal chemorepellent Semaphorin III, *Cell* 90 (1997) 739–751.

- [71] F. Nakamura, M. Tanaka, T. Takahashi, R.G. Kalb, S.M. Strittmatter, Neuropilin-1 extracellular domains mediate semaphorin D/III-induced growth cone collapse, *Neuron* 21 (1998) 1093–1100.
- [72] T. Kitsukawa, M. Shimizu, M. Sanbo, T. Hirata, M. Taniguchi, Y. Bekku, T. Yagi, H. Fujisawa, Neuropilin semaphorin III/D-mediated chemorepulsive signals play a crucial role in peripheral nerve projection in mice, *Neuron* 19 (1997) 995–1005.
- [73] A.L. Kolodkin, D.V. Levengood, E.G. Rowe, Y.T. Tai, R.J. Giger, D.D. Ginty, Neuropilin is a semaphorin III receptor, *Cell* 90 (1997) 753–762.
- [74] H. Chen, A. Chedotal, Z. He, C.S. Goodman, M. Tessier-Lavigne, Neuropilin-2, a novel member of the neuropilin family, is a high affinity receptor for the semaphorins Sema E and Sema IV but not Sema III, *Neuron* 19 (1997) 547–559.
- [75] T. Kitsukawa, A. Shimono, A. Kawakami, H. Kondoh, H. Fujisawa, Overexpression of a membrane protein, neuropilin, in chimeric mice causes anomalies in the cardiovascular system, nervous system and limbs, *Development* 121 (1995) 4309–4318.
- [76] S. Soker, H. Fidder, G. Neufeld, M. Klagsbrun, Characterization of novel vascular endothelial growth factor (VEGF) receptors on tumor cells that bind VEGF165 via its exon 7- encoded domain, *J. Biol. Chem.* 271 (1996) 5761–5767.
- [77] S. Soker, S. Takashima, H.Q. Miao, G. Neufeld, M. Klagsbrun, Neuropilin-1 is expressed by endothelial and tumor cells as an isoform-specific receptor for vascular endothelial growth factor, *Cell* 92 (1998) 735–745.
- [78] G. Fuh, K.C. Garcia, A.M. de Vos, The interaction of neuropilin-1 with vascular endothelial growth factor and its receptor flt-1, *J. Biol. Chem.* 275 (2000) 26690–26695.
- [79] B. Favier, A. Alam, P. Barron, J. Bonnin, P. Laboudie, P. Fons, M. Mandron, J.P. Herault, G. Neufeld, P. Savi, J.M. Herbert, F. Bono, Neuropilin-2 interacts with VEGFR-2 and VEGFR-3 and promotes human endothelial cells survival and migration, *Blood* 108 (2006) 1243–1250.
- [80] D.C. West, C.G. Rees, L. Duchesne, S.J. Patey, C.J. Terry, J.E. Turnbull, M. Delehedde, C.W. Heegaard, F. Allain, C. Vanpouille, D. Ron, D.G. Fernig, Interactions of multiple heparin binding growth factors with neuropilin-1 and potentiation of the activity of fibroblast growth factor-2, *J. Biol. Chem.* 280 (2005) 13457–13464.
- [81] T. Takahashi, A. Fournier, F. Nakamura, L.H. Wang, Y. Murakami, R.G. Kalb, H. Fujisawa, S.M. Strittmatter, Plexin-neuropilin-1 complexes form functional semaphorin-3A receptors, *Cell* 99 (1999) 59–69.
- [82] V. Castellani, E. De Angelis, S. Kenrick, G. Rougon, *Cis* and *trans* interactions of L1 with neuropilin-1 control axonal responses to semaphorin 3A, *EMBO J.* 21 (2002) 6348–6357.
- [83] M. Fukasawa, A. Matsushita, M. Korc, Neuropilin-1 interacts with integrin β 1 and modulates pancreatic cancer cell growth, survival and invasion, *Cancer Biol. Ther.* 6 (2007) 1173–1180.
- [84] H. Cai, R.R. Reed, Cloning and characterization of neuropilin-1-interacting protein: a PSD-95/Dlg/ZO-1 domain-containing protein that interacts with the cytoplasmic domain of neuropilin-1, *J. Neurosci.* 19 (1999) 6519–6527.
- [85] S.H. Hsieh, N.W. Ying, M.H. Wu, W.F. Chiang, C.L. Hsu, T.Y. Wong, Y.T. Jin, T.M. Hong, Y.L. Chen, Galectin-1, a novel ligand of neuropilin-1, activates VEGFR-2 signaling and modulates the migration of vascular endothelial cells, *Oncogene* 27 (2008) 3746–3753.
- [86] R. Mamluk, Z. Gerechtman, M.E. Kutcher, N. Gasianus, J. Gallagher, M. Klagsbrun, Neuropilin-1 binds vascular endothelial growth factor 165, placenta growth factor-2, and heparin via its b1b2 domain, *J. Biol. Chem.* 277 (2002) 24818–24825.
- [87] G.B. Whitaker, B.J. Limberg, J.S. Rosenbaum, Vascular endothelial growth factor receptor-2 and neuropilin-1 form a receptor complex that is responsible for the differential signaling potency of VEGF165 and VEGF121, *J. Biol. Chem.* 276 (2001) 25520–25531.
- [88] S. Soker, H.Q. Miao, M. Nomi, S. Takashima, M. Klagsbrun, VEGF(165) mediates formation of complexes containing VEGFR-2 and neuropilin-1 that enhance VEGF165-receptor binding, *J. Cell Biochem.* 85 (2002) 357–368.
- [89] R.E. Bachelder, A. Crago, J. Chung, M.A. Wendt, L.M. Shaw, G. Robinson, A.M. Mercurio, Vascular endothelial growth factor is an autocrine survival factor for neuropilin-expressing breast carcinoma cells, *Cancer Res.* 61 (2001) 5736–5740.
- [90] M. Murga, O. Fernandez-Capetillo, G. Tosato, Neuropilin-1 regulates attachment in human endothelial cells independently of vascular endothelial growth factor receptor-2, *Blood* 105 (2005) 1992–1999.
- [91] L. Wang, H. Zeng, P. Wang, S. Soker, D. Mukhopadhyay, Neuropilin-1-mediated vascular permeability factor/vascular endothelial growth factor (VPF/VEGF)-dependent endothelial cell migration, *J. Biol. Chem.* 281 (2003) 48848–48860.
- [92] L. De Vries, X. Lou, G. Zhao, B. Zheng, M.G. Farquhar, GIPC, a PDZ domain containing protein, interacts specifically with the C terminus of RGS-GAIP, *Proc. Natl. Acad. Sci. U. S. A.* 95 (1998) 12340–12345.
- [93] L. Wang, D. Mukhopadhyay, X. Xu, C terminus of RGS-GAIP-interacting protein conveys neuropilin-1-mediated signaling during angiogenesis, *FASEB J.* 20 (2006) 1513–1515.
- [94] M. Narazaki, G. Tosato, Ligand-induced internalization selects usage of common receptor Neuropilin-1 by VEGF165 and Semaphorin3A, *Blood* 107 (2006) 3892–3901.
- [95] A. Salikhova, L. Wang, A.A. Lanahan, M. Liu, M. Simons, W.P. Leenders, D. Mukhopadhyay, A. Horowitz, Vascular endothelial growth factor and semaphorin induce neuropilin-1 endocytosis via separate pathways, *Circ. Res.* 103 (2008) e71–e79.
- [96] D. Valdembrì, P.T. Caswell, K.I. Anderson, J.P. Schwarz, I. König, E. Astanina, F. Caccavari, J.C. Norman, M.J. Humphries, F. Bussolino, G. Serini, Neuropilin-1/GIPC1 signaling regulates α 5 β 1 integrin traffic and function in endothelial cells, *PLoS Biol.* 7 (2009) e25.
- [97] C. Prahst, M. Heroult, A.A. Lanahan, N. Uziel, O. Kessler, N. Shraga-Heled, M. Simons, G. Neufeld, H.G. Augustin, Neuropilin-1-VEGFR-2 complexing requires the PDZ-binding domain of neuropilin-1, *J. Biol. Chem.* 283 (2008) 25110–25114.
- [98] D. Krilleke, A. Deerkenez, W. Schubert, I. Giri, G.S. Robinson, Y.S. Ng, D.T. Shima, Molecular mapping and functional characterization of the VEGF164 heparin-binding domain, *J. Biol. Chem.* 282 (2007) 28045–28056.
- [99] M.E. Stauffer, N.J. Skelton, W.J. Fairbrother, Refinement of the solution structure of the heparin-binding domain of vascular endothelial growth factor using residual dipolar couplings, *J. Biomol. NMR* 23 (2002) 57–61.
- [100] T. Lange, N. Gutman-Raviv, L. Baruch, M. Machluf, G. Neufeld, VEGF162: a new heparin binding VEGF splice form that is expressed in transformed human cells, *J. Biol. Chem.* 278 (2003) 17164–17169.
- [101] C.J. Robinson, B. Mulloy, J.T. Gallagher, S.E. Stringer, VEGF165-binding sites within heparan sulfate encompass two highly sulfated domains and can be liberated by K5 lyase, *J. Biol. Chem.* 281 (2006) 1731–1740.
- [102] K. Ono, H. Hattori, S. Takeshita, A. Kurita, M. Ishihara, Structural features in glycan that interact with VEGF165 and modulate its biological activity, *Glycobiology* 9 (1999) 705–711.
- [103] R.V. Iozzo, Basement membrane proteoglycans: from cellar to ceiling, *Nat. Rev., Mol. Cell Biol.* 6 (2005) 646–656.
- [104] H. Gitay-Goren, S. Soker, I. Vlodavsky, G. Neufeld, The binding of vascular endothelial growth factor to its receptors is dependent on cell surface-associated heparin-like molecules, *J. Biol. Chem.* 267 (1992) 6093–6098.
- [105] B.I. Terman, L. Khandke, M. Dougher-Vermazan, D. Maglione, N.J. Lassam, D. Gospodarowicz, M.G. Persico, P. Böhlen, M. Eisinger, VEGF receptor subtypes KDR and FLT1 show different sensitivities to heparin and placenta growth factor, *Growth Factors* 11 (1994) 187–195.
- [106] J.B. Kaplan, L. Sridharan, J.A. Zaccardi, M. Dougher-Vermazan, B.I. Terman, Characterization of a soluble vascular endothelial growth factor receptor-immunoglobulin chimera, *Growth Factors* 14 (1997) 243–256.
- [107] S. Soker, D. Goldstaub, C.M. Svahn, I. Vlodavsky, B.Z. Levi, G. Neufeld, Variations in the size and sulfation of heparin modulate the effect of heparin on the binding of VEGF165 to its receptors, *Biochem. Biophys. Res. Commun.* 203 (1994) 1339–1347.
- [108] A.M. Dougher, H. Wasserstrom, L. Torley, L. Shridaran, P. Westdock, R.E. Hileman, J.R. Fromm, R. Anderberg, S. Lyman, R.J. Linhardt, J. Kaplan, B.I. Terman, Identification of a heparin binding peptide on the extracellular domain of the KDR VEGF receptor, *Growth Factors* 14 (1997) 257–268.
- [109] H. Gitay-Goren, T. Cohen, S. Tessler, S. Soker, S. Gengrinovitch, P. Rockwell, M. Klagsbrun, B.Z. Levi, G. Neufeld, Selective binding of VEGF121 to one of the three vascular endothelial growth factor receptors of vascular endothelial cells, *J. Biol. Chem.* 271 (1996) 5519–5523.
- [110] M.K. Chiang, J.G. Flanagan, Interactions between the Flk-1 receptor, vascular endothelial growth factor, and cell surface proteoglycan identified with a soluble receptor reagent, *Growth Factors* 12 (1995) 1–10.
- [111] M. Di Benedetto, A. Starzec, R. Vassy, G.Y. Perret, M. Crépin, Distinct heparin binding sites on VEGF165 and its receptors revealed by their interaction with a non sulfated glycoaminoglycan (NaPaC), *Biochim. Biophys. Acta* 1780 (2008) 723–732.
- [112] M.A. von Wronski, N. Raju, R. Pillai, N.J. Bogdan, E.R. Marinelli, P. Nanjappan, K. Ramalingam, T. Arunachalam, S. Eaton, K.E. Linder, F. Yan, S. Pochon, M.F. Tweedle, A.D. Nunn, Tuftsin binds neuropilin-1 through a sequence similar to that encoded by exon 8 of VEGF, *J. Biol. Chem.* 281 (2006) 5702–5710.
- [113] T.R. Binetruy-Tournaire, C. Demangel, B. Malavaud, R. Vassy, S. Rouyre, M. Kraemer, J. Plouët, C. Derbin, G. Perret, J.C. Mazie, Identification of a peptide blocking vascular endothelial growth factor (VEGF)-mediated angiogenesis, *EMBO J.* 19 (2000) 1525–1533.
- [114] A. Starzec, R. Vassy, A. Martin, M. Lecouvey, M. Di Benedetto, M. Crépin, G.Y. Perret, Antiangiogenic and antitumor activities of peptide inhibiting the vascular endothelial growth factor binding to neuropilin-1, *Life Sci.* 79 (2006) 2370–2381.
- [115] A. Starzec, P. Ladam, R. Vassy, S. Badache, N. Bouchemal, A. Navaza, C.H. du Penhoat, G.Y. Perret, Structure-function analysis of the antiangiogenic ATWLPFR peptide inhibiting VEGF165 binding to neuropilin-1 and molecular dynamics simulations of the ATWLPFR/neuropilin-1 complex, *Peptides* 28 (2007) 2397–2402.
- [116] M.A. von Wronski, M.F. Tweedle, A.D. Nunn, Binding of the C-terminal amino acids of VEGF121 directly with neuropilin-1 should be considered, *FASEB J.* 21 (2007) 1292.
- [117] Q. Pan, Y. Chanthery, Y. Wu, N. Rahtore, R.K. Tong, F. Peale, A. Bagri, M. Tessier-Lavigne, A.W. Koch, R.J. Watts, Neuropilin-1 binds to VEGF121 and regulates endothelial cell migration and sprouting, *J. Biol. Chem.* 282 (2007) 24049–24056.
- [118] W.J. Fairbrother, M.A. Champe, H.W. Christinger, B.A. Keyt, M.A. Starovasinik, Solution structure of the heparin-binding domain of vascular endothelial growth factor, *Structure* 6 (1998) 637–648.
- [119] R.C. Keck, L. Berleau, R. Harris, B.A. Keyt, Disulfide structure of the heparin binding domain in vascular endothelial growth factor: characterization of posttranslational modifications in VEGF, *Arch. Biochem. Biophys.* 344 (1997) 103–113.
- [120] K.P. Claffey, D.R. Senger, B.M. Spiegelman, Structural requirements for dimerization, glycosylation, secretion, and biological function of VPF/VEGF, *Biochim. Biophys. Acta* 1246 (1995) 1–9.
- [121] H. Kawamura, X. Li, K. Goishi, L.A. van Meeteren, L. Jakobsson, S. Cêbe-Suarez, A. Shimizu, D. Edholm, K. Ballmer-Hofer, L. Kjellen, M. Klagsbrun, L. Claesson-Welsh, Neuropilin-1 in regulation of VEGF-induced activation of p38MAPK and endothelial cell organization, *Blood* 112 (2008) 3638–3649.

- [122] M.A. McTigue, J.A. Wickersham, C. Pinko, R.E. Showalter, C.V. Parast, R.A. Tempczyk, M.R. Gehring, B. Mroczkowski, C.C. Kan, J.E. Villafranca, K. Appelt, Crystal structure of the kinase domain of human vascular endothelial growth factor receptor 2: a key enzyme in angiogenesis, *Structure* 7 (1999) 319–330.
- [123] H. Kawamura, X. Li, S.J. Harper, D.O. Bates, L. Claesson-Welsh, Vascular endothelial growth factor (VEGF)-A165b is a weak in vitro agonist for VEGF receptor-2 due to lack of coreceptor binding and deficient regulation of kinase activity, *Cancer Res.* 68 (2008) 4683–4692.
- [124] Z. Gluzman-Poltorak, T. Cohen, Y. Herzog, G. Neufeld, Neupilin-2 and neupilin-1 are receptors for the 165-amino acid form of vascular endothelial growth factor (VEGF) and of placenta growth factor-2, but only neupilin-2 functions as a receptor for the 145-amino acid form of VEGF, *J. Biol. Chem.* 275 (2000) 18040–18045.
- [125] Q. Pan, Y. Chanthery, W.C. Liang, S. Stawicki, J. Mak, N. Rathore, R.K. Tong, J. Kowalski, S.F. Yee, G. Pacheco, S. Ross, Z. Cheng, C.J. Le, G. Plowman, F. Peale, A.W. Koch, Y. Wu, A. Bagri, M. Tessier-Lavigne, R.J. Watts, Blocking neupilin-1 function has an additive effect with anti-VEGF to inhibit tumor growth, *Cancer Cell* 11 (2007) 53–67.
- [126] C.W. Vander Kooi, M.A. Jusino, B. Perman, D.B. Neau, H.D. Bellamy, D.J. Leahy, Structural basis for ligand and heparin binding to neupilin B domains, *Proc. Natl. Acad. Sci. U. S. A.* 104 (2007) 6152–6157.
- [127] L. Roth, C. Nasarre, S. Dirrig-Grosch, D. Aunis, G. Crémel, P. Hubert, D. Bagnard, Transmembrane domain interactions control biological functions of neupilin-1, *Mol. Biol. Cell* 19 (2008) 646–654.
- [128] M.J. Renzi, L. Feiner, A.M. Koppel, J.A. Raper, A dominant negative receptor for specific secreted semaphorins is generated by deleting an extracellular domain from neupilin-1, *J. Neurosci.* 19 (1999) 7870–7880.
- [129] H. Chen, Z. He, A. Bagri, M. Tessier-Lavigne, Semaphorin–neupilin interactions underlying sympathetic axon responses to class III semaphorins, *Neuron* 21 (1998) 1283–1290.
- [130] R.J. Giger, E.R. Urquhart, S.K. Gillespie, D.V. Levegood, D.D. Ginty, A.L. Kolodkin, Neupilin-2 is a receptor for semaphorin IV: insight into the structural basis of receptor function and specificity, *Neuron* 21 (1998) 1079–1092.
- [131] Y. Yamada, N. Takakura, H. Yasue, H. Ogawa, H. Fujisawa, T. Suda, Exogenous clustered neupilin 1 enhances vasculogenesis and angiogenesis, *Blood* 97 (2001) 1671–1678.
- [132] Y. Shintani, S. Takashima, Y. Asano, H. Kato, Y. Liao, S. Yamazaki, O. Tsukamoto, O. Seguchi, H. Yamamoto, T. Fukushima, K. Sugahara, M. Kitakaze, M. Hori, Glycosaminoglycan modification of neupilin-1 modulates VEGFR2 signaling, *EMBO J.* 25 (2006) 3045–3055.
- [133] L. Jakobsson, J. Kreuger, K. Holmborn, L. Lundin, I. Eriksson, L. Kjellen, L. Claesson-Welsh, Heparan sulfate in *trans* potentiates VEGFR-mediated angiogenesis, *Dev. Cell* 10 (2006) 625–634.
- [134] E. Chen, S.E. Stringer, M.A. Rusch, S.B. Selleck, S.C. Ekker, A unique role for 6-O sulfation modification in zebrafish vascular development, *Dev. Biol.* 284 (2005) 364–376.
- [135] I. Stalmans, Y.S. Ng, R. Rohan, M. Fruttiger, A. Bouche, A. Yuce, H. Fujisawa, B. Hermans, M. Shani, S. Jansen, D. Hicklin, D.J. Anderson, T. Gardiner, H.P. Hammes, L. Moons, M. Dewerchin, D. Collen, P. Carmeliet, P.A. D'Amore, Arteriolar and venular patterning in retinas of mice selectively expressing VEGF isoforms, *J. Clin. Invest.* 109 (2002) 327–336.
- [136] C. Galambos, Y.S. Ng, A. Ali, A. Noguchi, S. Lovejoy, P.A. D'Amore, D.E. Demello, Defective pulmonary development in the absence of heparin-binding vascular endothelial growth factor isoforms, *Am. J. Respir. Cell Mol. Biol.* 27 (2002) 194–203.
- [137] P. Carmeliet, Y.S. Ng, D. Nuyens, G. Theilmeier, K. Brusselmans, I. Cornelissen, E. Ehler, V.V. Kakkar, I. Stalmans, V. Mattot, J. Perriard, M. Dewerchin, W. Flameng, A. Nagy, F. Lupu, L. Moons, D. Collen, P.A. Amore, D.T. Shima, Impaired myocardial angiogenesis and ischemic cardiomyopathy in mice lacking the vascular endothelial growth factor isoforms VEGF164 and VEGF188, *Nat. Med.* 5 (1999) 495–502.
- [138] J. Grunstein, J.J. Masbad, R. Hickey, F. Giordano, R.S. Johnson, Isoforms of vascular endothelial growth factor act in a coordinate fashion to recruit and expand tumor vasculature, *Mol. Cell. Biol.* 20 (2000) 7282–7291.
- [139] J.M. Whitelock, J. Melrose, R.V. Iozzo, Diverse cell signaling events modulated by perlecan, *Biochemistry* 47 (2008) 11174–11183.
- [140] J.J. Zoeller, J.M. Whitelock, R.V. Iozzo, Perlecan regulates developmental angiogenesis by modulating the VEGF-VEGFR2 axis, *Matrix Biol.* 28 (2009) 284–291.
- [141] C. Savorè, C. Zhang, C. Muir, R. Liu, J. Wyrwa, J. Shu, H.E. Zhou, L.W. Chung, D.D. Carson, M.C. Farach-Carson, Perlecan knockdown in metastatic prostate cancer cells reduces heparin-binding growth factor responses in vitro and tumor growth in vivo, *Clin. Exp. Metastasis* 22 (2005) 377–390.
- [142] S. Gengrinovitch, B. Berlan, G. David, L. Witte, G. Neufeld, D. Ron, Glypican-1 is a VEGF165 binding proteoglycan that acts as an extracellular chaperone for VEGF165, *J. Biol. Chem.* 274 (1999) 10816–10822.
- [143] S. Iyer, D.D. Leonidas, G.J. Swaminathan, D. Maglione, M. Battisti, M. Tucci, M.G. Persico, K.R. Acharya, The crystal structure of human placenta growth factor-1 (PlGF-1), an angiogenic protein, at 2.0 Å resolution, *J. Biol. Chem.* 276 (2001) 12153–12161.
- [144] S. Iyer, P.D. Scotney, A.D. Nash, K.R. Acharya, Crystal structure of human vascular endothelial growth factor-B: identification of amino acids important for receptor binding, *J. Mol. Biol.* 359 (2006) 76–85.
- [145] Y.A. Muller, C. Heiring, R. Missetwitz, K. Wellfe, H. Wellfe, The cystine knot promotes folding and not thermodynamic stability in vascular endothelial growth factor, *J. Biol. Chem.* 277 (2002) 43410–43416.
- [146] Y.A. Muller, H.W. Christinger, B.A. Keyt, A.M. de Vos, The crystal structure of vascular endothelial growth factor (VEGF) refined to 1.93 Å resolution: multiple copy flexibility and receptor binding, *Structure* 5 (1997) 1325–1338.
- [147] C. Oefner, A. D'Arcy, F.K. Winkler, B. Eggimann, M. Hosang, Crystal structure of human platelet-derived growth factor BB, *EMBO J.* 11 (1992) 3921–3926.
- [148] M.P. Schlunegger, M.G. Grutter, An unusual feature revealed by the crystal structure at 2.2 Å resolution of human transforming growth factor-beta 2, *Nature* 358 (1992) 430–434.
- [149] K. Suto, Y. Yamazaki, T. Morita, H. Mizuno, Crystal structures of novel vascular endothelial growth factors (VEGF) from snake venoms: insight into selective VEGF binding to kinase insert domain-containing receptor but not to fms-like tyrosine kinase-1, *J. Biol. Chem.* 280 (2005) 2126–2131.
- [150] G. Fuh, B. Li, C. Crowley, B. Cunningham, J.A. Wells, Requirements for binding and signaling of the kinase domain receptor for vascular endothelial growth factor, *J. Biol. Chem.* 273 (1998) 11197–11204.
- [151] B. Olofsson, K. Pajusola, G.von Euler, D. Chilov, K. Alitalo, U. Eriksson, Genomic organization of the mouse and human genes for vascular endothelial growth factor B (VEGF-B) and characterization of a second splice isoform, *J. Biol. Chem.* 271 (1996) 19310–19317.
- [152] T. Mäkinen, B. Olofsson, T. Karpanen, U. Hellman, S. Soker, M. Klagsbrun, U. Eriksson, K. Alitalo, Differential binding of vascular endothelial growth factor B splice and proteolytic isoforms to neupilin-1, *J. Biol. Chem.* 274 (1999) 21217–21222.
- [153] P. Leonard, P.D. Scotney, T. Jabeen, S. Iyer, L.J. Fabri, A.D. Nash, K.R. Acharya, Crystal structure of vascular endothelial growth factor-B in complex with a neutralising antibody Fab fragment, *J. Mol. Biol.* 384 (2008) 1203–1217.
- [154] H.W. Christinger, G. Fuh, A.M. de Vos, C. Wiesmann, The crystal structure of PlGF in complex with domain 2 of VEGFR1, *J. Biol. Chem.* 279 (2004) 10382–10388.
- [155] V. Joukov, T. Sorsa, V. Kumar, M. Jeltsch, L. Claesson-Welsh, Y. Cao, O. Saksela, N. Kalkkinen, K. Alitalo, Proteolytic processing regulates receptor specificity and activity of VEGF-C, *EMBO J.* 16 (1997) 3898–3911.
- [156] V. Joukov, K. Pajusola, A. Kaipainen, D. Chilov, I. Lahtinen, E. Kukk, O. Saksela, N. Kalkkinen, K. Alitalo, A novel vascular endothelial growth factor, VEGF-C, is a ligand for the Flt4 (VEGFR-3) and KDR (VEGFR-2) receptor tyrosine kinases, *EMBO J.* 15 (1996) 290–298.
- [157] M. Jeltsch, T. Karpanen, T. Strandin, K. Aho, H. Lankinen, K. Alitalo, Vascular endothelial growth factor (VEGF)/VEGF-C mosaic molecules reveal specificity determinants and feature novel receptor binding patterns, *J. Biol. Chem.* 281 (2006) 12187–12195.
- [158] S.A. Stackler, K. Stenvers, C. Caesar, A. Vitali, T. Domagala, E. Nice, S. Roufaiil, R.J. Simpson, R. Moritz, T. Karpanen, K. Alitalo, M.G. Achen, Biosynthesis of vascular endothelial growth factor-D involves proteolytic processing which generates non-covalent homodimers, *J. Biol. Chem.* 274 (1999) 32127–32136.
- [159] P.I. Toivanen, T. Nieminen, L. Viitanen, A. Alitalo, M. Roschier, S. Jahniainen, J.E. Markkanen, O.H. Laitinen, T.T. Airenne, T.A. Salminen, M.S. Johnson, K.J. Airenne, S. Yla-Herttuala, Novel vascular endothelial growth factor D variants with increased biological activity, *J. Biol. Chem.* 284 (2009) 16037–16048.
- [160] M. Pieren, A. Prota, C. Ruch, D. Kostrewa, A. Wagner, K. Biedermann, F. Winkler, K. Ballmer-Hofer, Crystal structure of the Orf virus N22 variant of VEGF-E: implications for receptor specificity, *J. Biol. Chem.* 281 (2006) 19578–19587.
- [161] M.A. Starovassnik, H.W. Christinger, C. Wiesmann, M.A. Champe, A.M. de Vos, N.J. Skelton, Solution structure of the VEGF-binding domain of Flt-1: comparison of its free and bound states, *J. Mol. Biol.* 293 (1999) 531–544.
- [162] Y. Harpaz, C. Chothia, Many of the immunoglobulin superfamily domains in cell adhesion molecules and surface receptors belong to a new structural set which is close to that containing variable domains, *J. Mol. Biol.* 238 (1994) 528–539.
- [163] S. Takagi, T. Hirata, K. Agata, M. Mochii, G. Eguchi, H. Fujisawa, The A5 antigen, a candidate for the neuronal recognition molecule, has homologies to complement components and coagulation factors, *Neuron* 7 (1991) 295–307.
- [164] P. Bork, G. Beckmann, The CUB domain. A widespread module in developmentally regulated proteins, *J. Mol. Biol.* 231 (1993) 539–545.
- [165] C.C. Lee, A. Kreusch, D. McMullan, K. Ng, G. Spragg, Crystal structure of the human neupilin-1 b1 domain, *Structure* 11 (2003) 99–108.
- [166] B.A. Appleton, P. Wu, J. Maloney, J. Yin, W.C. Liang, S. Stawicki, K. Mortara, K.K. Bowman, J.M. Elliott, W. Desmarais, J.F. Bazan, A. Bagri, M. Tessier-Lavigne, A.W. Koch, Y. Wu, R.J. Watts, C. Wiesmann, Structural studies of neupilin/antibody complexes provide insights into semaphorin and VEGF binding, *EMBO J.* 26 (2007) 4902–4912.
- [167] K.P. Pratt, B.W. Shen, K. Takeshima, E.W. Davie, K. Fujikawa, B.L. Stoddard, Structure of the C2 domain of human factor VIII at 1.5 Å resolution, *Nature* 402 (1999) 439–442.
- [168] S. Macedo-Ribeiro, W. Bode, R. Huber, M.A. Quinn-Allen, S.W. Kim, T.L. Ortel, G.P. Bourenkov, H.D. Bartunik, M.T. Stubbs, W.H. Kane, P. Fuentes-Prior, Crystal structures of the membrane-binding C2 domain of human coagulation factor V, *Nature* 402 (1999) 434–439.
- [169] N. Ito, S.E. Phillips, C. Stevens, Z.B. Ogel, M.J. McPherson, J.N. Keen, K.D. Yadav, P.F. Knowles, Novel thioether bond revealed by a 1.7 Å crystal structure of galactose oxidase, *Nature* 350 (1991) 87–90.
- [170] W.L. DeLano, The PyMOL molecular graphics system, DeLano Scientific, 2002.
- [171] W. Rocchia, E. Alexov, B. Honig, Extending the applicability of the nonlinear Poisson–Boltzmann equation: multiple dielectric constants and multivalent ions, *J. Phys. Chem. B* 105 (2001) 6507–6514.
- [172] W. Rocchia, S. Sridharan, A. Nicholls, E. Alexov, A. Chiabrera, B. Honig, Rapid grid-based construction of the molecular surface and the use of induced surface charge to calculate reaction field energies: applications to the molecular systems and geometric objects, *J. Comput. Chem.* 23 (2002) 128–137.
- [173] D. Dell'Era Dosch, K. Ballmer-Hofer, Transmembrane domain-mediated orientation of receptor monomers in active VEGFR-2 dimers, *FASEB J.* 24 (2010) 32–38.

14 APPENDIX B

Author Manuscript Published OnlineFirst on June 28, 2011; DOI:10.1158/1078-0432.CCR-11-0379
Author manuscripts have been peer reviewed and accepted for publication but have not yet been edited.

Clinical Cancer Research



Novel functional germline variants in the vascular endothelial growth factor receptor 2 gene (*KDR*) and their effect on gene expression and microvessel density in lung cancer

Dylan M. Glubb, Elisa Cerri, Alexandra Giese, et al.

Clin Cancer Res Published OnlineFirst June 28, 2011.

Updated Version	Access the most recent version of this article at: doi: 10.1158/1078-0432.CCR-11-0379
Author Manuscript	Author manuscripts have been peer reviewed and accepted for publication but have not yet been edited.

E-mail alerts	Sign up to receive free email-alerts related to this article or journal.
Reprints and Subscriptions	To order reprints of this article or to subscribe to the journal, contact the AACR Publications Department at pubs@aacr.org .
Permissions	To request permission to re-use all or part of this article, contact the AACR Publications Department at permissions@aacr.org .

Author Manuscript Published OnlineFirst on June 28, 2011; DOI:10.1158/1078-0432.CCR-11-0379
Author manuscripts have been peer reviewed and accepted for publication but have not yet been edited.

1

**Novel functional germline variants in the vascular endothelial growth factor
receptor 2 gene and their effect on gene expression and microvessel density in lung
cancer**

Dylan M. Glubb^{1*}, Elisa Cerri^{1*}, Alexandra Giese², Wei Zhang³, Osman Mirza¹, Emma
E. Thompson⁴, Peixian Chen⁴, Soma Das⁴, Jacek Jassem⁵, Witold Rzyman⁶, Mark W.
Lingen⁷, Ravi Salgia¹, Fred R. Hirsch⁸, Rafal Dziadziuszko⁵, Kurt Ballmer-Hofer²,
Federico Innocenti^{1,9}

¹*Department of Medicine, University of Chicago, Chicago, Illinois*

²*Molecular Cell Biology, Paul Scherrer Institut, Villigen, Switzerland*

³*Department of Pediatrics, University of Illinois at Chicago, Chicago, Illinois*

⁴*Department of Human Genetics, University of Chicago, Chicago, Illinois*

⁵*Department of Oncology and Radiotherapy, Medical University of Gdansk, Gdansk,
Poland*

⁶*Department of Thoracic Surgery, Medical University of Gdansk, Gdansk, Poland*

⁷*Department of Pathology, University of Chicago, Chicago, Illinois*

⁸*Department of Medicine, University of Colorado Cancer Center, Aurora, Colorado*

⁹*Cancer Research Center, Committee on Clinical Pharmacology and Pharmacogenomics,
University of Chicago, Chicago, Illinois*

*These authors contributed equally

Running title: Novel functional *KDR* germline variations

2

Key-words: angiogenesis, *KDR*, resequencing, gene expression, NSCLC, functional validation

Financial support: NIH/NCI K07CA140390-01 (FI), Cancer Research Foundation Young Investigator Award (FI), American Cancer Society (FI), Grant ST-23 from Medical University of Gdansk (GD), NIH/NIGMS grant U01GM061393 (FI co-investigator, Ratain/Cox/Dolan PIs), NIH grant 5R01CA125541-04 (RS), Swiss National Science Foundation grant 3100A-116507 (KB-H).

Corresponding author: Federico Innocenti

Institute for Pharmacogenomics and Individualized
Therapy
University of North Carolina at Chapel Hill
CB 7361
120 Mason Farm Rd.
Chapel Hill
NC 27599-7361
Tel: 919-966-9422
Fax: 919-966-5863
E-mail: innocent@unc.edu

Word count: 4967

Number of figures and tables: 6

3

Translational relevance

Angiogenesis is a host-driven process which represents a crucial step in tumor development. The VEGFR-2 receptor mediates angiogenic endothelial cell responses via a downstream signaling pathway and its activity is targeted by several small molecule angiogenesis inhibitors. However, no biomarkers have yet been identified to guide the use of these drugs. We have characterized germline genetic variation of *KDR*, the gene encoding VEGFR-2, in three ethnic groups and identified functional variants which associate with *KDR* mRNA and protein levels, and microvessel density in non-small cell lung cancer tumor patient samples. These genetic variants provide strong candidates for the prospective testing of associations with patient outcome, the clinical effect of angiogenesis inhibitors, and other clinical cancer phenotypes related to angiogenesis.

Abstract

Purpose: VEGFR-2 plays a crucial role in mediating angiogenic endothelial cell responses via the VEGF pathway and angiogenesis inhibitors targeting VEGFR-2 are in clinical use. As angiogenesis is a host-driven process, functional heritable variation in *KDR*, the gene encoding VEGFR-2, may affect VEGFR-2 function, and ultimately, the extent of tumor angiogenesis.

Experimental Design: We resequenced *KDR* using 24 DNAs each from healthy Caucasian, African American and Asian groups. Non-synonymous genetic variants were assessed for function using phosphorylation assays. Luciferase reporter gene assays were used to examine effects of variants on gene expression. *KDR* mRNA and protein expression, and microvessel density (MVD) were measured in non-small cell lung cancer (NSCLC) tumor samples and matching patient DNA samples were genotyped to test for associations with variants of interest.

Results: *KDR* resequencing led to the discovery of 120 genetic variants, of which 25 had not been previously reported. Q472H had increased VEGFR-2 protein phosphorylation and associated with increased MVD in NSCLC tumor samples. -2854C and -2455A increased luciferase expression and associated with higher *KDR* mRNA levels in NSCLC samples. -271A reduced luciferase expression and associated with lower VEGFR-2 levels in NSCLC samples. -906C and 23408G, associated with higher *KDR* mRNA levels in NSCLC samples.

5

Conclusions: This study has defined *KDR* genetic variation in three populations and identified common variants that impact on tumoral *KDR* expression and vascularization. These findings may have important implications for understanding the molecular basis of genetic associations between *KDR* variation and clinical phenotypes related to VEGFR-2 function.

Introduction

VEGFR-2 (encoded by kinase insert domain receptor, *KDR*) is an important factor in tumor development and progression due to its pro-angiogenic effects (reviewed in (1)). VEGFR-2 levels correlate with tumor growth rate, microvessel density (MVD), proliferation, and tumor metastatic potential in several cancers (2, 3). Experimental blockage of the interaction between VEGF-A and VEGFR-2 inhibits tumor growth and metastasis (4). Indeed, angiogenesis inhibitors targeting the tyrosine kinase activity of VEGFR-2 are an effective class of anti-cancer drugs (5, 6). Although small molecule angiogenesis inhibitors interact with several targets, they are all characterized by a strong inhibitory activity of VEGFR-2 (7-9). In addition, the *in vivo* activity of one of them, sorafenib, is primarily mediated through VEGFR-2-mediated inhibition of angiogenesis (10).

Since gene expression in humans is in part determined by genetic factors (11) and angiogenesis is a host-mediated process (12), functional germline variation in *KDR* may contribute to variability in tumor endothelial function and, consequently, may affect cancer prognosis and the efficacy of VEGFR-2 inhibitors. Indeed, baseline soluble VEGFR-2 levels have been associated with a reduction in tumor size and clinical benefit in response to sunitinib treatment (13). Although no molecular marker is currently used to guide anti-angiogenesis therapy (14), the efforts towards identifying genetic prognostic biomarkers and predictive markers of response to VEGFR-2 inhibitors could be highly informed by studies characterizing *KDR* genetic variants. Furthermore, limited data are available on *KDR* germline genetic variation in the population, its ethnic differences and

7

its effect on gene function or tumoral expression. Hence, in this study, we defined common germline *KDR* variation in different ethnic groups and assessed the phenotypic impact of putative functional variants. These aims were achieved by resequencing healthy Caucasian, African American and Asian individuals; performing bioinformatic and *in vitro* functional analyses; and finally, rationally selecting variants to test their association with *KDR* expression and microvessel density (MVD) in non-small cell lung cancer (NSCLC) tumor specimens.

Materials and Methods

***KDR* resequencing**

Twenty-four germline DNA samples each from healthy Caucasians, Asian-Chinese, African-Americans obtained from the Coriell Institute Human Variation Collection* were chosen for resequencing. All 30 exons were sequenced (Figure 1). In addition, sequenced non-coding regions comprised flanking intronic sequences, promoter and the 5'-upstream region containing, evolutionarily conserved non-coding genomic regions (determined by comparative genomics using the UCSC genome browser – Supplementary Table S1), and regions determined to contain transcription factor binding sites according to computational prediction using Cluster-Buster†- Supplementary Table S2) (15). Primers used for PCR amplification are listed as in Supplementary Table S3. PCR reactions were set up using forward and reverse primers, HotStar DNA polymerase

*<http://www.coriell.org>

†<http://zlab.bu.edu/cluster-buster/>

8

(Qiagen, Hilden, Germany) and 10 ng of DNA. After initial 15 min of activation at 95°C, touch down cycles were performed at: 95°C for 30 s, touch down annealing from 65°C to 54.5°C (-1.5°C per cycle) for 30 s and 72°C for 1.5 min for 7 cycles, following the standard cycle of 95°C for 30 s, 55°C annealing for 30 s, and 72°C for 1.5 min for 30 cycles. PCR products were purified using the MultiScreen PCR Purification Kit (Millipore, Billerica, MA) and eluted in 30 µl elution buffer. DNA sequencing was performed at University of Chicago DNA Sequencing Core Facility by Sanger dye-terminator sequencing. Sequence analysis was performed using Sequencher (Gene Codes, Ann Arbor, MI), Version 4.7.

Linkage disequilibrium analysis and selection of tagging SNPs

Summary statistics of DNA sequence variation were calculated using SLIDER*. Linkage disequilibrium (LD) analysis of SNPs among the three ethnic groups was performed using the VG2 program†. For selection of haplotype tagging SNPs (tSNPs), SNPs were clustered using LD Select (16) integrated in the VG2 program. The parameters for the selection of tSNPs were $r^2 \geq 0.8$ and a minor allele frequency (MAF) $\geq 5\%$. Pair-wised LD analysis was done by the LD Plotter and r^2 values are calculated using an iterative EM algorithm (17).

* <http://genapps.uchicago.edu/slider>

† <http://pga.gs.washington.edu/VG2.html>

Bioinformatic analyses

The putative functional effects of SNPs were examined using FastSNP (18). The transcription factor binding site analysis of FastSNP was complemented by using PROMO (19). WWW Promoter Scan^{*} was used to predict functional *KDR* promoters. NCBI ORF finder[†] was used to determine open reading frames.

VEGFR-2 phosphorylation assays

The coding region of *KDR* was PCR amplified from cDNA using the following primers 5'-TTAAACTTAAGCTTGGTACCATGGAGAGCAAGGTGC-3' and 5'-TAGACTCGAGCGGCCGCTCACAGATCCTCTTC-3'. The pcDNA5 FRT vector (Invitrogen, California, USA) was PCR amplified using primers 5'-GCGGCCGCTCGAGTC-3' and 5'-GGTACCAAGCTTAAG-3'. Vector and insert were joined by In-Fusion Cloning (Clontech, Mountain View, CA, USA) according to kit instructions. The *KDR* variants R106W, V297I, Q472H and C482R were generated by using the QuikChange Site-Directed Mutagenesis Kit (Agilent Technologies, Santa Clara, CA, USA) as per the manufacturer's instructions.

HEK293 (ATCC) cells were grown for 24 h in DMEM with 10% FBS and transfected with $\text{Ca}_3(\text{PO}_4)_2$ precipitation. At 30 h after transfection, cells were starved overnight in DMEM

^{*} <http://www-bimas.cit.nih.gov/molbio/proscan/index.html>

[†] <http://www.ncbi.nlm.nih.gov/gorf/gorf.html>

10

supplemented with 1% BSA. Transfected cells were stimulated with 1.5 nM VEGF-A₁₆₅. Cell lysates were resolved on SDS gels, blotted to PVDF membranes, and immuno-decorated with phospho-specific pY1175 or VEGFR-2 55B11 antibodies (Cell Signaling, Danvers, MA, USA). All experiments were performed in triplicates, and immunoblots were quantified by densitometric scanning using ImageQuant RT ECL (Affymetrix-GE Healthcare, Freiburg, Germany).

Dual-Luciferase assays

A pGL2 plasmid (Promega, Madison, WI, USA) with *KDR* 5' upstream promoter region and *Firefly* luciferase gene was a gift from Dr. Patterson (20). Site-directed mutagenesis was performed by PCR according to the method of the QuikChange Site-Directed Mutagenesis Kit. Two allelic variations were introduced (-367C/T, -271G/A). Plasmids containing all major alleles (-367C, -271G), the -367T allele, the -271A allele and -367T/-271A alleles were generated.

To generate constructs containing variants at the -2854, -2455, -2008 and -1942 *KDR* loci, two PCRs of overlapping sequence were designed. Primers for the PCR amplifying the upstream region were the forward primer 5'-ACCCCAGTTCCTGGTTCAATGCCT-3' and the reverse primer 5'-GGGAAGCTTGTCTTTTACCTCCCAGA-3'. These primers were used to amplify human genomic DNA with Phusion High-Fidelity polymerase (NEB, Ipswich, MA, USA). This fragment was cloned into pGL4.20 (Promega) using

11

BglIII and HindIII sites. The second PCR was amplified using the forward primer 5'-GCAATTGTGGGAAGAGAAGGGTGAC-3' and the reverse primer 5'-GTAAGCTTCCGCAGCGCAGGACAGTT-3'. This PCR fragment was cloned into the construct containing the BglIII-HindIII fragment in pGL4.20 using the HindIII site in the reverse primer and an AseI site in the initial construct which was also present in the overlapping PCR fragment. The final construct contained a fragment between -2659 and +235 of *KDR*. Site-directed mutagenesis was performed as before and allelic variations were introduced: -2854 A/C (rs1551645), -2455 G/A (rs1551641), -2008 A/G (rs28517654) and -1942 A/G (rs28481683).

SVEC4-10 endothelial cells (a gift from Dr. Mark Lingen) were cultured in Dulbecco's Modified Eagle's medium with 10% FBS (fetal bovine serum). SVEC4-10 endothelial cells in 24 well plates were transfected by lipofectamine method (Invitrogen, Carlsbad, CA, USA) using the reporter gene plasmid construct of interest and a *Renilla* TK plasmid (Promega). Cells were lysed 40 h after transfection and the luciferase assays were then performed as per the manufacturer's instructions. Each construct was transfected three times for each experiment using triplicate wells. The ratio of *Firefly* to *Renilla* luciferase served as a measure of the luciferase activity. The luciferase activity in each experiment was normalized to the luciferase activity of the wild-type construct.

12

Non-small cell lung cancer (NSCLC) patients and tissue-microarray (TMA) preparation

The cohort consisted of 170 sequential Polish Caucasian patients who were systematically diagnosed with resectable NSCLC and from whom tumors were collected in tissue bank at the Medical University of Gdansk, Poland. The majority of patients were males, with squamous cell histology, smokers, and older than 60 years. Further details of the cohort are described in Dziadziuszko *et al.* (21). Primary tumors were fresh frozen at the time of surgery and stored at -80°C.

Representative regions of the blocks of consecutive NSCLC patients were selected from an archive of the Medical University of Gdansk (Poland) and microscopic diagnosis was verified by a board certified pathologist. Hematoxylin-eosin stained tissue sections with greater than 70% tumor cellularity were selected by the study investigator (RD) and verified by two pathologists at the University of Colorado Cancer Center. Three cylindrical tissue cores (1.5 mm in diameter) were punched from neoplastic areas by puncher provided by customized tissue microarray service (MaxArray, Invitrogen, South San Francisco, CA). Total RNA and genomic DNA were prepared from corresponding fresh-frozen tumor samples using AllPrep DNA/RNA kit (Qiagen).

VEGFR-2 and microvessel density (MVD) staining by immunohistochemistry

13

Immunohistochemical staining was performed using horseradish peroxidase (HRP)-labeled dextrose-based polymer complex bound to secondary antibody (DAKO Cytomation, Carpinteria, CA). In brief, four-micron TMA sections paraffin sections were deparaffinized in xylenes, rehydrated through graded ethanol solutions to distilled water and then washed in Tris-buffered saline. Antigen retrieval was carried out by heating sections in Citra Plus Buffer (Biogenex, San Ramon, CA, USA), pH=6, for 15 min in a microwave oven. Endogenous peroxidase activity was quenched by incubation in 3% H₂O₂ in methanol for 5 min. Non-specific binding sites were blocked using Protein Block (DAKO, Glostrup, Denmark) for 20 min. Then tissue sections were incubated for 1 h at room temperature with the rabbit polyclonal antibody against a 1:100 dilution of VEGFR-2 (Cat. No. 676488; Calbiochem, Merck, Darmstadt, Germany) for VEGFR-2 staining and with mouse monoclonal antibodies against CD31 (clone JC70A, 1:40, DAKO) for MVD. This step was followed by 30 min incubation with goat anti-rabbit IgG conjugated to a horseradish peroxidase (HRP)-labeled polymer (EnvisionTM System, DakoCytomation, Carpinteria, CA) for VEGFR-2 staining and with goat anti-mouse IgG conjugated to a horseradish peroxidase-labeled polymer (EnvisionTM+ System, DAKO) for MVD. Slides were then developed for 5 min with 3-3'-diaminobenzidine chromogen, counterstained with hematoxylin, and cover-slipped. Negative controls were performed by substituting primary antibody with non-immune rabbit immunoglobulins. The staining quantification was performed using the automated cellular imaging system at the Human Tissue Research Center at University of Chicago.

14

For the automated VEGFR-2 scoring, microarrays were scanned at 40X. Each core was analyzed separately by identifying the most representative tumoral area and scoring it. The average score among the three areas chosen was then calculated. Positive staining was calculated by applying two thresholds with one recognizing blue background (hematoxylin stained) cells and another recognizing brown positive cells. The percentage of positivity was the area detected by the brown threshold divided by the sum of the area detected by the brown and blue thresholds. The intensity was calculated by masking out all areas not selected by the brown threshold and calculating the integrated optical density of brown within the remaining area. This value was divided by the area in pixels of the brown mask to calculate an average intensity of a selected area.

For the automated MVD determination, CD31 was analyzed by an ACIS (ChromaVision Medical Systems, San Juan Capistrano, CA, USA). The image analysis system's MVD application was configured for vessel detection using CD31 stained slides. This was based on applying chromogen masks for high-chromogenic staining (brown threshold) and counterstaining (blue threshold), and the minimal and maximal size of the vessels. After selection of appropriate regions for MVD counting, the following measurements were captured digitally for each selected region of tissue: total vessel count, mean vessel area (μm^2 occupied by positively stained vessels), and vessel to tissue area ratio (vessel density percentage calculated by area of blood vessels occupying area of counterstained

15

tissue). The vessel count was then averaged for each case. MVD was calculated as positively staining vessel areas in μm^2 divided by total counterstained tissue area in μm^2 .

Genotyping of *KDR* SNPs

Patients from the NSCLC cohort (n=170) were genotyped for -2766A/T, -906T/C, 18487A/T (Q472H) and 23408T/G using Taqman® SNP genotyping assays (Applied Biosystems, Foster City, CA, USA), as per the manufacturer's instructions, using a CFX96 Real-Time System (Bio-Rad, Hercules, CA, USA). Genotyping of -271G/A was performed using a single base extension (SBE) genotyping assay using the following primers: 5'-CCACCCTGCACTGAGTCCC-3' (forward PCR primer) 5'-GCAGCGGAGGACAGTTGAG-3' (reverse PCR primer with one base edited from C to G) 5'-GAAACGCAGCGACCACACA-3' (downstream extension primer). Denaturing high performance liquid chromatography was used for separation of SBE products.

cDNA Synthesis and quantitative PCR (qPCR)

RNA extracted from lung tumor samples was reverse transcribed into cDNA using a High Capacity RT Kit as per the manufacturer's instructions (Applied Biosystems). *KDR* primers originally designed by An *et al.* (22) were used. *18S* served as a control gene as it exhibits stable expression in NSCLC tumor tissue (23) and was amplified with sense 5'-CGATGCTCTTAGCTGAGTGT-3' and antisense 5'-GGTCCAAGAATTCACCTCT-3' primers. qPCR of cDNA samples was completed in three independent experiments

16

using a Bio-Rad CFX96 Real-Time System, iQ SYBR Green Supermix (Bio-Rad) and 6 μ l cDNA. Thermal cycling parameters were followed by a disassociation step. Absolute quantification of mRNA levels was achieved using commercial human lung total RNA (Ambion, Applied Biosystems) converted to cDNA as above and serially diluted as an internal reference standard curve. mRNA levels were expressed as the ratio of *KDR* to *18S*.

Statistical analyses

For the luciferase reporter gene and phosphorylation assays, comparisons were made between the variant and the reference alleles by paired t-tests. The association between each SNP and either \log_2 -transformed *KDR* mRNA, VEGFR-2 or MVD levels was tested using univariate linear regression by assuming additive (AA=0, AB=1, BB=2), dominant (AA=0, AB/BB=1) and recessive (AA/AB=0, BB=1) models. As these are exploratory studies, a nominal p-value of 0.05 was regarded as significant. For the significant SNP-phenotype associations, we investigated whether age, sex, histology and pathological stage were potential confounding variables by multivariate regression in a model including significant SNPs and patient/tumor characteristics. For mRNA expression, the best combination of two associated SNPs was determined by multiple regression analysis. Since we had available only a smaller subset of samples (n=66) for mRNA analysis, and hence greater chance of detecting false discoveries than in the wider cohort of patients, for these analyses with SNP genotypes, false discovery rate estimates (q-values) were determined using the adaptive two-stage procedure defined by Benjamini et al. (24) and

17

the Excel-based calculator described by Pike (25). All other analyses were performed using the lm library in the R Statistical Package (26) and Prism (GraphPad, La Jolla, CA, USA).

RESULTS

KDR resequencing

KDR resequencing led to the identification of 113 SNPs and 7 insertion/deletions in the three ethnic groups (data summarized in Supplementary Table S4). Twenty five variants were not found in the dbSNP database* (build 132). In general, the available HapMap data showed that SNP MAFs in HapMap (matched by ethnic group) were similar to the MAFs generated by our resequencing (Supplementary Table S4). Fifteen SNPs were detected in the *KDR* coding region and eight of these variants were non-synonymous. R106W and P839L had not been previously reported in dbSNP.

Comparison of the variants across the different ethnic groups demonstrated inter-ethnic differences, with African-Americans carrying 94 variants compared with 58 for Asians and 51 for Caucasians. A stronger pattern of LD was found in Caucasians and Asians than African-Americans (Supplementary Figure S1). Thirty eight variants were found in all three groups. Out of the variants with MAF>5%, 45 were found in Caucasians, 49 in

* <http://www.ncbi.nlm.nih.gov/projects/SNP/>

18

Asians, and 53 in African-Americans. Overall, *KDR* genetic variation was characterized by a low level of LD and this study indicates that 20, 21, and 28 tSNPs should be used to interrogate *KDR* common variation in Caucasians, Asians, and African-Americans, respectively (Supplementary Figure S2).

Effect of non-synonymous SNPs on VEGFR-2 phosphorylation

Bioinformatic analysis of *KDR* variants (Supplementary Table S5) guided the prioritization of SNPs for *in vitro* functional testing. Of the non-synonymous variants, R106W, Q472H and C482R were predicted to affect protein function or be potentially damaging and so we examined their effects on VEGFR-2 phosphorylation. In addition, we also tested V297I, due to its high frequency in the three populations. In HEK293 cells, Q472H showed a 46% increase in VEGFR-2 phosphorylation after VEGF-A₁₆₅ stimulation ($p=0.035$) (Figure 2). The other non-synonymous variants did not show any effect on VEGFR-2 phosphorylation.

Effect of potential regulatory SNPs on *KDR* mRNA and protein expression

Bioinformatic analysis of the *KDR* variants identified 58 potential regulatory variants in non-coding gene regions (Supplementary Table S5). We were particularly interested in common SNPs in the 5' flanking and promoter regions of the gene, which could be assayed using reporter gene assays. We searched bioinformatically for the *KDR* promoter

19

and identified a region from -599 to -349 bp upstream of the start codon. The only two common SNPs identified in the promoter and the adjacent 5'UTR were -367T/C and -271G/A. Both SNPs were found to alter transcription factor binding sites after further bioinformatic analysis using PROMO (Supplementary Table S5). In reporter gene assays, we found that constructs containing -271A reduced expression to 49-55% ($p<0.0001$) of that from the construct with the reference, -271G, allele (Figure 3A). Presence of -367C did not alter expression ($p>0.05$).

We also examined the 5' flanking region of the gene and identified four SNPs which are predicted to alter transcription factor binding sites: -2854A/C, -2455T/A, -2008A/G and -1942A/G. The effect of these SNPs was tested singly but since two pairs of SNPs (-2854A/C and -2455T/A; -2008A/G and -1942A/G) were in perfect LD in all three ethnic groups (Supplementary Figures S1 and S2), reporter gene constructs were also created which contained the variants linked by LD. In SVEC4-10 cells, constructs containing -2455A, -2854C, or both variants, had 20% ($p<0.001$), 10% ($p<0.05$) and 10% ($p<0.01$) greater expression, respectively, than the reference construct (Figure 3B).

Association studies of *KDR* variants with *KDR* mRNA and protein expression, and MVD in a NSCLC cohort

Since the -271A, -2455A, -2854C and Q472H (18487T) variants had functional effects *in vitro*, we prospectively tested their effect on *KDR* gene expression and MVD in tumors.

20

We genotyped -271G/A, -2766A/T (a tagging SNP for both -2854A/C and -2455T/A; Supplementary Figure S2) and Q472H in a Caucasian NSCLC cohort. In addition, we also genotyped two further variants: -906T/C and 23408T/G. The -906C variant has been associated with serum VEGFR-2 levels and been shown to affect expression in reporter gene assays (27). Bioinformatic analysis predicted that the -906C allele introduces an IKZF2 binding site (Supplementary Table S5) so, as this transcription factor may be involved in mediating *KDR* expression, another *KDR* variant which introduces an IKZF2 binding site, the 23408T allele, was also genotyped to determine the impact of this binding site motif on expression. After genotyping in the NSCLC patients, the MAFs were determined to be 0.33 (n=169 patients), 0.46 (n=170), 0.44 (n=166), 0.29 (n=168) and 0.34 (n=169) for -2766A/T, -906T/C, -271G/A, Q472H and 23408T/G, respectively, which were comparable to the MAFs of Caucasians from our resequencing and HapMap (Supplementary Table S4). No significant deviation from Hardy-Weinberg equilibrium was observed for any of the SNPs.

We assayed tumoral VEGFR-2 protein and MVD levels in the same individuals by immunohistochemistry (n=170) and quantified *KDR* mRNA levels in a subset of these patients (n=66). Analysis of protein and mRNA levels determined that there was a very modest inverse correlation ($p=0.03$, $r^2=0.07$; Supplementary Figure S4); hence, we used both mRNA and protein levels to infer the molecular effects of *KDR* SNPs on gene expression. VEGFR-2 protein levels were positively correlated with MVD ($p=8e-09$; $r^2=0.18$; Supplementary Figure S5).

In univariate analyses of mRNA expression, the minor alleles of -2766A/T -906T/C, -271G/A, and 23408T/G correlated with significantly greater expression (Figure 4A-G). The association of -2766A/T and mRNA expression was consistent with the luciferase assay results of the -2854A/C and -2455T/A SNPs, which are tagged by -2766A/T. The minor allele of Q472H associated with significantly lower mRNA levels (Figure 4H-J), probably by altering the splicing machinery due to its vicinity (3 bp) to the intron/exon boundary. After false discovery rate analysis to control for the multiple comparisons, the only association not to maintain significance was -271G/A in the dominant genetic model ($q=0.05$; Figure 4F). However, the association of this SNP in the additive model remained significant as did all the other nominally significant associations with mRNA levels. Multivariate analyses were performed which incorporated combinations of SNP genotypes. However, possibly due to sample size limitations, the most significant model included only two SNPs: $0.98*\text{genotype} (-906 \text{ TC/CC}; p=0.037) + 1.74*\text{genotype} (\text{Q472H AA/AT}, p=0.007)$, overall $r^2=0.219$ and $p=0.0004$. The effect of these SNPs seems to be independent, as shown by the lack of LD between them (Supplementary Figure S3).

In univariate analyses of protein expression, no significant associations were found between the genotyped variants and VEGFR-2 protein levels. However, when testing the effect of patient/tumor characteristics, protein expression was lower in later stages of disease (Supplementary Figure S6). Controlling for early (I-II) versus late (III-IV) stage

22

of disease, we found that the tumors of patients with -271GG/GA genotypes had greater VEGFR-2 levels compared with tumors from patients with -271AA genotype: $-0.32 \times \text{stage (III\&IV; } p=0.02) + 0.36 \times \text{genotype (-271GG/GA; } p=0.03)$; overall $p=0.01$, $r^2=0.054$.

In univariate analysis of MVD, the major allele, A, of Q472H, coding for wild-type VEGFR-2, associated with lower MVD (additive and dominant: $p=0.036$ and $p=0.040$; Figure 5). After controlling for differences in tumor histology (Supplementary Figure S7), patients with the Q472H AA genotype (i.e. expressing only wild-type VEGFR-2) were shown to have tumors with lower MVD than patients with AT/TT genotypes: $0.57 \times \text{histology (adenocarcinoma and large cell carcinoma; } p=0.01) - 0.67 \times \text{genotype (Q472H AA; } p=0.05)$; overall $p=0.005$, $r^2=0.050$.

DISCUSSION

This report represents the most extensive molecular genetic study of *KDR*. Our resequencing study identified 120 *KDR* variants which included 25 previously unreported. Furthermore, there were considerable differences between the presence of specific variants and their corresponding frequencies among the three ethnic populations. This comprehensive assessment allowed the generation of haplotype-tagging SNPs for genotyping in subjects from Caucasian, African, or Asian backgrounds.

Statistical associations in genetic cancer risk or outcome studies should be supported with molecular mechanistic evidence of SNP function and the lack of mechanistically-based effects of clinical phenotypes is regarded as a major limitation for identifying biomarkers. Very few studies have focused on the identification of common functional *KDR* germline variants (27, 28). We have tested associations of twelve *KDR* SNPs and function in two different assays and with molecular phenotypes from tumor samples, and found five SNPs which have a significant association with at least one of these measures (Figure 6). We analyzed six SNPs in reporter gene assays and found three of these with significant effects. The -2455A and -2854C variants modestly increased reporter gene expression and these alleles were shown to be associated with increased *KDR* mRNA expression in NSCLC tumors, without an effect on VEGFR-2 protein levels. The -271A variant had a strong negative effect on expression in the reporter assay, and, supportive of this result, patients with the -271AA genotype had less tumor protein expression than subjects with -271GA/GG genotypes, after controlling for disease stage. Furthermore, the observation that VEGFR-2 levels in stages III-IV were significantly lower than in earlier stages appears to be a novel finding in NSCLC.

The decreased protein expression associated with -271A appears to be due to a post-transcriptional mechanism. The -271A allele creates a start codon which introduces an upstream open reading frame of 207 bp, in conjunction with an in frame stop codon in the 5'UTR, and thereby inhibits translation of *KDR* mRNA into protein (29). At the mRNA

24

level in our study, presence of an A allele was associated with greater tumor *KDR* expression, consistent with the previous association of the -271AA genotype with higher levels of *KDR* mRNA in NSCLC (30). We have also observed a modest negative correlation between mRNA and protein levels. Indeed, discordance between mRNA and protein levels of *KDR* has been found under low glucose conditions (31), which are common in the tumor microenvironment (32). The mechanistic explanation of this finding is that glucose depletion may up-regulate *KDR* mRNA expression through the unfolded protein response but down-regulate VEGFR-2 levels via a protein degradation mechanism (31).

We examined two other putatively regulatory SNPs, -906T/C and 23408T/G, for associations with *KDR* expression. The -906C variant introduces an IKZF2 binding site and increases reporter gene expression in human umbilical vein endothelial cells (27); in agreement with this observation, we found this variant associated with higher expression of mRNA in NSCLC tumors. Bioinformatic analyses predicted that 23408G disrupts an IKZF2 binding site but this allele was associated with higher mRNA levels. Therefore, it appears that the presence/absence of an IKZF2 binding site motif is not the cause of the differential expression. Instead, this effect may be due to the interaction of another transcription factor, such as GATA2, which putatively binds at this locus (Table S4). Alternatively, there may be a functional SNP in LD with 23408T/G which mediates this effect.

25

Q472H was predicted to have effects on protein function and this variant had increased phosphorylation after VEGF-A₁₆₅ stimulation. Wang *et al.*, examined VEGF-A₁₆₅ binding of VEGFR-2 and found that Q472H increased the binding efficiency (27). In univariate analysis, we observed greater MVD in patients with the Q472H TT genotype. Adenocarcinomas have been shown to have greater MVD (33) and we observed higher MVD in adenocarcinomas and large cell carcinomas (Figure S7). We controlled for tumor histology, and again found a correlation between patients expressing the Q472H variant and greater MVD. Although we observed an inverse relationship between Q472H and mRNA levels, Q472H did not associate with protein levels, measured by IHC of total VEGFR-2 (both phosphorylated and unphosphorylated). Therefore, the effect of Q472H on MVD is likely due to increased activation of the VEGFR-2 receptor through increased phosphorylation, as demonstrated by our finding from the phosphorylation assay. Moreover, this study has identified a germline variant as a potential determinant of increased tumor vasculature in NSCLC.

A potential drawback of this study is the lack of laser-capture microdissection, and the possibility that the molecular phenotypes of *KDR* in this study are not entirely representative of tumor vasculature. To minimize this effect, we used tumor blocks displaying greater than 70% tumor cellularity. Although it has been clearly shown that VEGFR-2 positive vessels are mainly absent or rare in normal lung vessels, and that VEGFR-2 expression is not detected in malignant lung cells (34), we cannot rule out that VEGFR-2 expression in the stromal cells may be a confounder. However, non-

26

microdissected lung cancer specimens are well accepted in the field as the material for molecular studies (35).

Our findings highlight the difficulty of identifying common germline variants with large effect sizes in genotype-phenotype association studies. Nevertheless, even small changes in gene expression may increase cancer susceptibility. In mice, a 20% reduction in expression of *Pten*, a gene involved in the regulation of angiogenesis (36), led to a dramatic rise in tumor incidence (37). Furthermore, we found that a combination of two SNPs can account for 22% of the variation in tumoral levels of *KDR* mRNA. The contribution of untested functional germline SNPs may partly explain the relatively small effect sizes. Also, we did not examine somatic DNA alterations such as gene amplification which could have significant effects on gene expression. Indeed, increased *KDR* copy number has been reported in some cancers (38, 39). However, the goal of this study was to characterize regions informative of function by focusing mainly on known regulatory regions.

We acknowledge that the results of this exploratory study are preliminary. The significant associations of SNP genotypes and *ex vivo* molecular phenotypes observed should be validated in an independent cohort with well-defined microdissected tissue. However, we believe this lack of validation may be somewhat mitigated by supportive findings from - 2854A/C, -2455T/A, -271G/A and Q472H in our *in vitro* reporter gene and

27

phosphorylation assays, and from the corroborative reports, discussed previously, of the functionality of -906T/C, -271G/A and Q472H.

We have generated the knowledge basis to guide the prospective evaluation of *KDR* variants for identification of clinical biomarkers and for validating their clinical utility. Our study will inform the selection of SNPs, in accordance with their functional effects and expected frequencies in the corresponding ethnic group. For example, Q472H, which increases VEGFR-2 phosphorylation, associates with MVD levels, and shows a large variation in allele frequencies, ranging from 0.10 in African Americans to 0.52 in Asians (Table S4). Our findings may have implications not only for the molecular genetics of angiogenesis in lung cancer but also in other tumors. Their effect on the outcome of treatment with VEGF-pathway inhibitors should be evaluated prospectively.

References

1. Ferrara N, Gerber HP, LeCouter J. The biology of VEGF and its receptors. *Nat Med.* 2003;9:669-76.
2. Takahashi Y, Kitadai Y, Bucana CD, Cleary KR, Ellis LM. Expression of vascular endothelial growth factor and its receptor, KDR, correlates with vascularity, metastasis, and proliferation of human colon cancer. *Cancer Res.* 1995;55:3964-8.
3. Hara H, Akisue T, Fujimoto T, Imabori M, Kawamoto T, Kuroda R, et al. Expression of VEGF and its receptors and angiogenesis in bone and soft tissue tumors. *Anticancer Res.* 2006;26:4307-11.
4. Hetian L, Ping A, Shumei S, Xiaoying L, Luowen H, Jian W, et al. A novel peptide isolated from a phage display library inhibits tumor growth and metastasis by blocking the binding of vascular endothelial growth factor to its kinase domain receptor. *J Biol Chem.* 2002;277:43137-42.
5. Rini BI, Flaherty K. Clinical effect and future considerations for molecularly-targeted therapy in renal cell carcinoma. *Urol Oncol.* 2008;26:543-9.
6. Minguéz B, Tovar V, Chiang D, Villanueva A, Llovet JM. Pathogenesis of hepatocellular carcinoma and molecular therapies. *Curr Opin Gastroenterol.* 2009;25:186-94.
7. Harris PA, Bloor A, Cheung M, Kumar R, Crosby RM, Davis-Ward RG, et al. Discovery of 5-[[4-[(2,3-dimethyl-2H-indazol-6-yl)methylamino]-2-pyrimidinyl]amino]-

29

2-methyl-b enzenesulfonamide (Pazopanib), a novel and potent vascular endothelial growth factor receptor inhibitor. *J Med Chem.* 2008;51:4632-40.

8. Mendel DB, Laird AD, Xin X, Louie SG, Christensen JG, Li G, et al. In vivo antitumor activity of SU11248, a novel tyrosine kinase inhibitor targeting vascular endothelial growth factor and platelet-derived growth factor receptors: determination of a pharmacokinetic/pharmacodynamic relationship. *Clin Cancer Res.* 2003;9:327-37.

9. Wilhelm SM, Carter C, Tang L, Wilkie D, McNabola A, Rong H, et al. BAY 43-9006 exhibits broad spectrum oral antitumor activity and targets the RAF/MEK/ERK pathway and receptor tyrosine kinases involved in tumor progression and angiogenesis. *Cancer Res.* 2004;64:7099-109.

10. Chang YS, Adnane J, Trail PA, Levy J, Henderson A, Xue D, et al. Sorafenib (BAY 43-9006) inhibits tumor growth and vascularization and induces tumor apoptosis and hypoxia in RCC xenograft models. *Cancer Chemother Pharmacol.* 2007;59:561-74.

11. Stranger BE, Nica AC, Forrest MS, Dimas A, Bird CP, Beazley C, et al. Population genomics of human gene expression. *Nat Genet.* 2007;39:1217-24.

12. Folkman J. Angiogenesis: an organizing principle for drug discovery? *Nat Rev Drug Discov.* 2007;6:273-86.

13. DePrimo SE, Bello C. Surrogate biomarkers in evaluating response to anti-angiogenic agents: focus on sunitinib. *Ann Oncol.* 2007;18 Suppl 10:x11-9.

30

14. Facchini G, Perri F, Caraglia M, Pisano C, Striano S, Marra L, et al. New treatment approaches in renal cell carcinoma. *Anticancer Drugs*. 2009;20:893-900.
15. Frith MC, Li MC, Weng Z. Cluster-Buster: Finding dense clusters of motifs in DNA sequences. *Nucleic Acids Res*. 2003;31:3666-8.
16. Carlson CS, Eberle MA, Rieder MJ, Yi Q, Kruglyak L, Nickerson DA. Selecting a maximally informative set of single-nucleotide polymorphisms for association analyses using linkage disequilibrium. *Am J Hum Genet*. 2004;74:106-20.
17. Hill WG. Estimation of linkage disequilibrium in randomly mating populations. *Heredity*. 1974;33:229-39.
18. Yuan HY, Chiou JJ, Tseng WH, Liu CH, Liu CK, Lin YJ, et al. FASTSNP: an always up-to-date and extendable service for SNP function analysis and prioritization. *Nucleic Acids Res*. 2006;34:W635-41.
19. Farre D, Roset R, Huerta M, Adsuara JE, Rosello L, Alba MM, et al. Identification of patterns in biological sequences at the ALGGEN server: PROMO and MALGEN. *Nucleic Acids Res*. 2003;31:3651-3.
20. Patterson C, Perrella MA, Hsieh CM, Yoshizumi M, Lee ME, Haber E. Cloning and functional analysis of the promoter for KDR/flk-1, a receptor for vascular endothelial growth factor. *J Biol Chem*. 1995;270:23111-8.
21. Dziadziuszko R, Merrick DT, Witta SE, Mendoza AD, Szostakiewicz B, Szymanowska A, et al. Insulin-like growth factor receptor 1 (IGF1R) gene copy number

31

is associated with survival in operable non-small-cell lung cancer: a comparison between IGF1R fluorescent in situ hybridization, protein expression, and mRNA expression. *J Clin Oncol.* 2010;28:2174-80.

22. An SJ, Nie Q, Chen ZH, Lin QX, Wang Z, Xie Z, et al. KDR expression is associated with the stage and cigarette smoking of the patients with lung cancer. *J Cancer Res Clin Oncol.* 2007;133:635-42.

23. Nguewa PA, Agorreta J, Blanco D, Lozano MD, Gomez-Roman J, Sanchez BA, et al. Identification of importin 8 (IPO8) as the most accurate reference gene for the clinicopathological analysis of lung specimens. *BMC Mol Biol.* 2008;9:103.

24. Benjamini Y, Krieger A, M., Yekutieli D. Adaptive linear step-up procedures that control the false discovery rate. *Biometrika.* 2006;93:491-507.

25. Pike N. Using false discovery rates for multiple comparisons in ecology and evolution. *Methods in Ecology and Evolution.* 2011;2:278-82.

26. Team RDC. R: A language and environment for statistical computing. In: *Computing RfFS*, editor. Vienna, Austria; 2010.

27. Wang Y, Zheng Y, Zhang W, Yu H, Lou K, Zhang Y, et al. Polymorphisms of KDR gene are associated with coronary heart disease. *J Am Coll Cardiol.* 2007;50:760-7.

28. Kariyazono H, Ohno T, Khajoev V, Ihara K, Kusuhara K, Kinukawa N, et al. Association of vascular endothelial growth factor (VEGF) and VEGF receptor gene

32

polymorphisms with coronary artery lesions of Kawasaki disease. *Pediatr Res.* 2004;56:953-9.

29. Calvo SE, Pagliarini DJ, Mootha VK. Upstream open reading frames cause widespread reduction of protein expression and are polymorphic among humans. *Proc Natl Acad Sci U S A.* 2009;106:7507-12.

30. An SJ, Chen ZH, Lin QX, Su J, Chen HJ, Lin JY, et al. The -271 G>A polymorphism of kinase insert domain-containing receptor gene regulates its transcription level in patients with non-small cell lung cancer. *BMC Cancer.* 2009;9:144.

31. Adham SA, Coomber BL. Glucose is a key regulator of VEGFR2/KDR in human epithelial ovarian carcinoma cells. *Biochem Biophys Res Commun.* 2009;390:130-5.

32. Henning T, Kraus M, Brischwein M, Otto AM, Wolf B. Relevance of tumor microenvironment for progression, therapy and drug development. *Anticancer Drugs.* 2004;15:7-14.

33. Ozbudak IH, Ozbilim G, Kucukosmanoglu I, Dertsiz L, Demircan A. Vascular endothelial growth factor expression and neovascularization in non--small cell lung carcinoma. *Int J Surg Pathol.* 2009;17:390-5.

34. Smith NR, Baker D, James NH, Ratcliffe K, Jenkins M, Ashton SE, et al. Vascular endothelial growth factor receptors VEGFR-2 and VEGFR-3 are localized primarily to the vasculature in human primary solid cancers. *Clin Cancer Res.* 2010;16:3548-61.

33

35. Eberhard DA, Giaccone G, Johnson BE. Biomarkers of response to epidermal growth factor receptor inhibitors in Non-Small-Cell Lung Cancer Working Group: standardization for use in the clinical trial setting. *J Clin Oncol*. 2008;26:983-94.
36. Castellino RC, Muh CR, Durden DL. PI-3 kinase-PTEN signaling node: an intercept point for the control of angiogenesis. *Curr Pharm Des*. 2009;15:380-8.
37. Alimonti A, Carracedo A, Clohessy JG, Trotman LC, Nardella C, Egia A, et al. Subtle variations in Pten dose determine cancer susceptibility. *Nat Genet*. 2010;42:454-8.
38. Holtkamp N, Ziegenhagen N, Malzer E, Hartmann C, Giese A, von Deimling A. Characterization of the amplicon on chromosomal segment 4q12 in glioblastoma multiforme. *Neuro Oncol*. 2007;9:291-7.
39. Hahtola S, Burghart E, Puputti M, Karenko L, Abdel-Rahman WM, Vakeva L, et al. Cutaneous T-cell lymphoma-associated lung cancers show chromosomal aberrations differing from primary lung cancer. *Genes Chromosomes Cancer*. 2008;47:107-17.

Figure legends

Figure 1. Genomic structure of *KDR* and SNPs investigated in this study. SNPs which were examined in our studies are shown with boxes indicating exons. SNPs are numbered in reference to the first base of the ATG start codon. Non-synonymous SNPs are shown with the appropriate amino acid variation. The figure is not to exact scale.

Figure 2. VEGFR-2 phosphorylation in HEK293 cells and effect of non-synonymous variants. The y axis corresponds to the ratio of phosphorylated VEGFR-2 to total VEGFR-2. Values are normalized to basal phosphorylation levels of reference sequence *KDR*. “-” refers to basal phosphorylation levels and “+” refers to VEGF-A₁₆₅ stimulation. Wt = reference sequence cDNA. The mean ± SEM of 3 experiments in triplicate is shown.

Figure 3. Function of -367T/C and -271G/A (A), and 2854A/C, -2455T/A, -2008A/G and -1942A/G (B) according to luciferase assays in SVEC4-10 endothelial cells. The mean ± SEM of experiments in triplicate is shown. Panel A shows assays examining the -367T/C and -271G/A variants; and panel B shows assays examining the -2854A/C, -2455G/A, -2008A/G and -1942A/G variants. The significant results of paired t-tests between the wild-type reference and variant alleles are shown.

Figure 4. Association between *KDR* genotypes and *KDR* mRNA expression in NSCLC tumor specimens. *KDR* mRNA expression was measured in 66 tumor

35

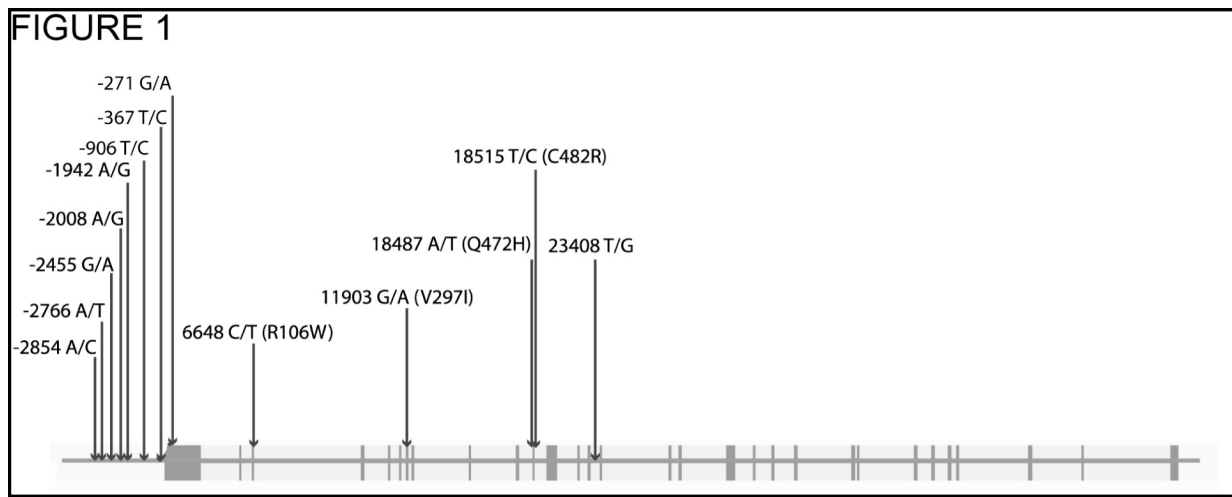
specimens. The relationship of -2766A/T and mRNA expression is shown in panels A and B in additive and dominant models, respectively; -906T/C genotype and mRNA expression is shown in panels C and D in additive and dominant models, respectively; -271G/A genotype and mRNA expression is shown in panels E and F in additive and dominant models, respectively; 23408T/G genotype and mRNA expression is shown in a dominant model in panel G; and Q472H genotype and mRNA expression is shown in additive, dominant and recessive models in panels H, I and J, respectively. Nominal statistical significance is denoted by p-values and the results of false discovery rate testing by q-values.

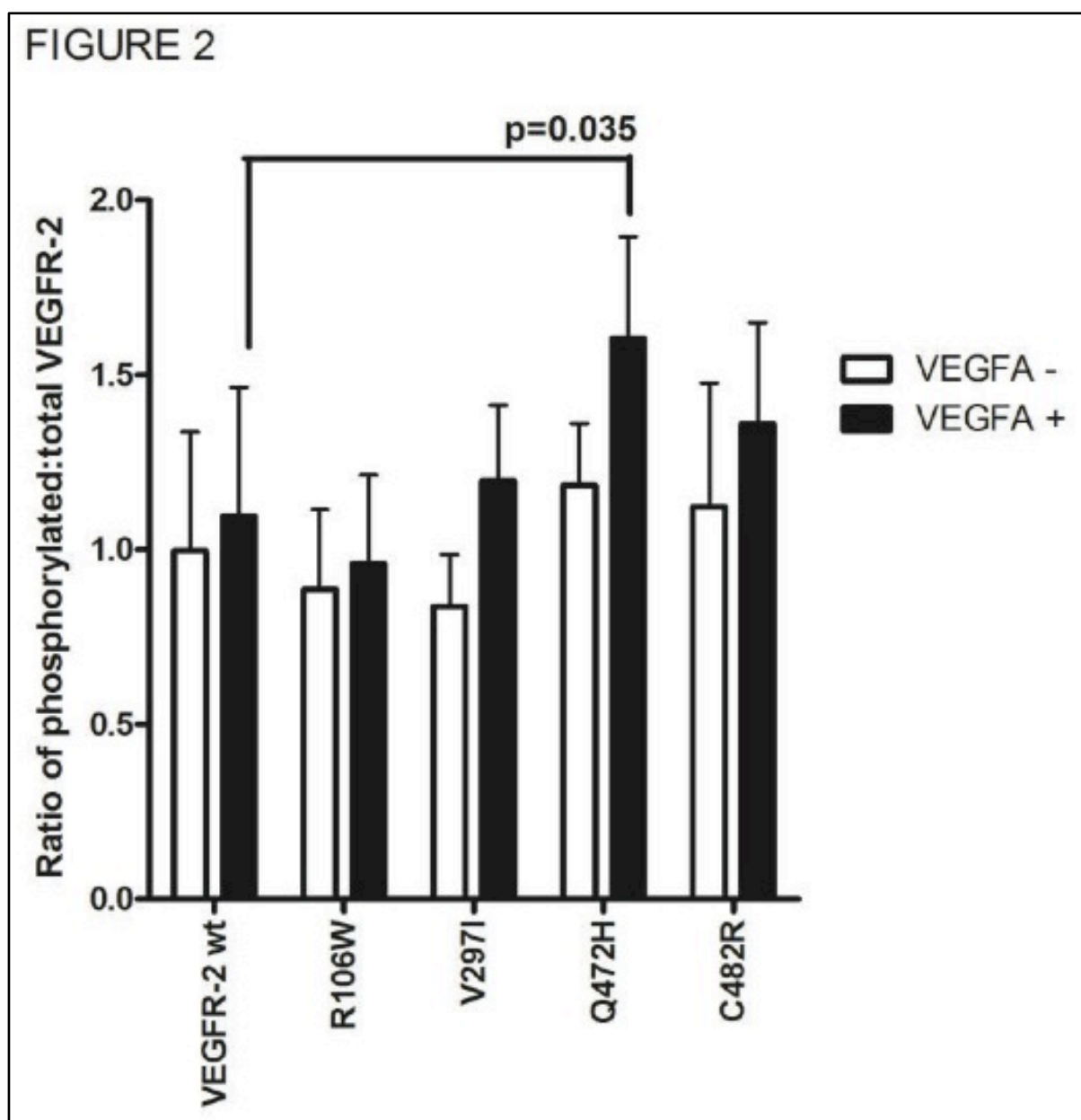
Figure 5. Association between Q472H genotypes and MVD in NSCLC tumor specimens. MVD was measured in 170 tumor specimens. The relationship between Q472H genotype and MVD is shown in panels A and B in additive and recessive models, respectively.

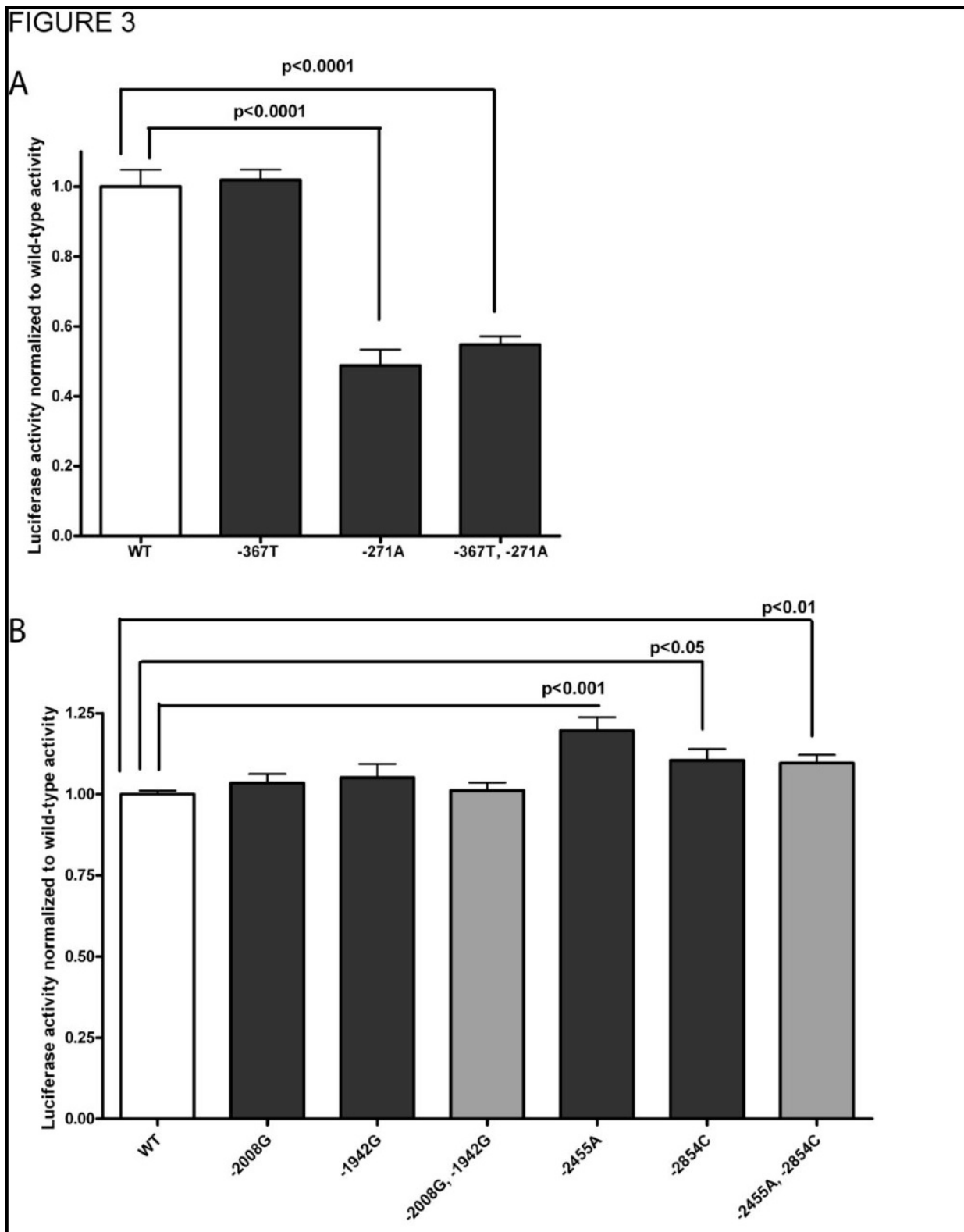
Figure 6. Summary of experimental and analytical approaches used, and significant findings. *KDR* was resequenced in three ethnic groups, each containing 24 healthy individuals. The genetic variants identified from the resequencing were analyzed for function using bioinformatic tools. Putatively functional SNPs were examined using reporter gene or VEGFR-2 phosphorylation assays. Functional SNPs, including two further putatively functional SNPs, were genotyped in a cohort of European NSCLC

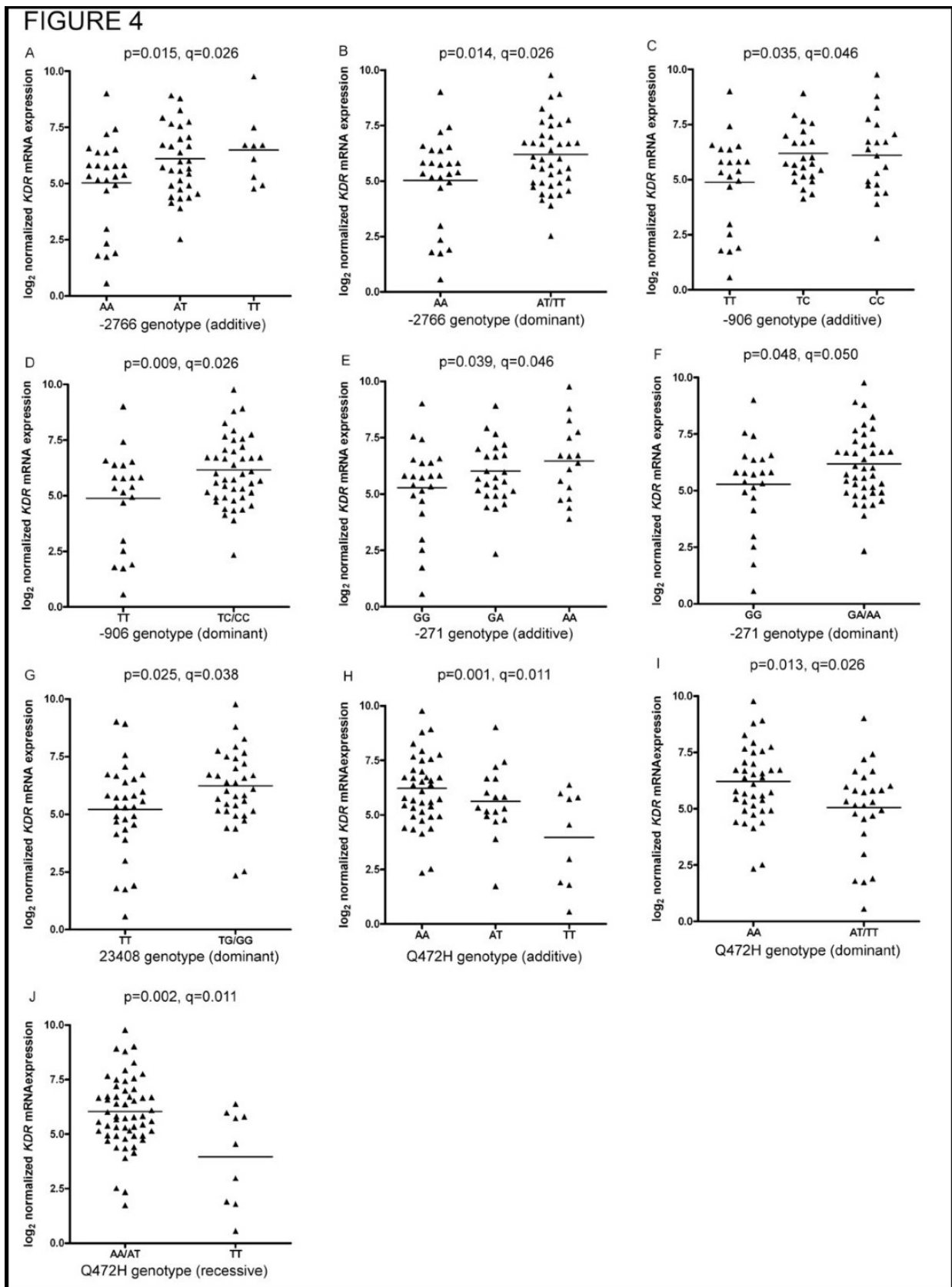
36

patients. These genotypes were tested for associations with *KDR* mRNA, VEGFR-2 protein and MVD levels from matching tumor samples. SNPs significantly ($p < 0.05$) associated with a phenotype of interest are designated by a block arrow. An up arrow indicates that the variant is associated with increased levels of the phenotype; conversely, a down arrow indicates that the variant is associated with decreased levels of the phenotype.









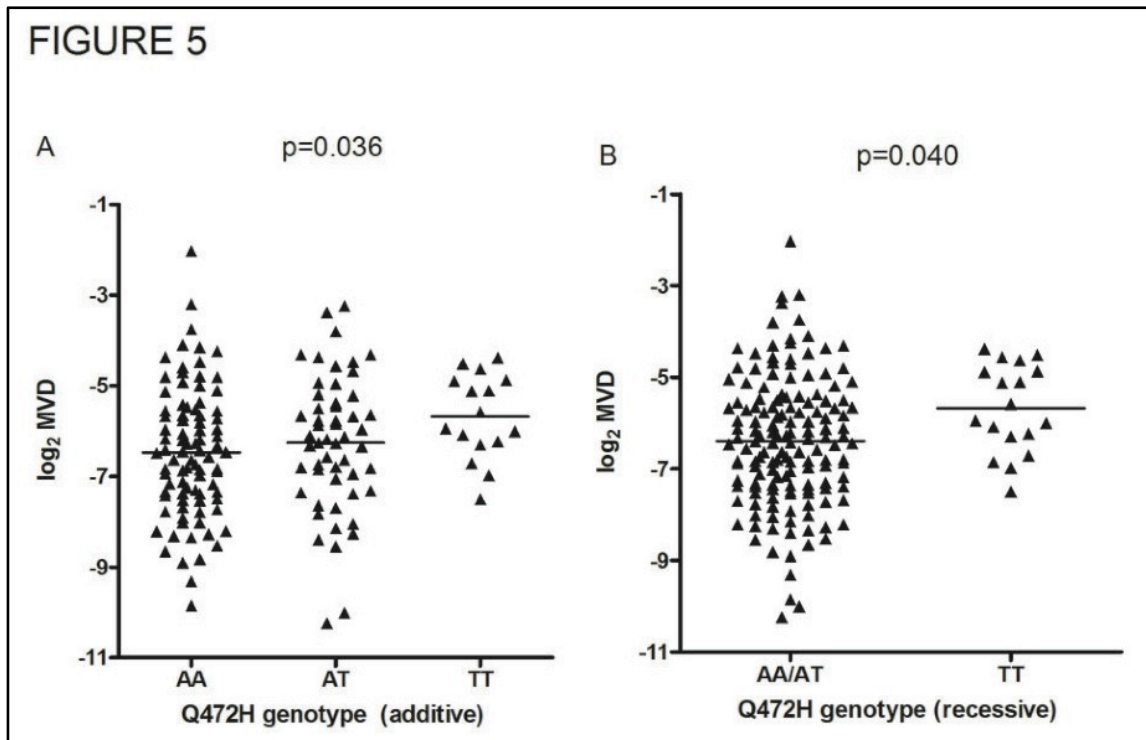
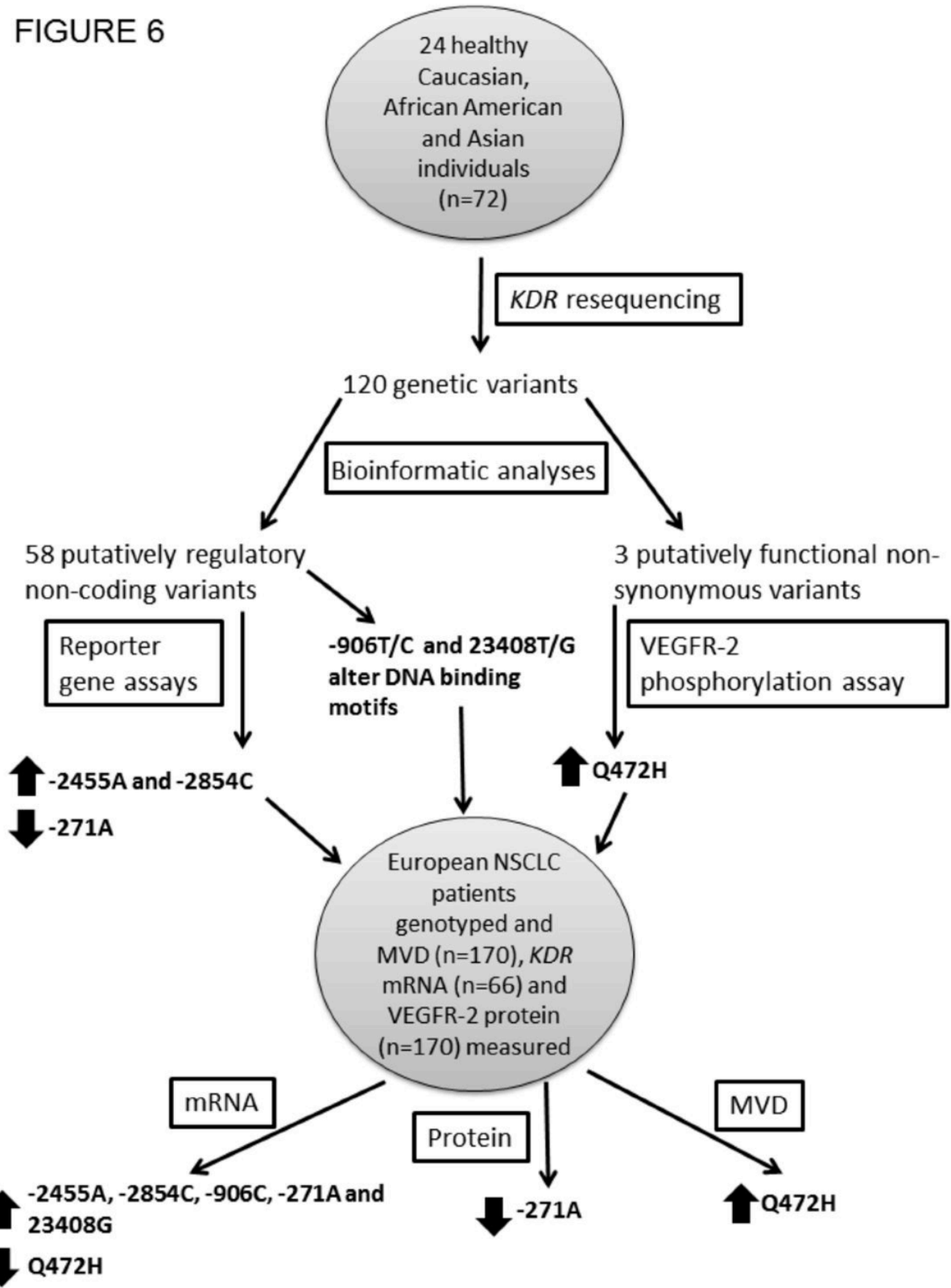


FIGURE 6



15 APPENDIX C

Monitoring Vessel Formation of Endothelial Cells on Micropatterned BiochipsA. Giese¹, C. Padeste², K. Ballmer-Hofer¹¹ Molecular Cell Biology, Paul Scherrer Institut, Villigen-PSI, Switzerland. ² Laboratory for Micro- and Nanotechnology, Paul Scherrer Institut, Villigen-PSI, Switzerland.

INTRODUCTION: Vascular Endothelial Growth Factors (VEGFs) constitute a family of proteins that regulate blood and lymphatic vessel development and homeostasis. In normal, healthy organisms vessel development is tightly regulated to maintain adequate blood supply and lymph drainage. Vessels are aberrantly stimulated in various diseases such as during tumor growth, in atherosclerosis, retinopathies and in lymphoproliferative or rheumatoid disease [1]. We are investigating the mechanisms responsible for vessel formation by VEGF family ligands in vitro using endothelial cells grown on micropatterned substrates. Patterned substrates are generated to mimic the extracellular milieu, in particular the extracellular matrix (ECM), of the cells.

METHODS:

Protein Immobilization: The ‘Molecular Assembly Patterning by Lift-Off (MAPL) technology’ developed at ETH Zürich [2] was adapted to the immobilization of VEGF. We use the natural affinity of VEGF-A₁₆₅ to heparin for indirect coupling. For this, we incubated commercially available heparin-biotin with neutravidin and bound the complex to the PLL-g-PEG biotin pattern. Further, VEGF-A₁₆₅ was immobilized via the heparin and visualized with an anti-VEGF antibody.

Cell assay: Porcine Aortic Endothelial (PAE) cells expressing the Vascular Endothelial Growth Factor Receptor 2 (VEGFR-2) were grown on VEGF patterns. Cells were fixed and immunostained with an anti-VEGFR-2 antibody.

RESULTS: In our study, we successfully immobilized VEGF-A₁₆₅ on patterned glass coverslips. Visualization with an anti-VEGF antibody showed the expected pattern (Fig. 1). Furthermore, we demonstrated that PAE cells are able to migrate and divide on the generated micropatterns (Fig.2).

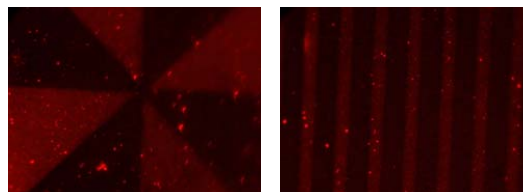


Fig. 1: VEGF-A₁₆₅ detection on PLL-g-PEG biotin patterns.

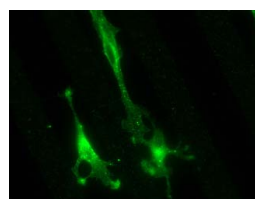


Fig. 2: PAE-VEGFR-2 cells on VEGF-patterned coverslips, stained with anti-VEGFR-2 antibody.

DISCUSSION & CONCLUSIONS: The purpose of this study was to establish a technology mimicking the extracellular milieu of endothelial cells. We were able to grow PAE cells on the heparin/VEGF-A₁₆₅ coated glass support. In a next step, we will culture pluripotent mouse stem cells and primary endothelial cells derived from human tissues as embryoid bodies [3] on our patterned substrates. Various isoforms of VEGF will be added as either soluble or matrix-bound material on the surface of glass coverslips. Further, we will monitor sprouting angiogenesis and vessel formation by live cell video microscopy and histologically after fixation.

REFERENCES: ¹ N. Ferrara (2001) *Am. J. Physiol Cell Physiol* 280, C1358-C1366. ² D. Falconnet, A. Koenig, F. Assi, M. Textor (2004) *Adv. Funct. Mat.* **14**, 749-756. ³ L. Jakobsson, J. Kreuger, L. Claesson-Welsh (2007) *J Cell Biol.* **177**(5):751.

ACKNOWLEDGEMENTS: This work is funded by Swiss National Science Foundation (SNSF).